Investigating the Role of Alternative Polyadenylation in Neuronal Differentiation and Neurodegeneration



Radhika Patel

Merton College

University of Oxford

A thesis submitted for the degree of Doctor of Philosophy

Trinity 2017

Abstract

Investigating the Role of Alternative Polyadenylation in Neuronal Differentiation and Neurodegeneration

Radhika Patel, Merton College, Doctor of Philosophy in Medical Sciences, Trinity 2017

Over 70% of human genes can undergo alternative polyadenylation (APA), whereby they utilise different polyadenylation (poly(A)) sites found in the 3'UTR (3'UTR-APA) or in the upstream coding region of the gene (upstream-APA). The 3'UTR harbours regulatory cis-elements which can mediate the stability, translatability and localisation of the mRNA. Therefore, modulating 3'UTR length through APA can affect downstream gene expression. The UTR landscape can be modified through altered poly(A) site choice during transcription, or in a post-transcriptional manner, via interaction with miRNAs or RNA binding proteins. Global shifts in UTR length have been identified in different tissues and cellular states. Using a combination of molecular biology and bioinformatics approaches, this thesis assesses changes in APA profiles regulated by transcriptional and post-transcriptional APA during neuronal differentiation, in neurodegeneration and in cellular stress. The BE(2)-M17 neuroblastoma cell line was used to model neuronal differentiation. Here, the trend to UTR lengthening in differentiation was attributed primarily to post-transcriptional not transcriptional APA regulation. APA in neurodegeneration was assessed using an *in vitro* model and publicly available RNA-seq datasets were bioinformatically interrogated to assess UTR length changes in Alzheimer's Disease, Parkinson's Disease and Amyotrophic Lateral Sclerosis. While global APA changes were not observed, genes associated with pathophysiological pathways were identified, highlighting the important role of APA mediated gene expression in neurodegenerative diseases. Exposure to cold shock and hypoxia showed differential APA regulation. Interestingly, moderate hypothermia caused a trend to 3'UTR lengthening, even in combination with other stress inducers. These UTR-lengthened genes exhibited binding sites for proteins that associate in stress granules. Therefore, APA regulation may contribute to the aggregation of mRNAs in stress granules during stress conditions. In conclusion, this thesis identifies an unprecedented role of post-transcriptional regulation of the UTR landscape, and identifies physiologically relevant genes regulated by APA during the changing cellular environment.

Acknowledgements

First and foremost, I would like to thank my supervisor André Furger, for envisioning this project and for his continuous guidance, enthusiasm and mentorship throughout the DPhil. I would like to extend my gratitude to the other members of the Furger Lab, particularly Jonathan Neve and Zhiqiao Wang, for their invaluable assistance with bioinformatic and experimental techniques.

In addition, I would like to thank Kieran Clarke, my college advisor, and Merton College for providing a diverse academic and social environment during my time in Oxford. Thank you to friends at Merton and beyond, for providing a life outside of the lab.

Most importantly, I would like to thank my parents Dakshesh and Bharati, and my brother Neeraj, for their eternal support.

Glossary

AD	Alzheimer's Disease
ADP	Adenosine Diphosphate
ALS	Amyotrophic Lateral Sclerosis
APA	Alternative Cleavage and Polyadenylation
ARE	AU-Rich Elements
ATP	Adenosine Triphosphate
BCA	Bicinchoninic Acid
bp	base pairs
BSA	Bovine Serum Albumin
cDNA	copy DNA
CFIm	Mammalian Cleavage Factor I
CFIIm	Mammalian Cleavage Factor II
CLIP	Cross Linked Immunoprecipitation
CNS	Central Nervous System
CPE	Cytoplasmic Polyadenylation Element
CPSF	Cleavage and Polyadenylation Specificity Factor
CR	Coding Region
CstF	Cleavage Stimulation Factor
CTD	Carboxyl Terminal Domain
DaPars	Dynamic Analysis of Alternative Polyadenylation from RNA-Seq
DMEM	Dulbecco's Modified Eagle Medium
DMSO	Dimethyl Sulfoxide
DNA	Deoxyribonucleic Acid
DNase	Deoxyribonuclease
dNTP	Deoxynucleotriphosphate
DREME	Discriminative Regular Expression Motif Elicitation
DSE	Downstream Element
dsRNA	double stranded RNA
ECL	Enhanced Chemiluminescence
EDTA	Ethylenediaminetetraacetic acid
EOAD	Early Onset Alzheimer's Disease
EJC	Exon Junction Complex
ER	Endoplasmic Reticulum
ERAD	ER Associated Degradation
ETC	Electron Transport Chain
FACS	Fluorescence Activated Cell Sorting
fAD	familial Alzheimer's Disease
fALS	familial Amyotrophic Lateral Sclerosis
FBS	Foetal Bovine Serum
FC	Fold Change
FCCP	Carbonyl cyanide-p-trifluoromethoxyphenylhydrazone

fPD	familial Parkinson's Disease
GO	Gene Ontology
GTP	Guanosine Triphosphate
HBSS	Hank's Balanced Salt Solution
HEK293	Human Embryonic Kidney 293 Cell Line
HIF-1	Hypoxia Inducible Factor 1
hnRNP	Heterogeneous Nuclear Ribonucleoproteins
HRE	Hypoxia Response Element
HRP	Horseradish Peroxidase
HSF1	Heat Shock Transcription Factor 1
HSP	Heat Shock Protein
IMM	Inner Mitochondrial Membrane
IMS	Inter Membrane Space
iPSC	induced Pluripotent Stem Cells
kb	kilo-base pairs
kDa	kilo Daltons
lncRNA	long noncoding RNA
LOAD	Late Onset Alzheimer's Disease
MA	Mean Average
Mbnl	Muscleblind-like
MEF	Mouse Embryonic Fibroblast Cell Line
MPP+	1-Methyl-4-phenylpyridinium
MPTP	1-methyl-4-phenyl-1,2,3,6-tetrahydropyridine
miRNA	micro RNA
mRNA	messenger RNA
mRNP	mRNA-protein complex
mtDNA	mitochondrial DNA
NLS	Nuclear Localisation Sequence
NMD	Nonsense Mediated Decay
OCR	Oxygen Consumption Rate
OMM	Outer Mitochondrial Membrane
ORF	Open Reading Frame
OXPHOS	Oxidative Phosphorylation
P-body	Processing body
PABPN1	Poly(A) Binding Protein Nuclear 1
PANTHER	Protein Analysis Through Evolutionary Relationships
PAR-CLIP	Photoactivatable Ribonucleoside enhanced Cross-Linking and Immunoprecipitation
PBS	Phosphate Buffered Saline
PBS+	PBS with $MgCl_2$ and $CaCl_2$
PCR	Polymerase Chain Reaction
PD	Parkinson's Disease
PDUI	Percentage of Distal Poly(A) site Usage Index
PHD	Prolyl hydroxylase

PI	Propidium Iodide
Pol II	RNA Polymerase II
Poly(A)	Polyadenylation
Pre-mRNA	Precursor messenger RNA
RA	Retinoic Acid
RAR	Retinoic Acid Receptor
RARE	Retinoic Acid Receptor Element
RBP	RNA Binding Protein
RISC	RNA induced silencing complex
RNA	Ribonucleic Acid
RNase	Ribonuclease
RNA-Seq	RNA sequencing
rRNA	ribosomal RNA
ROS	Reactive Oxygen Species
RPM	Reads Per Million
RRM	RNA Recognition Motif
RT-PCR	Reverse Transcription Polymerase Chain Reaction
RXR	Retinoid Receptor
sAD	sporadic Alzheimer's Disease
sALS	sporadic Amyotrophic Lateral Sclerosis
SDS	Sodium Dodecyl Sulphate
siRNA	small interfering RNA
snRNP	small nuclear Ribonucleoproteins
sPD	sporadic Parkinson's Disease
TBE	Tris/Borate/EDTA Buffer
TBS-T	Tris Buffered Saline with Tween20
TEMED	Tetramethylethylenediamine
TH	Tyrosine Hydroxylase
USE	Upstream Element
UTR	Untranslated Region
WT	Wild Type

List of Figures

Figure 1.1. Overview of pre-mRNA processing 3
Figure 1.2. Overview of Cleavage and Polyadenylation 6
Figure 1.3. Alternative Cleavage and Polyadenylation 10
Figure 1.4. Transcriptional and Post-Transcriptional Regulation of APA 12
Figure 1.5. Overview of miRNA Mediated Gene Repression 22

Figure 2.1 Outline of the Seahorse XF Mito Stress Assay 33

Figure 3.1. Retinoic acid (RA) Mediated Signalling 46
Figure 3.2. Characterising the Differentiation of BE(2)-M17 cells 49
Figure 3.3. Preparing libraries of Cytoplasmic and Nuclear RNA 52
Figure 3.4. Gene Expression Changes During Differentiation of BE(2)-M17 cells 54
Figure 3.5. A trend to 3'UTR Lengthening in the Differentiation of BE(2)-M17 cells 56
Figure 3.6. Greater 3'UTR Lengthening occurs in the Cytoplasm During the Differentiation of BE(2)-M17 cells 58
Figure 3.7. The Role of miRNAs in Mediating Cytoplasmic APA changes 62
Figure 3.8. *MAST1* Regulated by Upstream-APA During Differentiation of BE(2)-M17 cells 65
Figure 3.9. 3'UTR Lengthening During Differentiation in the *PRDX6* gene Correlates with Altered Protein Localisation 69
Figure 3.10. 3'UTR Shortening During Differentiation in the *CACYBP* gene Correlates with Reduced Protein Expression 73

Figure 4.1. Outline of the Ubiquitin Proteasome Pathway 92
Figure 4.2 Outline of Autophagy 94
Figure 4.3. Mitochondria and the Electron Transport Chain 96
Figure 4.4. *UBR1* and *OGDHL* show significant APA changes in LOAD 104
Figure 4.5. APA in Different Regions of the Brain 108
Figure 4.6. APA Regulation in fPD compared to sPD 112
Figure 4.7. APA Regulation in sPD 115
Figure 4.8. APA Regulation in c9ALS and sALS patients 120
Figure 4.9. APA Regulation in Motor Neurons in sALS 124
Figure 4.10 MPP+ Inhibits Complex I 135
Figure 4.11. Characterizing the BE(2)-M17 MPP+ *in vitro* model for PD 141
Figure 4.12. ER Stress Related Genes Upregulated with MPP+ Treatment 145
Figure 4.13. Post-transcriptional Regulation of 3'UTR APA profiles with MPP+ 147
Figure 4.14. 3'UTR Shortening in *PSMB2* 150
Figure 4.15. Global Regulation of APA through alternative UTR Cis-elements with MPP+ 154
Figure 4.16. Upstream-APA increases Full-length *NPM-1* Expression with MPP+ Treatment 157

Figure 4.17. Overlap of APA events in PD between *in silico* and *in vitro* Analysis 162

Figure 5.1. Outline of the Hypoxia Signalling Pathway 171
Figure 5.2. Characterisation of Cold Shock at 28°C for 24 h in BE(2)-M17 cells 175
Figure 5.3. Widespread Gene Expression Changes in Cold Shock 178
Figure 5.4. A Trend to 3'UTR Lengthening occurs in Cold Shock in BE(2)-M17 cells 181
Figure 5.5. 3'UTR Shortening in *RAB7A* Correlates with Increased Protein Output in Cold Shock 182
Figure 5.6. Role of RBM3 and CIRBP in Cold Shock in BE(2)-M17 cells 185
Figure 5.7. Let-7 family of miRNAs may Impact UTR landscape in Cold Shock 188
Figure 5.8. Cold Shock Mediated APA Changes in Differentiated BE(2)-M17 cells 191
Figure 5.9. 3'UTR Lengthening Observed in Cold Shock in HEK293 cells 195
Figure 5.10. Gene Expression Signature of Hypoxia in BE(2)-M17 cells 199
Figure 5.11. Greater Extent of Post-Transcriptional APA Regulation in Hypoxia 203
Figure 5.12. The Role of miRNAs in Mediating the UTR Landscape During Hypoxia 205
Figure 5.13. Differential Gene Expression in BE(2)-M17 cells Exposed to MPP+ or Hypoxia at Different Temperatures 209
Figure 5.14. Differential APA Regulation in BE(2)-M17 cells Exposed to MPP+ or Hypoxia at Different Temperatures 212
Figure 5.15. Stress Specific APA Changes at 28°C Compared to 37°C 214
Figure 5.16. Regulation of *ELAVL1* by APA correlates with Protein Output in Different Stress Conditions 217

List of Tables

Table 1.1.	The Proteins that Constitute the Core poly(A) Machinery	7
Table 1.2	Trans-factors that Influence Poly(A) Site Choice at the Point of Cleavage	15
Table 1.3.	Other Factors Affecting Poly(A) Site Choice at the Point of Cleavage	17
Table 1.4.	Regulatory Cis-elements identified in 3'UTRs	18
Table 2.1.	A Table outlining the Chemicals and Materials used	39
Table 2.2.	A Table outlining the Kits used	40
Table 2.3.	A Table listing the Composition of Buffers used	41
Table 2.4	Primer sequences used in RT-PCR	42
Table 2.5	Antibodies used for Western Blotting and Immunofluorescence	43
Table 2.6	GEO Accession Numbers of Publicly Available RNA-seq data	43
Table 4.1.	Genes Associated with AD	83
Table 4.2	Genes Associated with PD	85
Table 4.3.	Genes Associated with ALS	88
Table 4.4	Individual Genes Linked to APA Regulation in AD, PD and ALS	100
Table 4.5.	Background of RNA Samples from the LOAD RNA-seq Dataset	103
Table 4.6.	Background of RNA Samples from sPD and fPD RNA-seq Dataset	111
Table 4.7.	Background of RNA Samples from c9ALS and sALS RNA-seq Dataset	119
Table 4.8.	Methods to Model Neurodegenerative Diseases *in vitro*	132
Table 4.9.	The Effects of MPP+ on Different Cellular Pathways	136
Table 5.1.	*In vitro* Stress Inducers and Response Pathways	166

Table of Contents

Abstract i
Acknowledgements ii
Glossary iv
List of Figures vii
List of Tables ix

Chapter 1: Introduction **1**

1.1 Pre-mRNA processing 1
1.1.1 5' end capping 1
1.1.2 Splicing 2
1.1.3 Cleavage and Polyadenylation 4
1.1.3a The Cleavage and Polyadenylation Site 4
1.1.3b The Cleavage and Polyadenylation Machinery 5
1.1.3c The Role of the Poly(A) Tail 8
1.2 Alternative Cleavage and Polyadenylation 9
1.2.1 Transcriptional and Post-Transcriptional APA 11
1.3 Regulation of Transcriptional APA 13
1.3.1 Differential Poly(A) Site Architecture 13
1.3.2 Conservation of Poly(A) Site Usage 13
1.3.3 Factors Mediating Poly(A) Site Choice 14
1.4. Regulation of Post-Transcriptional APA 18
1.4.1 3'UTR and Stability 19
1.4.2 3'UTR and Translation 19
1.4.3 3'UTR and Localisation 20
1.4.4 miRNA Mediated Regulation 21
1.5 APA in Different Environments 23
1.5.1 APA in Different Tissues 23
1.5.2 APA in Different Cellular States 23
1.5.3 APA in Disease 24
1.5.4 APA in Stress 25
1.6 Thesis Objectives 26

Chapter 2: Materials and Methods **27**

2.1 Cell Culture 27
2.2 Cell Treatments 28
2.2.1 Retinoic acid (RA) Treatment 28
2.2.2 MPP+ Treatment 28
2.2.3 Cold Shock Exposure 28
2.2.4 Hypoxia Exposure 28
2.3 Subcellular RNA Isolation 29
2.4 Gel Electrophoresis 29

2.5 RT-PCR 30
2.6 Protein Isolation 30
2.7 SDS-PAGE and Western blotting 31
2.8 Immunofluorescence 31
2.9 Seahorse XF Mito Stress Assay 32
2.10 CYTO-ID kit Assay 34
2.11 MitoSOX™ Assay 34
2.12 Fluorescent Activated Cell Sorting (FACS) Analysis 34
2.13 Microscopy 35
2.14 QuantSeq 3' mRNA-Seq Library Preparation 35
2.15 hsDNA Bioanalyzer Assay 35
2.16 RNA-seq on Ion Proton Platform 35
2.17 Bioinformatics Pipeline to Assess Gene Expression and APA 36
2.18 Hierarchical Clustering Analysis 36
2.19 Panther Gene Ontology Analysis 36
2.20 Motif Enrichment Analysis 36
2.21 miRNA Enrichment Analysis 37
2.22 DaPars 37
2.23 Secondary Structure Prediction 38
2.24 Regulatory Cis-Element Identification 38

Chapter 3: APA in Differentiation 44

3.1 Introduction 44
3.1.1 APA in Differentiation 44
3.1.2 Retinoic acid Mediated Differentiation 45
3.1.3 BE(2)-M17 Neuroblastoma Cell Line 47
3.1.4 Chapter Aims 47
3.2 Results 48
3.2.1 Characterising the Differentiation of BE(2)-M17 cells 48
3.2.2 Isolation of Cytoplasmic and Nuclear RNA and Generation of 3'end libraries 50
3.2.3 Differentiation of BE(2)-M17 shows Widespread Gene Expression Changes 53
3.2.4 Modest APA changes Identified During Differentiation in Total RNA 55
3.2.5 Greater 3'UTR Lengthening in the Cytoplasm compared to the Nucleus 57
3.2.6 Altered miRNA Expression in Differentiation may Contribute to Cytoplasmic 3'UTR-APA Regulation 60
3.2.7 Upstream-APA shows a Trend to Longer Transcript Isoforms During Differentiation 63
3.2.8 A Shift to 3'UTR lengthening in *PRDX6* During Differentiation Correlates with Altered Protein Localisation 67
3.2.9 3'UTR Shortening in *CACYBP* During Differentiation Correlates with Reduced Protein Output 71

3.3 Discussion 74

3.3.1 Genome-wide Transcriptome Changes During Differentiation 74
3.3.2 3'UTR-APA in *PRDX6* correlated with Altered Protein Localisation 77
3.3.3 3'UTR-APA in *CACYBP* correlated with Reduced Protein Output 79
3.3.4 Conclusions and Future Outlook 80

Chapter 4: APA in Neurodegeneration **81**

4.1 Introduction 81
4.1.1 Alzheimer's Disease 82
4.1.2 Parkinson's Disease 84
4.1.3 Amyotrophic Lateral Sclerosis 87
4.1.4 Commonalities between Neurodegenerative Diseases 90
4.1.5 Pathways Associated with Neurodegenerative Diseases 91
4.1.5a Ubiquitin Proteasome Pathway 91
4.1.5b Autophagy 93
4.1.5c Mitochondrial Function 95
4.1.6 APA in Neurodegeneration 97
4.1.7 Chapter Aims 97

Chapter 4A: APA in Neurodegeneration: an *in silico* model **98**

4A.1 Introduction 98
4A.2 APA in Alzheimer's Disease 101
4A.2.1 APA Regulation in Hippocampi of LOAD Patients 102
4A.2.2 Comparison of APA in Different Regions of the AD brain 106
4A.3 APA in Parkinson's Disease 109
4A.3.1 APA in Sporadic and Familial PD 109
4A.3.2 APA in Different Sporadic PD Patients 113
4A.4 APA in ALS 116
4A.4.1 APA in the Frontal Cortex and Cerebellum of ALS Patients 117
4A.4.2 APA in Lumbar Spinal Cord Motor Neurons in Sporadic ALS Patients 122
4A.5 Discussion 125
4A.5.1 The Use of DaPars 125
4A5.2. APA in AD 126
4A.5.3 APA in PD 128
4A.5.3 APA in ALS 129
4A.5.4 Conclusions and Future Outlook 130

Chapter 4B: APA in Neurodegeneration: an *in vitro* model 132

4B.1 Introduction 132
4B.1.1 *In vitro* Model of PD using MPP+ 133
4B.2. Results 139
4B.2.1 Characterizing the MPP+ Model of PD in BE(2)-M17 cells 139
4B.2.2 MPP+ Treatment Upregulates Genes of the ER Stress Pathways 143
4B.2.3 Protein Degradation Genes Regulated by APA in MPP+ Treated Cells 146
4B.2.4 Regulatory Cis-elements may Mediate Cytoplasmic APA Profiles with MPP+ Treatment 152
4B.2.5 Upstream-APA in *NPM1* with MPP+ Treatment Increases Abundance of Transcript Encoding Functional Protein 156
4B.3 Discussion 159
4B.3.1 Characterisation of MPP+ to Model PD *in vitro* 159
4B.3.2 Gene Expression Changes with MPP+ Treatment 159
4B.3.3 APA Changes in the MPP+ Model 160
4B.3.4 Cis-element Regulation of APA in MPP+ Model 161
4B.3.5 Comparison of *in silico* and *in vitro* APA Analysis 162
4B.3.6 Conclusions and Future Outlook 163

Chapter 5: APA in cellular stress 164

5.1 Introduction 164
5.1.1 Types of Cellular Stress 164
5.1.2 Cold Shock 167
5.1.3 Hypoxia 169
5.1.4 Effect of Combined Stress Inducers 172
5.1.5 Chapter Aims 173
5.2 APA in Cold Shock 174
5.2.1 Cold Shock at 28°C does not Alter Cell Morphology or the Cell Cycle 174
5.2.2 Gene Expression Changes with Cold Shock 176
5.2.3 A Trend to 3'UTR Lengthening Observed in the Nuclear and Cytoplasmic Fractions 179
5.2.4 RBM3 and CIRBP do not widely affect APA Profile Changes in Cold Shock in BE(2)-M17 cells 183
5.2.5 Let-7 miRNA Family Associated with Cytoplasmic APA Profile Changes During Cold Shock 186
5.2.6 A Significant Trend to 3'UTR Lengthening in the Nucleus but not the Cytoplasm During Cold Shock in Differentiated BE(2)-M17 cells 189
5.2.7 Cold Shock Induces Cell Type Specific APA Changes between BE(2)-M17 and HEK293 cells 193

5.3. APA in Hypoxia 197
5.3.1 Characterisation of Hypoxia in BE(2)-M17 197
5.3.2 Hypoxia does not Mediate a Shift to either 3'UTR Lengthening or 3'UTR Shortening 201
5.3.3 Cis-elements in alternative UTRs may Mediate Cytoplasmic APA Profiles 204
5.4. APA in combined stresses 206
5.4.1 Moderate Hypothermia Reduces Impact of Differential Gene Expression Induced by MPP+ and Hypoxia 206
5.4.2 Different Cohorts of Genes are Regulated by APA under Different Stress Conditions 211
5.4.3 The Extent of 3'UTR Shortening of *ELAVL1* is Correlated with the Level of Increased Protein Expression 215
5.5 Discussion 218
5.5.1 APA in Cold Shock 219
5.5.2 APA in Hypoxia 222
5.5.3 APA in Combined Stresses 225
5.5.4 Role of RBM3 and CIRBP in Stress 229
5.5.5 Conclusions and Further Work 230

Chapter 6: Discussion **233**

6.1 Introduction 233
6.2 The Importance of Subcellular Fractionation to Investigate APA 234
6.3 Post-transcriptional APA Regulation in Changing Cellular States 235
6.4 The Importance of APA in Neurodegeneration 236
6.5 Conclusions and Future Outlook 238

Chapter 7: Supplementary Data **239**
7.1 Supplementary Figures 239
7.2 Supplementary Tables 251

Chapter 8: References **256**

Chapter 1: Introduction

1.1 Pre-mRNA processing

All protein coding genes are transcribed by RNA Polymerase II (Pol II) to produce pre-messenger RNAs (pre-mRNAs). These pre-mRNAs have a 5' to 3' direction and require processing to produce a mature mRNA for nuclear export to the cytoplasm. Mature mRNAs consist of an open reading frame (ORF) that encodes the protein, which is flanked by an untranslated region (UTR) at both the 5' and 3'end (Figure 1.1A).

For most pre-mRNAs in eukaryotes, three processing mechanisms are required: 5'end capping, splicing and 3'end cleavage and polyadenylation. Initially, these processes were thought to occur after transcription in the nucleoplasm, however it is now widely accepted that mRNAs can also be processed co-transcriptionally (Proudfoot, Furger, and Dye 2002), and the processing machinery has been shown to interact with Pol II itself (Bentley 2014; Saldi et al. 2016), making the mRNA processing mechanism more efficient.

1.1.1 5'end capping

The addition of the 5'cap is the first processing step of pre-mRNA. In this process, a guanosine cap structure is added to the first nucleotide via a 5'-5' triphosphate linkage catalysed by Guanylyl transferase. This terminal guanosine residue is then methylated by Guanylyl-7-methyltransferase (Figure 1.1B). Capping enzymes interact with the Pol II enabling capping of nascent RNA (McCracken et al. 1997). The 5'cap is important for nuclear mRNA export and protection against degradation by 5'-3' exoribonucleases. In addition, the 5'cap interacts with translation initiation factor eIF4E to facilitate the binding of ribosomes to the transcript for translation (Lewis and Izaurralde 1997).

1.1.2 Splicing

Most eukaryotic genes encode transcripts containing alternating exons and introns. In protein coding genes, only exons encode the amino acid sequence of the protein whereas introns need to be removed from the pre-mRNA. This occurs through splicing, which is the most studied pre-mRNA processing mechanism. A large multi-protein-RNA complex is required for this two-step reaction which removes all the non-coding regions of the gene, and fuses the exons together forming the ORF, which is the template for protein synthesis. An overview of splicing is given in Figure 1.1C. Proteins are deposited at the junction between two exons forming an exon-junction complex (EJC), which can influence the localisation and translation of the transcript.

Splicing occurs in all eukaryotes, although lower eukaryotes such as yeast have far fewer intron-containing genes than mammalian or plant genomes. In humans, approximately 97% of genes contain introns and undergo splicing (Grzybowska 2012). Alternative splicing, defined as the inclusion of different subsets of introns and exons in the mature mRNA, occurs in approximately 95% of mammalian genes, contributing significantly to increase transcriptome and proteome diversity. Furthermore, alternative splicing has been identified to be tissue specific and crucial for proper differentiation and development (de Klerk and 't Hoen 2015). Mechanisms of alternative splicing are outlined in Figure 1.1D.

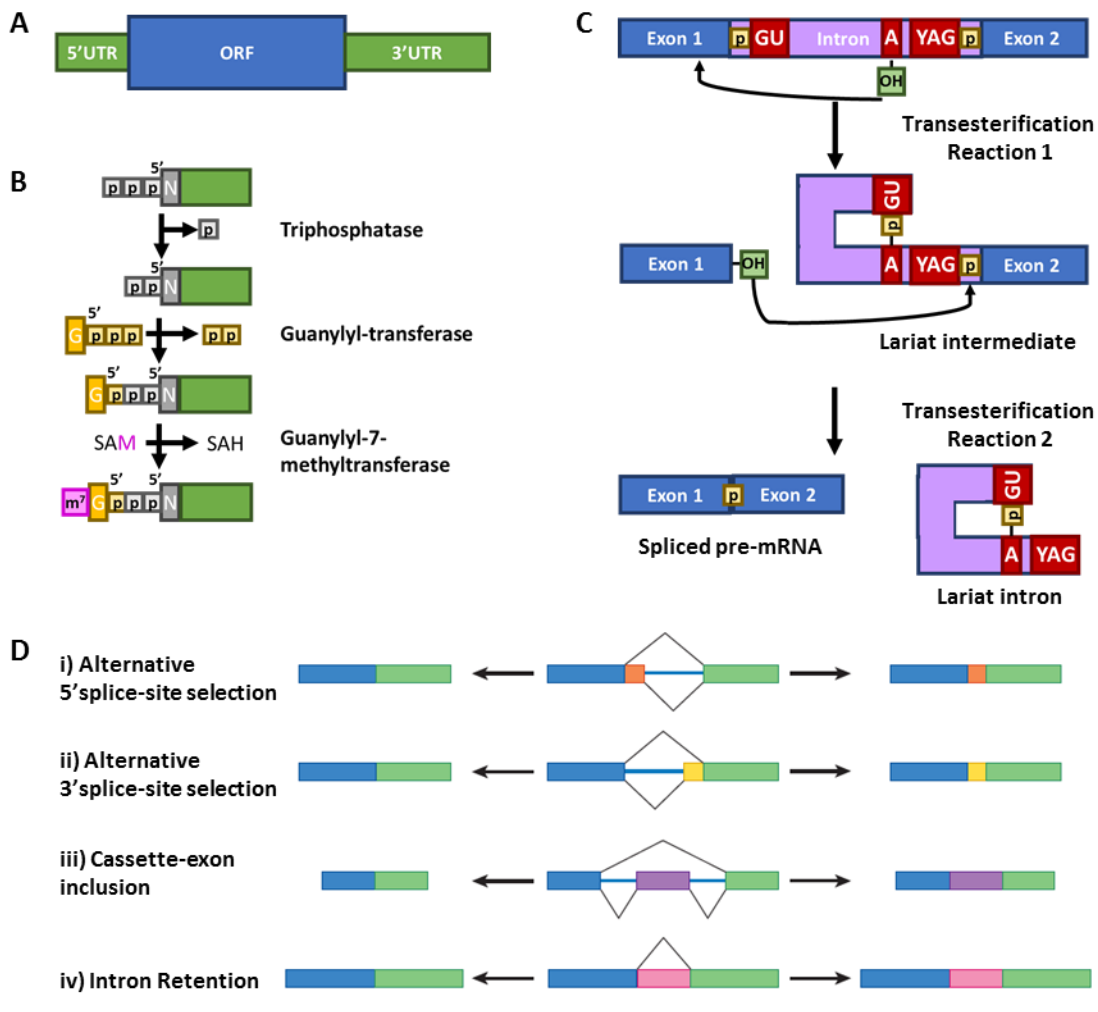


Figure 1.1. Overview of pre-mRNA processing.

A. Schematic of mature mRNA. The open reading frame (ORF, blue), is flanked by untranslated regions (UTRs, green) at the 5' and 3'end.

B. A schematic to show 5' capping. The gamma phosphate (grey) of the terminal residue (N) on the nascent RNA (green) is removed by a triphosphatase. A free GTP residue (G) is added by guanylyl transferase forming a 5'-5' triphosphate linkage. Finally, a methyl group is transferred to the terminal G from an S-adenosyl-L-methionine (SAM), which is converted to S-adenosyl-L-homocysteine (SAH).

C. A schematic to show the two-step splicing reaction. First, a hydroxyl group on an adenine residue in a consensus sequence at the 3'end of the intron, attacks the phosphate before a GU dinucleotide at the 5'end of the intron sequence. This first transesterification reaction forms a lariat intermediate. The hydroxyl group, now at the 3'end of Exon 1 attacks the nucleotide at the 5'end of Exon 2 in another transesterification reaction yielding a spliced pre-mRNA and a lariat intron.

D. Mechanisms of alternative splicing, modified from (Nilsen and Graveley 2010). The middle panel represents the pre-mRNA and the black lines show potential routes of splicing. The mRNAs resulting from exclusion or inclusion of intronic sequences are shown on the left and right respectively. Alternative 5' splice site (i) or 3' splice site (ii) selection can include or exclude partial intronic sequences. Middle segments of the intron can be included through cassette exon inclusion (iii), or the whole intron can be retained (iv).

1.1.3 Cleavage and Polyadenylation

The final step of pre-mRNA processing occurs at the 3'end, known as cleavage and polyadenylation. Almost all protein coding genes in metazoans are processed at the 3'end in the same manner, providing a uniform 3'end of all mRNAs in a two-step mechanism. First, an endonucleolytic cleavage reaction occurs at a specific site in the transcript. This is followed by the addition of a chain of adenosine residues (up to 250 in humans), known as the poly(A) tail, catalysed by an evolutionary conserved enzyme, poly(A) polymerase (Figure 1.2) (Nick J. Proudfoot 2011). This process, termed cleavage and polyadenylation, which also occurs in some long noncoding RNAs (lncRNAs), is closely linked to transcript termination.

1.1.3a The Cleavage and Polyadenylation Site

The cleavage and polyadenylation site (poly(A) site) is found in the 3'UTR of the pre-mRNA. It is defined by a bi-partite cis-element in the 3'UTR of the pre-mRNA, consisting of a conserved A-rich hexamer, 21 nucleotides upstream of the cleavage site, known as the poly(A) signal, and a less conserved U or GU-rich downstream element (DSE), found 10-30 nucleotides downstream of the cleavage site (Figure 1.2A). This poly(A) site is recognised by a complex machinery which enables the two-step cleavage and polyadenylation reaction.

The most common hexamer sequence is AAUAAA or AUUAAA, known as the canonical poly(A) signal, which is found at 70-75% of poly(A) sites (Beaudoing and Gautheret 2001; Neve et al. 2016). More than 10 variations of this hexamer have been found (Tian et al. 2005) but not all non-canonical poly(A) signals have been identified. The cleavage site itself in humans usually occurs at a UA dinucleotide in between the hexamer and DSE. Upstream auxiliary elements (USEs) can also be found around poly(A) sites which aid efficient cleavage and polyadenylation. These can be G-rich quadruplex structures downstream of the cleavage site that can enhance efficient cleavage, or U-rich regions up or downstream of the cleavage site (Neve et al. 2017).

Mutations in the hexamer sequence can significantly reduce cleavage and polyadenylation at that poly(A) site. The DSE was thought to be less sensitive to mutations, but studies have suggested this may not always be the case (Nunes et al. 2010). Numerous factors contribute to the strength of a poly(A) site, including the presence of the canonical

hexamer sequence, the composition and distance of the DSE from the hexamer and the presence of additional USEs, which can enhance the recruitment of cleavage and polyadenylation factors (Neve et al. 2017).

1.1.3b The Cleavage and Polyadenylation Machinery

Over 80 proteins have been identified to mediate mRNA 3'end processing (Y. Shi et al. 2009), although far fewer constitute the core poly(A) machinery (Table 1.1). The hexamer and the downstream GU rich region, are bound by Cleavage and Polyadenylation Specificity Factor (CPSF) and Cleavage Stimulation Factor (CstF) respectively, which initiate 3'end processing. CPSF and CstF are composed of multiple subunits as outlined in Figure 1.2B. The endonuclease cleavage reaction itself, that occurs between the hexamer signal and the DSE, is mediated by the CPSF-73/100 (Mandel et al. 2006). The 3'end RNA product of the cleavage reaction is degraded by hPcf11, while the 5'end-product remains bound by the machinery. CPSF-160 and hFip1 enable recruitment of poly(A) polymerase to catalyse the addition of adenosine residues to the 3'end of the pre-mRNA. The addition of adenosine residues is initially slow, but is accelerated upon recruitment of the nuclear poly(A) binding protein, PABPN1 (Wahle 1991). The cleavage and polyadenylation reaction is outlined in Figure 1.2C.

As with 5'end capping and splicing, the 3'end machinery interacts with the transcriptional machinery, specifically the C-terminal domain (CTD) of Pol II, which increases the efficiency of pre-mRNA processing (Bentley 2014).

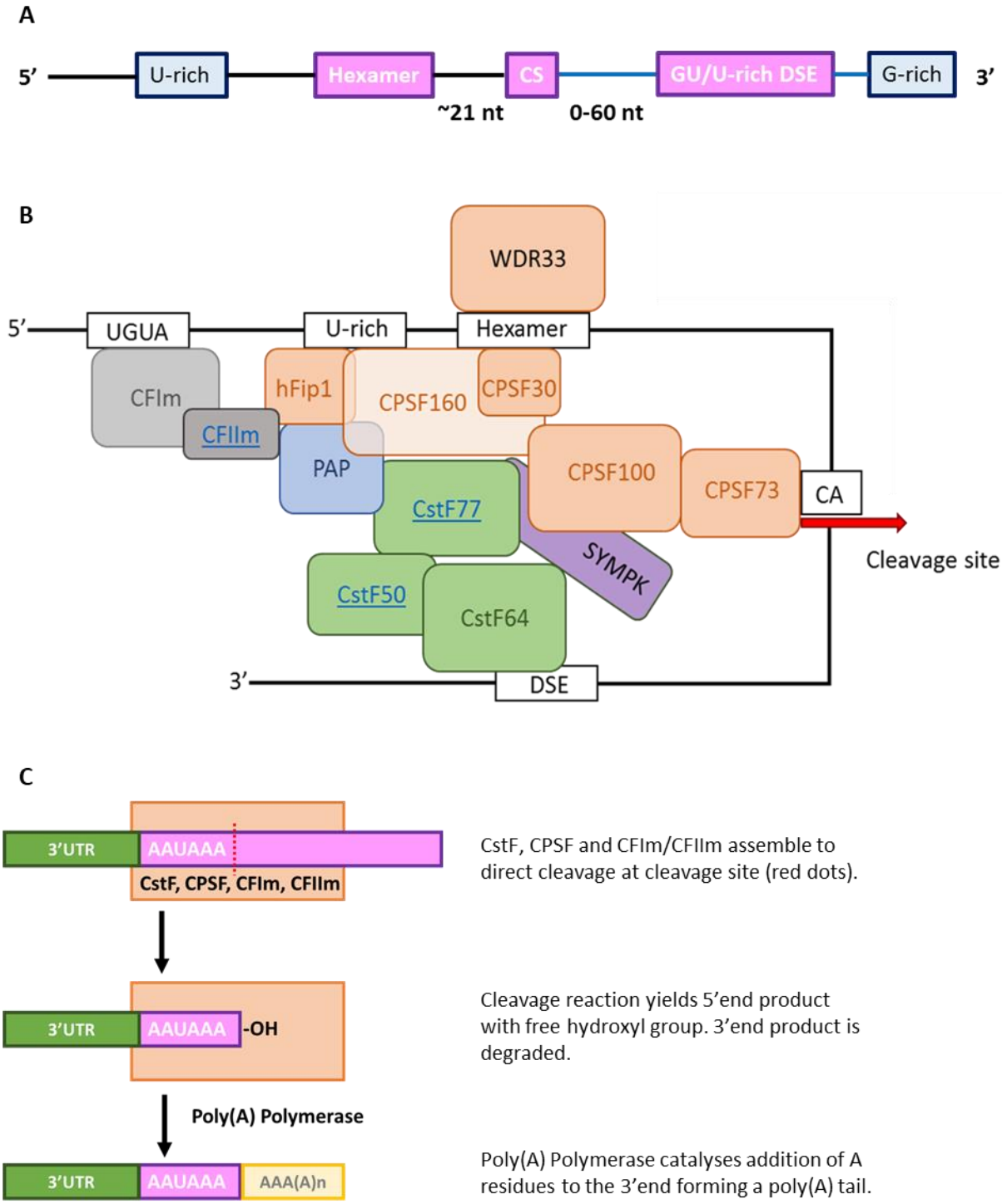


Figure 1.2. Overview of Cleavage and Polyadenylation. Figures modified from (Neve et al. 2017).

A. Cis-elements at the mRNA 3'end which mediate cleavage and polyadenylation. The cleavage site is denoted by CS.

B. The core factors in the poly(A) machinery. The subunits of CstF are labelled in green and the subunits of CPSF are labelled in peach.

C. Schematic to outline the cleavage and polyadenylation reaction in 3'end formation.

Table 1.1. The Proteins that Constitute the Core poly(A) Machinery.

Abbreviations: RRM, RNA Recognition Motif. Reviewed (Neve et al. 2017)

Factor	Function
CPSF	Cleavage and Polyadenylation Specificity Factor. Recognises the hexamer poly(A) signal.
CPSF-160	Mediates interaction with hexamer sequence. Important for interaction with CstF. Interacts with poly(A) polymerase.
CPSF-100	Has endonuclease activity to perform cleavage reaction.
CPSF-73	Has endonuclease activity to perform cleavage reaction.
CPSF-30	Interacts with the hexamer sequence *in vitro*.
hFip1	Interacts with the poly(A) polymerase. Binds the RNA at upstream or downstream U-rich regions
WDR33	Large protein of 146 kDa. Interacts directly with AAUAAA hexamer (Schönemann et al. 2014). Contains WD40 domains to mediate protein-protein interactions with other subunits of CPSF.
CstF	Cleavage Stimulation Factor. Recruited to the DSE. Essential for cleavage but not polyadenylation.
CstF-64	Has RNA Recognition Motif (RRM) which mediates interaction between CstF and pre-mRNA downstream of poly(A) signal. Binds strongly to U-rich region.
CstF-50	Contains WD40 repeat motifs which mediate protein-protein interactions with Pol II CTD.
CstF-77	Role in connecting CstF-64 and CstF-50 subunits forming CstF complex. Mediates interaction between CstF and other proteins including CPSF-160.
CFIm	Cleavage Factor I (mammalian) Stabilizes binding of CPSF to pre-mRNA. Aids recognition of noncanonical poly(A) signals Four subunits: CFIm-68, CFIm-59, CFIm-25, CFIm-72. CFIm-68 and CFIm-25 interact with the RNA via an RRM.
CFIIm	Cleavage Factor II (mammalian). Required for cleavage but not polyadenylation.
CFIIAm	Contain components for cleavage reaction.
CFIIBm	Stimulates cleavage reaction.
hPcf11	Role in degradation of RNA associated with Pol II after cleavage.
hClp1	Interacts with CFIm and CPSF so may bridge these two proteins during the cleavage reaction.
Symplekin	Role in scaffolding the 3'end machinery, and role in histone 3'end formation. Required for cytoplasmic polyadenylation.
Poly(A) Polymerase	Catalyses addition of adenosine residues to the 3'end of the pre-mRNA after the cleavage reaction. Recruited to processing machinery by CPSF and hFip1. Several human isoforms. Uses ATP as a substrate.
PABPN1	Recruited to CPSF and poly(A) polymerase to enhance the addition of adenosines to the poly(A) tail. May interact with the poly(A) signal itself, or CPSF and poly(A) polymerase to modulate this function.
RPB1	The large subunit of CTD of Pol II. Provides platform to bridge transcription with pre-mRNA processing.

1.1.3c The Role of the Poly(A) Tail

Although between 200-250 adenosines are added by the poly(A) polymerase in the nucleus, the length of poly(A) tails in the mammalian cytoplasm has been reported to be as low as 50-100 nucleotides (Chang et al. 2014). A cytoplasmic poly(A) binding protein, PABPC, regulates the length of the poly(A) tail in the cytoplasm (Goss and Kleimann 2013). Short poly(A) tails are associated with dormant transcripts, whereas long poly(A) tails are associated with transcripts ready for translation (Crawford et al. 1997). Dysregulation of poly(A) tail length has been associated with disease, for example, global increase in cytoplasmic adenylation has been identified in cancer, increasing global protein expression levels (Weill et al. 2012). The poly(A) tail prevents 3'end exonucleolytic degradation of the mRNA and is important in mRNA export. In the cytoplasm, the poly(A) tail modulates transcript stability and promotes ribosome assembly by interacting with the 5'cap via PABPC to form a circular mRNA (Reviewed (Weill et al. 2012; Goss and Kleimann 2013)).

Histone coding genes are the only exception to this uniform 3'end processing, which have their own distinct 3'end processing machinery (Dominski and Marzluff 2007). However, a proportion of histone coding genes have been shown to be cleaved and polyadenylated in the same manner as all other nuclear encoded genes in human cell lines (Shepard et al. 2011) and in *C. elegans* (Mangone et al. 2010).

1.2 Alternative Cleavage and Polyadenylation

Constitutive polyadenylation is when a single poly(A) site in the 3'UTR is used for cleavage and polyadenylation in every transcript encoded by that gene (Figure 1.3A). However, approximately 70% of human genes harbour multiple poly(A) sites, with over 50% of genes using 3 or more poly(A) sites (Derti et al. 2012). This means that these genes can undergo alternative cleavage and polyadenylation (APA), whereby differential poly(A) sites can be utilised in different transcripts of the same gene, increasing transcriptome diversity. The mechanism of APA is conserved from yeast to humans. Alternative splicing, which also increases transcriptome diversity, is very rare in yeast, whereas APA is common, suggesting APA pre-dates alternative splicing as a regulatory mechanism.

There are two types of APA: 3'UTR-APA, where alternative poly(A) sites are found in the 3'UTR (Figure 1.3B); or upstream-APA, where the proximal poly(A) site lies upstream in the coding region (CR), in an exonic or intronic region (Figure 1.3C). 3'UTR-APA does not affect the coding potential of the transcript, therefore increases diversity at the transcriptome but not proteome level. On the other hand, upstream-APA modifies the message of the transcript, thereby encoding a different protein. The isoforms that arise from upstream-APA do not introduce a premature translational termination codon, and are consequently not targeted by the Nonsense Mediated Decay (NMD) degradation pathway, enabling translation of a truncated protein, with a potentially altered function (Lejeune and Maquat 2005).

3'UTRs harbour numerous regulatory cis-elements, which can influence the stability, nuclear export, localisation and translatability of the transcript. Regulatory cis-elements only found in the longer, or alternative UTR, as oppose to the constitutive UTR, would enable specific regulation of the longer transcript isoform. Furthermore, altered poly(A) site usage could result in different secondary structures of the mRNA which could mask or expose regulatory elements. Therefore, usage of different poly(A) sites within the 3'UTR is a crucial mechanism which can affect downstream gene expression. Reports suggest that highly expressed genes utilise proximal poly(A) sites and therefore have shorter 3'UTRs, whereas lowly expressed genes are more likely to use the distal poly(A) sites (Zhe Ji et al. 2009; Zhe Ji et al. 2011).

A classic example of upstream-APA is found in the gene encoding the antibody IgM. In resting B cells, the poly(A) site in the terminal exon is used to produce a longer membrane bound protein. However, upon B cell activation CstF-64 enables a switch to use a poly(A) site in an upstream exon, which produces a truncated protein that is secreted (Takagaki et al. 1996). Over 40% of APA events in mice were identified to be upstream-APA events (Hoque et al. 2013), yet most studies in the APA field have focussed on 3'UTR-APA.

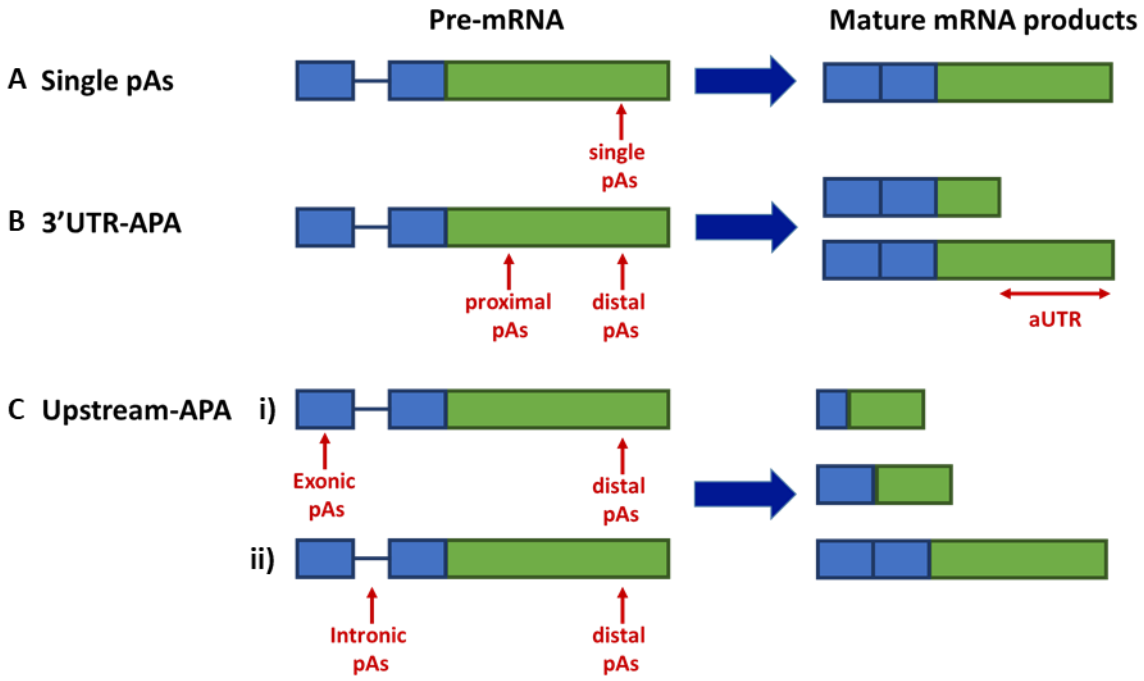


Figure 1.3. Alternative Cleavage and Polyadenylation.

A. Fewer than 30% of mRNAs have a single poly(A) site, where all transcripts have the same UTR length.

B. 3'UTR-APA. Usage of an upstream poly(A) site in the UTR will not affect the encoded protein, but will affect UTR length to modulate the presence of regulatory cis-elements, including miRNA target sites, and RBP binding sites found in the alternative UTR (aUTR).

C. Upstream-APA. An upstream poly(A) site can be found in i) an upstream exon or ii) an upstream intron. Usage of these upstream poly(A) sites affects the coding potential of the transcript. Exons in ORF indicated in blue, 3'UTR indicated in green.

1.2.1 Transcriptional and Post-transcriptional APA

The choice of poly(A) site selection can occur during transcription, referred to as transcriptional APA, where the cleavage and polyadenylation machinery assembles around a poly(A) site to select its usage. Transcriptional APA is modulated by the changes in availability of cleavage and polyadenylation factors which can enhance or repress usage of a poly(A) site, to influence the nuclear APA profile (Figure 1.4A). However, the levels of the short and long 3'UTRs transcribed in the nucleus can be very different in the cytoplasm due to nuclear export rates or post-transcriptional mechanisms to stabilize or degrade one of the transcript isoforms. This process, post-transcriptional APA, can lead to a different transcriptome in the cytoplasm compared to the nucleus (Figure 1.4B).

The nucleus, in general, shows an increased usage of the distal poly(A) sites compared to the cytoplasmic transcriptome (Neve et al. 2016; Djebali et al. 2012), which suggests that either the longer 3'UTR isoforms are retained in the nucleus, or they are targeted for degradation once they are exported into the cytoplasm.

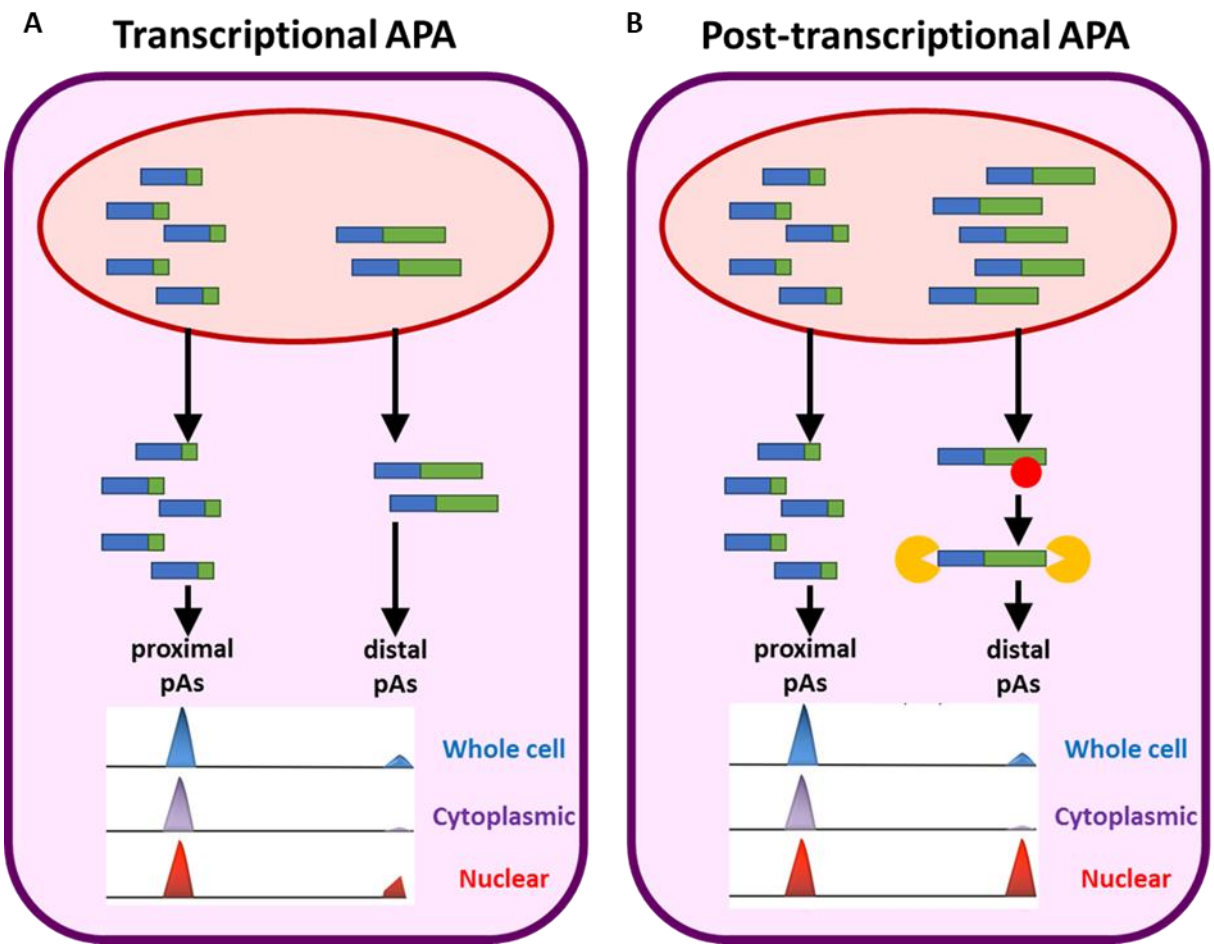


Figure 1.4. Transcriptional and Post-Transcriptional Regulation of APA.

A schematic to show how APA profiles can differ through either Transcriptional (**A**) or post-transcriptional APA (**B**). In transcriptional APA, the abundance of short and long 3'UTRs is determined at the point of cleavage in the nucleus, influencing the whole-cell APA profile. In post-transcriptional APA, the abundance of short and long 3'UTRs is determined by post-transcriptional regulatory mechanisms in the cytoplasm. Here, the binding of an RBP (red circle) to the 3'UTR (green) targets the longer isoform for degradation by exonucleases (yellow Pacman). Therefore, although the whole-cell APA profile appears to be the same as in part **A**, the transcriptome is regulated in a different manner. Figure modified from (Neve et al. 2017).

1.3 Regulation of Transcriptional APA

1.3.1 Differential Poly(A) Site Architecture

The strength of a poly(A) site can be determined by the presence of canonical cis-elements. Generally, stronger poly(A) sites display increased usage compared to weaker ones. The distal poly(A) site has been shown to be more likely to display the canonical hexamer poly(A) signal, and have a GU or U-rich DSE. However, upstream proximal poly(A) sites are more likely to lack these signals but instead have noncanonical structure including G-rich and CU-rich elements (Beaudoing and Gautheret 2001; Martin et al. 2012; Shepard et al. 2011). This makes proximal poly(A) sites weaker, as the polyadenylation machinery may not recognise these signals as efficiently. This phenomenon is conserved from yeast to humans (Smibert et al. 2012). There is an array of evidence to suggest that distal poly(A) sites are default, whereas proximal poly(A) sites are used to exclude the regulatory elements found in the UTRs (Di Giammartino, Nishida, and Manley 2011).

1.3.2 Conservation of Poly(A) Site Usage

The usage of poly(A) sites between different tissues varies considerably. In the testes, global usage of proximal poly(A) sites has been reported (W. Li et al. 2015), while in the central nervous system (CNS) and the brain, there is a shift to usage of distal poly(A) sites, and therefore longer UTRs, in both invertebrates and mammals (Smibert et al. 2012; Miura et al. 2013; Lianoglou et al. 2013). The usage of proximal or distal poly(A) sites is more conserved between tissues of different species than different tissues within a single species (Derti et al. 2012).

Despite the high conservation of most genes between humans and mice, fewer than 500 poly(A) sites are conserved (Ara et al. 2006). However, the distal poly(A) sites, which are more likely to contain the canonical hexamer, are more likely to be conserved between species (Martin et al. 2012). This suggests that the distal poly(A) sites are the default site whereas the proximal sites are used to remove regulatory elements and modulate gene expression (Y. Shi 2012).

1.3.3 Factors Mediating Poly(A) Site Choice

Over 80 proteins have been associated with the cleavage and polyadenylation machinery but the mechanism of poly(A) site choice it is still largely unclear. This is primarily due to the large variety of factors that influence poly(A) site choice, including the strength of the poly(A) site determined by its architecture and numerous trans-factors that can preferentially utilise or repress a poly(A) site. Further, the concentration of trans-factors present can influence poly(A) site usage (W. Li et al. 2015). An overview of RNA Binding Proteins (RBPs) that influence poly(A) site choice at the point of cleavage are shown in Table 1.2. In addition, tissue specific expression of trans-factors can contribute to tissue specific APA profiles. For example, the expression of β-CstF-64, a neuron-specific variant of Cst-F64, contributes to altered poly(A) site choice during neuron development by increasing the usage of weaker poly(A) sites (Shankarling and MacDonald 2013; MacDonald and McMahon 2010).

The overlapping roles of RBPs in both splicing and cleavage and polyadenylation are becoming more evident, highlighting the coordinated nature of the stages of pre-mRNA processing (Licatalosi and Darnell 2010). For example, U1snRNP, a member of the family of small nuclear ribonucleoproteins (snRNPs) that constitute the spliceosome, interacts with poly(A) polymerase to inhibit polyadenylation (Gunderson, Polycarpou-Schwarz, and Mattaj 1998). U1snRNP was more recently shown to influence poly(A) site choice by suppressing the usage of upstream cryptic poly(A) sites whose usage would produce truncated transcripts (Kaida et al. 2010).

In addition to RBPs, the surrounding chromatin environment and transcriptional regulatory mechanisms such as the Pol II elongation rate can also contribute to the poly(A) site choice (Table 1.3). The combination of these different factors will inevitably mediate poly(A) site usage during 3'end processing of the pre-mRNA.

Table 1.2 Trans-factors that Influence Poly(A) Site Choice at the Point of Cleavage.

Factor	Role	Reference
Associated with poly(A) machinery		
CstF-64	Binds U-rich regions in 3'UTR. In B cells, increased CstF-64 levels increase usage of upstream poly(A) site in upstream exon which enables switch of membrane bound IgM form to the secreted form. Enhances usage of weaker proximal poly(A) site. Novel role in promoting usage of noncanonical poly(A) sites.	(Takagaki et al. 1996) (Hwang et al. 2016)
βCstF-64	Neuron specific variant which has an extra 49 amino acids in PG rich domain of CstF-64. Ubiquitous function in vertebrate nervous system. Interaction with CstF enhances usage of proximal poly(A) sites.	(Shankarling and MacDonald 2013)
τCstF-64	Specific but dispensable role in brain and in testis. Promotes usage of proximal poly(A) site. Depletion leads to usage of distal poly(A) site.	(MacDonald and McMahon 2010)
CstF-77	Associated in negative feedback loop to regulate its own expression. Increased levels of CstF-77 activates intronic poly(A) site to produce truncated transcript.	(Luo et al. 2013)
hFip1	Promotes usage of weaker proximal poly(A) sites. Low levels reduce proximal poly(A) site usage.	(Lackford et al. 2014)
CFIm-25	Suppresses proximal poly(A) site usage as knockdown leads to global switch to using proximal poly(A) site. Binds to proximal suboptimal poly(A) sites to repress their usage which promotes usage of distal poly(A) sites.	(Masamha et al. 2014) (Martin et al. 2012)
hPcf11	Increases proximal poly(A) site usage.	(W. Li et al. 2015)
PABPN1	Interacts with and suppress the proximal poly(A) signal. Its absence or mutation in Oculopharyngeal Muscular Dystrophy leads to global 3'UTR shortening.	(Jenal et al. 2012) (De Klerk et al. 2012)
PTB	Binds DSE in competition with CstF-64 which inhibits usage of the corresponding poly(A) site.	(Castelo-Branco et al. 2004)
Other RBPs		
αCP	Enhances usage of poly(A) sites that are close to C-rich motifs.	(X. Ji et al. 2013)
CIRBP/ RBM3	Binds to GNNGNNG motif in 3'UTR. Increased expression in cold shock inhibits usage of the proximal poly(A) site causing 3'UTR lengthening.	(Y Liu et al. 2013)
CPEB1	Cytoplasmic poly(A) element (CPE) binding protein which can shuttle into the nucleus and mediate usage of poly(A) sites close to CPEs. Recruits poly(A) machinery to use proximal poly(A) site during proliferation.	(Bava et al. 2013)
ELAVL1	Member of ELAVL family which binds AU-rich elements (AREs) in 3'UTR. Influences poly(A) site usage of its own transcript. Inhibits poly(A) site usage close to binding by preventing the interaction between RNA and CPSF-160 and CstF-64. In the cytoplasm, can bind UTRs to stabilise target mRNAs.	(Mansfield and Keene 2012) (H. Zhu et al. 2007).
FUS	Binds UGGUU motif. FUS binding downstream of poly(A) site enables recruitment of CPSF160 and enhances usage of that poly(A) site causing transcriptional termination.	(Masuda et al. 2015)
hnRNP A2/B1	Binds to UAGG motif in 3'UTR. Has predominantly nuclear localisation. Depletion in human induced Pluripotent Stem Cells (iPSC) derived motor neuron cells showed 3'UTR lengthening.	(Martinez et al. 2016)

hnRNP C	Its binding to U-rich sequences masks nearby poly(A) sites suppressing their usage.	(A. J. Gruber et al. 2016)
hnRNP H	hnRNP H1 binds DSE to promote usage of proximal poly(A) sites. hnRNP H2 binds G-rich regions to enhance CstF-64 binding. High expression of hnRNP H2 in proliferating cells enhances usage of proximal poly(A) sites. Reduced expression of hnRNP H2 in differentiated cells encourages usage of distal poly(A) sites.	(Katz et al. 2010) (Bagga, Arhin, and Wilusz 1998) (Shepard et al. 2011)
hnRNP F	Binds to G-rich DSE which competes with CstF-64, repressing usage of the nearby poly(A) site.	(Alkan, Martincic, and Milcarek 2006)
hnRNP K	Binds a UCCCUU motif in 3'UTR which reduces usage of nearby poly(A) site. Competes with CFI for pre-mRNA binding site.	(Naganuma et al. 2012)
Mbnl	Binds to R/YGCY motif. Location of motif relative to poly(A) site mediates effect of Mbnl binding. Mbnl binding close to poly(A) site inhibits its usage due to steric hindrance. Binding upstream of the poly(A) site enhances its usage. Binding of Mbnl to 3'UTR can also alter localisation of transcript.	(Batra et al. 2014) (Taliaferro et al. 2016)
Nova	Brain specific protein regulating neuronal APA. Nova1 associates with YCAY elements in the 3'UTRs. Poly(A) site usage depends on surrounding architecture: suppresses usage of sites close to binding perhaps through steric inhibition; enhances usage of poly(A) sites distant from Nova binding site. Binding in constitutive UTR causes 3'UTR lengthening; binding in alternative UTR causes 3'UTR shortening.	(Licatalosi et al. 2008) (Wenchao Hu, Liu, and Yan 2014)
PABPC1	Promotes distal poly(A) usage.	(W. Li et al. 2015)
U1 snRNP	Suppresses the usage of cryptic poly(A) sites found in the gene body enabling transcription of the full-length gene.	(Kaida et al. 2010)

Table 1.3. Other Factors Affecting Poly(A) Site Choice at the Point of Cleavage

Factor	Mechanism	Reference
Chromatin state	An open chromatin state favours usage of the proximal poly(A) site resulting in 3'UTR shortening by transcriptional APA regulation.	(W. Li et al. 2016)
H3K36me3	Creates more open chromatin state which was associated with increased usage of proximal poly(A) site.	(Z Ji et al. 2011)
H3K4me3	Increased H3K4me3 correlated with increased use of proximal poly(A) sites in 3'UTR-APA as seen during spermatogenesis. Open chromatin state associated with usage of proximal poly(A) site.	(W. Li et al. 2016) (Z Ji et al. 2011)
CpG islands	Allele-specific DNA methylation affected usage of poly(A) sites in the mouse H13 gene to affect upstream-APA.	(Wood et al. 2008)
Dicer	In the nucleus, Dicer can modify the chromatin environment to alter the Pol II elongation rate which can affect poly(A) site usage. In closed chromatin conditions, Pol II transcribes slowing enhancing proximal poly(A) site usage.	(Neve et al. 2016)
Nucleosome positioning	Depletion of nucleosomes can increase usage of exposed poly(A) sites.	(Spies et al. 2009) (Huang et al. 2013)
Pol II elongation rate	Slow elongation rate encourages usage of proximal poly(A) sites. G-rich sequences which cause transcriptional pausing can also enhance use of nearby poly(A) site.	(Pinto et al. 2011).
Transcription Factors	Transcription Factor E2F can preferentially increase usage of proximal poly(A) sites.	(Elkon et al. 2012)
Transcriptional start site	Transcriptional start site choice has been linked to usage of certain poly(A) sites.	(Nagaike and Manley 2011) (Z Ji et al. 2011)

1.4. Regulation of Post-Transcriptional APA

Cis-elements found in the UTR are critical for post-transcriptional regulation of mRNAs (Table 1.4). Usage of different poly(A) sites at the point of cleavage affects which regulatory elements are present in the UTR. These play an important role in mRNA stability, localisation and translation influencing the cytoplasmic UTR landscape and consequently regulating gene expression.

Binding of trans-factors, primarily miRNAs and RBPs, to these cis-elements can influence transcript stability, protein output and localisation. While miRNAs bind complementary regions in the UTR, RBPs bind target motifs, which can be specific sequences, or a range of consensus sequences (Batra, Manchanda, and Swanson 2015). In addition, RBPs can bind RNA secondary structures, in a sequence independent manner, such as through stem loop structures. RBPs can be promiscuous in their function such as ELAVL1, whose binding to mRNA can impact poly(A) site usage at the point of cleavage as well as mRNA stability (Reviewed in (C. Mayr 2016)).

Table 1.4. Regulatory Cis-elements Identified in 3'UTRs (Reviewed in (Matoulkova et al. 2012))

Cis-element	Motif	Function
miRNA binding site	NNNNNNNN	miRNA sequence is complementary to that in the 3'UTR. miRNA binding recruits the RISC complex which facilitates translational repression or degradation of target mRNA.
AU-rich element (ARE)	AUUUA	A balance of binding by stabilizing RBPs such as ELAVL (Hu) protein family, and destabilising RBPs such as hnRNP D (AUF1), TTP and KSRP, mediate mRNA stability. Destabilising RBPs cause de-adenylation and consequently mRNA decay by exoribonucleases.
GU-rich element (GRE)	Overlapping GUUUG pentamer motif	Found in 5% of mRNA 3'UTRs (Sandberg et al. 2008) Destabilizing element that recruits RBPs to cause mRNA decay.
CU-rich element	(C/U)CCANxCCC	Bound by RBPs including PTB causing mRNA decay.
CA-rich element	(CA)n	Stabilizing effects through binding of RBPs such as hnRNP L.
U-rich		Affect mRNA stability during spermatogenesis (W. Li et al. 2016).
Alu element	-	Interact with lncRNAs causing mRNA decay via Stau1, a dsRNA, which recruits NMD factors. Inverted Alu elements in 3'UTR can hybridise forming double stranded UTR structure that is translationally repressed (Capshew, Dusenbury, and Hundley 2012).

1.4.1 3'UTR and Stability

Initially the regulatory elements found in the UTR were considered to be more destabilizing and therefore caused degradation of the transcript. These destabilizing elements included both miRNA target sites, and motifs for RBP whose binding recruited RNA degradation machinery. Therefore, shorter 3'UTRs which use the proximal poly(A) site were thought to be more stable than longer 3'UTRs using the distal poly(A) site (C. Mayr and Bartel 2009; W. Li et al. 2016). However, numerous stabilizing cis-elements have now been identified, and other studies showed that 40% of longer UTR isoforms were more stable than their shorter counterparts due to the binding of stabilising RBPs (Spies et al., 2013). Therefore, although up to 35% of alternative 3'UTRs have significantly different half-lives (C. Mayr 2016), there is no significant correlation between UTR length and mRNA stability (Spies et al., 2013) or mRNA abundance (Lianoglou et al. 2013; Jia et al. 2017).

Investigation into UTR stability in yeast suggested that single nucleotide changes in 3'UTR length could affect transcript stability (Geisberg et al. 2014; I. Gupta et al. 2014), however mammalian UTRs have not been found to be as sensitive.

The RNA turnover pathway NMD has been associated with targeting longer 3'UTR isoforms for degradation, influencing the transcriptome, on both an individual gene (Martins et al. 2012; Hogg and Goff 2010) and genome-wide basis (Bao et al. 2016). Competition between stabilizing RBPs such as PTPB1 and UPF1, the RNA helicase that initiates of NMD, binding to the 3'UTR can mediate transcript stability (Ge et al. 2016).

1.4.2 3'UTR and Translation

The 3'UTR length was first suggested to have a clear relationship with protein output. Shorter 3'UTRs were proposed to lack negative regulatory elements, which are bound by RBPs such as Pumilio, Maskin, TIAR and Musashi that mediate translational repression (C. Mayr 2016). Additionally, shorter 3'UTR isoforms were proposed to be more stable and consequently resulted in increased translation and protein expression (Sandberg et al., 2008; Mayr & Bartel 2009). However, more recent studies have suggested UTR length has a minimal effect on protein output (A. R. Gruber et al. 2014), and certain transcripts with shorter UTRs have

lower translation efficiency than their longer UTR counterparts (Pinto et al. 2011). Thus, the correlation between UTR length and translation efficiency is not linear.

1.4.3 3'UTR and Localisation

In the cytoplasm, the localisation of mRNAs can enable localised protein synthesis within a cell, which is particularly important for neurons, where different regions of the same cell have very different protein requirements (Andreassi and Riccio 2009). Different 3'UTR isoforms of the same mRNA can be localised to different places such as the *BDNF* transcript, where the short isoform is localised to the cell soma, but the longer 3'UTR isoform is localised to the dendrites (An et al. 2008). Localisation of mRNAs in neurons was recently explored on a genome wide scale, where a more distal alternative last exon was found to be utilised in transcripts that were localised to neurite outgrowths in two different mouse neuronal cell lines (Taliaferro et al. 2016).

3'UTRs can mediate mRNA localisation to organelles including the Endoplasmic Reticulum (ER) (Loya et al. 2008), mitochondria (Marc et al. 2002), and also to cytoplasmic RNA granules, to sequester transcripts from the translation machinery (Han et al. 2012). A novel function of UTRs mediating localisation was observed in the *CD47* gene, where the longer UTR isoform localised to the plasma membrane whereas the protein produced by shorter UTR isoform was retained in the ER (Berkovits and Mayr 2015). The authors suggested that the longer 3'UTR formed a scaffold during translation to recruit ELAVL1, which bound the nascent protein and directed its transport to the cell surface.

The 3'UTR has also been linked to nuclear export. The splicing factors SRSF3 and SRSF7 were shown to bind and regulate 3'UTR length, and recruit the mRNA export factor NXF1. Consequently the 3'UTR could determine the extent of nuclear retention of the transcript and influence transcript abundance in the cytoplasm (Müller-McNicoll et al. 2016).

1.4.4 miRNA Mediated Regulation

MicroRNAs (miRNAs) are small noncoding RNAs that are 21-23 nucleotides in length, which bind to 3'UTRs of mRNAs at sites complementary to their own sequence. In animals, only the seed region of the miRNA, usually between bases 2-8, is required to effectively interact with the mRNA target. This interaction recruits the RNA induced silencing complex (RISC) which either represses translation or initiates degradation of the corresponding transcript (Fabian, Sonenberg, and Filipowicz 2010) (Figure 1.5). A single miRNA can target hundreds of mRNAs, while mRNAs can be targeted by numerous miRNAs. Over 60% of mammalian protein coding genes are regulated by miRNAs (Bartel 2009), implying widespread regulation of gene expression.

Differential poly(A) site usage can mediate the presence of miRNA binding sites in the 3'UTR. For example, miRNA binding sites found only in the alternative UTR can specifically result in the inhibition of longer transcript isoforms. Indeed it was reported that there are 30% more miRNA target sites found in alternative UTRs than in constitutive UTRs (Zhe Ji et al. 2009). Therefore changes in the 3'UTR landscape can alter the ability of miRNAs to regulate gene expression of their target genes (Nam et al. 2014), and conversely altered miRNA expression can greatly influence the 3'UTR landscape (Legendre et al. 2006). Evidence suggests that miRNA target sites are more functional when near the 3'end of a transcript (Nam et al. 2014). A recent study suggested that 3'UTR shortening can therefore activate miRNA target sites found in the constitutive UTR to regulate gene expression of the target transcript (Hoffman et al. 2016).

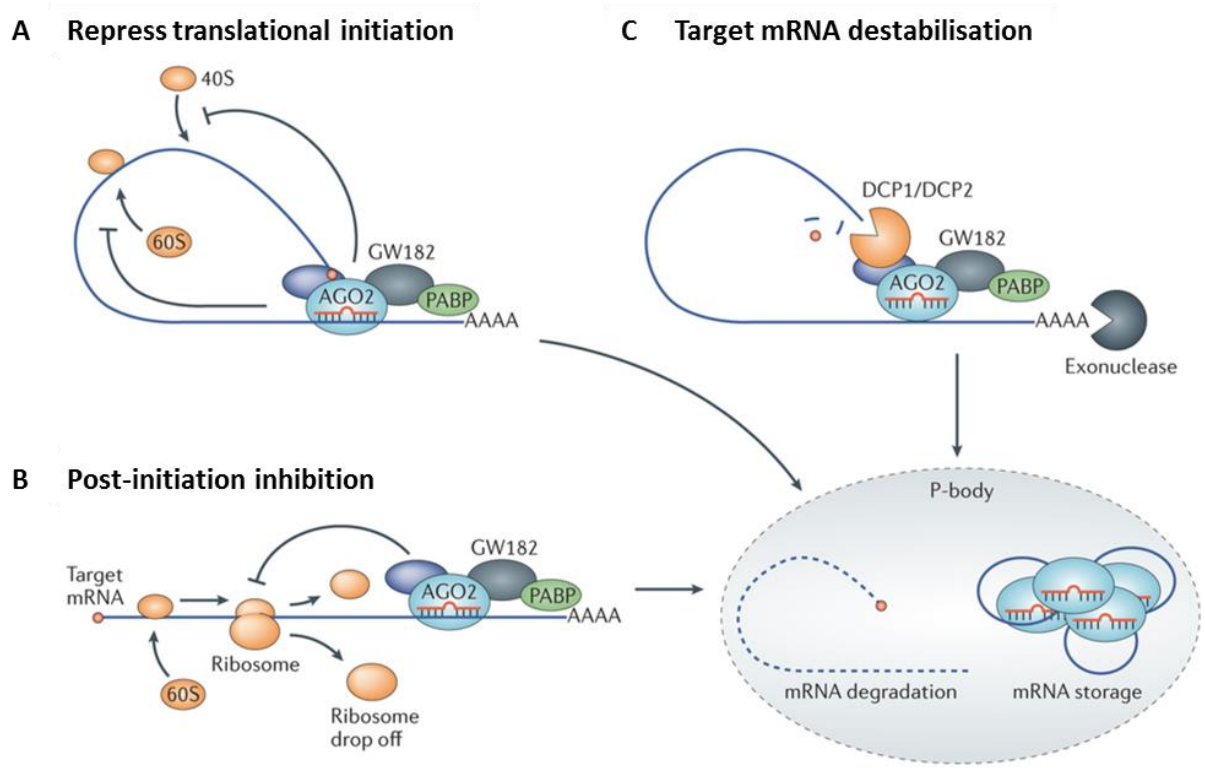


Figure 1.5. Overview of miRNA Mediated Gene Repression. miRNAs are carried to their target via RISC. Argonaute 2 (AGO2) contains the catalytic activity of the RISC to cleave the mRNA target. miRNAs (red) complementarily bind to their target mRNA to repress its expression via three main mechanisms. PABP (poly(A) binding protein) stabilises transcripts but its dissociation is enhanced by GW182, a protein that interacts with AGO2.

A. Repress translational initiation. The RISC can prevent the assembly of the 40S and 60S ribosomal complexes to inhibit translational initiation.

B. Post-initiation inhibition. Translational elongation can be inhibited by the RISC complex by promoting ribosome disassembly.

C. Target mRNA destabilization. miRNA binding to the target mRNA can initiate deadenylation at the 3'end and/or de-capping by DCP1/DCP2. De-capped and deadenylated transcripts are unstable and degraded by exoribonucleases.

The consequence of miRNA targeting and translational repression in **A, B** and **C**, can lead to transcripts being targeted to Processing bodies (P-bodies) which are sites of mRNA decay via the NMD pathway. Some mRNAs bound to RISC from **A** can be stored in P-bodies and later be signalled to resume translation. Figure modified from (Z. Li and Rana 2014).

1.5 APA in Different Environments

1.5.1. APA in Different Tissues

3'UTR isoform usage is tissue and cell type specific to allow post-transcriptional regulation to modulate protein expression. Tissue specific genes and housekeeping genes, such as genes associated with energy metabolism, are more likely to have single UTR isoforms, whereas genes expressed in multiple tissues are more likely have multiple UTR isoforms. Thus these genes can be regulated by APA to fine-tune their expression in different tissues (Lianoglou et al. 2013).

APA has tissue specificity that is conserved from drosophila to humans (Smibert et al. 2012). An in depth APA study in five mammalian species showed significant conservation of tissue specific rather than species specific poly(A) site usage (Derti et al. 2012). For example, in the testis and ovaries, global usage of proximal poly(A) sites has been identified (H. Zhang, Lee, and Tian 2005; W. Li et al. 2016), while in the brain extended 3'UTRs have been observed (Miura et al. 2013; Wehrspaun, Ponting, and Marques 2014; Ulitsky et al. 2012). In the frontal cortex, genes showing extended 3'UTRs encoded proteins associated with ion channels and transporters (Wehrspaun, Ponting, and Marques 2014). These proteins regulate the membrane potential, playing a crucial role in the brain. Interestingly, the alternative UTRs of these genes were enriched in miRNA target sites for miRNAs highly expressed in the frontal cortex, providing a mechanism to regulate gene expression (Wehrspaun, Ponting, and Marques 2014).

1.5.2 APA in Different Cellular States

As well as tissue specificity, the cellular state appears to play an important role in the usage of poly(A) sites. Cells undergoing proliferation (Sandberg et al. 2008; Elkon et al. 2012), or stem cells maintaining pluripotency (Zhe Ji and Tian 2009) have shown an increased usage of proximal poly(A) sites limiting the length of their 3'UTRs. The absence of miRNA target sites in shorter UTRs was initially proposed to increase transcript stability (Sandberg et al. 2008), however subsequent studies have shown a reduced correlation between UTR length and transcript stability (Spies, Burge, and Bartel 2013). Another study suggested that the reasoning behind 3'UTR shortening in proliferation is to save energy by eliminating regulation

in longer UTRs and preventing downstream effects of transcript regulatory networks such as association with the cell cycle (A. R. Gruber et al. 2014). Increased usage of upstream poly(A) sites in exonic and intronic regions has also been observed during proliferation (Elkon et al. 2012; Hoque et al. 2013).

The phenomenon of 3'UTR lengthening during development and differentiation is conserved amongst species (Ulitsky et al. 2012; Zhe Ji et al. 2009; Hoque et al. 2013; Wenyan Hu et al. 2017). An increase in the use of distal poly(A) sites in differentiation and development was first identified in murine C2C12 myoblast cells (Zhe Ji et al. 2009). It was proposed that the lengthening of the 3'UTR increases the presence of regulatory elements in the transcript which enables fine-tuning of gene expression. Interestingly, 3'UTR shortening was observed when differentiated cells were reverted back to stem cells (Zhe Ji and Tian 2009). 3'UTR lengthening was also seen during the differentiation of mouse Embryonic Stem Cells to neurons, where APA regulated genes were associated in neuronal functions, suggesting APA is a key regulator in neuron specific gene expression (Shepard et al. 2011). Changes in upstream-APA upon differentiation have also been observed, but the trend to increased mRNA length through usage of the terminal exon poly(A) site is contentious (Hoque et al. 2013; Shepard et al. 2011).

A novel mechanism of modulating cellular processes was identified in a study investigating membrane depolarisation in synapse development of hippocampal rat neurons. Upstream-APA in target genes of the MEF2 transcription factor family was reported due to increased Pol II pausing at upstream poly(A) sites (Flavell et al. 2008). The truncated transcripts, whose genes were associated with synaptic control, encoded truncated proteins lacking regulatory CTDs. The resulting proteins had altered functions to their longer counterparts, providing an example of how upstream-APA can globally regulate the transcriptome and subsequently proteome during synapse development (Flavell et al. 2008).

1.5.3 APA in Disease

Mutations in poly(A) site cis-elements (Bennett et al. 2001) or in genes encoding the cleavage and polyadenylation machinery (Jenal et al. 2012; Batra et al. 2014) have been implicated in disease (Reviewed in (Tian and Manley 2013; Curinha et al. 2014)). APA changes

in individual genes have also been linked to disease states. An extended 3'UTR in the *SNCA* transcript correlated with altered localisation of the α-synuclein protein from synaptic terminals to the mitochondria, and increased α-synuclein accumulation, which is observed in Parkinson's Disease (PD) patients (Rhinn et al. 2012). This protein is key to PD pathology, therefore its regulation by APA may be crucial to understanding mechanisms of PD. However, global changes in APA in PD have not been investigated.

Global 3'UTR shortening has been well documented in cancers (C. Mayr and Bartel 2009; Xia et al. 2014), however other studies suggest this is not the case in all cancerous cell lines (Fu et al. 2011), highlighting the complexity of APA regulation in cancer. Widespread APA changes were also observed in different brain regions of patients with Amyotrophic Lateral Sclerosis (ALS), though an overall trend to 3'UTR lengthening or shortening was not identified in the disease state (Prudencio et al. 2015). Global analysis of APA in other sporadic neurodegenerative diseases has not been performed.

1.5.4 APA in Stress

Stress conditions require an adaptive response to enable cell survival. While gene expression changes in stress have been assessed, few studies have explored the contribution of APA to the stress response. Temperature stress was shown to cause global 3'UTR lengthening upon exposure to cold temperatures (Y Liu et al. 2013), while individual heat shock protein genes showed 3'UTR shortening in heat shock to increase protein output (Tranter et al. 2011; Kraynik et al. 2015).

Other stress types have shown distinctly different APA changes. UV induced DNA damage caused widespread 3'UTR lengthening and upstream-APA with increased usage of the terminal exon poly(A) site (Graber et al. 2013), whereas viral infection induced stress saw a global switch to 3'UTR shortening (B. Hu et al. 2016; Jia et al. 2017). In addition, drug inhibition of protein synthesis resulted in increased usage of downstream intergenic poly(A) sites and repression of intronic poly(A) sites (Hollerer et al. 2016). Therefore, there is no consensus that stress causes altered APA profiles with trends to either 3'UTR lengthening or shortening.

1.6 Thesis Objectives

The aim of this project was to investigate changing APA profiles regulated by transcriptional and post-transcriptional APA, using a subcellular fractionation approach, during cell differentiation, in neurodegeneration and during exposure to cellular stress. Numerous factors contribute to poly(A) site choice at the point of cleavage, while the cytoplasmic transcriptome can be modulated further by post-transcriptional regulatory mechanisms to influence downstream gene expression. Furthermore, many studies investigating APA on a global scale focus on the bioinformatics of APA changes and fail to explore the physiological impact of these APA shifts, particularly at a gene specific level. This thesis aimed to identify physiologically relevant APA events occurring in different cellular states and understand how this may contribute or be consequential of the changing environment.

Chapter 2: Materials and Methods

A combination of experimental and computational methods was employed throughout this thesis. For experimental methods, a list of chemicals and kits used and the corresponding manufacturer's details are outlined in Table 2.1 and Table 2.2, and composition of buffers used are outlined in Table 2.3. The pH of buffers was adjusted using pellets of sodium hydroxide or 5 M hydrochloric acid.

2.1 Cell Culture

The neuroblastoma cell line BE(2)-M17 was a gift from Prof. Matthew Wood's Lab (DPAG, University of Oxford). BE(2)-M17 cells were cultured in Opti-MEM, supplemented with 10% v/v FBS (Fetal Bovine Serum), 1% Penicillin-Streptomycin and grown in an incubator at 37°C, with 5% CO_2. HEK293 cells were cultured in DMEM supplemented with 10% FBS, 1% L-Glutamine and 1% Penicillin-Streptomycin (complete media) at 37°C, with 5% CO_2.

During passaging, cells were washed with PBS, and the Trypsin was used to detach the cells. Complete media was added to the cells, which were centrifuged at 1000 rpm, and the cell pellet was re-suspended in an appropriate volume of complete media. Cells were passaged at ratios of 1:10 for experiments and 1:20 for maintain the cell culture. Cells were grown to 80% confluency before harvesting.

2.2 Cell Treatments

2.2.1 Retinoic acid (RA) Treatment

RA was diluted to 50 mM in DMSO and 100 µL aliquots were stored at -80°C in the dark for long term storage. The aliquot was further diluted with ethanol to get a working stock concentration of 10 mM, stored at -20°C in the dark for up to 1 week. 24 hours after seeding the cells in T225 flasks, RA was added to BE(2)-M17 cells at a final concentration of 10 µM. The media was changed every 48 hours since cells were seeded, and RA was added every 24 hours for a total of 72 hours.

2.2.2 MPP+ Treatment

The active metabolite MPP+ was diluted in cell culture grade water to 100 mM. Aliquots of 500 µL were stored at -20°C in the dark. BE(2)-M17 cells were seeded in T225 flasks, and a final concentration of 0.5 mM MPP+ was added at a cell confluency of 60-80%, for 24 hours.

2.2.3 Cold Shock Exposure

Cells were seeded in T225 flasks and grown at 37°C and 5% CO_2 until reaching 60-80% confluency. Flasks were then transferred to an incubator with a temperature of 28°C and 5% CO_2 for 24 hours. For cold shock in differentiated cells, BE(2)-M17 cells were differentiated with RA for 72 hours at 37°C and then transferred to an incubator at 28°C and 5% CO_2 for 24 hours.

2.2.4 Hypoxia Exposure

BE(2)-M17 cells were seeded in T225 flasks and grown at 37°C and 5% CO_2 until reaching 60-80% confluency. Flasks were then transferred to an incubator with a temperature of 37°C, 5% CO_2 and 2% O_2 for 24 hours. Nitrogen comprised the remaining gaseous environment.

For all treatments, cells were lysed for RNA and/or protein immediately after the time point (72 hours after RA treatment and 24 hours after stress treatments).

2.3 Subcellular RNA Isolation

Cells grown in 2 x T225 flasks were detached with trypsin and washed twice with ice-cold PBS. The cell pellet was re-suspended in 1 mL of Lysis Buffer (Table 2.2). 100 µL of the lysate was taken out as the whole-cell RNA fraction. The remaining lysate was centrifuged at 1,000 g for 3 minutes at 4°C and the supernatant was removed as the cytoplasmic fraction. This was purified by centrifuging at 12,000 g for 2 minutes at 4°C. The nuclear pellet was re-suspended in 1 mL Lysis Buffer and 100 µL Detergent Stock was added in a drop-wise manner under slow vortexing. The sample was left on ice for 5 minutes, then centrifuged at 1000 g for 3 minutes at 4°C. The supernatant was removed and the pellet was washed in 1 mL Lysis Buffer. The remaining pellet was re-suspended in 1 mL Trizol® by passing through a 21-gauge needle until fully dissolved. Equal volumes of Trizol® were added to the cytoplasmic and whole-cell lysate, and all three fractions were left at room temperature for 5 minutes. A 20% ratio of chloroform was added and samples were vigorously vortexed before being centrifuged at 12,000 g for 15 minutes at 4°C. The upper aqueous layer was transferred to a new tube with an equal volume of isopropanol and left to precipitate for >1 hour at -20°C. RNA was collected by centrifuging samples at 13,000 rpm for 30 minutes at 4°C.

The RNA pellet was DNase I-treated as per manufacturer's instructions. RNA was subsequently purified through phenol-chloroform extraction and the aqueous layer was added to 2.5 x volume of ethanol and 10% sodium acetate and left to precipitate at -20°C for >1 hour. RNA was finally collected by centrifuging at 13,000 rpm for 30 minutes at 4°C and the pellet was re-suspended in RNase-free water. The RNA concentration was measured on a NanoDrop 1000.

2.4 Gel Electrophoresis

A denaturing 1% formaldehyde/agarose gel was used to assess the quality of RNA. The gel was made with 1 x formaldehyde gel running buffer, 3.3% formaldehyde and 1% agarose. Two micrograms of RNA were mixed with formamide, formaldehyde gel running buffer and formaldehyde. Samples were denatured for 15 minutes at 65°C, and subsequently mixed with formaldehyde gel loading buffer and ethidium bromide. The gel was run for 2 hours at 65 V in 1 x formaldehyde gel running buffer.

DNA fragments were run on 1.5% agarose gels for analysis of RT-PCRs. The gel was made with 1.5% agarose, 1 x TBE buffer and 0.5 µg/mL ethidium bromide. Samples were mixed with 6 x Loading Dye before loading onto the gel along with a DNA ladder. The gel was run for 1 hour at 110 V in 1 x TBE. A DNA ladder was run in parallel to quantify band sizes. Both RNA gels and DNA gels were visualised under $UV_{320\ nm}$ light and pictured on a Kodak Gel Camera System.

2.5 RT-PCR

Reverse transcription was performed with 1 µg of RNA which was primed using an oligod(T) primer using RevertAid Reverse Transcriptase as per the manufacturer's guidelines. PCR was performed with 1 µl of cDNA template with Taq Polymerase as per manufacturer's instructions. The annealing temperature was modified depending on the melting temperature of the two primers used in the reaction. Primers were designed using the online tool Primer Blast (www.ncbi.nlm.nih.gov/tools/primer-blast) so that the intended region was amplified. MWG Eurofins was used to synthesise primers. The sequences of primers used are listed in Table 2.4. Band intensities were quantified using ImageJ software.

2.6 Protein Isolation

For whole-cell isolation, cell pellets were re-suspended directly in 100 µL Lysis Buffer. For isolating cytoplasmic and nuclear proteins, the subcellular fractionation protocol for RNA isolation was followed using 500 µL of Lysis Buffer instead of 1 mL up until the addition of Trizol®. Instead, of Trizol®, the nuclear pellet was re-suspended in 100 µL Lysis Buffer. Samples were incubated with 1 µL Benzonase® Nuclease for 30 min at 37°C to degrade nucleic acid content. Protein concentration was measured using the Qubit® Protein Assay Kit as per manufacturer's instructions.

2.7 SDS-PAGE and Western blotting

Protein samples (15 µg) were mixed with 4 x Laemmli Buffer and boiled for 5 minutes at 90°C, before loading on to an SDS-PAGE gel (5% acrylamide stacking gel at pH 6.8; 10% or 12% acrylamide resolving gel at pH 8.8) alongside a protein ladder. The gel was run in 1 x SDS running buffer for 20 minutes at 65 V and then 2-3 hours at 150V.

The gel was placed onto PVDF blotting membrane and sandwiched between three layers of Whatman blotting paper. Wet-transfer was performed in 1 x Transfer Buffer, in an electroblotting system (Bio-Rad), at a constant current of 250 mA for 3 hours in an ice bucket at 4°C.

Membranes were pre-blocked in 5% non-fat milk powder in TBS-T under agitation for 1 hour at room temperature. Primary and horseradish peroxidase (HRP)-conjugated secondary antibody incubations were done for 1 hour at room temperature. After each antibody incubation, membranes were washed 3 x for 10 minutes with TBS-T. Antibodies and corresponding dilutions used are outlined in Table 2.5. Proteins were detected using an ECL kit. Band intensities were quantified using ImageJ software.

2.8 Immunofluorescence

BE(2)-M17 cells were grown in 6-well plates. Three wells were treated with 10 µM RA for 72 hours to induce differentiation. Cell media was aspirated and cells were washed in warm PBS^+. Cells were submerged in 4% formaldehyde diluted in warm PBS and left for 15 minutes at room temperature to be fixed. The formaldehyde/PBS^+ mix was aspirated and cells were washed once with ice cold PBS^+.

Cells were permeabilised by incubation with 0.2% Triton X-100 diluted in PBS^+ for 5 minutes. Cells were then washed 2 x 5 minutes with PBS. Cells were incubated in Blocking buffer (Table 2.3) for 30 minutes gently shaking at room temperature.

The primary anti-PRDX6 antibody was diluted 1:1000 in 1% BSA in PBS-T and applied for 1 hour at room temperature with gentle shaking. Cells were rinsed 3 x 5 min with PBS. The fluorochrome-conjugated secondary antibody was applied at a dilution of 1:1000 in in 1% BSA in PBS-T for 1 hour at room temperature with gentle shaking in the dark. Cells were rinsed 3 x 5 min with PBS in the dark.

Nuclei were stained by incubation with 300 nM DAPI for 5 minutes at 37°C. Cells were rinsed once with PBS and then submerged in PBS for imaging on ZOE™ Fluorescent Cell Imager.

2.9 Seahorse XF Mito Stress Assay

The Seahorse XF Mito Stress Assay was used with the help of Dr. Brent Ryan (Wade-Martins Lab, DPAG, University of Oxford), to measure the extent of mitochondrial dysfunction in MPP+ treated cells. To measure the change in mitochondrial respiration, cells were plated in an X96F Seahorse Plate at 1000 cells per well. 24 hours later, 0-1 mM MPP+ was added for 24 hours. The assay was performed as per manufacturer's instructions. Briefly, the Oxygen Consumption Rate (OCR) and Extracellular Acidification Rate (ECAR) were measured initially measured, and then 3 measurements were taken after injection of Oligomycin, FCCP, Rotenone and Antimycin (Figure 2.1). The OCR is proportional to the level of mitochondrial respiration, and the ECAR is indicative of glycolysis. Figure 2.1 explains what each of the injections indicates about the mitochondrial metabolism of the cells. The Basal Respiration Rate and the Maximal Respiratory Capacity were taken to be the two key parameters which measured mitochondrial dysfunction with MPP+ treatment. The mitochondrial respiration rates in each well were normalised to the total protein content using a Pierce™ BCA Protein Assay as per manufacturer's instructions. Mean respiration rates and standard deviations were calculated from three replicate samples.

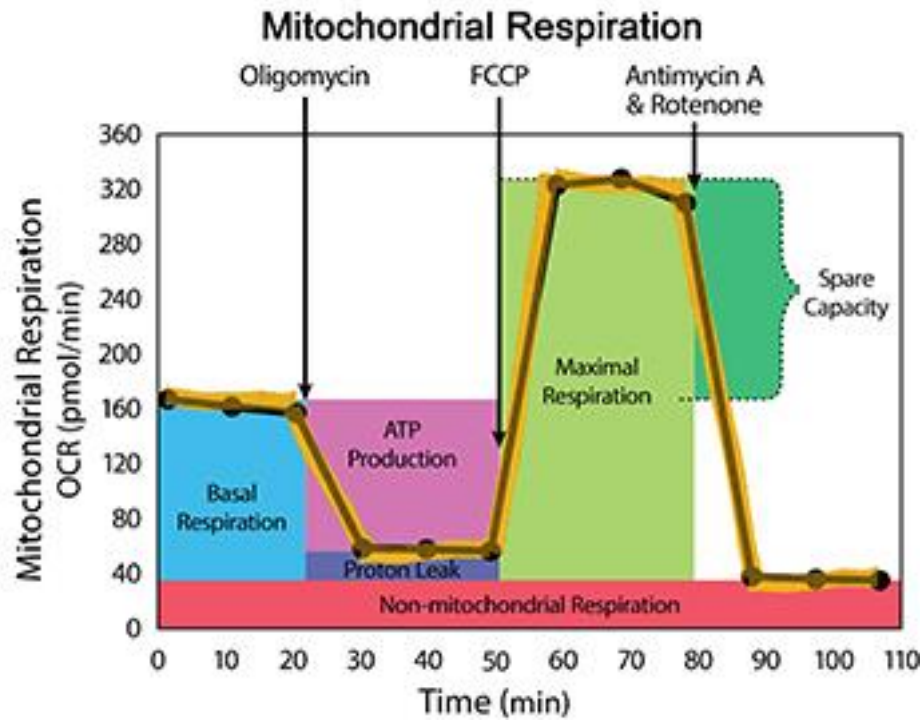


Figure 2.1 Outline of the Seahorse XF Mito Stress Assay.

Cells are subjected to five drugs to affect the mitochondrial electron transport chain (ETC) and bioenergetics of the cell to measure the oxygen consumption rate (OCR). The basal respiration rate is measured initially and the maximal respiratory capacity is measured after the injection of FCCP. Image taken from the Agilent website (http://www.agilent.com/en-us/products/cell-analysis-(seahorse)/mitochondrial-respiration-the-xf-cell-mito-stress-test)

2.10 MitoSOX™ Assay

BE(2)-M17 cells were plated in a 24-well plate. After 24 hours, 0 mM or 0.5 mM MPP+ was added. Media was aspirated from cells and they were washed once with pre-warmed HBSS. Cells were incubated with a final concentration of 5 µM MitoSOX™ diluted in pre-warmed HBSS for 20 minutes at 37°C in the dark. Cells were gently washed twice with pre-warmed HBSS. Hoechst stain was diluted 1:1000 in HBSS and applied to cells for 10 minutes at 37°C in the dark. The stain was removed and cells were kept in HBSS for visualisation. MitoSOX™ was visualised at an emission of 590 nm and Hoechst stain was visualised using the DAPI channel on ZOE™ Fluorescent Cell Imager.

2.11 CYTO-ID kit Assay

The CYTO-ID kit assay was employed to measure levels of autophagy with MPP+ treatment. Cells were plated in chamber slides in 5 mL complete media. After 24 h, MPP+ was added at a final concentration of 0.5 mM, and an equal volume of cell culture grade water was added to the negative control. Rapamycin (a gift from Prof. Lynne Cox's Lab, Department of Biochemistry, University of Oxford), was added in a separate chamber slide at a final concentration of 70 nM as a positive control. The assay was performed as per manufacturer's instructions. Cells were visualised by wide-field fluorescence microscopy to detect the 488nm-excitable green-emitting fluorescent probe to highlight vacuolar components of the autophagy pathway using the ZOE™ Fluorescent Cell Imager.

2.12 Fluorescent Activated Cell Sorting (FACS) Analysis

Cells were grown in T25 flasks, and trypsinised as normal to collect the cell pellet. The cell pellet was washed once with PBS and then re-suspended in 0.5 mL PBS, which was added to 4.5 mL ice cold 70% ethanol and kept on ice. Cells were kept in ethanol at 4°C for 2 hours to fix. The cell pellet was then collected through centrifugation at 2000 rpm for 5 minutes. The cell pellet was incubated in 50 uL RNase A solution (100 µg/mL in PBS) at 37°C for 30 min. Next 400 µL of propidium iodide (PI) (50 µg/mL in PBS) was added and the tubes were kept in the dark for 30 min. The samples were transferred to flow cytometry tubes and cell fluorescence was measured using default settings on the PI channel. The percentage of cells in

each stage of the cell cycle were calculated by measuring the areas underneath the curve representing the G0/1, S and G2/M phases of the cell cycle. Mean percentages and standard deviations were calculated from three replicates.

2.13 Microscopy

The EVOS XL Core Cell Imaging System (ThermoFisher Scientific) was used to take live cell images of cells before and after treatments with a 20 X magnification.

The ZOE™ Fluorescent Cell Imager was used to observe fluorescently labelled cells using default settings for the colour channels.

2.14 QuantSeq 3' mRNA-Seq Library Preparation

Libraries for RNA sequencing were prepared with the Lexogen QuantSeq 3' mRNA-Seq kit as per manufacturer's instructions. Input RNA was 500 ng for nuclear fractions and 5 µg for cytoplasmic fractions. 13 PCR cycles were used for amplification.

2.15 hsDNA Bioanalyzer Assay

The quality of libraries generated from the Quant-Seq kit were assessed using a high sensitivity DNA (hsDNA) chip on the Agilent 2100 Bioanalyzer as per manufacturer's instructions. The concentration of libraries was quantified by selecting the region between 50 bp and 1000 bp from the Bioanalyzer output profile.

2.16 RNA-seq on Ion Proton Platform

Libraries quantified on the Bioanalyzer were diluted to a final concentration of 300 pM. The Ion PI™ Hi-Q™ Chef Kit was used with the Ion Chef™ System for template preparation and Ion Proton™ System for sequencing as per the manufacturer's instructions. FASTQ files were aligned to the human genome (hg19) using STAR (Spliced Transcripts Alignment to a Reference). Each BAM file for further processing had a minimum of 1 million reads.

2.17 Bioinformatics pipeline to Assess Gene Expression and APA

All RNA-seq experiments were done with biological replicates of samples processed weeks apart. The filtered reads from these two samples were combined and processed through an established bioinformatics pipeline to perform gene expression and APA analysis on samples (Hoque et al. 2013; Neve et al. 2016). Gene expression values were calculated from the combined reads of poly(A) sites mapping to a single gene, and normalised to reads per million (RPM). Significant gene expression changes were defined by $p<0.01$ Fisher's exact Test and a fold change greater than 2. Significant APA changes were defined as $p<0.01$ Fisher's exact Test, with a minimum of 5% change in APA isoform abundance as defined in previous studies (Hoque et al. 2013; Neve et al. 2016). APA isoform usage was visualised on the IGV Browser using auto-scaling settings.

2.18 Hierarchical Clustering Analysis

Heatmaps were generated using reads per million (RPM) from gene expression analysis using the Morpheus tool (https://software.broadinstitute.org/morpheus/). Hierarchical clustering analysis was performed using the one minus Pearson correlation distance metric for clustering.

2.19 Panther Gene Ontology Analysis

Gene Ontology analysis was done with the PANTHER (Protein Analysis through Evolutionary Relationships) Classification system (Blake et al. 2015). Lists of genes showing differential expression of APA regulation were submitted and analysed for enrichment in 'Biological Processes' using the statistical overrepresentation test with default parameters. A significant enrichment was defined by $p<0.05$.

2.20 Motif Enrichment Analysis

BED files of the alternative UTRs of lengthened and shortened genes were converted to FASTA files with unique names. DREME (Discriminative Regular Expression Motif Elicitation) was utilised to search for enrichment of regulatory motifs in APA regulated gene alternative UTRs compared to the alternative UTRs of genes which did not exhibit APA

(Bailey 2011). The e-value is the enrichment p-value (Fisher's exact Test) multiplied by the number of candidate motifs tested, which indicates the probability of the enrichment of the motif being identified by chance.

The identified enriched motifs were processed through the TOMTOM motif comparison tool (S. Gupta et al. 2007) to identify RBPs that bind to the enriched motifs. Motif input parameters were RNA (DNA-encoded) using the Ray2013 Homo sapiens (DNA-encoded) motif database.

2.21 miRNA Enrichment Analysis

miRNA enrichment in alternative UTRs was based on work by Gruber and colleagues (A. R. Gruber et al. 2014). Briefly, miRNA high confidence target predictions were taken from the EIMMo database (Gaidatzis et al. 2007), and the number of target sites found in the alternative UTRs were counted for each miRNA. Next, the miRNA target site labels were randomised. This produced a randomised dataset as the target site no longer corresponded to the correct miRNAs. This was iterated 500 times, and a z-score for each miRNA was calculated from this random dataset. Therefore, the z-score, which is the number of standard deviations a value is from its mean, is consequently a measure of how many times the miRNA target site is enriched compared to the randomised dataset. A positive z-score indicates that the miRNA is enriched in the alternative UTRs because its target site is present more frequently than it would be at random. A z-score greater than 2 was considered to be significant. Individual miRNAs enriched in both shortened and lengthened alternative UTRs were omitted from further analysis as they are unlikely to mediate trends in APA profile changes.

2.22 DaPars

Raw sequencing data in the form of FASTQ files and alignment information was downloaded from the Sequence Read Archive (SRA). GEO Accession numbers of datasets used are outlined in Table 2.6. FASTQ files were groomed and filtered reads were aligned to the human genome (hg19) using TopHat using Galaxy (https://usegalaxy.org/). The aligned BAM files were converted to Bedgraph files and subjected to Dynamic Analysis of Alternative Polyadenylation from RNA-Seq (DaPars) (Masamha et al. 2014; Xia et al. 2014). The code is

available at https://code.google.com/p/dapars. This python script enables de novo identification and analysis of dynamic poly(A) sites from RNA-Seq data. The relative usage of proximal and distal poly(A) sites can be assessed by looking at the percentage of reads which use the distal instead of the proximal poly(A) site (percentage of distal poly(A) site usage index, PDUI). The PDUI is calculated in multiple data sets and the difference in PDUI between different data sets is calculated. Genes with more than a 25% change between patient and control are highlighted as being statistically significant changes in poly(A) site usage. The output from DaPars was coupled to known poly(A) site coordinates ensuring false poly(A) sites are not identified. An additional filter in the DaPars script was added so that the predicted proximal poly(A) site was present within 250 nucleotides of a previously annotated poly(A) site, rather than 500 nucleotides as initially proposed by the authors (Masamha et al. 2014; Xia et al. 2014). Bedgraph files were converted to bigwig files for visualisation of the 3'UTRs on the IGV Browser.

2.23 Secondary Structure Prediction

The sequence of the short or full length 3'UTR isoforms were submitted to the 'Predict a Secondary Structure Web Server' using default parameters to predict a maximum free energy structure.
(http://rna.urmc.rochester.edu/RNAstructureWeb/Servers/Predict1/Predict1.html)

2.24 Regulatory Cis-Element Identification

TargetScan (http://www.targetscan.org/vert_71/) was used to scan 3'UTR genes to identify miRNA target sites, and to identify target genes of miRNAs.

The CLIP database was used to identify RBP binding sites in 3'UTRs.
(http://lulab.life.tsinghua.edu.cn/postar/).

Table 2.1. A Table outlining the Chemicals and Materials used.

Chemicals & Materials	Supplier	Supplier Code
10 x Taq polymerase buffer with $MgCl_2$	NEB	MO267
2-mercaptoethanol	Sigma	M6250
Acrylamide	Sigma	A3574
Agarose	Sigma	A9539
Alternative NP-40	Merck Millipore	492016
Ammonium Persulphate	Sigma	A3678
Benzonase® Nuclease	Merck	70746
Boric Acid	Sigma	B6768
Bovine Serum Albumin (BSA)	NEB	B9001S
Bromophenol Blue	Sigma	B0126
Cell Culture Grade Water	Sigma	W3500
Chloroform	Fisher Scientific	C/4920/17
ColorPlus™ Prestained Protein Ladder	NEB	P7711S
DAPI	Sigma	D9542
Deoxynucleoside triphosphate set (dNTPs)	Thermo Fisher	R0181
DMEM (Dulbecco's Modified Eagle's Medium)	Sigma	D6546
DMSO	Sigma	D8418
DNA Ladder	Thermo Scientific	SM0403
DNase I	Roche	4716728001
EDTA	Sigma	E6758
Ethanol	VWR	20831.33
Ethidium Bromide	Sigma	E1510
FBS	Sigma	F7524
Formaldehyde (37%)	Sigma	F8775
Formamide	Sigma	F9037
Glycerol	Fisher Scientific	10579570
Glycine	Sigma	G8898
HBSS	Life Tech	14025092
Hoechst 33342	Thermo Fisher	H3570
Hydrochloric Acid	Sigma	320331
Hydrogen Peroxide Solution (30% w/v)	Sigma	H1009
Isopropanol	Fisher Scientific	P/7500/17
L-Glutamine	Sigma	G7513
Magnesium Chloride	Sigma	M8266
Methanol	VWR	20847.307
MOPS (4-Morpholinepropanesulphonic acid)	Sigma	M1254
MPP+	Sigma	D048
Nonfat milk powder	Bio Rad	1706404
OptiMEM	Life Tech	319850054
PBS	Sigma	D8537
PBS+ (PBS with $MgCl_2$ and $CaCl_2$)	Sigma	D8662
Penicillin/Streptomycin	Sigma	P0781
Phenol	Sigma	P1037
Propidium Iodide	Sigma	P4864
PVDF blotting membrane	GE Healthcare	10600021
Retinoic Acid	Sigma	R2625
RevertAid Reverse Transcriptase	Thermo Scientific	EP0441

RNaseA	Thermo Fisher	88518
RnaseOUT	Thermo Fisher	10777019
Rotenone	Sigma	R8875
Sodium Acetate	Sigma	S2889
Sodium Chloride	Sigma	S9625
Sodium Citrate	Merck Millipore	567446
Sodium Deoxycholate	VWR	43053P
Sodium Dodecyl Sulphate (SDS)	Sigma	L4390
Sodium Hydroxide	Fisher Scientific	S318
Taq polymerase	NEB	M0273S
TEMED	Sigma	T9281
Tris (Tris-hydroxymethyl-aminomethane)	Sigma	252859
Triton X-100	Sigma	X100
Trizol®	Thermo Fisher	15596-026
Trypsin	Sigma	T3924
Tween 20	Sigma	P9416
Tween 40	Sigma	P1504
Whatman Paper	GE Healthcare	3030-917
Xylene Cyanol	Sigma	X4126

Table 2.2. A Table outlining the kits used.

Kit	**Supplier**	**Supplier Code**
2100 Bioanalyzer high sensitivity DNA kit	Agilent	5067-4626
CYTO-ID Kit	Enzo	ENZ-51031
Enhanced chemiluminescence (ECL) kit	Perkin Elmer	NEL104001EA
Ion PI™ HiQ™ Chef Kit	Thermo Fisher	A27198
MitoSOX™	Thermo Fisher	M36008
Pierce™ BCA Protein Assay	Thermo Fisher	23225
QuantSeq 3'mRNA-seq Library Prep Kit	Lexogen	0.12.24
Qubit® Protein Assay Kit	Life Tech	Q33211

Table 2.3. A Table listing the Composition of Buffers used.

* 5% Acrylamide used for the stacking gel; 10-12% Acrylamide used for the Resolving gel

Buffer	**Concentration**	**Chemical**
1 x Formaldehyde gel running buffer	8 mM	Sodium Acetate
	1 mM	EDTA
	20 mM	MOPS
1 x SDS-PAGE Running Buffer	25 mM	Tris
	192 mM	Glycine
	0.10%	SDS
1 x TBE Buffer	100 mM	Tris
	100 mM	Boric Acid
	1 mM	EDTA
1 x Transfer Buffer	25 mM	Tris-HCl
	192 mM	Glycine
	20%	Methanol
4 x Laemmli Buffer	20%	2-mercaptoethanol
	40%	Glycerol
	8%	SDS
	0.01%	Bromophenol blue
	125 mM	Tris-HCl pH 6.8
6 x Loading Dye	0.25% (w/v)	Bromophenol Blue
	0.1 M	EDTA
	30%	Glycerol
Acrylamide Gel	x% *	Acrylamide
	400 mM	Tris pH 8.8 or pH 6.8
	0.10%	SDS
	0.10%	APS
	0.10%	TEMED
Blocking Buffer	22.52 mg/mL	Glycine
	1%	BSA
	0.10%	Tween20
	1x	PBS
ECL	90 mM	Coumaric Acid
	250 mM	Luminol
	100 mM	Tris-HC pH 8
	0.03%	30% Hydrogen Peroxide Solution
Detergent Stock	3.30%	Sodium Deoxycholate
	6.60%	Tween 40
Formaldehyde Gel Loading Buffer	50%	Glycerol
	1 mM	EDTA pH 8
	0.25%	Bromophenol Blue
	0.25%	Xylene cyanol
Lysis Buffer	10 mM	Tris
	140 mM	NaCl
	1.5 mM	$MgCl_2$
	0.50%	NP-40
PBS-T	1 x	PBS
	0.10%	Tween20
TBS-T	50 mM	Tris
	150 mM	NaCl
	0.05%	Tween20

Table 2.4 Primer sequences used in RT-PCR

Primer	5'-3' Sequence
AP oligo dT	GCCCACGCGTCGACTAGTACTTTTTTTTTTTTTTT
CACYBP dF1	ACTGACATCAGCTTCCACCAG
CACYBP dR1	TGAGCATAGGAATAGACGGGC
CACYBP F1	GCTCCCATTACAACGGGCTAT
CACYBP R1	GTGTCTCCTTTGGCTTGCTTC
ENO2 F1	TCCCACTGATCCTTCCCGAT
ENO2 R1	CCAGGCAAGCAGAGGAATCA
GAPDH F1	GGTGAAGGTCGGAGTCAACG
GAPDH R1	TGGTTCACACCCATGACGAA
HIF1a_F1	CCTGAAAGCGCAAGTCCTCA
HIF1a_R1	TGATCGTCTGGCTGCTGTAATA
MALAT F1	agagaattcCCTGCAAATTGTTAACAGAA
MALAT R1	TCAGCTTCCGCTAAGATGCTAGCTT
NPM1-01_F1	GCTTCCGGATGACTGACCAA
NPM1-01_F1	GCTTCCGGATGACTGACCAA
NPM1-01_R1	GAGGGCAGGGACATTCTCAT
NPM1-03_F1	CATTGAACAGTCCTGGGCAC
NPM1-03_R1	CAAGGGACTTTGGCAGAATCA
PRDX6 dF1	TGCAGGGCTTGTGACCAATG
PRDX6 dR1	GCCTTTTCTGCAATCTCCCC
PRDX6 F1	GGGACTTTACCCCAGTGTGC
PRDX6 R1	TGGTGAAGACTCCTTTCGGG
PSMB2 CR F1	CCGACTATGTTCTTGTCGCC
PSMB2 CR R1	CCTAAGGAGTTCCACTGCCC
PSMB2 dF1	CCCACGTTCTACTCCATGCTT
PSMB2 dR1	GCAGGAAGCAGATGACTGGAT
TUBG1 F1	AGGACGAGATGAGCGATGTG
TUBG1 R1	ACCAGTAAGGCAGATGAGGGT
VEGF_F1	GCCATCCAATCGAGACCCTG
VEGF_R1	ATTAGACAGCAGCGGGCAC

Table 2.5 Antibodies used for Western Blotting and Immunofluorescence

Antibody	Host	Concentration	Supplier	Supplier Number
For Western Blotting				
Anti-CIRBP	Rabbit	1:1000	GeneTex	GTX120184
Anti-CACYBP	Rabbit	1:1000	Bethyl	A302-904A
Anti-ELAVL1	Rabbit	1:2000	Abcam	Ab200342
Anti-GAPDH	Rabbit	1:1000	Bethyl	A300-640A
Anti-Gamma-Tubulin	Rabbit	1:1000	Bethyl	A302-631A
Anti-PRDX6	Rabbit	1:2000	GeneTex	GTX115262
Anti-PSMB2	Rabbit	1:1000	Bethyl	A303-817A
Anti-RAB7A	Rabbit	1:1000	GeneTex	GTX130847
Anti-Rabbit IgG HRP	Goat	1:4000	Sigma	A6154
Anti-RBM3	Rabbit	1:1000	Protein Tech	14363-1-AP
Anti-SAM68	Rabbit	1:1000	Bethyl	A302-110A
For Immunofluorescence				
Anti-PRDX6	Rabbit	1:1000	GeneTex	GTX115262
Anti-Rabbit IgG Alexa Fluor® 568 conjugate	Donkey	1:1000	ThermoFisher	A10042

Table 2.6 GEO Accession Numbers of Publicly Available RNA-seq data

GEO/SRA Accession Number	Background to Dataset	Use in the Thesis	Reference
GSE24565	Small RNA-seq in SK-N SH and RA differentiated SK-N-SH. Two biological repeats per sample	Comparison with miRNA enriched targets in RA differentiation of BE(2)-M17 cells	N/A
GSE67333	RNA sequencing on RNA samples extracted from the hippocampi of 4 LOAD patients and 4 age-matched controls	DaPars analysis in AD	(Magistri et al. 2015)
SRX034874	Total mRNA from Capital Biosciences sequenced from Total Brain, Frontal Lobe and Temporal Lobe from Normal individuals and AD patients	DaPars analysis in AD	(Twine et al. 2011)
GSE62642	Total RNA extracted from dopaminergic neurons derived from iPSCs from healthy controls, sporadic PD patient, and monozygotic twins where one individual has PD and one does not. Two technical repeats per sample	DaPars analysis in PD	(Woodard et al. 2014)
ERA589991	Total RNA extracted from dopaminergic neurons derived from iPSCs of sporadic PD patients and healthy individuals. Two technical replicates per sample.	DaPars analysis in PD	N/A
GSE67196.	Total RNA sequencing from RNA extracted from the Frontal Cortex and Cerebellum of c9ALS and sporadic ALS patients and control individuals	DaPars analysis in ALS	(Prudencio et al. 2015)
GSE76220	Total RNA-sequencing on RNA from Motor Neuron Populations Isolated from sALS	DaPars analysis in ALS	(Batra et al. 2016)

Chapter 3: APA in differentiation

3.1 Introduction

3.1.1 APA in Differentiation

Global shifts in APA in different cellular states has been implied as a mechanism of gene regulation. During proliferation and in cancer, a shift towards using proximal poly(A) sites has been observed (Sandberg et al. 2008; Mayr and Bartel 2010). This switch to proximal poly(A) site usage through transcriptional APA is proposed to reduce the regulatory elements such as miRNA or RBP target sites in the UTRs of affected transcripts and so impact stability and final protein output. miRNA profiles also change during cancer progression, which can post-transcriptionally target and degrade longer UTR isoforms (Liaw et al. 2013).

During differentiation, 3'UTR lengthening has been observed in different cell types (Zhe Ji et al. 2009; Hoque et al. 2013; Shepard et al. 2011). Studies investigating APA in differentiation have not distinguished between transcriptional APA occurring at the point of cleavage, or post-transcriptional APA which arises due to alterations of regulatory elements in the cytoplasm. The observed lengthening during differentiation is generally assumed to be due to the suppression of the proximal poly(A) site at the point of cleavage. Given that widespread miRNA expression changes have been observed during neuronal differentiation (Stallings et al. 2011), it is important to distinguish between mechanisms that affect APA profiles at the co- or post transcriptional level during differentiation. This approach would enable insight into how APA profiles are established and regulated.

3.1.2 Retinoic Acid Mediated Differentiation

Neuroblastoma cell lines can be differentiated by serum starvation or addition of differentiation factors, such as retinoic acid (RA), to produce a more neuronal phenotype (Filograna et al. 2015). Interestingly, different neuronal phenotypes are determined based on the differentiation factor used (Filograna et al. 2015). RA, a retinoid that is a derivative of vitamin A (Figure 3.1A), inhibits cell growth and induces morphological differentiation of neuroblastoma cell lines (Abemayor and Sidell 1989), though the effect of RA on different cell lines can vary.

There are two types of endogenous RA, all-trans-RA and 9-cis-RA, which bind to different RA receptors (RARs). Upon ligand binding, RARs heterodimerize with a retinoid receptor (RXR), to form a functional transcription factor. This is transported into the nucleus where it binds RA response elements (RAREs) in gene promoters to mediate transcription (Figure 3.1B) (Reviewed in (Maden 2007).

RA induced changes can affect mRNA expression profiles within 12 hours although morphological changes only become visible after 24 hours. The Wnt signaling pathway and protein kinase A pathway (S. N. Kim et al. 2000), among others, have been identified to mediate the neurite outgrowth process during RA mediated differentiation of neuroblastoma cell lines. RA can affect transcription of 20% of both coding and noncoding genes during differentiation of an embryonic carcinoma cell line, NCCIT (Cawley et al. 2004).

Changing miRNA expression profiles have been observed with RA treatment in the murine P19 and human NT2/D1 embryonic pluripotent cell lines (Sempere et al. 2004). Notably some of these miRNAs were those found enriched in the brain indicating the validity of these observations made in tissue culture cells. Furthermore, down-regulation of the miR-17 family, which is involved in regulating neuronal differentiation, and upregulation of brain enriched miRNAs has also been seen with RA mediated differentiation of SH-SY5Y neuroblastoma cells (Beveridge et al. 2009). This is significant as miRNA profile changes could shape APA profiles post-transcriptionally by targeting and degrading specific transcript isoforms during differentiation.

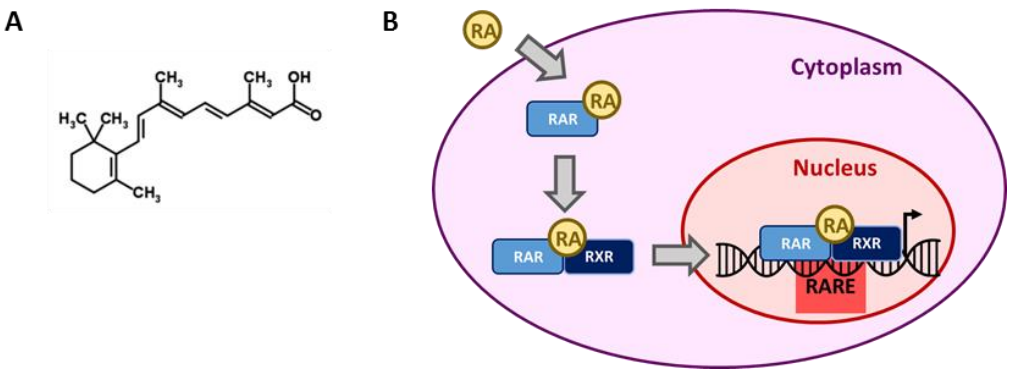


Figure 3.1. Retinoic acid (RA) mediated signalling.

A. Molecular structure of all-trans RA.

B. RA mediated signalling pathway to mediate gene expression changes. RA (yellow) enters the cell and binds to its receptor (RAR, light blue). RAR can then heterodimerise with RXR (navy), forming a complex which translocates to the nucleus, where it binds promoter regions containing RAREs (red) to initiate transcription of target genes.

3.1.2 BE(2)-M17 Neuroblastoma Cell Line

Neuroblastoma cell lines, which originate from cancerous neural crest cells, are commonly used in neuronal research as primary neuronal cells are difficult to grow (Reviewed in (Datta et al. 2013)). They are also a useful system to study neuronal differentiation.

The neuroblastoma BE(2)-M17 cell line originates from a clone of SK-N-BE(2) cells, taken from a 2-year-old male cancer patient. BE(2)-M17 cells are increasingly used in neurobiology, particularly in the *in vitro* modelling of Parkinson's disease (Keane et al. 2015). Treatment of BE(2)-M17 cells with RA induced differentiation to a mature neuronal cell state, including typical morphological changes such as extended neurite growth. Additionally, increased expression of neuron specific proteins, such as neuron specific enolase and synapsin were observed. Expression levels of cancer related genes which are highly expressed in neuroblastoma cells were also shown to decrease upon differentiation (Andres et al. 2013).

3.1.4 Chapter Aims

The aim of this chapter was to understand the impact of RA mediated differentiation in BE(2)-M17 cells on transcriptional and post-transcriptional APA regulation. The strategy used isolated nuclear and cytoplasmic RNA to compare the subcellular APA profiles during differentiation. Many studies on APA focus on global changes, rather than physiologically relevant APA events. Therefore, this chapter also aimed to identify APA events which may contribute to neuronal differentiation of the BE(2)-M17 cell line.

3.2 Results

3.2.1. Characterising the Differentiation of BE(2)-M17 cells

The neuroblastoma cell line BE(2)-M17 was chosen to study APA in neuronal differentiation. Treatment of BE(2)-M17 cells with RA results in neurite outgrowth and cell cycle arrest producing neuronal like cells that no longer divide. BE(2)-M17 cells were differentiated with 10 µM RA for 72 hours, after which morphological changes, such as neurite outgrowth, were visible (Figure 3.2A). To quantify the differentiation process, FACS analysis of propidium iodide treated cells was performed to assess and quantify changes in the cell cycle progression between the RA treated and untreated cells. After RA exposure, the proportion of cells in mitosis dropped from 31% in untreated cells to 21% in differentiated cells, while the proportion of cells in G1 increased from 52% to 70%, suggesting a tendency for increased cell cycle arrest upon RA treatment (Figure 3.2B). Furthermore, increased expression of neuron specific genes, such as *ENO2*, previously shown to be induced during BE(2)-M17 differentiation (Andres et al. 2013) were confirmed by RT-PCR using RNA from the respective cells (Figure 3.2C). Collectively these results show that BE(2)-M17 cells treated with RA for 72 hours show classic indicators of neuronal differentiation.

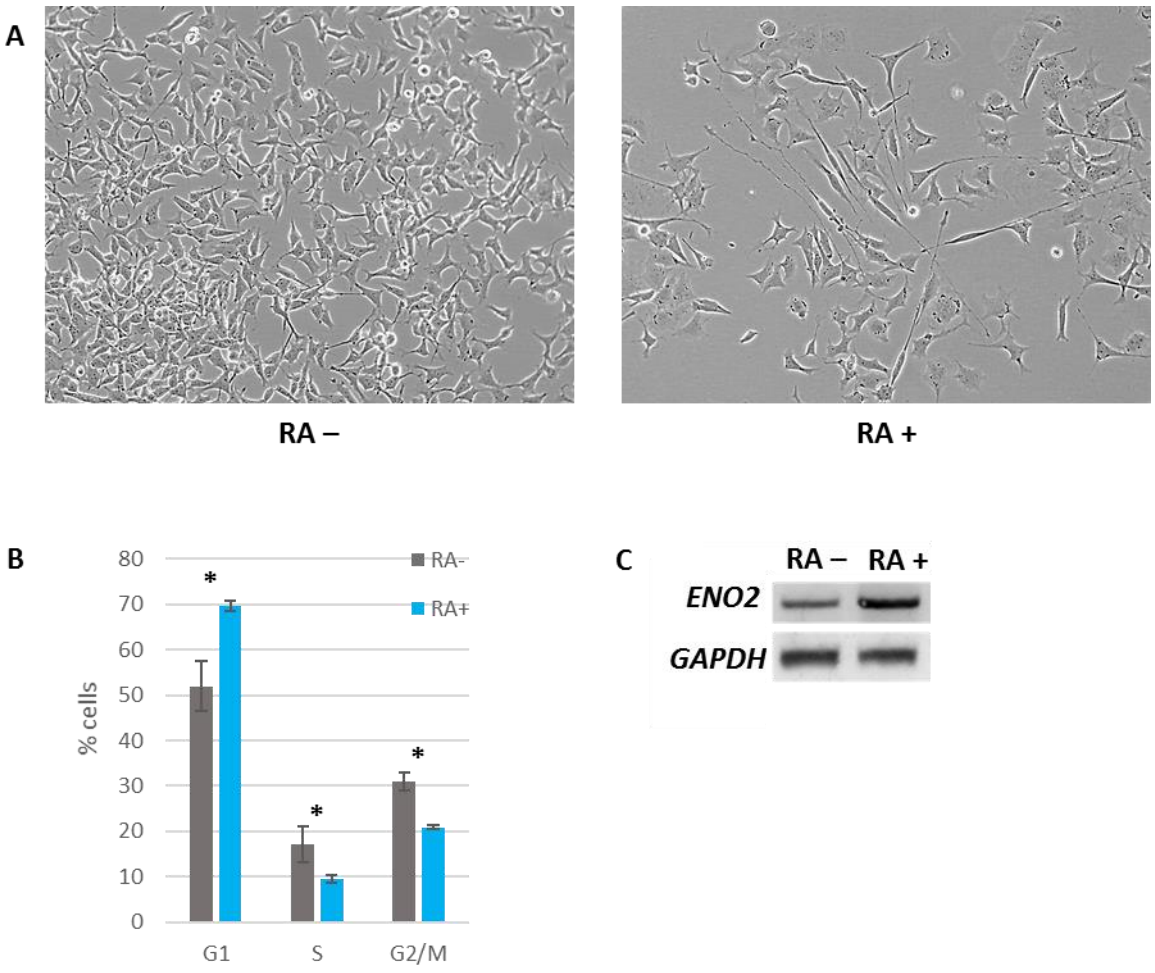


Figure 3.2. Characterising the Differentiation of BE(2)-M17 cells.

A. BE(2)-M17 cells were treated with or without 10 µM RA for 72 hours. Compared to untreated cells (RA-), neurite outgrowth was observed RA treatment of BE(2)-M17 cells (RA+). Images were taken with a EVOS xl Core Cell Imaging System (20x magnification).

B. Quantification of the cell cycle. A bar chart to show the proportion of cells in the G1, S and G2/M phases of the cell cycle identified through FACS analysis. Error bars show standard deviation, n = 3. T-test, * = $p<0.05$.

C. RT-PCR using total RNA to show increased expression of *ENO2*, a neuron specific enolase, in differentiated (RA+) versus non-differentiated (RA-) cells. *GAPDH* used as a housekeeping control gene.

3.2.2. Isolation of Cytoplasmic and Nuclear RNA and Generation of 3'end libraries

APA changes are almost exclusively assessed using whole-cell RNA, which cannot discriminate between changes in APA profiles that occur at the co-transcriptional level in the nucleus or are due to post-transcriptional events that happen in the cytoplasm. To get a deeper insight into the mechanisms that shape APA profile changes, RNA was isolated from the cytoplasm and nucleus of cells (Chapter 2.3). In addition, total RNA was isolated from the same cells. To verify the integrity of the RNA fractions and ensure that there was no cross-contamination of cytoplasmic RNA in the nuclear RNA fraction, and vice versa, two quality control steps were taken. Firstly, RNA samples were run on a denaturing agarose gel, where intact ribosomal RNA (rRNA) signifies no RNA degradation. In the cytoplasm, there should be 1.8x more 28S rRNA than 18S rRNA, as seen in Figure 3.3A. As rRNA is processed in the nucleus, the precursor rRNAs of 45S and 32S are also present in the nuclear fraction. The absence of precursor rRNAs in the cytoplasm indicates its purity. Total RNA shows a predominantly 'cytoplasmic' profile, but in contrast to the cytoplasmic fraction, the rRNA precursors are faintly visible (Figure 3.3B).

Secondly, the expression of *MALAT1*, a highly expressed, nuclear-retained noncoding RNA, was determined in the cytoplasmic and nuclear fractions. An RT-PCR reaction confirmed that this noncoding RNA was only present in the nucleus, further verifying the successful separation of the nuclear and cytoplasmic RNA fractions (Figure 3.3C).

Numerous RNA-seq techniques have been developed to assess differential poly(A) site usage (Supplementary Table 1). Libraries for sequencing the different fractions were prepared using a 3'Quant-Seq kit (Lexogen), which extracts the 3'end of transcripts (Figure 3.3D). This enables a higher resolution of poly(A) site usage than whole transcriptome sequencing, where reads are often disproportionately from the coding region of the transcript. In addition, since each transcript generates one sequencing fragment, this method also allows accurate assessment of gene expression. This protocol maintains strand specificity enabling accurate sequencing around overlapping genes. Furthermore, sequencing only the terminal 200 bases is highly cost-efficient. Library quality was verified and quantified using a High Sensitivity dsDNA Bioanalyzer kit (Figure 3.3E), and libraries were sequenced on the Ion Proton platform. The RNA-seq data was processed through a well-established bioinformatics pipeline (Hoque et

al. 2013; Neve et al. 2016), which analyses both statistically significant gene expression changes (Fisher's exact Test, $p<0.01$) and quantifies and identifies statistically significant changes in APA.

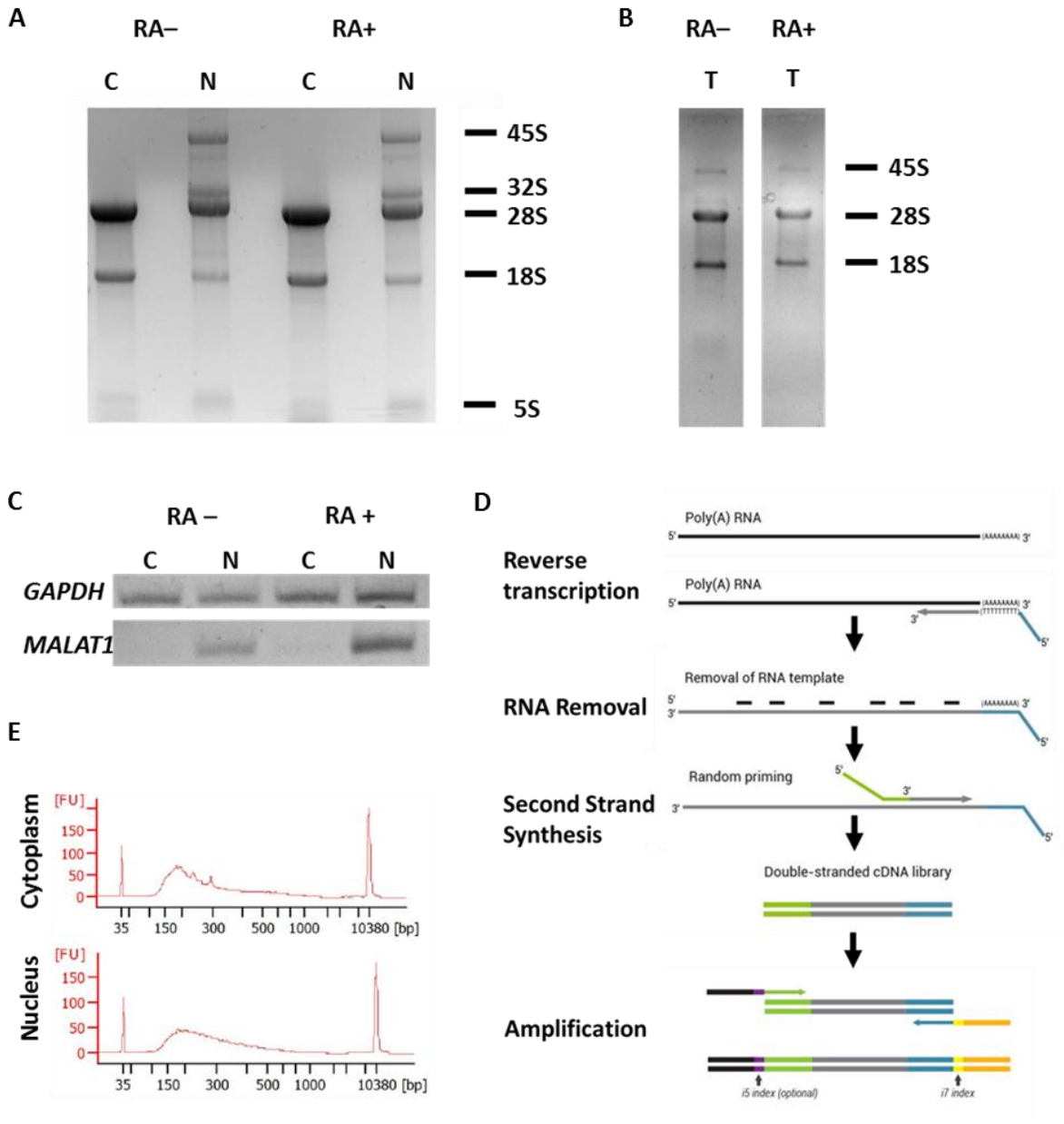


Figure 3.3. Preparing Libraries of Cytoplasmic and Nuclear RNA.

A. Representative agarose gels assessing rRNA composition in the different cytoplasmic (C) and nuclear (N) fractions. The rRNA precursors (45S and 32S) are only observed in the nuclear fraction.

B. Agarose gel to verify quality of Total RNA (T). The 45S and 32S rRNA precursors are faintly visible.

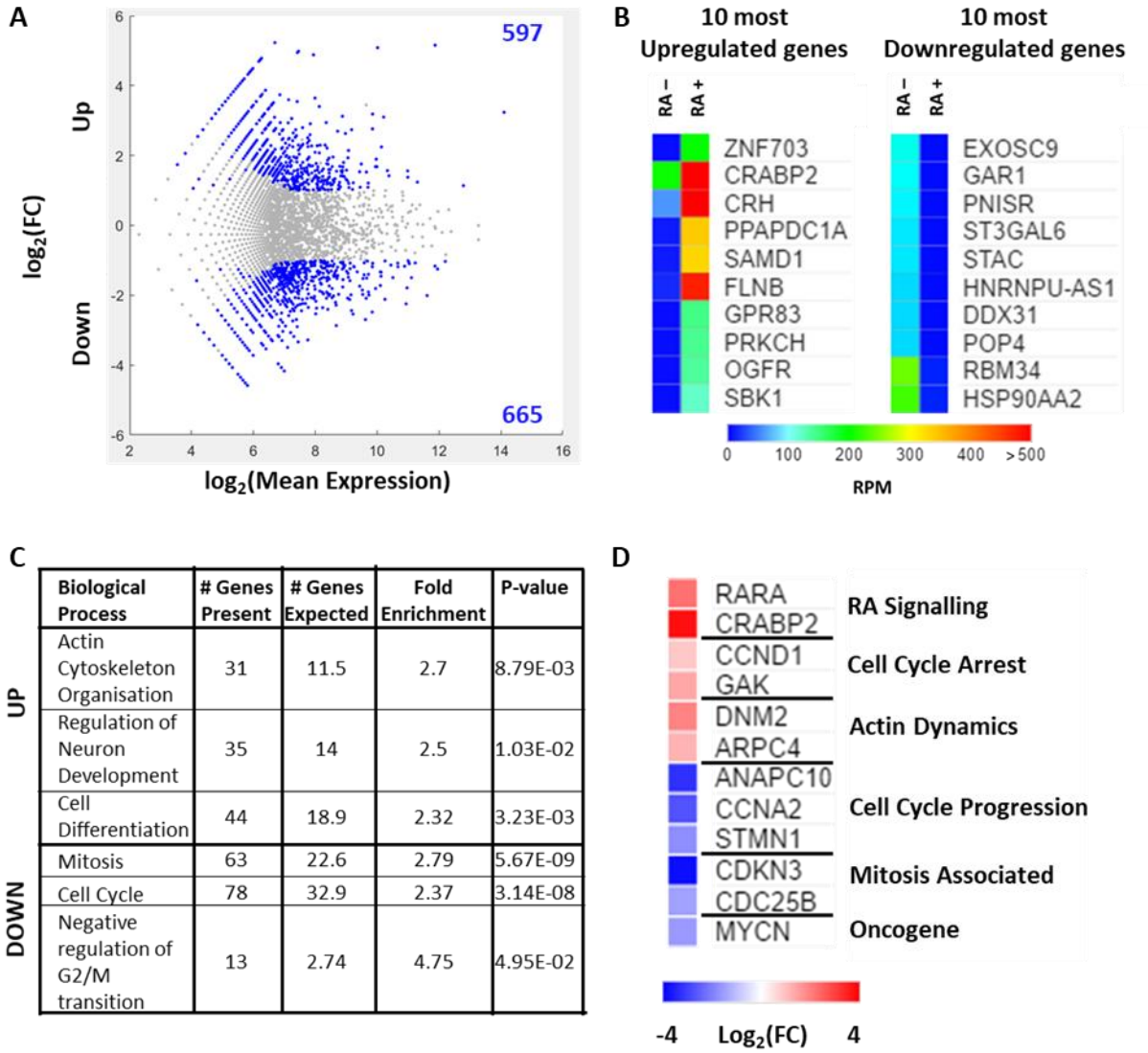
C. RT-PCR analysis probing the presence of *MALAT1* showing that this nuclear retained gene is only present in the nucleus, confirming the successful separation of the nuclear and cytoplasmic fractions. *GAPDH* used as a housekeeping control gene, and is present in both nuclear and cytoplasmic fractions.

D. Schematic depicting the principles of 3'end extraction by the 3'Quant-Seq library preparation kit. The polyadenylated (poly(A)) RNA is reverse transcribed using an oligo dT primer. The parent RNA strand is then degraded and the second strand is synthesized using random primers to produce a double stranded cDNA library. Amplification with PCR produces sufficient material for RNA-seq. Image modified from https://www.lexogen.com/quantseq-workflow.

E. Representative libraries for cytoplasmic and nuclear fractions were subsequently assessed for quality on a Bioanalyzer. Marker peaks observed at 35 bp and 10380 bp.

3.2.3. Differentiation of BE(2)-M17 cells shows Widespread Gene Expression Changes

Altered expression of specific genes has been identified in differentiated neuroblastoma cells (Andres et al. 2013) but this has not previously been done on a genome wide scale in BE(2)-M17 cells differentiated with RA. The impact of 72 hour treatment of RA on global gene expression in BE(2)-M17 cells was first assessed using total RNA of treated and untreated cells. A total of 597 and 665 genes were significantly up- and down-regulated respectively ($p<0.01$, Fisher's exact Test, Fold Change (FC) >2) (Figure 3.4A, B). Gene ontology (GO) analysis of the upregulated genes showed an enrichment in actin cytoskeleton organization, axon development and cell differentiation while downregulated genes were associated with mitosis and the cell cycle (Figure 3.4C). These transcriptomic changes would be expected as there is increased cell cycle arrest during neurite outgrowth. In addition, genes specifically encoding proteins associated with RA signaling, such as the RA binding protein CRABP2, and the RA receptor RARα, were upregulated, and those associated with the cancerous state of neuroblastoma cells such as *MYCN* were downregulated. The changes in expression of a selection of these genes is shown in Figure 3.4D. This analysis further confirms that upon RA treatment, BE(2)-M17 cells differentiate into neuron-like cells.



Biological Process	# Genes Present	# Genes Expected	Fold Enrichment	P-value
Actin Cytoskeleton Organisation	31	11.5	2.7	8.79E-03
Regulation of Neuron Development	35	14	2.5	1.03E-02
Cell Differentiation	44	18.9	2.32	3.23E-03
Mitosis	63	22.6	2.79	5.67E-09
Cell Cycle	78	32.9	2.37	3.14E-08
Negative regulation of G2/M transition	13	2.74	4.75	4.95E-02

Figure 3.4. Gene Expression Changes During Differentiation of BE(2)-M17 cells.

A. An MA (Mean Average) plot to show significantly (Fisher's exact Test, $p<0.01$; FC >2) upregulated and downregulated genes identified through RNA-seq in total RNA isolated from undifferentiated cells and differentiated cells treated with 10 µM RA for 72 hours.

B. A heatmap of the top 10 most upregulated (left) and downregulated (right) genes are shown in differentiated (RA+) compared to undifferentiated (RA-) cells. Colour spectrum shows reads per million (RPM) normalized to housekeeping gene *GAPDH*.

C. A table to show biological processes enriched in differentially expressed genes identified by GO analysis.

D. Log_2(FC) in expression of selected genes associated with pathways related to differentiation. Expression is normalized to the housekeeping gene *GAPDH*.

3.2.4 Modest APA Changes Identified During Differentiation in Total RNA

The CNS has been shown to utilise more distal poly(A) sites than other tissues, to provide increased regulation of the transcriptome (Miura et al. 2014). However, APA changes during the differentiation of neuroblastoma cells have not previously been investigated on a global scale.

An established bioinformatics pipeline (Hoque et al. 2013; Neve et al. 2016) was used to assess APA changes during differentiation. To assess trends in UTR length, the $\log_2$ ratio of the proximal APA isoform in RA treated samples was compared to untreated samples, and plotted against the $\log_2$ ratio of the distal APA isoform between the two samples. Where multiple poly(A) sites were present, the two most abundant poly(A) sites were selected for analysis. Comparing total RNA in RA treated and untreated cells, a total of 4275 APA events were identified, but only 100, fewer than 2.5%, of these showed significant APA changes ($p<0.01$ Fisher's exact Test, with a minimum 5% change in APA isoform abundance, as defined in previous studies (Hoque et al. 2013; Neve et al. 2016)) (Figure 3.5A). This suggests that there are not widespread changes during the differentiation of BE(2)-M17 cells as previously proposed in differentiation of other cell lines (Zhe Ji et al. 2009; Shepard et al. 2011). However, a significant increase to 3'UTR lengthening was observed in the cohort that changed (Fisher's exact Test, $p<0.05$), indicating increased usage of the distal poly(A) site upon differentiation or post-transcriptional stabilisation of the longer isoforms, which is in agreement with studies in other cell lines (Zhe Ji et al. 2009; Shepard et al. 2011).

An example of a 3'UTR lengthening event was identified in *ICMT* (Figure 3.5B). This gene encodes an enzyme which localises to the ER, where it modifies cysteine residues on proteins that are required to be targeted to the cell membrane. A binding site for miR-17 is found in the alternative UTR of *ICMT*, which is an miRNA known to be downregulated during differentiation of another neuroblastoma cell line, SH-SY5Y (Beveridge et al. 2009). This altered miRNA expression could explain the upregulation of the longer *ICMT* transcript, which may alter the protein output or localisation of this transcript.

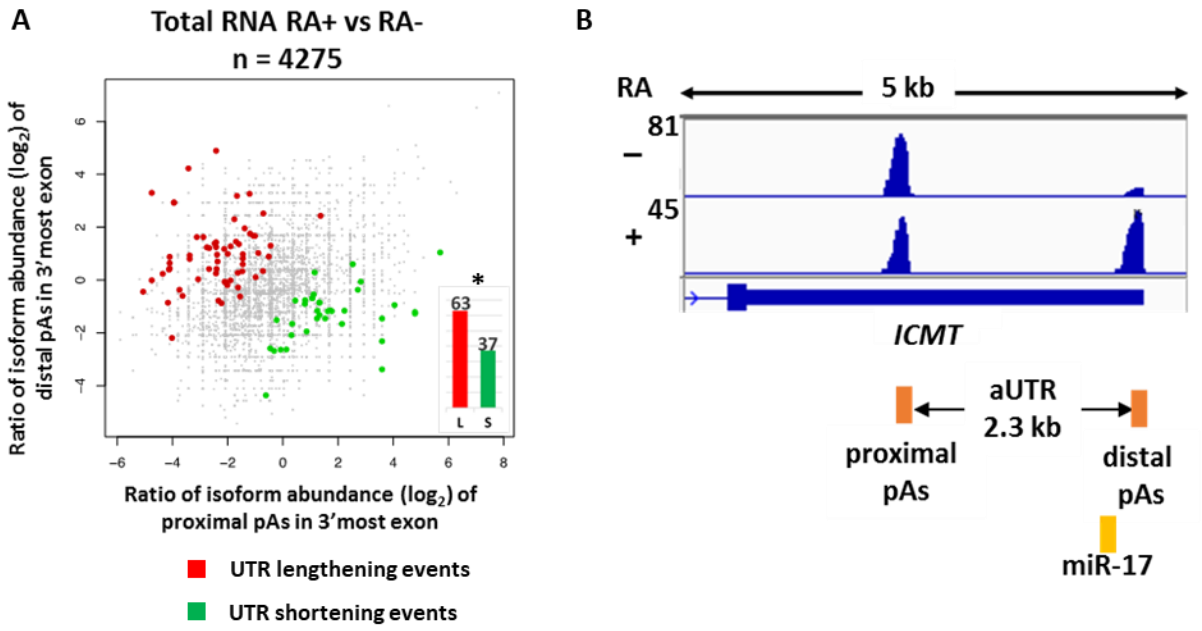


Figure 3.5. A trend to 3'UTR Lengthening in the Differentiation of BE(2)-M17 cells.

A. A total of 4275 expressed genes were identified to be regulated by APA in total RNA isolated from BE(2)-M17 cells differentiated for 72 hours with 10 µM RA compared to undifferentiated cells. Each dot represents an APA event displayed as a $\log_2$ ratio identified from 3'end RNA-seq. 100 of these APA events were statistically significant (Fisher's exact Test, $p<0.01$, with a minimum 5% change in APA isoform abundance). Red dots and bar indicate 3'UTR lengthening (L) events, while green dots and bar indicate 3'UTR shortening (S) events. The trend to 3'UTR lengthening was significant (Fisher's exact Test, * = $p<0.05$).

B. 3'UTR lengthening was seen in *ICMT*, which encodes a protein involved in post-translational modifications of proteins to target them to the cell membrane. Read numbers in reads per million (RPM) of the most abundant isoform from sequencing data are indicated on the left. The tracks are visualised using auto-scale settings on the IGV Browser. The proximal and distal poly(A) sites (pAs) are indicated by orange boxes. The yellow box indicates the location of the miR-17 binding site for miR-17 in the alternative UTR.

3.2.5 Greater 3'UTR Lengthening in the Cytoplasm compared to the Nucleus

As discussed, most studies only assess APA profile changes during differentiation using total RNA. To distinguish between APA changes at the point of cleavage or post-transcriptionally, poly(A) site usage and therefore UTR length was compared between RNA isolated from the nucleus and cytoplasm of undifferentiated and differentiated cells (Figure 3.6A and B). Remarkably, the trend to 3'UTR lengthening in the nucleus was much less significant than in the cytoplasm. This suggests there is a lesser tendency to favour proximal or distal poly(A) site usage at the co-transcriptional level, as suggested in the literature, but the 3'UTR lengthening in differentiation appears to be mediated by post-transcriptionally acting mechanisms in the cytoplasm. These are likely to involve regulatory events, that control the stability of the longer isoforms. However, 12 of the 3'UTR lengthening events and 2 of the 3'UTR shortening events in the cytoplasm were also identified as changing in the nucleus (Figure 3.6C), suggesting these are likely to be co-transcriptionally regulated events.

Comparison of APA events in the cytoplasm compared to the nucleus tends to see a shift to 3'UTR shortening due to the presence of miRNAs and RBPs that target transcripts for degradation in the cytoplasm (Neve et al. 2016). This shift to 3'UTR shortening was also seen in undifferentiated cells, but importantly, upon differentiation, the ratio of 3'UTR lengthening to shortening events was reduced from 1:4.8 in undifferentiated cells to 1:2.7 in differentiated cells (Figure 3.6D). This suggests that an increased number of longer isoforms are stabilized in the cytoplasm of differentiated cells due to regulatory mechanisms that function in the cytoplasm.

In conclusion, the separate analysis of APA changes in the cytoplasm and nucleus during differentiation of BE(2)-M17 cells highlights that stabilisation of longer UTRs in the cytoplasm is more prevalent than increased usage of the distal poly(A) site at the point of cleavage.

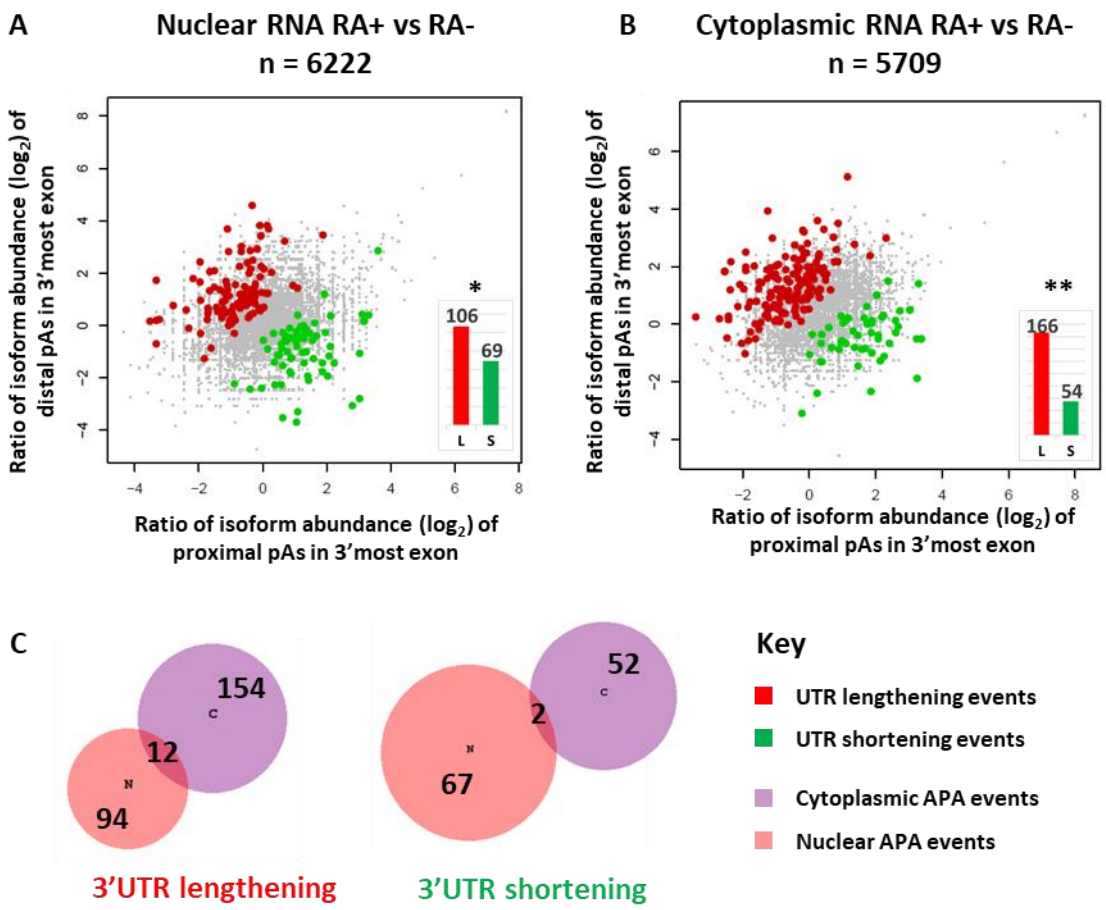

A
Nuclear RNA RA+ vs RA-
n = 6222
Ratio of isoform abundance (log2) of distal pAs in 3'most exon
Ratio of isoform abundance (log2) of proximal pAs in 3'most exon
*
106
69
L
S
B
Cytoplasmic RNA RA+ vs RA-
n = 5709
Ratio of isoform abundance (log2) of distal pAs in 3'most exon
Ratio of isoform abundance (log2) of proximal pAs in 3'most exon
**
166
54
L
S
C
154
C
12
N
94
3'UTR lengthening
52
C
2
N
67
3'UTR shortening
Key
UTR lengthening events
UTR shortening events
Cytoplasmic APA events
Nuclear APA events
D
RA- Cytoplasm vs Nucleus
n = 6089
Ratio of isoform abundance (log2) of distal pAs in 3'most exon
Ratio of isoform abundance (log2) of proximal pAs in 3'most exon
X 4.8
355
74
L
S
RA+ Cytoplasm vs Nucleus
n = 6240
Ratio of isoform abundance (log2) of distal pAs in 3'most exon
Ratio of isoform abundance (log2) of proximal pAs in 3'most exon
X 2.7
367
137
L
S

Figure 3.6. Greater 3'UTR Lengthening occurs in the Cytoplasm During the Differentiation of BE(2)-M17 cells.

A. A scatter plot to show that there are more 3'UTR lengthening events (red) than 3'UTR shortening events (green) in BE(2)-M17 cells differentiated with 10 µM RA for 72 hours compared to undifferentiated cells in the nuclear fraction (* = $p<0.05$, Fisher's exact Test) identified through 3'end RNA-seq.

B. A scatter plot to show that the trend to increased 3'UTR lengthening events (red) than 3'UTR shortening events (green) in RA differentiated compared to undifferentiated BE(2)-M17 cells is stronger in the cytoplasmic fraction (** = $p<0.001$, Fisher's exact Test), identified through 3'end RNA-seq.

C. A Venn diagram to show the overlap of significant 3'UTR lengthening (left) and 3'UTR shortening (right) APA events between the cytoplasm (purple) and nucleus (red).

D. APA events in the cytoplasm compared to the nucleus in undifferentiated (left, RA-) and differentiated (right, RA+) cells. The ratio of lengthened (L) to shortened (S) UTRs is reduced from RA- to RA+ cells suggesting increased stabilisation of longer UTRs in the cytoplasm. Red indicates 3'UTR lengthening (L) events, green indicates 3'UTR shortening (S) events; n = the number of APA events identified in each comparison.

3.2.6 Altered miRNA Expression in Differentiation may Contribute to Cytoplasmic 3'UTR-APA regulation

The changes in miRNA expression have been explored during the RA mediated differentiation of mouse and human embryonic stem cells to neurons and neuroblastoma cell lines to neuronal like cells (Sempere et al. 2004; Beveridge et al. 2009; Stallings et al. 2011).

Given that miRNA target sites are predominantly found in the 3'UTRs, alterations in poly(A) site usage to change the 3'UTR length could include or exclude miRNA target sites. The enrichment of miRNA binding sites in the alternative UTRs of genes showing significantly different cytoplasmic APA profiles upon RA mediated differentiation, was assessed using an miRNA enrichment analysis developed by Gruber and colleagues (A. R. Gruber et al. 2014) (Chapter 2.21).

In this analysis, a z-score of greater than 2 is considered to represent a significant enrichment of a miRNA in the set of alternative UTRs tested. In the cohort of lengthened genes, 13 miRNAs showed a significant enrichment, while 17 miRNAs were significantly enriched in shortened alternative UTRs (Figure 3.7A). The miRNAs were found to target up to 23% of the genes showing APA, though there was no correlation between the percentage of genes targeted and the z-score enrichment (Figure 3.7A).

Enrichment of these miRNA binding sites in the cohorts of genes assessed could explain the 3'UTR length changes. Although miRNA expression changes have not been assessed in the BE(2)-M17 cell line, small RNA-seq has been conducted in another neuroblastoma cell line, SK-N-SH, in both undifferentiated and RA-mediated differentiated cells (GEO accession GSE24565). Expression changes of miRNAs enriched in the alternative UTRs of APA regulated genes in BE(2)-M17 cells were investigated in the small RNA-seq dataset. With the lengthened alternative UTR cohort, only 8 of the 13 enriched miRNAs were expressed, and only 3, all members of the let-7 family, showed significantly reduced expression in differentiated cells (Figure 3.7B). Therefore, the 3'UTR lengthening of genes targeted by the let-7 family could be explained through reduced miRNA expression. However, the other lengthened alternative UTRs are unexplained through miRNA expression levels. Similarly, only two miRNAs, miR-363 and miR-195, were significantly upregulated in differentiated SK-N-SH cells that were enriched in the shortened alternative UTRs, while 2 were not expressed and 4 were

significantly downregulated (Figure 3.7B). This analysis consequently suggests that the influence of miRNAs on mediating cytoplasmic APA profiles may be limited during the during differentiation of neuroblastoma cells.

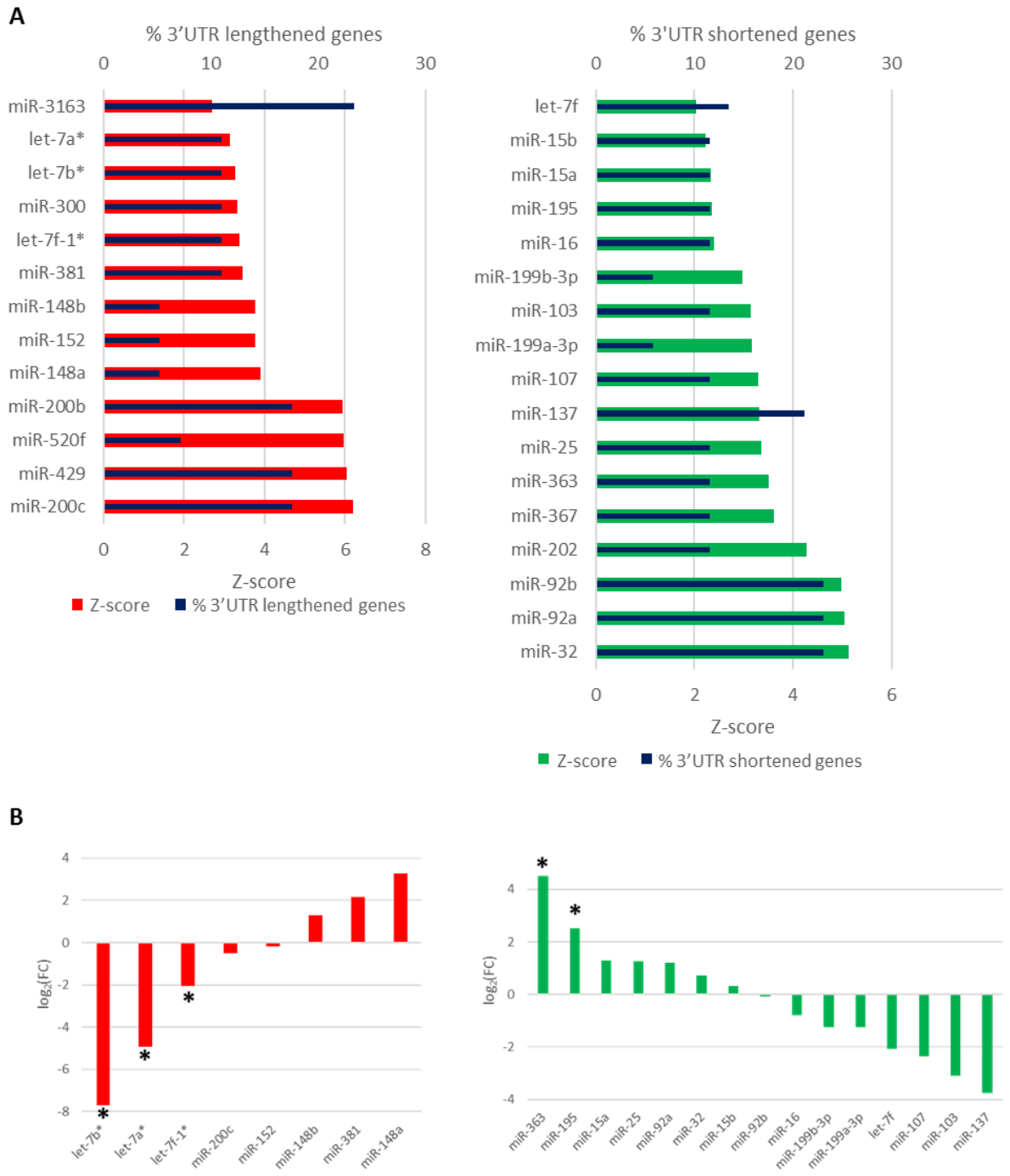


Figure 3.7. The Role of miRNAs in Mediating Cytoplasmic APA Changes.

A. A bar chart to show the miRNAs that were significantly enriched (z-score >2) in lengthened alternative UTRs (left, red bars) and shortened alternative UTRs (right, green bars) in RA differentiated cells compared to undifferentiated cells. The percentage of APA regulated genes with the corresponding miRNA target site are indicated by navy bars.

B. Bar charts to show the fold change (FC) of miRNAs that were enriched in lengthened (left, red) and shortened (right, green) alternative UTRs in RA differentiated compared to undifferentiated SK-N-SH cells. The statistically significant expression changes that could explain UTR lengthening (left) or UTR shortening (right) are indicated by asterisks ($p<0.01$ Fisher's exact Test, FC >2).

3.2.7. Upstream-APA shows a Trend to Longer Transcript Isoforms During Differentiation

Whilst UTR-APA has been extensively studied in the context of differentiation and development, changes in upstream-APA, where an upstream poly(A) site in an upstream exon or intron is utilised, have not been extensively investigated. Usage of this upstream poly(A) site alters the message and therefore impacts the protein produced.

Fewer upstream-APA events were observed in both the nuclear and cytoplasmic fractions upon differentiation than UTR-APA events (Figure 3.8A), in agreement with other studies (Shepard et al. 2011). However, in both fractions, a trend to using the terminal exon poly(A) site, and therefore produce longer transcripts, was observed with RA treatment (Figure 3.8A, red bars). Upstream-APA events occurring in the nucleus are likely to be mediated by an increased usage of the terminal exon poly(A) site at the point of cleavage. However, only four genes showed an altered APA profile in both the cytoplasmic and nuclear fractions (Figure 3.8B), which suggests that the other transcript isoforms are retained in the nucleus or degraded upon entry into the cytoplasm.

Comparison of the upstream-APA events in the cytoplasm will have a greater physiological impact, since these transcripts will be translated. A gene encoding a microtubule associated serine/threonine kinase, *MAST1*, showed an increased presence of the full-length transcript in differentiation in the cytoplasm, but this was not statistically significant when comparing the nuclear fractions (Figure 3.8C). There was no significant change in gene expression of *MAST1* at the RNA level. The protein encoded by the full length *MAST1* gene has a central domain with kinase activity and a C-terminal PDZ domain, as outlined in Figure 3.8D (Garland et al. 2008). MAST1 is enriched in the brain and is associated with the cytoskeleton. The PDZ domain is important in anchoring proteins to the cytoskeleton, and can also interact with syntrophin. This adaptor protein that connects signalling molecules to the protein dystrophin and its associated complex, which connects the extracellular matrix to the intracellular cytoskeleton for construction and maintenance of post synaptic structures in the CNS.

The full-length gene encodes a 170 kDa protein. A splice variant of this gene, with a truncated C-terminus encoding a 124 kDa protein, has been identified, which showed altered

localisation in the rat brain (Yano et al. 2003). However, the shorter isoform identified here would encode a smaller, 49 kDa, protein. The full catalytic site of the kinase domain and the C-terminal PDZ domain are absent in the shorter isoform (Figure 3.8D). Therefore, the truncated protein cannot be fully functional. During differentiation, a shift from the shorter isoform to the longer isoform at the level of APA may be a regulatory mechanism to increase the amount of functional protein, which may be important in cytoskeletal reorganisation that occurs during the differentiation process. Differentiated BE(2)-M17 cells have been shown to develop synaptic maturation (Andres et al. 2013), which may be aided by the increased expression of functional MAST1.

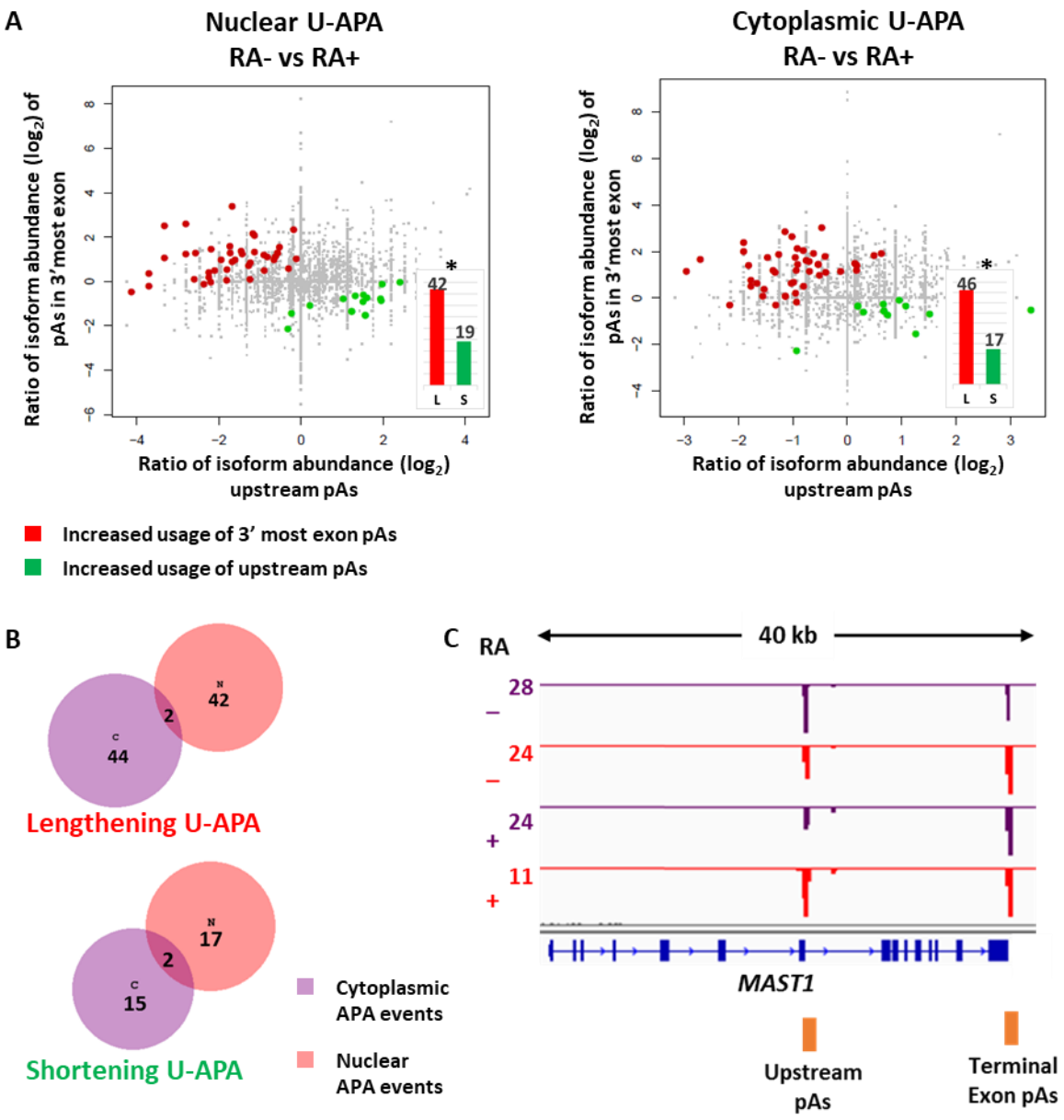

A
Nuclear U-APA
RA- vs RA+
Cytoplasmic U-APA
RA- vs RA+
Ratio of isoform abundance (log2) of pAs in 3'most exon
Ratio of isoform abundance (log2) upstream pAs
42
19
46
17
L
S
Increased usage of 3' most exon pAs
Increased usage of upstream pAs
B
N 42
C 44
2
Lengthening U-APA
N 17
C 15
2
Shortening U-APA
Cytoplasmic APA events
Nuclear APA events
C
RA
40 kb
28
24
24
11
MAST1
Upstream pAs
Terminal Exon pAs
D
1570 aa
Protein kinase domain
PDZ domain
433 aa
Nucleotide binding domain
ATP binding site
H+ acceptor active site
Protein sequence in truncated same as full length

Figure 3.8. *MAST1* Regulated by Upstream-APA During Differentiation of BE(2)-M17 cells.

A. A scatter plot to visualise upstream-APA events in the nucleus (left) and the cytoplasm (right) during 72 hour differentiation of BE(2)-M17 with 10 µM RA. The $\log_2$ ratio of all the reads identified in an upstream poly(A) site in the RA treated compared to untreated cells are plotted against the $\log_2$ ratio of all of the reads identified in the 3' most terminal exon between the two samples. Red dots and bars indicate genes where more of the full-length transcript was present, while green dots and bars indicate where more of the upstream poly(A) site was used. A significant trend to using the terminal exon poly(A) site over the upstream poly(A) site was observed (Fisher's exact Test, * = $p < 0.05$).

B. Overlap between identified events in the nucleus (red) and cytoplasm (purple) shows only 2 lengthening and 2 shortening upstream-APA events occur in both fractions.

C. *MAST1* showed increased expression of the longer isoform in the cytoplasm (purple tracks), but the switch in the nucleus (red tracks) was not statistically significant ($p<0.01$, Fisher's exact Test). Numbers on the left indicate the read numbers (RPM) from sequencing data of the most abundant isoform in the track. Tracks have been visualised using auto-scale settings.

D. Schematic to show the protein domains and functional regions of the full length (1570 amino acids) and truncated (433 amino acids) MAST1 protein. The truncated isoform lacks the full Protein Kinase domain and the PDZ domain.

3.2.8 A Shift to 3'UTR Lengthening in *PRDX6* During Differentiation Correlates with Altered Protein Localisation

The *PRDX6* gene, which shows significant lengthening of its 3'UTR in the cytoplasm of differentiated cells (Figure 3.9A), was selected to explore whether RA induced APA changes have downstream effects on gene expression in differentiation. *PRDX6* encodes a member of the peroxiredoxin family of proteins, which are antioxidant enzymes that scavenge reactive oxygen species (ROS).

First, the 3'UTR lengthening event upon differentiation was verified with RT-PCR, using two primers sets that monitor the ratio between the distal UTR containing isoforms versus all *PRDX6* transcripts (Figure 3.9B). This showed that RA treated cells indeed expressed a greater proportion of the distal transcript than undifferentiated cells (Figure 3.9C). Extension of 3'UTRs has been associated with altered protein output. Western blot analysis was employed to assess the effect on protein output of the 3'UTR lengthening event. This showed no expression change in PRDX6 protein with RA treatment (Figure 3.9D), therefore 3'UTR lengthening had no effect on PRDX6 protein output.

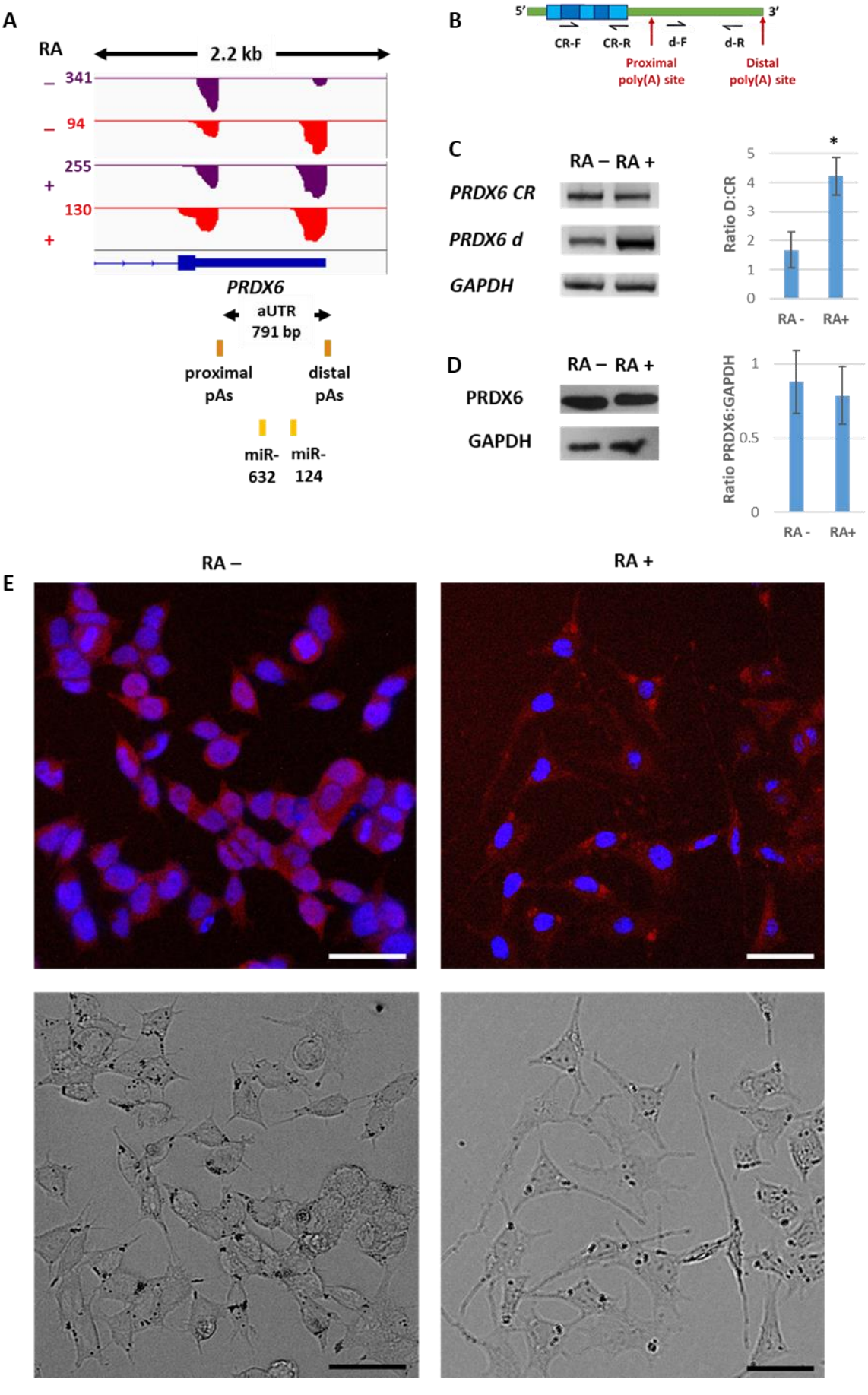
Since alternative UTRs have been implicated in determining protein localisation (Berkovits and Mayr 2015; An et al. 2008), the effect of the 3'UTR lengthening event on the destination of the PRDX6 protein was investigated using immunofluorescence. In undifferentiated cells PRDX6 was uniformly expressed in the cells (Figure 3.9E upper left panel, RA–). However, in differentiated cells, PRDX6 appeared to cluster, particularly close to the nuclear region, although PRDX6 was also detected throughout the cell including in the neurite outgrowth regions (Figure 3.9E upper right panel, RA+). This indicates that PRDX6 shows differential protein localisation in differentiated cells, which correlates with the 3'UTR lengthening event of its mRNA.

The differential protein localisation of PRDX6 could be a result of the longer transcript in RA treated cells being differentially localised to enable localised protein expression. To explore how *PRDX6* mRNA transport may vary between the long and the short isoforms, cis-elements in the alternative UTR were investigated to identify RBP binding sites. From the CLIP database (Chapter 2.24), two binding sites for IGF2BP3 were identified in the alternative UTR sequence.

The IGF2BP family of proteins are involved in binding mRNAs forming a protein-RNA cage complex, which binds to a motor protein that is transported along the cytoskeleton (Wächter et al. 2013). This protein-RNA complex also protects the mRNA from endonucleases and miRNA mediated degradation. Furthermore, this transient storage mechanism regulates the translatability of the transcript. IGF2BP1, which is important in axonal regeneration, is involved in mRNA transport to neurite outgrowth regions enabling localised translation (Gaynes et al. 2015). RNA-seq data showed that IGF2BP1 is not expressed in BE(2)-M17 cells, but its paralog IGF2BP3 showed constant RNA expression during differentiation at the RNA level. The presence of IGFBP3 binding sites in the longer *PRDX6* mRNA isoform could aid its transport enabling localised protein synthesis, and may contribute to the differential protein expression of PRDX6 observed through immunofluorescence.

RBPs can also bind to secondary structure motifs created in the UTR. To investigate the secondary structure of the short and long UTR isoforms, the two UTR sequences were submitted to an RNA fold Web Server (Chapter 2.23). This analysis showed that the two UTRs exhibit very different secondary structure (Figure 3.9F). The longer UTR isoform has numerous stem loop structures that are missing in the shorter UTR isoform, which nonspecific RBPs could use as a scaffold. This gives further insights into how the two *PRDX6* isoforms may be regulated, although the RBPs that bind these scaffold regions need to be investigated.

In conclusion, these results show that the 3'UTR lengthening of *PRDX6* observed during the differentiation of BE(2)-M17 cells is correlated with altered protein localisation.


A
RA
2.2 kb
– 341
– 94
+ 255
+ 130
PRDX6
aUTR
791 bp
proximal
pAs
distal
pAs
miR-
632
miR-
124
B
5′
3′
CR-F
CR-R
d-F
d-R
Proximal
poly(A) site
Distal
poly(A) site
C
RA – RA +
PRDX6 CR
PRDX6 d
GAPDH
Ratio D:CR
5
4
3
2
1
0
*
RA -
RA+
D
RA – RA +
PRDX6
GAPDH
Ratio PRDX6:GAPDH
1
0.5
0
RA -
RA+
E
RA –
RA +

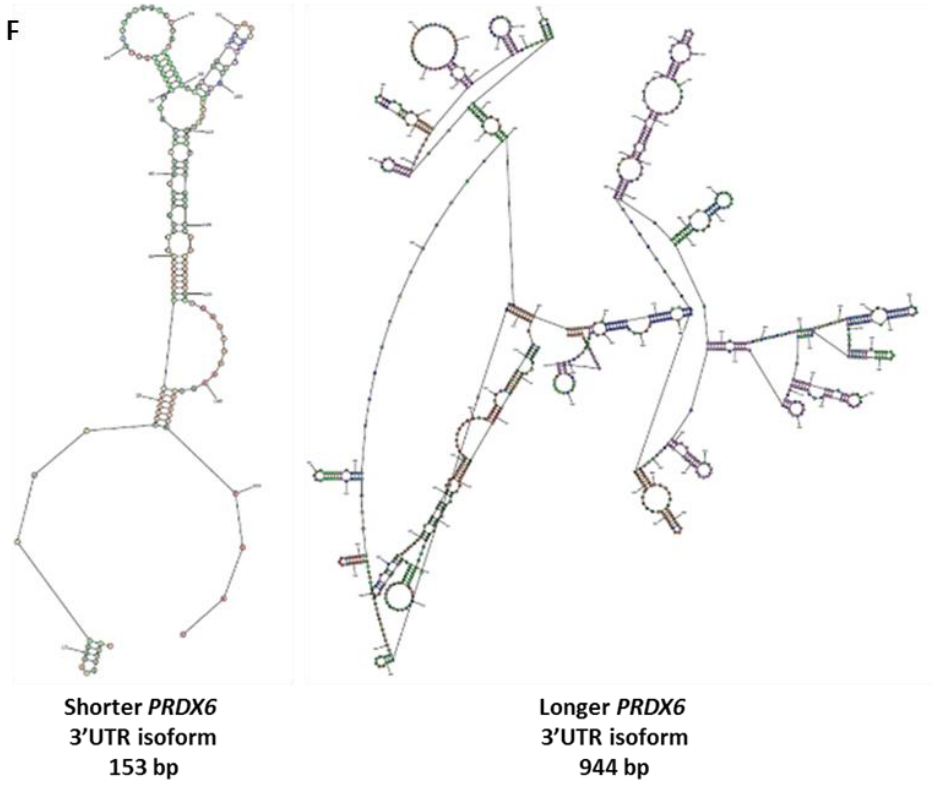


Figure 3.9. The *PRDX6* gene shows 3'UTR Lengthening During Differentiation which Correlates to Altered Protein Localisation.

A. An increased usage of the distal poly(A) site in BE(2)-M17 cells treated with 10 µM RA for 72 hours (RA+) compared to untreated cells (RA-) in the cytoplasm (purple tracks) but not the nucleus (red tracks). miRNA target sites indicated by yellow boxes. The read numbers (RPM) from sequencing data of the most abundant isoform are shown on the left.

B. A schematic to show the primers used in RT-PCR to amplify all *PRDX6* transcripts in the coding region (CR) and only the distal isoform (D). Exons are indicated by alternating blue and light blue boxes; the UTR region is indicated in green.

C. Left panel: RT-PCR using cytoplasmic RNA of total mRNA output (PRDX6 CR), distal PRDX6 isoform (PRDX6 d) and control GAPDH. No change in PRDX6 expression of the coding region (CR) but upregulation of the alternative UTR region with RA treatment was observed. Right panel: a bar chart indicating the change in ratio of the long to short isoform in RA– and RA+ cells calculated from the intensities of the bands quantified by ImageJ. * = $p<0.05$, T-test.

D. Left panel: a western blot showing no significant change in PRDX6 protein isolated from the whole cell fraction during differentiation. Right panel: a bar chart indicating ratio of PRDX6 with and without RA treatment calculated from intensities of bands quantified by ImageJ. In part C and D, error bars in bar charts indicate standard deviation, n = 3.

E. Differential distribution of PRDX6 in BE(2)-M17 cells with and without RA treatment. Upper left panel shows uniform localisation of PRDX6 in undifferentiated (RA –) cells. Upper right panel shows PRDX6 accumulates in clusters in differentiated (RA+) cells. PRDX6 is stained red, nuclei are stained blue with Hoechst stain. Lower panels show light images of the RA– and RA+ cells. Scale bar = 50 µM.

F. Predicted secondary structure with the lowest free energy of the shorter (left) and longer (right) *PRDX6* UTR isoforms.

3.2.9 3'UTR Shortening in *CACYBP* During Differentiation Correlates with Reduced Protein Output

An interesting APA event upon RA exposure of BE(2)-M17 cells was observed in transcripts of the *CACYBP* gene (Figure 3.10A). *CACYBP* moves against the overall trend and undergoes shortening upon RA mediated differentiation in BE(2)-M17 cells. The observed shortening in this gene may be physiologically significant as previous studies have suggested that CACYBP has an important role during cell line differentiation (Au et al. 2006; Schneider et al. 2010) and also acts as a positive modulator of the cell cycle in tumours (H. Shi et al. 2014; Niu et al. 2016; Zhai et al. 2017; N. Wang et al. 2010; X. Chen et al. 2011).

The observed 3'UTR shortening in RA treated compared to untreated cells was first verified with RT-PCR using two primers sets that monitor the ratio between the distal UTR containing isoforms versus all *CACYBP* transcripts (Figure 3.10B). This analysis showed that the overall *CACYBP* mRNA levels remained constant between treated and untreated cells and importantly confirmed the increased frequency of the shorter UTR containing isoform in RA treated cells (Figure 3.10C). To test whether shortening affected protein output, western blot analysis of whole-cell protein extracts was performed from RA treated and untreated cells. As can be seen in Figure 3.10D, CACYBP protein level is significantly reduced in RA treated cells.

CACYBP has been reported to have both cytoplasmic and nuclear roles (Topolska-Woš, Chazin, and Filipek 2016). To investigate whether the reduction in protein output compromises the subcellular distribution, CACYBP protein levels in the nuclear and cytoplasmic fractions were analysed. In contrast to previous reports (J. Wu et al. 2003), CACYBP was only weakly expressed in the nucleus in both undifferentiated and differentiated cells. Its expression in the cytoplasm was reduced upon differentiation, as observed in the whole-cell protein lysate (Figure 3.10E). This suggests that there are no changes in CACYBP localisation between the cytoplasm and the nucleus during differentiation in BE(2)-M17 cells.

To understand the mechanism of the 3'UTR shortening event, the 3'UTR was scanned for the presence of regulatory cis-elements using TargetScan to identify miRNA target sites and the CLIP database to identify presence of RBP binding sites (Chapter 2.24). From this analysis, no miRNAs were identified in the alternative UTR to specifically target the longer

UTR isoform. However, a binding site for MOV10, which is associated with miRNA mediated translational repression by the RISC complex, was observed in the alternative UTR. MOV10 could therefore mediate selective degradation of the longer isoform, although the miRNA mediated repression may be from miRNA target sites for miR-27-3p, miR-128-3p or miR-31-5p, which are found in the constitutive UTR (Figure 3.10A, yellow boxes).

These results show that RA induced differentiation causes 3'UTR shortening of the *CACYBP* mRNA resulting in a reduction of protein expression. The reduction in CACYBP protein is likely to be linked to suppressing the cell cycle during differentiation.

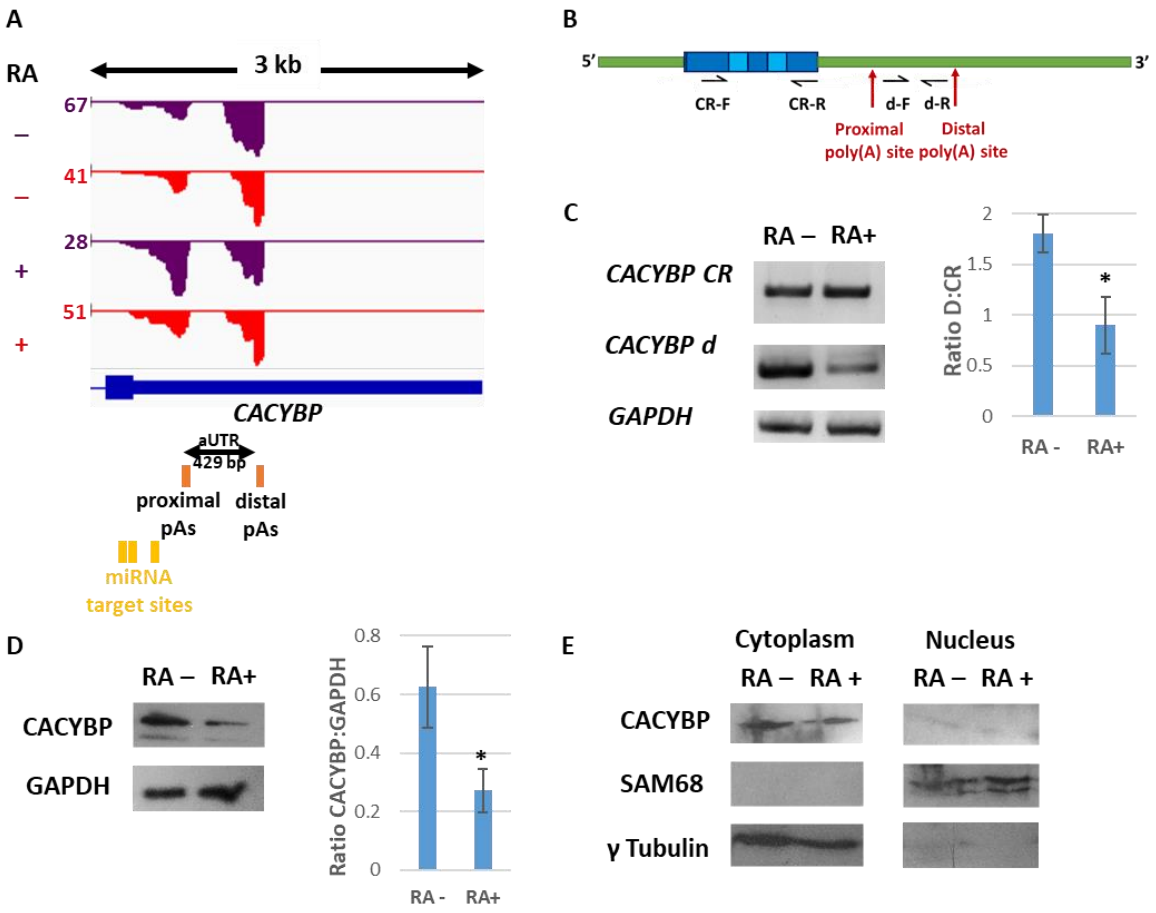


Figure 3.10. 3'UTR Shortening During Differentiation in the *CACYBP* gene Correlates with Reduced Protein Expression

A. An increased usage of the proximal poly(A) site was observed in BE(2)-M17 cells treated for 72 hours with 10 µM RA in the cytoplasm (purple tracks) but not the nucleus (red tracks). miRNA target sites for miR-27-3p, miR-128-3p and miR-31 are indicated by yellow boxes. The numbers on the left indicate RPM of the most abundant isoform of that track visualised on IGV using auto-scale settings.

B. Schematic to show the primers used in RT-PCR to amplify all *CACYBP* transcripts in the coding region (CR) and only the distal isoform (D).

C. Left panel: RT-PCR result using cytoplasmic RNA of total mRNA output (CACYBP CR), distal CACYPB isoform (CACYBP d) and control GAPDH mRNA in undifferentiated (RA–) and differentiated (RA+) cells. No change in total *CACYBP* expression, but reduced expression of the alternative UTR region upon RA treatment was observed. Right panel: a bar chart indicating a ratio of the long to short isoform with and without RA treatment calculated from the intensities of the bands quantified by ImageJ. Error bars on bar charts show standard deviation, n = 3, * = $p<0.05$, T-test.

D. Left panel: Western blot showing reduced CACYBP expression in whole cell fraction protein samples isolated from differentiated cells compared to undifferentiated cells. Right panel: a bar chart indicating ratio of CACYBP to GAPDH with and without RA treatment calculated from intensities of bands quantified by ImageJ. Error bars on bar charts show standard deviation, n = 3. * = $p<0.05$, T-test.

E. Western blot showing expression of CACYBP in undifferentiated (RA –) and differentiated (RA +) cells in the cytoplasm (left) and nucleus (right). SAM68 was used as a loading control for nuclear fractions and γ-Tubulin was used a protein loading control for the cytoplasmic fractions.

3.3 Discussion

The neuroblastoma cell line BE(2)-M17 can be differentiated using RA to produce a more neuronal phenotype as characterised by Andres and colleagues (Andres et al. 2013). The differentiation of a neuronal precursor cell requires many genotypic and phenotypic changes. Here, changes in the transcriptome during the RA mediated differentiation of BE(2)-M17 cells were investigated genome wide using 3'end RNA-seq.

3.3.1 Genome wide Transcriptome Changes During Differentiation

Altered transcription is known to mediate neuronal differentiation, and previous studies have shown 'global' 3'UTR lengthening in the differentiation of stem cells to neuronal cells (Shepard et al. 2011), although the extent of the global effect has not clearly been defined. Previous studies investigating APA in differentiation have always assessed changes in the total transcriptome rather than the cytoplasmic and nuclear transcriptomes. This does not give an insight into whether the APA change is occurring due to differential poly(A) site choice during transcription or altered regulation in the cytoplasm. Furthermore, it is more informative to look at polyadenylation changes in the cytoplasm instead of in total RNA, as cytoplasmic changes can affect the stability, localisation and translation of the transcript and have a downstream effect of gene expression. However, the extent to which APA influences the proteome has been contentious (Sandberg et al. 2008; A. R. Gruber et al. 2014).

During the differentiation of BE(2)-M17 cells, a trend to 3'UTR lengthening was observed compared to undifferentiated cells in both subcellular fractions. However, the proportion of 3'UTR lengthening events to shortening events was more significant in the cytoplasm compared to the nucleus, suggesting a large influence of post-transcriptional regulation on APA during differentiation. Many of the 3'UTR lengthening events observed in the cytoplasm were not present in the nucleus, which suggests increased stabilization of the longer transcript isoforms in the cytoplasm. The usage of more distal poly(A) sites during differentiation and development is conserved in different organisms (Hoque et al. 2013; Shepard et al. 2011; Ulitsky et al. 2012; Zhe Ji et al. 2009; Wenyan Hu et al. 2017), but this is the first time this trend has been observed in the cytoplasmic APA profile during differentiation.

Only 12 of the 3'UTR lengthened genes in the nucleus also showed lengthening in the cytoplasm. The remaining lengthened transcript isoforms may be retained in the nucleus, and therefore have no impact on final protein production, or may be subjected to rapid degradation in the cytoplasm. Co-transcriptional changes influencing poly(A) site choice have previously been associated with alterations in the cleavage and polyadenylation machinery (Zhe Ji et al. 2009). Altered expression of trans-factors such as hnRNP H may suppress usage of the proximal poly(A) site during differentiation (Shepard et al. 2011) leading to increased usage of the canonical distal poly(A) site. While this may have also contributed to poly(A) site choice in differentiated BE(2)-M17 cells, few of these co-transcriptional changes were carried into the cytoplasm.

The separation of APA events between the nucleus and the cytoplasm is crucial in determining the reasons behind changes in the APA landscape. Subcellular fractionation in the context of APA has recently shown to reveal important changes occurring in the cytoplasmic APA landscape in different tissues (Neve et al. 2016). Transcript localisation is particularly important in neurons, where the neurites and the cell soma have different requirements, thus need differential protein expression. Individual gene examples of APA mediating transcript localisation have been identified (An et al. 2008). More recently a genome wide study into APA in the cell soma compared to neurites highlighted the importance of alternative cis-elements in the UTR enabling differential regulation in different regions of the neuron (Taliaferro et al. 2016). Transcripts in the cell soma used proximal poly(A) sites while those in the neurites used distal poly(A) sites found in an alternative terminal exon, where the UTRs were enriched in binding sites for Muscleblind-like (Mbnl) proteins, enabling mRNA localisation (Taliaferro et al. 2016). Motif enrichment analysis of the lengthened alternative UTRs was conducted in BE(2)-M17 cells using DREME (Chapter 2.20), identifying enrichment of three motifs in this cohort of genes (Supplementary Figure 1). However, no physiologically relevant RBPs were found to bind to these motifs, suggesting no global regulation by known RBPs in stabilizing longer UTR isoforms during differentiation of BE(2)-M17 cells.

The 3'UTR also harbours miRNA binding sites which can regulate transcript stability. During differentiation, increased expression of an miRNA may target a cohort of genes for degradation, and conversely decreased miRNA expression can stabilise its target mRNAs. For

example, increased expression of miR-124 is crucial for the differentiation process of neurons to degrade transcripts associated with cell proliferation (Makeyev et al. 2007). miRNA enrichment analysis was performed to identify which miRNAs may globally mediate the UTR landscape. These identified miRNAs were compared to miRNA expression changes during RA mediated differentiation of the SK-N-SH neuroblastoma cell line. The let-7 family of miRNAs were enriched in the lengthened alternative UTRs and showed reduced expression changes in differentiation of SK-N-SH cells. This may be a potential regulatory mechanism that enables stabilisation of longer UTR isoforms during differentiation. This is contradictory to previous reports where increased expression of let-7 miRNAs was observed during embryonic development and reduced let-7 expression increased cell proliferation (Roush and Slack 2008). Therefore, APA profile changes mediated by the let-7 family during the differentiation of BE(2)-M17 cells should be investigated further by assessing expression of these miRNAs in undifferentiated and differentiated BE(2)-M17 cells through small RNA-seq.

This chapter investigated alterations in APA profiles during differentiation. For the first time, the known trend to 3'UTR lengthening during differentiation was identified to be more significant in the cytoplasm than in the nucleus, suggesting post-transcriptional mechanisms can affect APA more than poly(A) site choice at the point of cleavage during transcription.

3.3.2 3'UTR-APA in *PRDX6* correlated with Altered Protein Localisation

Widespread 3'UTR lengthening has been observed in different cell types during cell differentiation and development (Shepard et al. 2011; Zhe Ji et al. 2009), however the physiological implication of these lengthening events has rarely been assessed on a gene by gene basis.

In BE(2)-M17 cells, increased usage of the distal poly(A) site in the *PRDX6* gene was observed in the cytoplasm but not the nucleus, strongly suggesting that a post-transcriptional regulatory mechanism mediates this switch. This may be through increased nuclear export of the longer isoform, or through increased stabilisation in the cytoplasm. 3'UTR lengthening events have been suggested to decrease protein output, but no impact on protein expression was observed in differentiated BE(2)-M17 cells.

Cytoplasmic APA profiles can also be mediated by miRNAs. miRNA binding sites for miR-632 and miR-124 were identified in the *PRDX6* alternative UTR (Figure 3.9A, yellow boxes). The 3'UTR lengthening is unlikely to be explained by miR-124 regulation, as this miRNA is downregulated in proliferative states (Y. Wang et al. 2016) and upregulated in differentiation (Makeyev et al. 2007), therefore would target the longer isoform for degradation. The miR-124 binding site here may be masked by the binding of an RBP. Alternatively, miR-124 mediated regulation may fine-tune the expression of this gene during differentiation.

Few studies have investigated the role of miR-632, however its expression has been increased in breast cancer to promote cell proliferation and invasion (Mitra et al. 2012). Reduced expression of miR-632 during differentiation may stabilise the longer isoform contributing to the 3'UTR lengthening event in *PRDX6*. However, small RNA-seq data from SK-N-SH cells did not show high expression of this miRNA in undifferentiated or differentiated cells. This suggests it may not affect APA profile changes in neuroblastoma cells, however its expression needs to be verified in BE(2)-M17 cells.

PRDX6 encodes a peroxiredoxin, which has a role in scavenging ROS. Its upregulation has been linked to tumorigenesis (Yun et al. 2015) and neurodegeneration (Power et al. 2008) but its function has not been associated with neuronal differentiation. Previous studies have suggested altered localisation of PRDX6 during development of the mouse spinal cord, with increased expression in neurite outgrowth regions during development (Pirson and Knoops

2015). Though increased expression in the neurite outgrowth region was not observed in BE(2)-M17 cells, the 3'UTR lengthening event of the *PRDX6* transcript correlated with a change in PRDX6 protein localisation, as observed through immunofluorescence (Figure 3.9E).

mRNAs are exported from the nucleus in an mRNA-protein (mRNP) complex. Once entering the cytoplasm, the mRNP complex interacts with other RBPs and noncoding RNAs to mediate the transport and/or stability of the transcript. RBPs that bind to the mRNA can facilitate the interaction with the motor proteins enabling the translocation of the mRNA in the cell (Reviewed in (Eliscovich and Singer 2017)). The alternative UTR of *PRDX6* contains binding sites for the RBP IGF2BP3 which may increase the stability of the longer isoform, while playing a role in its translocation to enable localised translation during BE(2)-M17 differentiation.

mRNA transport is important for spatial and temporal regulation of gene expression, particularly in polarised neuronal cells, where different regions of the cell have distinctly different requirements. Transporting mRNAs is far more efficient than transporting proteins to enable localised gene expression as a single RBP can bind multiple mRNAs which can be transported simultaneously. Furthermore, transcripts which encode proteins of similar function can be transported and therefore localised together. While transcripts were initially thought to be translationally silent during transport, recent evidence suggests that protein synthesis can occur during mRNA localisation (B. Wu et al. 2016). To verify that the longer *PRDX6* transcript is differentially localised, the transport of the mRNA could be assessed using techniques such as single molecule Fluorescence in situ Hybridisation.

To conclude, a cytoplasmic 3'UTR lengthening event in the *PRDX6* gene during the differentiation of BE(2)-M17 cells may enable the longer transcript to be differentially translocated, resulting in localised PRDX6 protein expression.

3.3.3 3'UTR-APA in *CACYBP* correlated with Reduced Protein Output

While there have been numerous genome wide studies investigating the role of 3'UTR lengthening during differentiation, few have identified the physiological effect of these lengthening events on a gene by gene basis. Examples such as *BDNF* (An et al. 2008) have shown an importance in 3'UTR lengthening, however the physiological impact of genes showing 3'UTR shortening on the differentiation process have never been investigated.

A 3'UTR shortening event was observed in the cytoplasm but not the nucleus in the *CACYBP* gene, suggesting a post-transcriptional APA profile change. Despite no expression change at the RNA level, a reduction in protein expression was observed, which correlates with the 3'UTR shortening event. CACYBP has an established role in promoting G1/S transition of the cell cycle in cancer (H. Shi et al. 2014; Niu et al. 2016; X. Chen et al. 2011; Zhai et al. 2017), therefore its reduced expression may contribute to the cell cycle arrest during differentiation of BE(2)-M17 cells.

A role for CACYBP has previously been proposed during the differentiation of neuronal cells (Ding and Cantor 2004; Schneider et al. 2007; Schneider et al. 2010), but this is the first study that links altered CACYBP expression with an APA event. This is an example of how APA may be linked to altered protein expression to enable the differentiation process. Increased usage of the proximal poly(A) site has been associated with increased protein output (Sandberg et al. 2008), however the *CACYBP* gene showed reduced protein expression alongside 3'UTR shortening. The shorter mRNA may be kept translationally silent, resulting in reduced protein expression in differentiated BE(2)-M17 cells. However, RBPs that might mediate this regulation have not yet been identified and post-translational regulation of CACYBP during differentiation of BE(2)-M17 cells cannot be excluded.

The change in APA profile may be mediated by MOV10, which has a binding site in the alternative UTR as identified by PAR-CLIP, and promotes miRNA mediated mRNA decay by the RISC complex (Kenny et al. 2014). This could enable the miRNAs that target the constitutive UTR to specifically cause degradation of the longer *CACYBP* isoform during differentiation.

There is contention regarding the localisation of CACYBP during the differentiation of neuroblastoma cells as some studies show it is translocated to the nucleus (Ding and Cantor

2004; J. Wu et al. 2003), whereas others suggest that it is localised to neurite outgrowth regions (Schneider et al. 2007; Schneider et al. 2010). However, in BE(2)-M17 cells, CACYBP was not expressed in the nucleus, and its expression was reduced in the cytoplasm during differentiation. Post-translational phosphorylation of CACYBP was observed to inhibit its phosphatase activity, which enabled ERK1/2 kinase mediated activation of CREB, a transcription factor associated with cell differentiation (Rosinska, Lesniak, and Filipek 2016). In BE(2)-M17 cells, the inhibition of CACYBP activity may instead be at the translational level rather than through post-translational modifications.

In conclusion, CACYBP undergoes specific APA during differentiation possibly involving the action of MOV10. The shift was confirmed by PCR and importantly the shift to a shorter UTR correlates with a reduced protein output, which could contribute to the overall suppression of cell cycle progression.

3.3.4 Conclusions and Future Outlook

This chapter identified a trend to 3'UTR lengthening during the differentiation of BE(2)-M17 cells induced by RA. For the first time, the APA profile changes in the nucleus and the cytoplasm were assessed separately to identify that 3'UTR lengthening during differentiation was more significant in the cytoplasm. This work consequently highlights the importance of post-transcriptional mechanisms over poly(A) site choice at the point of cleavage to regulate the UTR landscape during differentiation. In addition, the impact of APA on gene expression was assessed on an individual gene basis in *PRDX6* and *CACYBP* where the APA event may contribute to the differentiation process.

Future studies investigating APA during differentiation and development should explore the contribution of transcriptional and post-transcriptional APA regulation that mediate the trend to 3'UTR lengthening, and assess the impact of APA events on the genes, including those that show 3'UTR shortening. Furthermore, the changing expression of miRNAs and RBPs during the differentiation process should be investigated to get a deeper insight into the mechanisms behind the cytoplasmic regulation of the UTR landscape.

Chapter 4: APA in neurodegeneration

4.1 Introduction

Neurodegeneration is defined as the progressive loss of neurons in the central nervous system (CNS) and the brain. Neurodegenerative diseases are complex and arise from a combination of environmental and genetic factors. While neurodegenerative diseases can be inherited, these familial cases account for fewer than 10% for the three most common diseases: Alzheimer's Disease (AD), Parkinson's Disease (PD) and Amyotrophic Lateral Sclerosis (ALS). Interestingly, the sporadic (non-inherited) and familial cases often exhibit the same symptoms, despite the cause of disease in sporadic patients being largely unknown. Decades of research have been invested in understanding neurodegenerative diseases, however no cure has been found.

Despite the AD, PD and ALS exhibiting very different symptoms and affecting different parts of the CNS, at the cellular level, many similarities have been identified that contribute to neuronal loss. This includes compromised mitochondrial function and protein aggregation to form plaques or inclusion bodies that impair neuronal function. Furthermore, genes associated with the same biological pathways show differential expression and regulation. Details of each of the main sporadic neurodegenerative diseases, AD, PD and ALS, are discussed below.

4.1.1 Alzheimer's Disease

Alzheimer's Disease (AD) is the most common neurodegenerative disease, where age is the greatest risk factor. AD is characterised by memory loss and cognitive defects in both familial AD (fAD) and sporadic AD (sAD) cases. At a molecular level, affected neurons in the brain show increased levels of protein aggregates that form plaques. These plaques, which can be intracellular or extracellular, are composed of an insoluble form of amyloid ß protein (Aß) or neurofibrillary tangles produced from hyperphosphorylated tau, a protein involved in microtubule formation and dynamics. The production of the Aß peptide is regulated by the cleavage of the amyloid precursor protein (APP) by beta-secretase cleavage enzyme 1 (BACE1) and a gamma-secretase complex (O'Brien and Wong 2011).

fAD is categorised into Early Onset AD (EOAD) and Late Onset AD (LOAD). EOAD arises in middle age, and can be linked to mutations in *APP*, *PSEN1* or *PSEN2.* The only gene associated with LOAD, which typically occurs in patients over the age of 65, is *APOE*, a lipoprotein associated with neuronal maintenance and repair. Mutations in this gene are linked to structural changes of the protein which can lead to neuronal death. Numerous genes associated with fAD have been identified, some of which have also been associated as risk factors to drive sAD. The main genes associated with AD are outlined in Table 4.1.

Table 4.1. Genes associated with AD

(Reviewed in (O'Brien and Wong 2011; C. C. Zhang et al. 2016; Jungsu Kim, Basak, and Holtzman 2009))

Key Genes	Protein	Mutations	Function and role in disease
APOE	ApoE	R112Q Risk variants	The *APOE E4* allele increases risk of AD and is associated with increased binding to Aβ. Associated with regulating Aβ aggregation and clearance. Lipoprotein with roles in brain physiology. Cholesterol carrier involved in neuronal maintenance and repair. Role in receptor mediated endocytosis of lipoprotein particles. R112Q mutation leads to structural changes.
APP	Amyloid β A4	At least 32 mutations linked to EOAD	Single pass transmembrane protein with large N-terminal extracellular domain. Processed by BACE1 protease and γ-secretase to produce smaller proteins and peptides, including the amyloid β ($A\beta_{1\text{-}40}$) peptide. $A\beta_{1\text{-}40}$ is soluble and important in synaptic physiology. Mutations linked to AD are found around the γ-secretase or BACE1 cleavage site. Improper processing of APP produces the toxic $A\beta_{1\text{-}42}$ which is insoluble and aggregates forming senile plaques in combination with neurofibrillary tangles, and is associated with oxidative damage.
MAPT	Tau	At least 55 mutations linked to neuro-degeneration	Soluble monomeric protein which promotes assembly and stabilization of microtubules. Mainly expressed in neurons, specifically axonal regions. Mutations can disrupt structure of tau and lead to hyper-phosphorylation, which increases insolubility and therefore aggregation, resulting in formation of neurofibrillary tangles. Mutations in C-terminus disrupt tau binding to microtubules so impair its ability to stabilize and assemble microtubules. N-terminal mutations disrupt tau binding to dynein causing disordered axonal transport, including transport of mitochondria. Abnormal tau also linked to Aβ induced toxicity.
PSEN1	Presenilin 1	Over 180 identified mutations Linked to EOAD	Component of the catalytic core of γ-secretase involved in cleavage of the Aβ precursor. Mutations alter amino acid composition. Associated with increased production of toxic $A\beta_{1\text{-}42}$ peptide.
PSEN2	Presenilin 2	14 identified mutations linked to EOAD	Component of the catalytic core of γ-secretase involved in cleavage of Aβ precursor Mutations alter amino acid composition. Associated with increased production of toxic $A\beta_{1\text{-}42}$ peptide.

4.1.2 Parkinson's Disease

Parkinson's Disease (PD) is the second most common neurodegenerative disease, characterised by bradykinesia (slowdown of movement), tremors and stiffness of movement, due to a loss of dopaminergic neurons in the substantia nigra region of the brain. These neurons use dopamine as their neurotransmitter, which has reduced levels in PD. Further, genes involved in dopamine metabolism show altered expression in PD (Poewe et al. 2017). PD is also characterised by the accumulation of cytoplasmic protein aggregates, mostly composed of insoluble α-synuclein forming structures called Lewy bodies (Spillantini et al. 1997). Over 90% of PD cases are sporadic, but much of the research has been focussed on familial cases of the disease. Sporadic PD (sPD) patients exhibit the same symptoms, and in some cases, mutations have been seen in the same causative genes as in familial PD (fPD). These genes have been studied extensively (Reviewed in (Bogaerts, Theuns, and Van Broeckhoven 2008; Poewe et al. 2017)) and are summarized in Table 4.2.

Table 4.2 Genes associated with PD.

Gene	Function	Role in PD
ATP13A2	Encodes ATPase that is present in lysosomes and autophagosomes.	Mutations associated with hereditary parkinsonism. (Poewe et al. 2017).
DJ-1	Redox sensor mediated by cysteine residues that are important in cytoprotection. Anti-oxidant properties and ROS scavenger. Translocates to the mitochondrial matrix during oxidative stress. Influences ERK1/2 signalling pathway (G. Wang, Pan, and Chen 2012).	Reduced expression leads to increased oxidative stress and cell death. Mutations linked to mitochondrial fission cause autosomal recessive PD (Bonifati et al. 2003). Overexpression linked to neuroprotection by increasing elongated mitochondria (G. Wang, Pan, and Chen 2012). Mice lacking DJ-1 gene had increased dopaminergic neuronal loss (Subramaniam and Chesselet 2013).
GBA	Encodes glucocerebrosidase, which has a role in the lysosomal pathway.	Mutations, including N370S, are thought to prevent degradation of α-synuclein via the lysosomal pathway, increasing α-synuclein expression and aggregation (Woodard et al. 2014; Bendor, Logan, and Edwards 2013; Poewe et al. 2017).
HTRA2	Mitochondrial protease involved in mitochondrial quality control mechanism.	Mutations identified in sPD patients. Deletion of *HTRA2* correlated to increased ROS production and misfolded proteins in the mitochondria (Desideri and Martins 2012). Induces apoptosis if released into the cytoplasm
LRRK2	LRRK2 protein is a GTPase and Serine/threonine kinase containing MAPKKK.	Mutations cause increased autophagy and cell death, and are most common in fPD. Localization to mitochondria increases mitochondrial dysfunction.
PARK2	Encodes Parkin, an ubiquitin E3 ligase associated with outer mitochondrial membrane. Parkin is involved in proteasome mediated degradation of proteins. Role in mitochondrial biogenesis. Protects against apoptosis, decreases cellular ROS (Subramaniam and Chesselet 2013).	Mutations cause mitochondrial structural alterations. Knockout models show dopaminergic neurodegeneration. Loss of PARK2 causes accumulation of toxic protein aggregates (Subramaniam and Chesselet 2013).
PINK1	Mitochondrial serine/threonine kinase, localised to inner mitochondrial membrane, inter-membrane space, and the outer mitochondrial membrane. Cytoprotective role. (Subramaniam and Chesselet 2013). Regulates mitophagy and release of Ca^{2+} from mitochondria (Perier and Vila 2012).	Mutations linked to increased apoptosis; Mutants in drosophila have reduced ATP levels and mtDNA content so are more sensitive to mitochondrial stress. Silencing PINK1 expression led to elongated mitochondria. Over expression restores normal mitochondrial morphology and inhibits ROS production (Subramaniam and Chesselet 2013).
POLG1	Mitochondrial polymerase gamma 1 Controls mtDNA synthesis, replication and repair.	Mutations associated with mitochondrial pathology and DNA deletions.

SNCA	Encodes α-synuclein. Localised to axon terminal. Interacts with membranes of synaptic vesicles via N-terminal domain which may aid its localisation to the nerve terminal. Regulates synaptic vesicles and neurotransmitter release (including dopamine) (Bendor, Logan, and Edwards 2013) Interacts with numerous proteins including tubulin, ERK2/MAPK (Gomez-Santos et al. 2002; Banerjee et al. 2009). Found associated in vesicles but also free in the cytosol.	Increased expression specifically in the substantia nigra but not in other brain regions in PD (Chiba-Falek, Lopez, and Nussbaum 2006). Overexpression of WT α-synuclein inhibited dopamine release and increased dopamine mediated toxicity (Bisaglia et al. 2010; Lundblad et al. 2012), increased its localisation to mitochondria where it increased mitochondrial fragmentation (M. Zhu, Li, and Lu 2012; Nakamura et al. 2011), and caused cytochrome c release to induce apoptosis (Parihar et al. 2008). Unstructured protein has an α-helical conformation on membrane binding, but mis-folding in neuro-degeneration causes aggregation in a β-sheet which aggregates to 5-10 nm filaments forming Lewy bodies. Has prion like properties. (Spillantini et al. 1997). Missense mutations A53T, A30P, E46K associated with PD (Polymeropoulos et al. 1997). A30P mutation disrupts presynaptic location of α-synuclein in neurons and disrupts association with membranes *in vitro* and *in vivo* (Banerjee et al. 2009; Subramaniam and Chesselet 2013).
TFAM	Mitochondrial transcription factor A Regulates mtDNA transcription (Banerjee et al. 2009).	Mutations which abrogate function associated with PD.
VPS35	Vacuolar protein sorting associated protein. Retromer for endosomal trafficking	Mutations associated with autosomal dominant familial PD leading to accumulation of α-synuclein and impairment of mitochondrial fusion and fission (F. L. Tang et al. 2015)

4.1.3 Amyloid Lateral Sclerosis

Amyotrophic Lateral Sclerosis (ALS), also known as Motor Neuron Disease, is a debilitating disease which affects upper and lower motor neurons in the motor cortex of the brain, brain stem and spinal cord. The motor neurons span from the brain, to the spinal cord and to muscles throughout the body. Death of these neurons, which control voluntary muscles, leads to muscle stiffness, weakness and eventually loss of voluntary movement. Like AD and PD over 90% of cases are sporadic, while approximately 10% are related to inherited genetic mutations. However, both familial (fALS) and sporadic (sALS) cases exhibit similar neuropathologies with loss of motor neuron function resulting in loss of movement. Furthermore, both fALS and sALS patient samples have shown similar dysregulation of miRNA and gene expression (Butovsky et al. 2015).

ALS has been closely linked to defects in RNA metabolism. Mutations in *FUS* and *TARDBP*, two genes that encode RBPs associated with RNA processing, are linked to fALS. FUS, which has a role in alternative splicing (Masuda, Takeda, and Ohno 2016), can also interact with the Pol II CTD to regulate phosphorylation of Ser2 (Schwartz et al. 2012) and can control mRNA turnover (Kapeli et al. 2016). Furthermore, FUS knockdown altered mRNA expression of genes associated with mitochondrial function and increased proximal poly(A) site usage (Schwartz et al. 2012). FUS therefore functions in many aspects of mRNA regulation. TDP-43, which is encoded by the *TARDBP* gene, was shown to autoregulate the splicing and poly(A) site selection of its own transcript (Koyama et al. 2016), although its role in global poly(A) site choice has not been investigated. Thus, the regulation of RNA metabolism by these RBPs is crucial in ALS.

The mutations in FUS that are associated with ALS are found in the nuclear localisation sequence (NLS) of the protein, causing its mis-localisation to the cytoplasm and subsequent aggregation (Blokhuis et al. 2013). Protein aggregates form inclusion bodies, which can consist of a variety of proteins including TDP-43, FUS and SOD1. The protein aggregates found in the motor neurons of ALS patients are a consequence of dysfunctional protein degradation pathways. While gene mutations have been linked to increased protein aggregation in fALS, inclusion bodies have also been observed in sALS. Key genes associated with ALS pathology are summarised in Table 4.3.

Table 4.3. Genes associated with ALS.
(Reviewed in (Parakh and Atkin 2016; Blokhuis et al. 2013; S. Chen et al. 2013)

Gene	Protein	Function and Role in Disease
ATXN2	Ataxin-2	Ataxin-2 has a role in polyadenylation, stress granule formation and polyribosome assembly. Increased accumulation seen in cytoplasm of spinal cord tissue of sALS patients. PolyQ repeat region increased from 21-22 to between 27-32 are associated with ALS. This increase in polyQ repeats does not alter protein localisation but may induce stress induced activation of caspase 3.
C9ORF72	C9ORF72	Unknown protein function – homology to DENN, a Guanine Exchange Factor that activates Rab GTPases. Potential role in endosomal trafficking and autophagy. Over 30% of fALS cases are linked to intronic hexanucleotide (GGGGCC) repeat expansion (from 25 to several hundred). The repeat expansion mRNA may sequester RBPs which can then no longer fulfil their role.
FUS	FUS	Nuclear RBP that mediates DNA repair, transcription, splicing, mRNA export. Interacts with intronic region of pre-mRNAs (Masuda, Takeda, and Ohno 2016). Over 40 mutations, mostly in the NLS, identified in up to 5% of fALS cases, causing cytoplasmic protein localisation. Accumulation in the cytoplasm causes toxicity. N-terminal RRM and RGG domains mediate cytosolic aggregation.
HNRNPA2B1	hnRNP A2/B1	Interacts with UAGG motif in 3'UTRs to mediate alternative splicing and APA. Mutation associated with fALS. Depletion in mouse spinal cord promoted usage of distal poly(A) site in target genes suggesting it promotes usage of proximal poly(A) sites (Martinez et al. 2016)
OPTN	Optineurin	Inhibitor of NFkB signalling pathway. Acts as autophagy receptor and involved in vesicle trafficking of the Golgi. Rare mutations associated with fALS where truncated protein has lost its function. Found in inclusions in the cytoplasm in sALS cases, and also in inclusion bodies in AD and PD.
PFN1	Profilin 1	Small actin-binding protein associated with actin polymerisation. Overexpression correlated to increased insoluble protein aggregates that interact with TDP-43. Mutations linked to reduced actin polymerisation and therefore inhibition of axonal outgrowth.
SOD1	Superoxide Dismutase 1	Ubiquitous cytoplasmic enzyme that scavenges of superoxide radicals. Over 160 identified mutations account for 20% of fALS cases. Mutations destabilise SOD1 and can increase its aggregation. Loss of a disulphide bond between two critical cysteine residues increase its propensity to aggregate. Loss of function leads to increased Reactive Oxygen Species (ROS) abundance, increasing oxidative stress.
SQSTM1	p62	Role in protein degradation in binding ubiquitinated proteins and the autophagosomal marker LC3. Associated with NFkB pathway. Mutations associated with dysregulated autophagy.

TARDBP	TDP-43	Nuclear RBP with roles in splicing, polyadenylation and transcription termination. Interacts with intronic region and 3'UTR of pre-mRNAs and noncoding RNAs (Sreedharan et al. 2008). WT protein aggregates in spinal cord motor neurons, hippocampal neurons, frontal cortex neurons, glial cells in sporadic ALS patients Over 40 mutations associated with fALS, accounting for up to 5% of fALS cases. Mutations identified in the C-terminal glycine rich domain affect the splicing activity of TDP-43. TDP-43 is cleaved to produce C-terminal fragments that are prone to aggregation, forming protein inclusions. The full length TDP-43 protein can also aggregate, particularly when hyper-phosphorylated. Abnormal disulphide bonds associated with aggregation. TDP-43 overexpression shows dose dependent toxicity without protein aggregation.
UBQLN2	Ubiquilin-2	Protein in the ubiquitin proteasome pathway. Delivers ubiquitinylated proteins to the proteasome. Mutations linked to dysfunctional ubiquitin proteasome pathway are linked to ALS. WT and mutant protein aggregates in sALS cases.
VCP	Valosin-containing protein	Ubiquitously expressed hexameric ATPase important in the ubiquitin proteasome pathway and in ER associated degradation (ERAD) pathways. Facilitates delivery of ubiquitinylated proteins from the ER to the proteasome. Also has a role in autophagy in fusing lysosomes to autophagosomes. Mutations and loss of protein inhibit protein degradation pathways, increasing aggregation of misfolded proteins.

4.1.4 Commonalities between neurodegenerative diseases

Although AD, PD and ALS have distinctly different symptoms as described above, the three diseases share pathways that contribute to pathology including mitochondrial dysfunction and protein aggregation. Protein aggregates, often consisting of misfolded proteins, are usually degraded via the ubiquitin proteasome pathway or through the autophagy pathway. Deregulation of these pathways is associated with neurodegeneration. However, it is unclear if deregulation of protein degradation pathways is a cause or consequence of neurodegeneration (Dennissen, Kholod, and van Leeuwen 2012).

As well as common pathways, specific disease-associated genes have been linked with different neurodegenerative diseases. For example, the tau protein, which is key to AD pathogenesis, has an implicated role in PD (C. C. Zhang et al. 2016) and the *MAPT* transcript is upregulated in some sALS patients (Batra et al. 2016). In addition, plaques found in AD have been shown to contain aggregation of α-synuclein fragments and formation of Lewy bodies have been identified in AD (Bendor, Logan, and Edwards 2013). Although mutations in *TARDBP* are uniquely linked to ALS, the formation of protein aggregates of the TDP-43 protein in the cytoplasm, have also been identified in some AD patients (Blokhuis et al. 2013).

4.1.5 Pathways associated with Neurodegenerative Diseases

4.1.5a Ubiquitin Proteasome Pathway

Damaged or misfolded proteins need to be degraded to prevent cellular damage. The ubiquitin-proteasome pathway is a major protein degradation pathway which regulates protein quality control and protein turnover. Proteins are marked for degradation by addition of a small protein called ubiquitin which forms a covalent bond with a lysine residue. Ubiquitin chains are built up on target proteins, and this process is conducted by three enzymes: a ubiquitin activating enzyme, E1; a ubiquitin conjugating enzyme E2; and a ubiquitin ligase E3. This ubiquitin chain is recognised by the 26S proteasome, which is a large protein complex that degrades the target protein (Goldberg 2000). This pathway is outlined in Figure 4.1.

Dysregulation of all stages of this pathway have been identified in neurodegeneration (McKinnon and Tabrizi 2014). Failure to remove ubiquitinated proteins suggests defects in the proteasome, however, mutations in ubiquitination enzymes are linked to AD, PD and ALS suggesting both stages of the pathway may be impaired. In addition, mutations in the gene that codes for the ubiquitin protein itself have been linked to neurodegeneration (McKinnon and Tabrizi 2014).

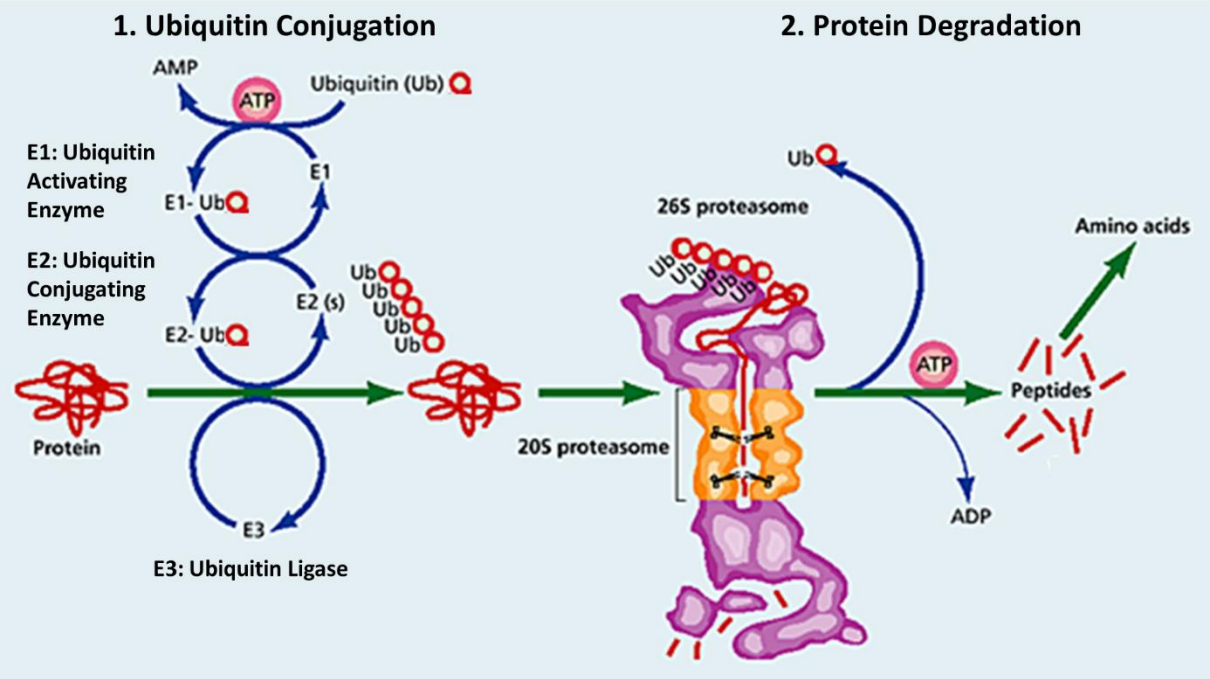


Figure 4.1. Outline of the Ubiquitin Proteasome Pathway.

This pathway has two parts. 1. Ubiquitin Conjugation and 2. Protein Degradation. First, Ubiquitin (Ub) is first activated by E1, which enables it to bind to the Ubiquitin Carrier E2. The binding of Ubiquitin to target proteins is mediated by the E3 ligase, which adds multiple Ubiquitin residues for recognition by the proteasome. The second step involves delivery of the substrate to the proteasome where the Ubiquitin chain interacts with the 26S proteasome. The Ubiquitin chain is dissembled and the core 20S proteasome degrades the protein target to peptides, which are subsequently further hydrolysed to amino acids. Image modified from (Goldberg 2000).

4.1.5b Autophagy

Autophagy is another important catabolic pathway which has a role in the degradation of misfolded proteins. While the ubiquitin proteasome pathway typically targets short-lived proteins, autophagy is associated with the turnover of organelles and removal of long-lived proteins. Double-membraned vesicles called autophagosomes form around a portion of the cytoplasm or around damaged organelles. Autophagosomes are transported along microtubules and subsequently fuse with lysosomes, forming an autolysosome, where the pH drops and the contents are degraded by hydrolytic enzymes (Figure 4.2). While constitutive autophagy is critical for normal neuronal function, increased autophagy, due to oxidative stress (Kalivendi et al. 2004), or deregulation of the autophagy pathway is associated with neurodegenerative diseases, (Cheung and Ip 2011; Metcalf et al. 2012).

As with the ubiquitin proteasome pathway, different stages in the autophagy pathway have been associated with neurodegeneration (Metcalf et al. 2012). AD and PD brains show accumulation of autophagosomes, whereas mutations in autophagy pathway proteins including VCP, CHMP2B and UBQLN2 have been associated with ALS (Blokhuis et al. 2013).

Autophagy may be neuroprotective with low levels of stress because it removes aggregated proteins (Pan et al. 2009) and damaged mitochondria. Indeed, in *in vivo* models of PD, induction of autophagy improved neuron survival (Dehay et al. 2010). However in prolonged oxidative stress conditions, autophagy could remove functional mitochondria causing cell death (Hung et al. 2014). Rapamycin, an antibiotic that induces autophagy, was shown to protect SH-SY5Y cells against rotenone induced apoptosis (Pan et al. 2009). However increased autophagic activation in PD models, has also resulted in neuronal cell loss (Cheung and Ip 2011).

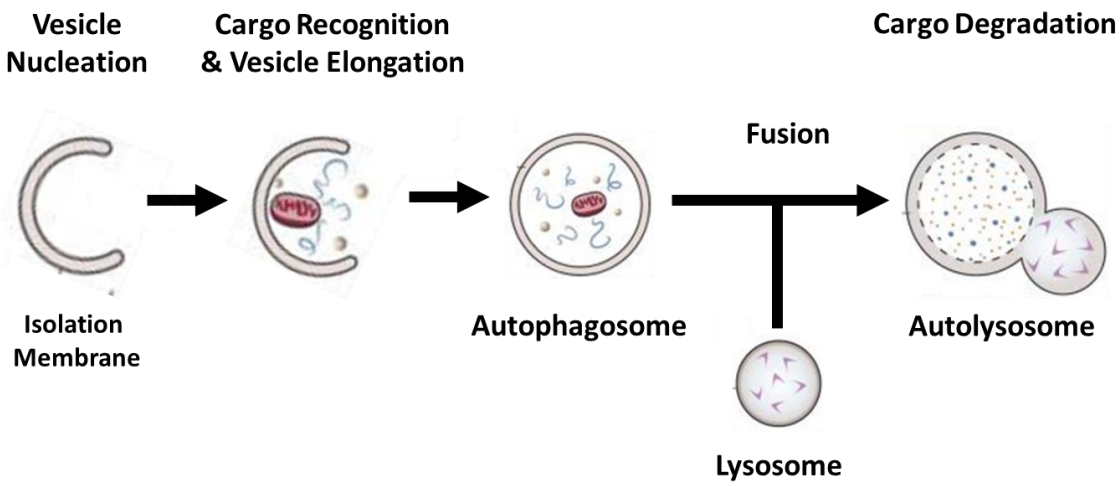


Figure 4.2 Outline of Autophagy.

A double membrane is first formed (nucleation). The vesicle elongates around target cargo forming an autophagosome. The autophagosome then fuses with a lysosome forming an autolysosome which contains the hydrolases required to degrade the cargo. Image modified from (Levine, Mizushima, and Virgin 2011).

4.1.5c Mitochondrial Function

Mitochondria are the powerhouses of cells, responsible for ATP production through oxidative phosphorylation (OXPHOS). Mitochondria also have crucial roles in apoptotic signalling and calcium homeostasis. Neurons have a high ATP requirement, therefore compromises in mitochondrial function which reduce total ATP output largely contributes to neuronal cell death.

A schematic of mitochondrial structure is shown in Figure 4.3A. OXPHOS involves a series of redox reactions involving five multimeric proteins located in the inner mitochondrial membrane. Protons are released into the intermembrane space during the transfer of electrons from donors NADH and $FADH_2$ by Coenzyme Q and Cytochrome C respectively through the Electron Transport Chain (ETC). This builds a proton gradient across the inner mitochondrial membrane that enables the synthesis of ATP from ADP by ATP synthase (Complex V). The final electron acceptor is oxygen, which is reduced to water. The process of OXPHOS is outlined in Figure 4.3B.

Approximately 1% of electrons that pass through the ETC escape from Complex I and Complex III (Desideri and Martins 2012). This release of electrons during OXPHOS prematurely reduces oxygen producing the superoxide anion ($O_2^{\bullet -}$), hydrogen peroxide (H_2O_2) and the hydroxyl radical ($OH^{\bullet}$). Together, these are known as reactive oxygen species (ROS) which are damaging as they cause oxidation of lipids and proteins. Loss of Complex I and Complex III activity, which impairs ATP production, also increases ROS production, and is associated with neurodegeneration (Desideri and Martins 2012; Perier and Vila 2012)

Abnormalities in mitochondrial DNA (mtDNA), which encodes 13 polypeptides of the ETC, accumulate with age and have been linked to neurodegeneration. mtDNA is more susceptible to insults from ROS due to proximity to the site of ROS production and unlike nuclear DNA, mtDNA is not protected by histones (Perier and Vila 2012).

Mitochondria are dynamic organelles that undergo balanced fusion and fission. During neurodegeneration, disruption of this balance has been observed, mostly through increased mitochondrial fragmentation, which impairs mitochondrial function (Itoh et al. 2013; Yana, Wang, and Zhu 2013). Defective mitochondria are removed in a specific autophagy pathway known as mitophagy. Mutations in PINK1 and Parkin in fPD are associated with disrupting

mitophagy (Perier and Vila 2012), through insufficient removal of dysfunctional mitochondria, or overstimulation of mitophagy where functional mitochondria are also removed.

Impaired transport of mitochondria to axons is linked to loss of synaptic activity, which also contributes to neuronal dysfunction. In AD, hyperphosphorylated tau disrupts microtubule dynamics to prevent efficient mitochondrial transport, while in ALS, mutant SOD1 can impair mitochondrial transport (Yana, Wang, and Zhu 2013; Filosto et al. 2011)

Many mutant genes linked to familial cases of neurodegeneration are associated with deregulating mitochondrial function. As described in this section, all aspects of mitochondrial function have been linked to neurodegeneration, making this organelle critical in understanding reasons behind neuronal loss.

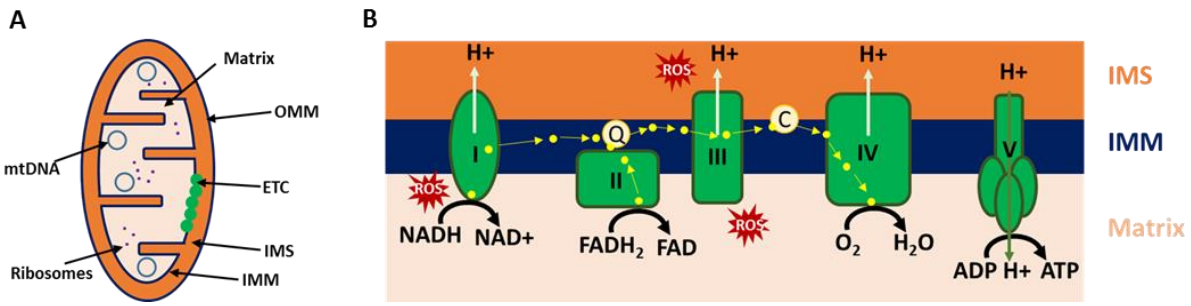


Figure 4.3. Mitochondria and the Electron Transport Chain (ETC).

A. A schematic of mitochondria. OMM: outer mitochondrial membrane; IMM: inner mitochondrial membrane; ETC: Electron Transport Chain; IMS: inter membrane space; mtDNA: mitochondrial DNA.

B. A schematic of the ETC. Electrons are donated by NADH and flow into Complex I (I). They are then carried by Coenzyme Q (Q) to Complex II (II) where coenzyme Q picks up more electrons donated by $FADH_2$. Electrons are delivered to Complex III (III) where Cytochome C (C) which is present in the IMS transports electrons to Complex IV (IV). Here oxygen accepts the electrons and is reduced to water. Protons (H+) are pumped into the IMS during the ETC which builds a proton gradient. H+ then flow back into the mitochondrial matrix via Complex V (V) which enables synthesis of ATP from ADP. Complexes of the ETC are shown in green, while the flow of electrons (yellow circles) is shown by yellow arrows. Red stars indicate where ROS are generated during the ETC.

4.1.6 APA in Neurodegeneration

APA has been linked to neurological diseases. For example, a triplet repeat expansion in the *PABPN1* gene produces a dysfunctional protein in Oculopharyngeal Muscular Dystrophy. PABPN1 promotes the usage of distal poly(A) sites, so loss of PABPN1 activity from the dysfunctional protein, caused increased proximal poly(A) site usage in 10% of APA regulated genes (Jenal et al. 2012).

Individual genes exhibiting APA in PD (Rhinn et al. 2012) and AD (Dickson et al. 2013) have been identified, but genome wide analysis has not previously been explored in these two diseases. Global analysis of APA has been assessed in ALS, where defects in RNA processing have been associated with the disease. Widespread 3'UTR shortening was observed in the frontal cortex in fALS but not sALS patients (Prudencio et al. 2015). However, the frontal cortex is not specifically compromised in ALS therefore APA changes in this region of the brain may not be linked directly to motor neuron loss.

4.1.7 Chapter Aims

Widespread changes in the transcriptome and proteome have been identified in neurodegeneration, however the role played by APA in the regulation of gene expression remains underexplored. Understanding the contribution of APA in the gene expression changes may give new insights into molecular changes and their contribution to the pathological state in neurodegenerative diseases. This chapter explores changes in APA during neurodegeneration using a bioinformatics approach on publicly available RNA-seq data from patients (Chapter 4A) and data obtained from a tissue culture based PD model system (Chapter 4B).

Chapter 4A:
APA in Neurodegeneration: an *in silico* model

4A.1 Introduction

The usage of alternative splicing and alternative promoter usage have been implicated in the brain to achieve the complexity required (Twine et al. 2011). APA has also been investigated, with UTRs globally appearing to be lengthened in the brain compared to other tissues (Miura et al. 2013). However, the possibility of changes in poly(A) site usage in neurodegeneration has not been extensively investigated at a global level.

ALS is associated with alterations in RNA metabolism as mutations in two RBPs, TDP-43 and FUS, which mediate pre-mRNA splicing, are strongly linked to the disease. Given the overlap in proteins associated in splicing and cleavage and polyadenylation during pre-mRNA processing (Licatalosi and Darnell 2010), the choice of poly(A) site usage may be impacted by defects in TDP-43 and FUS. Indeed, FUS can affect poly(A) site usage depending on the proximity of its binding site to the poly(A) site (Masuda et al. 2015).

Changes in the 3'UTR length in both sALS and a *C9orf27* mutant case of ALS have been assessed globally through RNA-seq (Prudencio et al. 2015). Differential poly(A) site usage was observed in ALS patients compared to healthy controls, and different regions of the brain showed different poly(A) site usage (Prudencio et al. 2015). Depletion of *HNRNPA2B1*, mutations in which are associated with ALS, promoted usage of distal poly(A) sites (Martinez et al. 2016).

Multiple poly(A) sites have also been identified in genes associated with AD and PD as outlined in the Table 4.4. *SNCA* showed 3'UTR lengthening in PD patients compared to healthy controls. This longer transcript was suggested to translate a protein that was more prone to aggregation and association with the mitochondria (Rhinn et al. 2012). In AD, APA has been shown in the *APP* gene (Mbella et al. 2000), however the changes in poly(A) site usage in the disease state have not been assessed.

The transcriptome of patients with neurodegenerative diseases has been investigated with RNA-seq to assess changes in gene expression (Dumitriu et al. 2016), splicing (Twine et

al. 2011), and changes in miRNAs (Lau et al. 2013; Butovsky et al. 2015) and lncRNAs (Magistri et al. 2015). In RNA-seq, reads are mostly in the exonic coding regions, with only a small percentage found in the 3'UTR, making it more difficult to investigate changes in 3'UTR-APA. Recently, a bioinformatic pipeline was developed to assess the usage of poly(A) sites from existing RNA-seq data (Xia et al. 2014). This method, Dynamic Analysis of Alternative Polyadenylation from RNA-seq (DaPars), enables de novo identification and analysis of dynamic poly(A) sites from existing RNA-Seq data retrospectively (Chapter 2.22).

In DaPars, the distal poly(A) site is considered to be the default poly(A) site in the transcript, and de novo poly(A) sites are identified using a linear regression model. The read intensities are modelled as a linear combination of proximal and distal poly(A) sites at single nucleotide resolution. Changes in poly(A) site usage are calculated as a change in the ratio of proximal to distal poly(A) site usage, which is quantified with a percentage of the distal poly(A) site usage index, PDUI. Positive or negative PDUIs determine whether a statistically significant APA event is identified as 3'UTR lengthening or shortening respectively between two samples (Xia et al. 2014).

Assessing APA changes in the affected regions of neurodegenerative disease patients through wet-lab experiments is difficult due to the scarcity of post-mortem patient RNA. However, using DaPars, APA can be investigated from RNA-seq data from existing studies. Here, RNA-seq datasets from AD, PD, and ALS were investigated for alterations in APA. While widespread changes in APA were not seen in any of the diseases, examples of genes which may contribute to the disease state were identified and different APA profiles were observed in different regions of the brain.

Table 4.4 Individual Genes Linked to APA Regulation in AD, PD and ALS

Disease	Gene	Protein	APA Change in Disease	Reference
AD	*APP*	Amyloid β A4	The longer 3'UTR has a higher translation efficiency than the shorter 3'UTR. Ratio change between long and short *APP* UTR-isoforms has not been identified in AD.	(Mbella et al. 2000)
	MAPT	Tau	Causes neurofibrillary tangles in AD pathogenesis. Shorter isoform more highly expressed in disease state.	(Goedert et al. 1988; Dickson et al. 2013)
	PTGS2	COX-2	Increase distal poly(A) site usage in AD.	(Hall-Pogar et al. 2005; Lukiw and Bazan 1997)
PD	*SNCA*	α-synuclein	Extended 3'UTR observed in PD which increased accumulation of the α-synuclein protein and directed it away from synaptic terminals to mitochondria.	(Rhinn et al. 2012)
ALS	*TARDBP*	TDP-43	TDP-43 autoregulates poly(A) site choice in its own mRNA. TDP-43 inhibits usage of the proximal poly(A) site producing a longer *TARDBP* transcript that is regulated by NMD in the cytoplasm. When TDP-43 levels are low, the proximal poly(A) site is used to increase TDP-43 production. In ALS, increased TDP-43 levels may be due to increased usage of the proximal poly(A) site in *TARDBP*.	(Koyama et al. 2016)

4A.2 APA in Alzheimer's Disease

Dysregulated RNA processing in AD has been identified in isolated cases, such as the extracellular aggregation of U1snRNP, a factor associated with regulation of splicing and polyadenylation, in AD brains (Bai et al. 2013). However, there have been no genome-wide studies investigating the role of APA in AD, although certain genes associated with AD such as *COX-2* (Lukiw and Bazan 1997) and *APP* (Mbella et al. 2000) utilise different 3'UTRs.

APA in the *MAPT* gene has been implied in the regulation of tau expression, a protein which is a key component of neurofibrillary tangles in AD pathogenesis. Papers almost 30 years ago gave evidence that the shorter *MAPT* 3'UTR isoform is more highly expressed in the frontal cortex of AD patients than controls (Goedert et al. 1988). The longer *MAPT* isoform has miR-34a target sites which inhibit tau protein expression (Dickson et al. 2013). APA may therefore regulate *MAPT* gene expression in AD pathogenesis, though it is not clear if miR-34 levels are altered in AD. Many miRNAs have been associated with AD, as outlined in Supplementary Table 2.

Here, to investigate APA at a global scale, two datasets were interrogated using DaPars to identify alterations in APA in RNA isolated from post-mortem brain tissue of AD patients compared to control individuals. Different cohorts of genes were identified to be regulated by APA in the two AD datasets, however APA regulated genes were associated in pathways linked to AD pathology. Therefore, APA may play an important role in influencing gene expression in AD.

4A.2.1 APA Regulation in Hippocampi of LOAD Patients

The first RNA-seq dataset for AD was taken from a study on transcriptomics of LOAD patients and control individuals (Magistri et al. 2015) (Table 4.5). RNA was isolated from the hippocampus, the region of the brain important for memory, which is one of the first damaged regions in AD, and sequenced at a high depth (read numbers in Supplementary Table 3).

The 4 patient samples were taken from individuals whose brain tissue was classified as fully developed AD (Braak stage V or VI). Braak stage denotes the degree of pathology in AD. In AD, stages I – VI are based on the extent of neurofibrillary tangle involvement. In stages I and II, neurofibrillary tangles are only in the trans-entorhinal region (between the hippocampus and neocortex) of the brain, whereas in stage III and IV, they are present in the hippocampus. In stages V and VI, there is extensive neocortical involvement (Braak and Braak 1995). The control samples had clinically silent AD symptoms which categorises them into Braak Stage I and II. Ideally, the controls should be Braak stage 0, with no AD phenotype.

Each of the 4 LOAD patients was compared to each of the control samples yielding 16 comparisons. Between 7223 and 8419 APA events were identified, where between 0.7-3.3% of genes showed statistically significant APA changes between the LOAD and control samples although there was no trend toward either 3'UTR shortening or lengthening. Figure 4.4A shows the mean percentage of significant APA events for each LOAD sample compared to each of the controls. As indicated by the size of the error bars which represent standard deviation, there was great variability between the number of significant APA changes identified between the LOAD sample and the different controls.

GO analysis showed that all genes exhibiting 3'UTR lengthening were enriched in mitochondrial pathways (Figure 4.4B), while an enrichment in genes associated with protein catabolic processes was identified in genes showing 3'UTR shortening. Both biological processes are closely linked to neurodegeneration. Therefore, changes in gene regulation through APA of these pathways may contribute or be consequential of AD pathology.

The large differences in the number of significant events between LOAD and control comparisons may be attributed to biological variation. Therefore, for each patient, genes that showed significant APA compared to at least 3 of the 4 controls were selected as the cohort of genes for further analysis. These genes are more likely to actually have altered 3'UTRs due to

the disease state. Interestingly, this suggested a trend towards 3'UTR lengthening, however this was only significant for LOAD3 and LOAD4 (Fisher's exact Test, $p<0.05$) (Figure 4.4C).

Only 10 genes showed 3'UTR lengthening and 10 genes showed 3'UTR shortening in 2 or more LOAD samples (Figure 4.4D). One example identified was the ubiquitin ligase *UBR1,* which showed 3'UTR shortening in AD in two patient vs control comparisons (Figure 4.4E). Protein turnover and degradation is compromised in AD and altered expression of proteins in the ubiquitin proteasome pathway could contribute to protein turnover dysregulation. The 3'UTR shortening event could be explained by the presence of target sites for miR-26 and miR-128 in the alternative UTR, which are miRNAs known to be upregulated in temporal cortex and hippocampus respectively in AD patients (Absalon et al. 2013; Lukiw 2007)

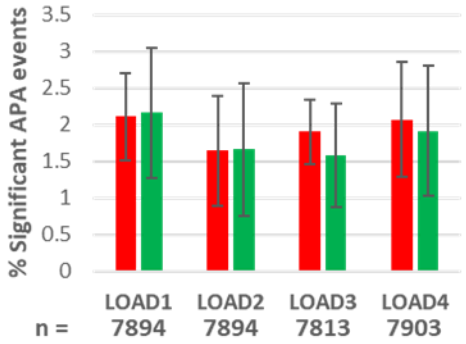
3'UTR lengthening was observed in *OGDHL*, which encodes a brain specific isoenzyme for oxoglutarate dehydrogenase in the mitochondrial Krebs cycle (Figure 4.4F). Downregulation of this protein has been observed in an AD mouse model (Ciavardelli et al. 2010) and its decreased expression can contribute to reduced ATP production.

These results show that there is great variability in APA between patients and control samples, however individual genes that may be connected to AD pathology, including *UBR1* and *OGDHL*, show significant and reoccurring APA events. The impact of these UTR length changes on downstream gene expression, including protein output, should be further investigated to understand the importance of APA regulation of these genes in AD.

Table 4.5. Background of RNA Samples from the LOAD RNA-seq dataset

	Age	**Gender**	**Braak stage**
LOAD 1	82	F	VI
LOAD 2	87	F	V
LOAD 3	83	M	VI
LOAD 4	82	F	VI
CTRL 1	77	F	I
CTRL 2	83	M	II
CTRL 3	>90	M	II
CTRL 4	85	F	II

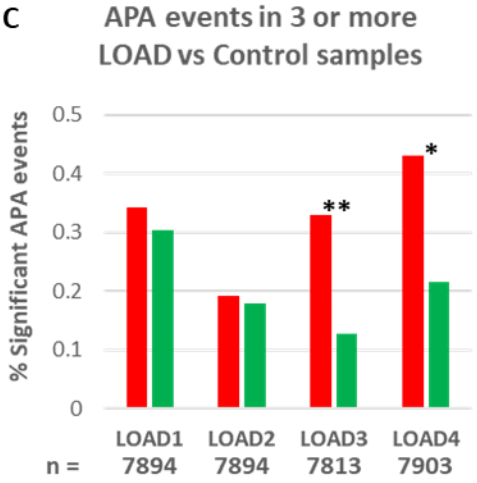
A



B

	Biological Process	# Genes Present	# Genes Expected	Fold Enrichment	P-value
UTR Lengthened	Protein targeting to mitochondrion	13	2.64	4.92	3.40E-02
	Mitochondrial Translational Termination	19	4.21	4.52	8.34E-04
	Mitochondrial Translational Elongation	18	4.16	4.33	3.28E-03
UTR Shortened	Regulation of protein stability	28	10.19	2.75	2.24E-02
	Regulation of protein catabolic processes	42	16.48	2.55	6.02E-04
	Regulation of Translation	36	15.37	2.34	3.34E-02

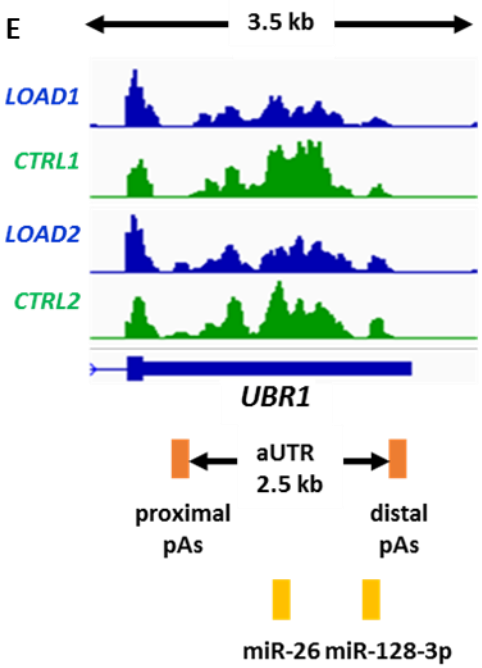
C



D

Shortening	Lengthening
ALDOC	ABCA3
C10orf10	EIF83
GABARAPL2	MSTO2P
KAT2A	OGDHL
POLR3A	PARP6
SH3BGRL2	SLC33A1
TIMM23	SUPV3L1
TMC6	TAF3
UBR1	WASH7P
UNC80	JAK1

E



F

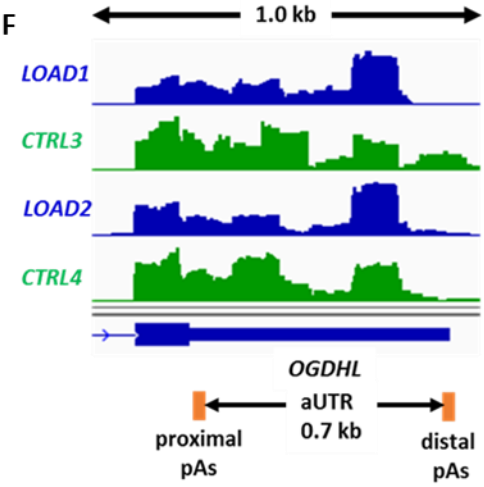


Figure 4.4. *UBR1* and *OGDHL* show significant APA changes in LOAD.

A. A bar chart to show mean percentage of significant 3'UTR lengthening (red bars) and 3'UTR shortening (green bars) events between each LOAD patient and the 4 control samples identified through DaPars analysis (PDUI >0.25, Fisher's exact test, $p<0.05$). The error bars indicate standard deviation. The mean number (n) of identified APA events for each LOAD patient are indicated underneath the chart.

B. A table to show the enrichment of biological processes identified with GO analysis in genes exhibiting 3'UTR lengthening (upper) and 3'UTR shortening (lower).

C. A bar chart to show significant APA events identified in LOAD compared to at least 3 control samples. Red bars indicate UTR lengthening events; green bars indicate UTR shortening events. * = $p<0.05$, ** = $p<0.01$, Fisher's exact Test.

D. A list of shortening (green) and lengthening events (red) identified in at least two LOAD samples from the graph in 4.4C.

E. *UBR1* shows 3'UTR shortening and **F.** *OGDHL* shows 3'UTR lengthening in LOAD (blue tracks) compared to control (CTRL, green tracks). In **E,** miRNA target sites indicated by yellow boxes.

4A.2.2 Comparison of APA in Different Regions of the AD brain

The above study assessed RNA from the hippocampus, which is reported to be the first region affected in AD, however other regions of the brain are also compromised during disease progression. RNA-seq on the frontal lobe and temporal lobe regions of the brain investigated changes in gene expression and alternative splicing (Twine et al. 2011). This study provided evidence that different genes were up- and down-regulated in the temporal lobe, which is involved in memory formation, compared to the frontal lobe, which has a role in intelligence, behaviour and judgement. Here, DaPars was used on these datasets to assess APA changes in these regions of the brain in AD.

There was only one sample from each brain region so a cross comparison of different patients and controls could not be conducted. DaPars usually requires a 30 fold coverage over the 3'UTR which requires approximately 50 million reads per sample with a read length of 50 bp. However, this dataset only had between 13.4-15.8 million reads with a lower read length of 36 bp (Supplementary Table 3). This reduced sequencing depth meant that only 270-700 genes were investigated for APA by the DaPars algorithm. This is a large limitation to this analysis as all the potentially APA regulated genes in these regions of the brain may not be analysed.

It must also be noted that the samples from the temporal and frontal lobe and whole brain were taken from different patients, and the control samples were a mixture of different individuals. As highlighted in the previous AD RNA-seq dataset, variation between different control samples can skew the number of APA events identified.

Bearing these limitations in mind, the data showed between 6-12% of genes that undergo APA had lengthened 3'UTRs whereas fewer than 2% showed 3'UTR shortening (Figure 4.5A). Interestingly, most APA regulated genes only showed significant UTR length changes in one region of the brain (Figure 4.5B). This indicates that APA is differentially regulated between the temporal and frontal lobes in AD.

GO analysis in genes showing significant changes in 3'UTR length showed an enrichment of synaptic plasticity regulation, modulation of synaptic transmission and regulation of neuron apoptotic processes. This suggests that APA mediated regulation of the transcriptome could affect synaptic activity, which may contribute to altered neuronal function

observed in AD. The *BIN1* gene, whose protein is involved in synaptic vesicle endocytosis, showed 3'UTR lengthening in the temporal and frontal lobe samples (Figure 4.5C). Importantly, this gene has been identified as a risk locus for AD (Tan, Yu, and Tan 2013) and increased expression has been linked to modulating tau pathology in LOAD (Chapuis et al. 2013).

Only 6 genes showed 3'UTR shortening, and only one of these, *VAMP2*, showed APA in each region of the brain (Figure 4.5D). The encoded protein is involved in neurotransmitter release during the fusion of synaptic vesicles to the pre-synaptic membrane. Decreased protein expression of VAMP2 is seen during progression of AD (Vallortigara et al. 2015), which may contribute to AD pathology.

This study shows that different genes exhibit significant APA in different regions of the AD brain, but all show a significant trend to 3'UTR lengthening. Altered protein expression of BIN1 and VAMP2 has been associated with AD (Chapuis et al. 2013; Vallortigara et al. 2015), but the role of APA in their gene regulation has not been linked. This analysis provides a novel mechanism of potential gene regulation of *BIN1* and *VAMP2* genes through 3'UTR changes which could impact protein output.

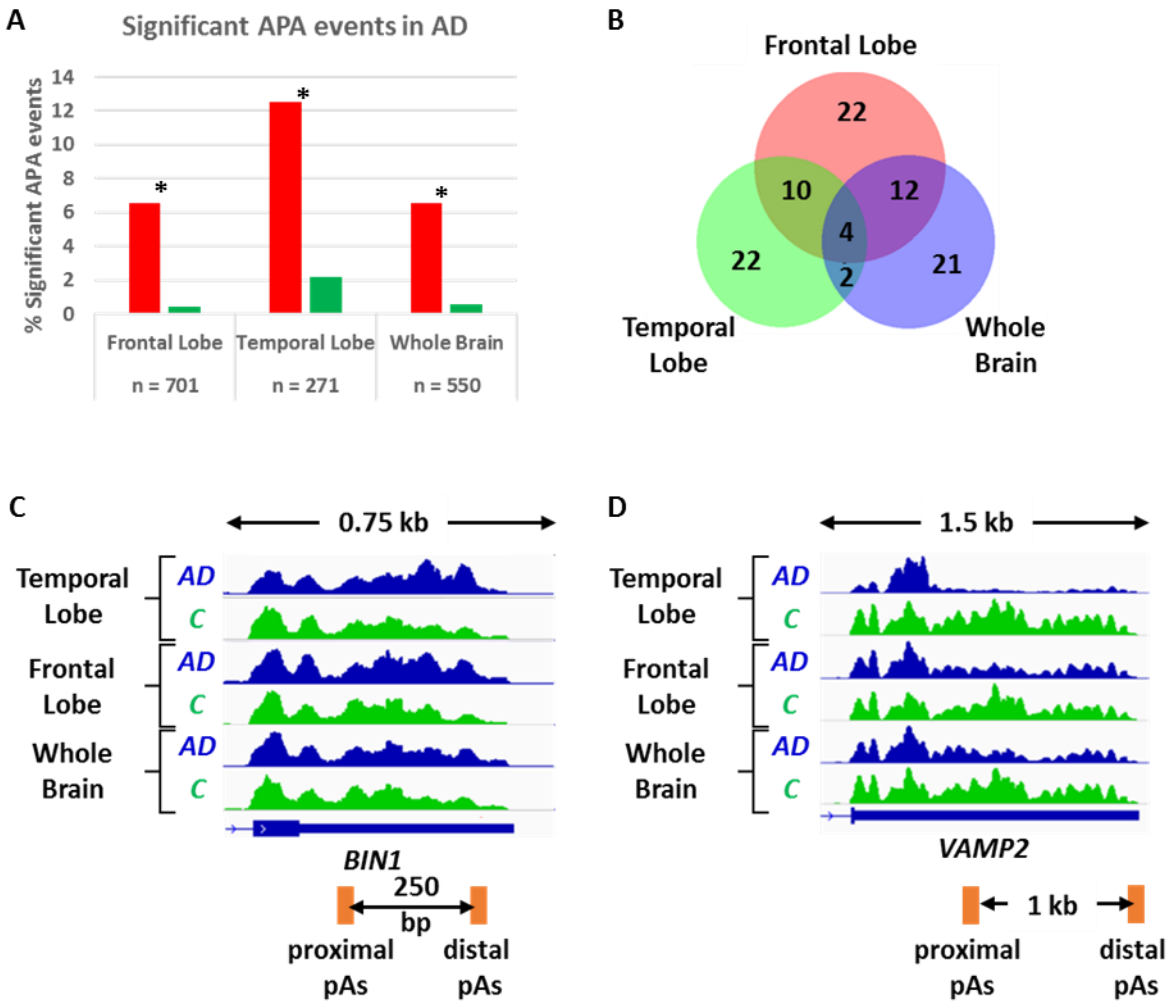


Figure 4.5. APA Regulation in Different Regions of the Brain in AD.

A. Significant 3'UTR lengthening observed in all regions of the brain in AD compared to control samples identified with DaPars analysis (PDUI >0.25, Fisher's exact Test, p<0.05). Red and green bars indicate number of identified UTR-APA lengthening and shortening events respectively. n = number of identified APA events in the comparison. * = p<0.01, Fisher's exact Test.

B. Different genes undergo APA in different regions of the brain in AD.

C. 3'UTR lengthening in *BIN1* and **D.** 3'UTR shortening in *VAMP2* in AD (blue tracks) compared to control (C, green tracks).

4A.3 APA in Parkinson's Disease

To date, only one study has assessed the role of APA in PD. Rhinn and colleagues showed an increased usage of the distal poly(A) site of *SNCA*, a gene crucial to PD pathogenesis, in the brains of PD patients. These longer isoforms produced proteins that were localised to the mitochondria and were more likely to aggregate suggesting a critical role of APA in α-synuclein regulation (Rhinn et al. 2012).

Here, two RNA-seq datasets were analysed to assess genome-wide APA changes in both fPD and sPD patients. APA events in fPD were far less prevalent than in sPD, where genes associated with mitochondrial function showed altered UTR length. Given the importance of mitochondrial function in PD pathology, APA may be an important regulator of the transcriptome in PD.

4A.3.1 APA in sporadic and familial PD

Woodard and colleagues analysed transcriptomic changes between monozygotic twins carrying a N370S mutation in the *GBA* gene, where only one of the twins had developed PD, aged 63 (Woodard et al. 2014). Mutations in *GBA* are linked to increased α-synuclein aggregation in fPD, and *GBA* mutations have also been seen in sPD patients (Sidransky and Lopez 2012).

Induced pluripotent cells (iPSCs) were derived and differentiated to midbrain dopaminergic neurons from fibroblasts isolated from the twins (Non-F-PD and F-PD), a healthy control with no family history of PD (C1), a healthy control with a family history of PD (C2), and a patient with sporadic PD (S-PD) (Table 4.6). Total RNA was isolated from biological replicates and RNA-seq was performed to look at the global transcriptome. DaPars analysis on this RNA-seq dataset enabled investigation of poly(A) site usage between the twins as well as in the sPD patient and healthy control individuals.

Initially, the F-PD and S-PD samples were compared with each of the healthy controls. There was no trend to 3'UTR shortening or lengthening and fewer than 0.9% of APA events were significant (Figure 4.6A), indicating that global APA changes do not occur in PD. However, GO analysis of all of the genes that show 3'UTR shortening presented an enrichment in mitochondrial organisation (Figure 4.6B). Altered regulation of these genes through shorter

3'UTRs may have a role in mediating mitochondrial dysfunction, which is an established phenotype in PD. Genes showing 3'UTR lengthening were associated with 'macromolecular complex subunit organisation', including genes associated with protein turnover (Figure 4.6B). Aggregation of misfolded proteins is an important hallmark of PD pathogenesis, therefore altered regulation of these genes through 3'UTR lengthening may contribute to PD pathology.

A prominent candidate gene showing 3'UTR shortening in S-PD, but not F-PD, is *LONP1* (Figure 4.6C), which encodes a mitochondrial matrix protease that mediates degradation of misfolded or oxidatively damaged proteins. Given the association of misfolded protein aggregation in PD, including in the mitochondria (Desideri and Martins 2012), alterations in the regulation of the *LONP1* could affect mitochondrial function. One study showed that *LONP1* knockdown caused an increase in PINK1 accumulation, which increased mitophagy (Jin and Youle 2013). PINK1 is associated with fPD along with Parkin, which together regulate the removal of dysfunctional mitochondria. Consequently, alterations in LONP1 protein levels in the mitochondrial matrix, may contribute to PD pathogenesis. RBPs or regulatory elements in the alternative UTR that could influence transcript stability, protein output or localization were not identified by scanning the UTR.

An example of a 3'UTR lengthening event in F-PD was seen in *NELFA* (Figure 4.6D). *NELFA* encodes a component of the negative elongation factor complex, which has a role in transcriptional pausing and regulating Pol II mediated transcription. This gene appears to show 3'UTR lengthening in the S-PD patient, but this was not identified as a statistically significant event by DaPars. A target site for miR-133 family of miRNAs is found in the alternative UTR which may mediate the isoform expression in the cytoplasm. miR-133b was shown to be deficient in the midbrain of PD patients (Jongpil Kim et al. 2007), which could contribute to this 3'UTR lengthening event.

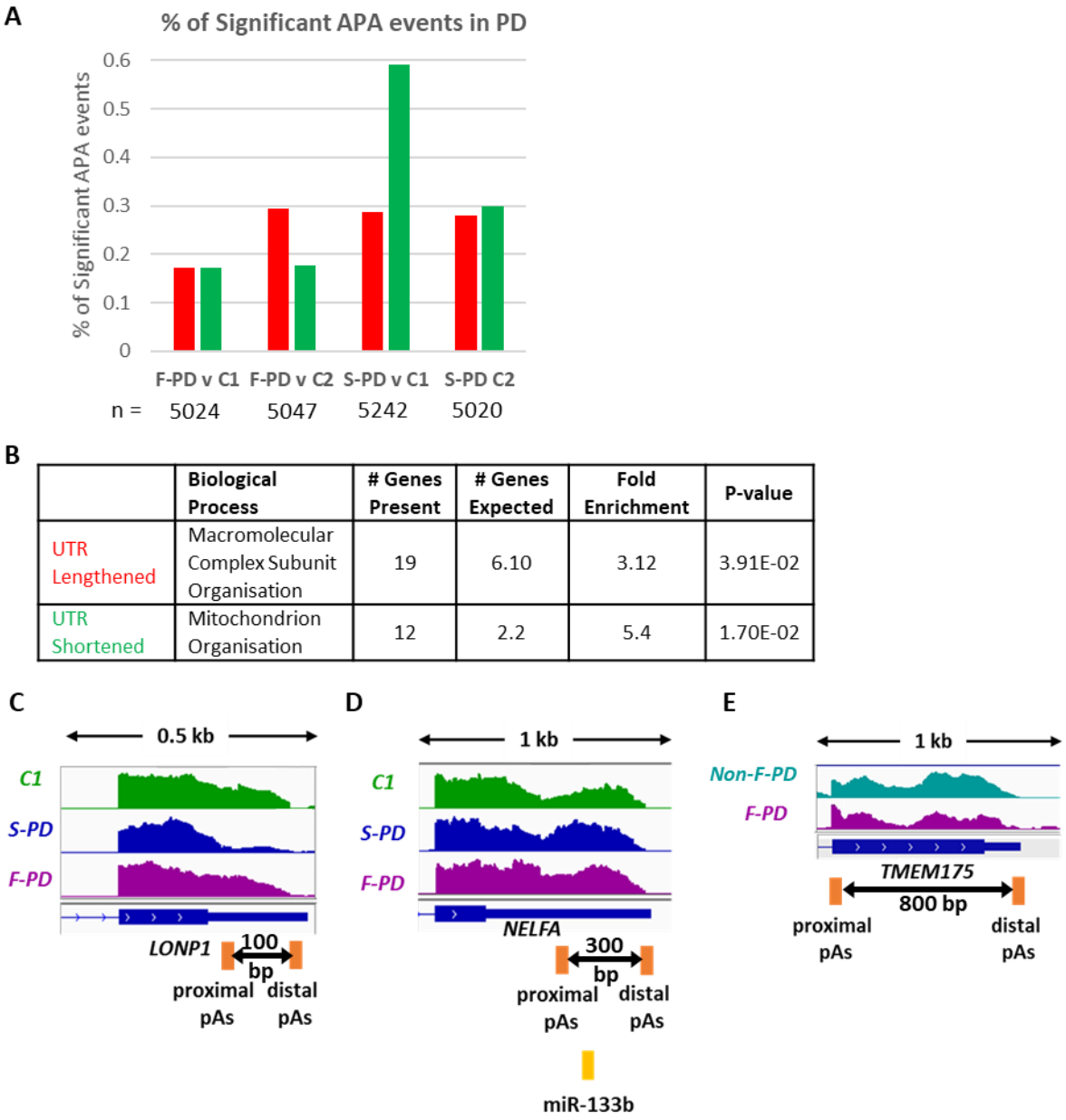
Next, APA was assessed between the monozygotic twins. Surprisingly, only two genes, *TMEM175* and *INPP5E* showed 3'UTR shortening, and none showed 3'UTR lengthening, between the Non-PD or PD twin. This suggests that APA does not play a crucial role in disease pathology in this case of fPD. Although both *TMEM175* and *INPP5E* were identified as statistically significant shortening events in F-PD, visualisation of the reads in Bigwig files shows that the read depletion is not in the 3'UTR but rather over the terminal exon coding

region (as exemplified for *TMEM175* in Figure 4.6E). Therefore, this does not constitute as a UTR-APA event. *TMEM175* encodes a lysosomal potassium channel, so alterations in the regulation of this gene could have implications for autophagosome-lysosome fusion in the autophagy pathway, which is known to be dysregulated in PD. However, changes in the regulatory mechanisms of this gene are not clearly identified through DaPars.

These results do not show widespread APA changes in S-PD or F-PD compared to controls, however identification of genes associated with mitochondrial function and protein degradation may be regulated by APA to contribute to PD pathology.

Table 4.6. Background of RNA samples from sPD and fPD RNA-seq dataset

Sample	Description	Gender	Age
C1	Healthy individual – no family history of PD	Male	37
C2	Healthy individual – family history of PD	Male	54
S-PD	Sporadic PD Patient	Female	65
Non-F-PD	N370S mutation, without PD	Male	68
F-PD	N370S mutation, with PD	Male	68



	Biological Process	# Genes Present	# Genes Expected	Fold Enrichment	P-value
UTR Lengthened	Macromolecular Complex Subunit Organisation	19	6.10	3.12	3.91E-02
UTR Shortened	Mitochondrion Organisation	12	2.2	5.4	1.70E-02

Figure 4.6. APA Regulation in fPD compared to sPD.

A. The percentage of 3'UTR shortening (green) and 3'UTR lengthening (red) events in F-PD and S-PD compared to the two healthy controls identified by DaPars analysis (PDUI >0.25, Fisher's exact Test, $p<0.05$) are shown. n = indicates the total number of APA events identified in each comparison.

B. A table to show biological processes identified through GO analysis in APA regulated genes in PD.

C. 3'UTR shortening was observed in *LONP1* in S-PD but not F-PD.

D. 3'UTR lengthening was observed in *NELFA* in F-PD.

E. One of two significant APA events identified between the monozygotic twins which carry the *GBA* N370S mutation; F-PD: Twin with PD, Non-F-PD: Twin without PD. Reads are depleted in F-PD over the coding region in the terminal exon.

For figures **C-E**, control tracks are indicated in green (C1), S-PD in blue, Non-PD in teal and F-PD in purple.

4A.3.2 APA in Different Sporadic PD patients

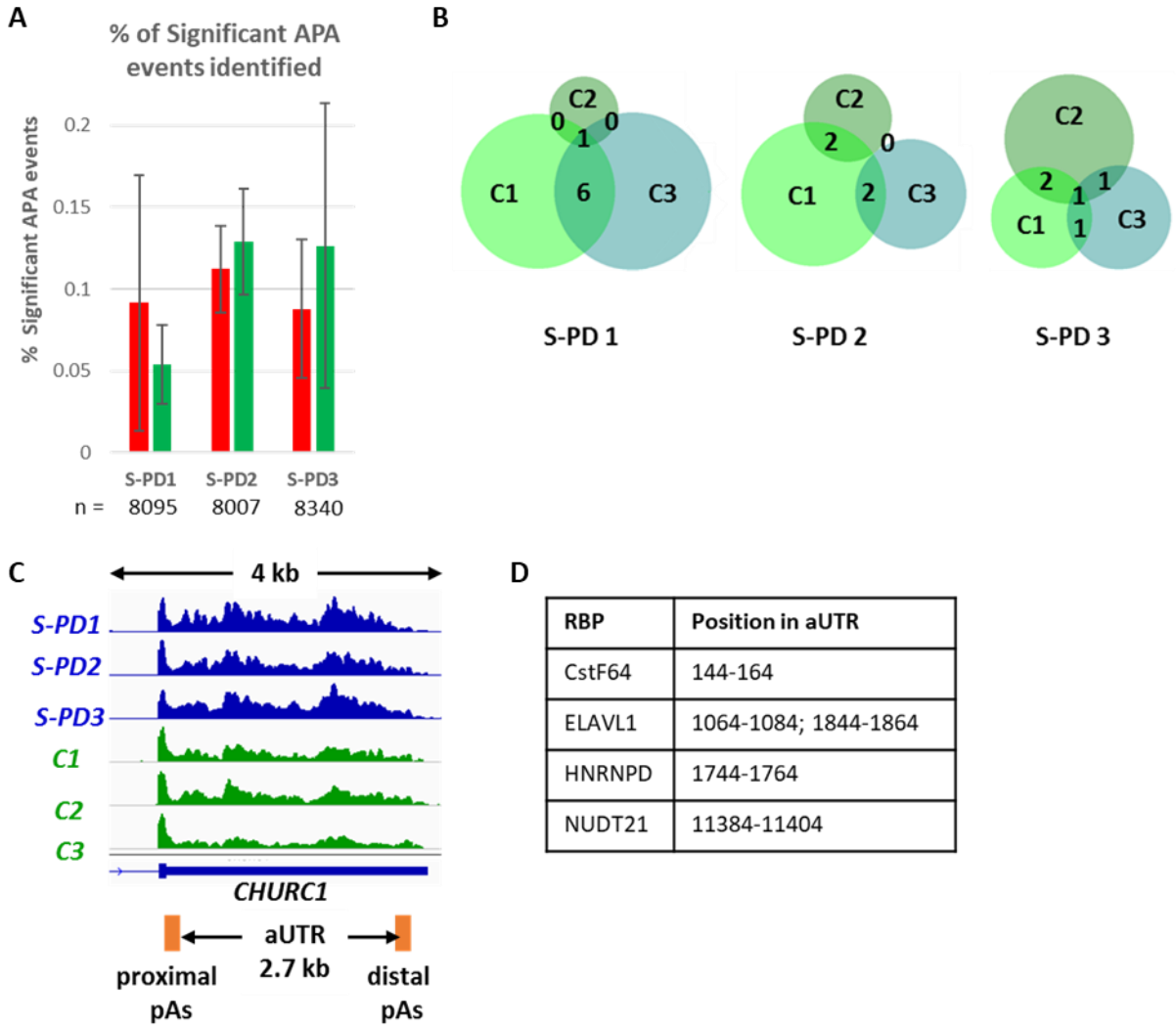
The above section suggested that APA changes are not widespread in PD patients compared to controls, but genes that are affected are enriched in physiologically relevant pathways. To explore this further, APA was assessed in an additional RNA-seq dataset where RNA had been isolated from midbrain dopaminergic neurons derived from sPD patient iPSCs. Here, a further three patient samples were cross compared to three control samples. These dopaminergic neurons showed signs of oxidative stress and altered neuronal activity, as observed in the PD disease state (GEO ERA589991).

APA analysis was conducted on combined biological replicates of each of the three sPD patient (S-PD) with three control RNA samples from derived dopaminergic neurons. The mean of the total number of APA events was calculated per S-PD vs control comparison, which resulted in fewer than 0.2% of genes showed significant APA changes (Figure 4.9A). This suggests that APA has a limited influence on transcriptome changes observed in S-PD. In addition, there was great variation between the number of APA events identified between the different comparisons as highlighted by the standard deviation. Further, as seen in previous AD datasets, there was little overlap between the genes exhibiting APA between different comparisons (Figure 4.9B), suggesting few APA changes may be specifically correlated to PD.

The *CHURC1* gene showed 3'UTR lengthening in each of the S-PD patients compared to at least 2 of the control samples (Figure 4.9C). This gene encodes a transcriptional activator that is involved in neuronal development, but has not been previously associated with neurodegeneration. The *CHURC1* alternative UTR region was scanned to identify any regulatory elements that could explain the 3'UTR lengthening event observed in S-PD samples. PAR-CLIP data from the CLIP database (Chapter 2.24) identified binding sites for CstF-64, ELAVL1, HNRNPD and NUDT21 (Figure 4.9D). NUDT21, which encodes a subunit of CFIm, and CstF-64 have roles in modulating poly(A) site choice. CstF-64 enhances proximal poly(A) site usage, while a novel role for NUDT21 in promoting usage of a distal poly(A) site has been identified (Gennarino et al. 2015). Although increased expression of NUDT21 was reported in AD (Wong 2013), expression changes in NUDT21 or CstF-64 have not been associated with PD.

HNRNPD, also known as AUF1, binds to AREs and targets them for degradation (Demaria and Brewer 1996). ELAVL1, which also binds to AREs, has been shown to displace HNRNPD to stabilise the transcript (C.-Y. A. Chen, Xu, and Shyu 2002). These RBPs may mediate the 3'UTR lengthening observed in the *CHURC1* transcript, however altered ELAVL1 and AUF1 expression in PD has not been reported.

These data suggest that the regulation of APA in sPD may be limited, however different poly(A) site usage in the *CHURC1* gene, which is associated with neuronal development, may contribute to transcriptome changes in sPD. RBPs that target the *CHURC1* alternative UTR were identified, but further investigation into RBP expression changes in PD are required to understand the mechanism behind this 3'UTR lengthening event in sPD.



RBP	Position in aUTR
CstF64	144-164
ELAVL1	1064-1084; 1844-1864
HNRNPD	1744-1764
NUDT21	11384-11404

Figure 4.7. APA Regulation in sPD.

A. A bar chart to showing the mean percentage of 3'UTR lengthening (red) and shortening (green) APA events in SP-D compared to each of the three control samples identified by DaPars analysis (PDUI >0.25, Fisher's exact Test, $p<0.05$). The mean number of identified APA events (n) is indicated under the chart. Error bars show standard deviation.

B. Venn diagrams to show little overlap between the identified APA events in each of the S-PD vs control samples. Each shade of green represents a different control sample C1, C2 or C3.

C. A screenshot to show 3'UTR lengthening in the *CHURC1* gene in S-PD (blue tracks) compared to control (C, green tracks).

D. A table summarising the RBPs identified to target the *CHURC1* alternative UTR (aUTR) and their predicted binding sites along the alternative UTR.

4A.4 APA in ALS

ALS is characterized by the deterioration of motor neurons which control voluntary muscles. This neurodegenerative disease has been linked to changes in RNA metabolism as mutations in two RBPs, FUS and TDP-43 have been associated with fALS. They both regulate alternative splicing of genes involved in neuronal development and neurodegeneration, but there is not a significant overlap in the genes they regulate (Rogelj et al. 2012).

FUS has a nuclear role mediating alternative splicing and APA, but has also been found to have a cytoplasmic function in mRNA localisation and synaptic transmission (Udagawa et al. 2015) as well as mRNA turnover (Kapeli et al. 2016). This RBP can modulate co-transcriptional mRNA processing by interacting with other core transcription machinery proteins such as TFIID, splicing factors, Pol II CTD and to the transcription start site of actively transcribed genes (Masuda, Takeda, and Ohno 2016; Schwartz et al. 2012).

FUS also interacts with multiple APA factors including CPSF-160, CstF-64 and WDR33. FUS binding downstream of a poly(A) site recruits CPSF-160 and enhances usage of that poly(A) site causing transcriptional termination (Masuda et al. 2015). However, binding of FUS in the nascent RNA upstream of a poly(A) site caused premature transcription termination producing un-polyadenylated transcripts. Knockdown of FUS resulted in widespread changes in mRNA length, including in genes specifically associated with neuronal activities and synaptic transmission (Masuda et al. 2015; Schwartz et al. 2012). Mutations in the NLS of FUS, causing cytoplasmic accumulation and subsequently impaired mRNA processing, are associated with ALS pathology (Masuda, Takeda, and Ohno 2016).

In addition to FUS, the RBP HNRNPA2B1, which can harbour fALS associated mutations, was recently shown to interact with a UAGG motif in the 3'UTR to affect APA (Martinez et al. 2016). TDP-43 autoregulates its own expression through a negative feedback loop involving alternative splicing and APA (Avendaño-Vázquez et al. 2012; Koyama et al. 2016). Increased TDP-43 levels have been associated with ALS, therefore understanding the mechanisms of TDP-43 production are important to characterize ALS pathology. Together, this suggests the regulation of RNA metabolism by these RBPs is crucial in ALS.

APA has been investigated in ALS genome wide showing many APA events between the control and sALS or fALS patients in the frontal cortex and cerebellum (Prudencio et al.

2015). While these regions of the brain show early neuropathological markers of ALS, it is the motor neurons whose function is mainly compromised. Here, these APA changes in the frontal cortex and cerebellum of ALS patients are analysed and compared to APA events identified with DaPars in motor neurons of the lumbar spinal cord from another RNA-seq dataset.

4A.4.1 APA in the Frontal Cortex and Cerebellum of ALS Patients

The only neurodegenerative disease where APA has previously been investigated genome wide is ALS (Prudencio et al. 2015). Prudencio and colleagues performed RNA-seq on RNA samples isolated from the frontal cortex and cerebellum of sALS and fALS patients, which had a hexameric repeat expansion of GGGGCC in the *C9ORF27*, referred to herein as c9ALS patients. This mutation is the most common known cause of fALS, found in over 30% of familial ALS and over 5% of sALS cases (Parakh and Atkin 2016). The sALS patients had no mutations in the genes most commonly related to ALS, while control samples were taken from individuals with no known neurological disease.

The authors of this study used RNA-seq to investigate gene expression changes and alterations in splicing in ALS. In addition, changes in APA were investigated using DaPars analysis. Widespread changes were seen in poly(A) site usage between ALS patients and control individuals, and sALS and c9ALS patients showed different APA profiles. Different trends to 3'UTR lengthening and shortening were observed in the frontal cortex and cerebellum, which also differed between the c9ALS and sALS patients. APA changes were identified in genes associated with oxidative stress in sALS and RNA processing in c9ALS. However, individual gene analysis was not performed and the overlap of APA events in different regions of the brain were not investigated. Furthermore, this study was not clear on the extent of overlap in APA events between different patient samples compared to control samples.

To investigate APA regulated genes in both sALS and c9ALS, and in both frontal cortex and cerebellum, DaPars analysis was performed on RNA-seq data from two different age-matched patient and control samples (Table 4.7).

Firstly, APA changes between the frontal cortex and the cerebellum in sALS and c9ALS compared to the age matched control were assessed. In Set 1, a significant trend to

3'UTR shortening ($p<0.01$ Fisher's exact Test) was observed in the cerebellum in both sALS and c9ALS. In the frontal cortex, overwhelming 3'UTR shortening was observed in sALS but 3'UTR lengthening was observed in c9ALS (Figure 4.8A, left). This suggests differences in APA profiles in sALS and c9ALS patients. In Set 2, far fewer significant APA events were identified and the trends to 3'UTR lengthening or shortening did not hold true (Figure 4.8A, right). This suggests a large degree of variation between samples with regards to APA, which was not explored in the original study by Prudencio and colleagues.

Next, an overlap of the APA events between the cerebellum and frontal cortex was performed to identify common APA events in different regions of the brain. A greater proportion of APA events occurred in both regions in sALS compared to c9ALS in Set 1 (Figure 4.8B), again suggesting distinctly different APA regulation in the two patients compared to controls. An overlap of the APA events between the c9ALS and sALS showed more differences in APA changes in the frontal cortex than the cerebellum in Set 1 (Figure 4.8C). However, these differences were not observed in the second set (Supplementary Figure 2). This indicates large variability in APA regulation between the two datasets.

To assess this further, the number of APA events identified in the two datasets were compared. Between just 9 and 21 APA events were identified in the same region in the two datasets assessed (Figure 4.8D). This suggests a strong degree of patient and/or control specific variation, and that very few APA events are causative or consequential of the ALS phenotype.

USP21 showed 3'UTR shortening in both sALS patients (Figure 4.8E). This gene encodes a deubiquitinating enzyme, which is important in ubiquitin turnover and protein degradation. Although *USP21* has not directly been associated with ALS, alterations in the ubiquitin proteasome pathway in ALS are well established. Therefore, APA mediated regulation of this gene in sALS may affect protein turnover pathways.

In both c9ALS and sALS patients, 3'UTR lengthening was observed in the *PLXNA2* gene, which encodes a receptor protein that is associated with axon guidance and cytoskeleton remodelling during neuron development. The alternative UTR spans 4.5 kb, but only two RBPs, ELAVL1 and YTHFD2, have binding sites in this region as identified by PAR-CLIP (Chapter 2.24). In the nucleus, ELAVL1 can modulate poly(A) site choice (Mansfield and Keene 2012; H. Zhu et al. 2007), while in the cytoplasm, ELAVL1 contributes to transcript

stability of its target mRNAs (Gorospe et al. 2011). Stabilizing the longer transcript isoform could cause this 3'UTR lengthening event, however alterations in ELAVL1 expression in ALS have not been observed.

In conclusion, this section highlights the importance of assessing APA changes in multiple patient and control samples to identify true APA events in the disease state. Through this stringent analysis, two APA regulated genes *USP21* and *PLXNA2* were identified that have direct links to pathways that are affected in ALS pathology.

Table 4.7. Background of RNA samples from c9ALS, sALS and Control individuals selected for APA analysis using DaPars. * = closest aged control sample available.

Sample		**Age**
Set 1	c9ALS 1	64
	sALS 1	64
	C 1	65
Set 2	c9ALS 2	49.5
	sALS 2	48
	C 2	55*

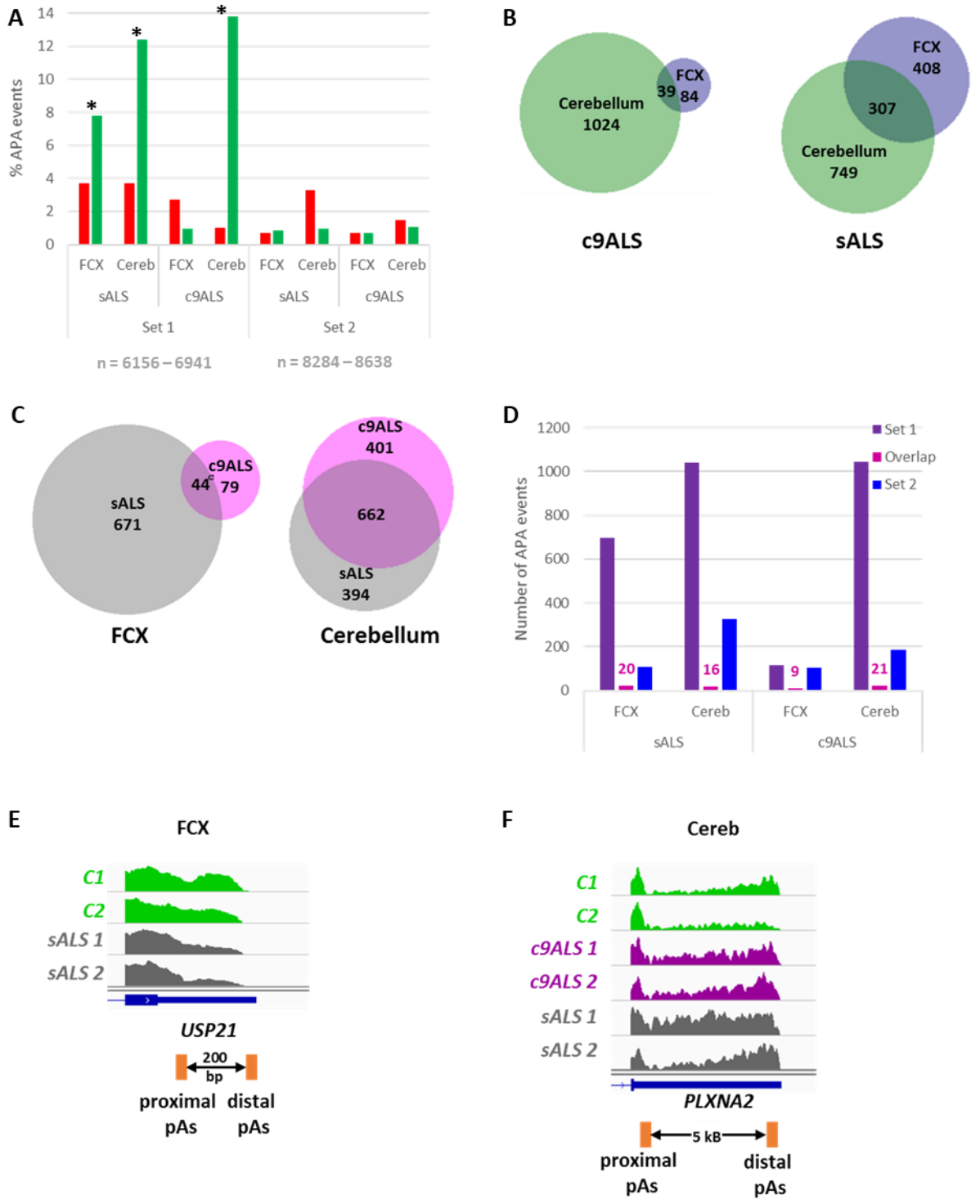

A
% APA events
14
12
10
8
6
4
2
0
*
*
*
FCX
Cereb
FCX
Cereb
FCX
Cereb
FCX
Cereb
sALS
c9ALS
sALS
c9ALS
Set 1
Set 2
n = 6156 – 6941
n = 8284 – 8638
B
Cerebellum
1024
FCX
39
84
c9ALS
FCX
408
307
Cerebellum
749
sALS
C
sALS
671
c9ALS
44
79
FCX
c9ALS
401
662
sALS
394
Cerebellum
D
Number of APA events
1200
1000
800
600
400
200
0
Set 1
Overlap
Set 2
20
16
9
21
FCX
Cereb
FCX
Cereb
sALS
c9ALS
E
FCX
C1
C2
sALS 1
sALS 2
USP21
200
bp
proximal
pAs
distal
pAs
F
Cereb
C1
C2
c9ALS 1
c9ALS 2
sALS 1
sALS 2
PLXNA2
5 kB
proximal
pAs
distal
pAs

Figure 4.8. APA Regulation in c9ALS and sALS Patients.

A. A bar chart to show the proportion of significantly changing 3'UTR lengthening (red bars) and 3'UTR shortening (green bars) events in the frontal cortex (FCX) and cerebellum (Cereb) in sALS and c9ALS patients compared to age-matched controls. * = $p<0.01$, Fisher's exact Test. Changes in UTR length were identified using DaPars analysis. The range of the total number of identified APA events (n) for each set are indicated under the bar graph.

B. Venn diagrams of Set 1 to show the overlap of APA events between the FCX (blue) and cerebellum (green) in c9ALS and sALS patients. A greater overlap was observed in sALS compared to c9ALS.

C. Venn diagrams to show a greater overlap of APA events in the cerebellum than the FCX between sALS (grey) and c9ALS (purple) of Set 1. For **B** and **C**, data for Set 2 is shown in (Supplementary Figure 2).

D. A bar chart to show the number of overlapping events (pink) in the two age-matched Sets of ALS and control samples assessed.

E. A screenshot to show the 3'UTR shortening event in the *USP21* gene in sALS (grey tracks) compared to control samples (green tracks).

F. A screenshot to show the 3'UTR lengthening event in *PLXNA2* in both c9ALS (purple tracks) and sALS (grey tracks) in both sets compared to control samples (green tracks).

4A.4.2 APA in Lumbar Spinal Cord Motor Neurons in Sporadic ALS patients

Gene expression changes in the CNS of ALS patients has been investigated extensively but often these studies do not consider the fact that the brain has a heterologous population of cells which may have differential gene expression changes in disease. The previous study assessed APA changes in the cerebellum and frontal cortex, however these regions are not primarily affected in ALS. A recent pre-print, unpublished study, extracted total RNA from motor neurons from ALS patients which had not been fully degenerated (Batra et al. 2016). The authors reported transcriptome wide changes that deviated from those reported in tissue analysis of other brain regions indicating that regions of the CNS are differentially affected in ALS.

DaPars was employed to assess APA changes in samples from motor neurons in the lumbar spinal region between 13 sALS and 9 control individuals. Samples with fewer than 20 million reads, which fall below the chosen threshold requirements for DaPars were omitted, yielding 10 sALS and 8 control patients (Read numbers in Supplementary Table 3).

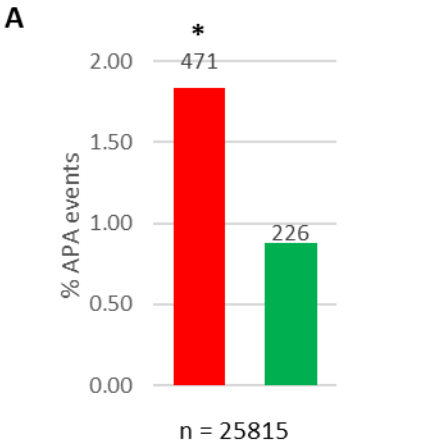
Each of the selected sALS patient samples were compared to each of the controls, yielding 80 comparisons. On average, 2.7% of genes showed significant APA, with twice as many 3'UTR lengthening than shortening events seen (Figure 4.9A). GO analysis for UTR lengthened genes identified an enrichment for genes involved in negative regulation of neuron projection development as well as genes associated with cytoskeleton intracellular transport (Figure 4.9B). Therefore, although global changes are not seen in sALS, APA may be important in the regulation of transcripts encoding proteins that contribute to neuropathology. The biological processes identified here differ from those identified in the Prudencio et al., dataset, which adds to the evidence that APA affects different genes in different regions of the CNS during ALS.

To investigate the key changing genes further, 3'UTR shortening or lengthening events occurring in at least 3 different sALS vs control comparisons were selected, yielding 22 genes for further analysis. *UCHL1*, which encodes an abundant neuron specific enzyme associated with the ubiquitin proteasome pathway, shows 3'UTR lengthening in 4 sALS compared to 4 different control samples (Figure 4.9C). UCHL1 is a regulator of ubiquitin turnover as it has both hydrolase activity to remove ubiquitin (Osaka et al. 2003) and ubiquitin ligase activity

(Yichin Liu et al. 2002). Its crucial role in maintaining healthy motor neurons was demonstrated in a mouse knockout model where loss of UCHL1 increased ER stress causing motor neuron degeneration (Jara et al. 2015). Furthermore, reduced UCHL1 protein levels (J. Choi et al. 2004), and loss of its activity have been reported in PD and AD (Ristic, Tsou, and Todi 2014).

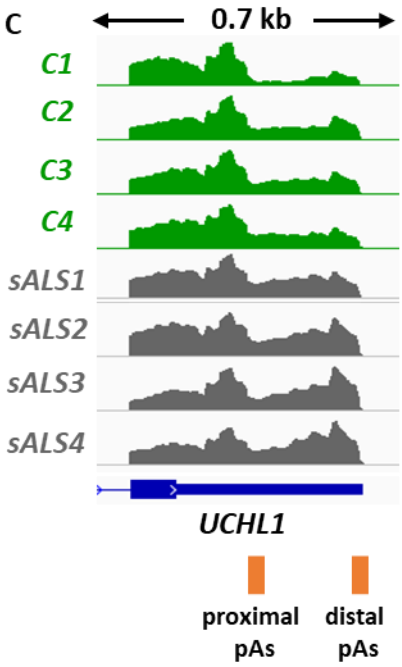
Analysis of the *UCHL1* UTR using a CLIP database identified 21 RBPs that interact with the UTR, but only 3 of these, CstF-64, WDR33 and TARDBP, uniquely interact with the alternative UTR (Figure 4.9D). CstF-64 promotes usage of a proximal poly(A) site, while WDR33, though crucial for cleavage and polyadenylation, does not have an established role in APA. Mutations in *TARDBP*, which mediates splicing, are linked to fALS cases but there is no evidence that it influences APA in genes apart from its own transcript. Further, no miRNAs have been identified to target the *UCHL1* UTR. It is therefore unclear how the 3'UTR lengthening event in *UCHL1* may arise in sALS, yet dysregulation of this gene by APA may affect its protein output or localisation, which could contribute to pathology in sALS.

This section assessed APA changes in the motor neurons of the spinal cord of sALS patients compared to control individuals. In comparison to the frontal cortex and cerebellum of the brain, few significant APA events were identified in sALS patients. However, 3'UTR lengthening was identified in *UCHL1*, which is important in the ubiquitin proteasome pathway and is associated with neurodegeneration. APA regulation of this gene may be crucial to its expression in sALS. Subsequently, the mechanism behind APA and its impact on protein output will be interesting for further investigation.



B

Biological Process	# Genes Present	# Genes Expected	Fold Enrichment	P-value
Protein folding	9	1.06	8.49	1.12E-02
Negative Regulation of Neuron Projection	7	0.67	10.37	4.96E-02
Cytoskeletal Intracellular Transport	21	6.06	3.46	4.05E-03



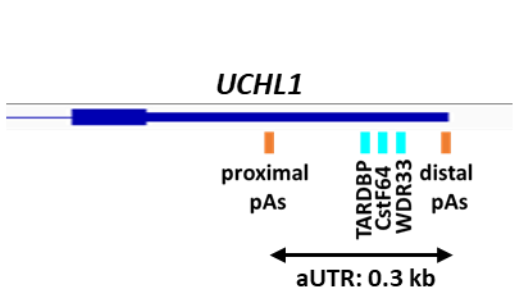


Figure 4.9. APA Regulation in Motor Neurons in sALS.

A. A bar chart to show 1.8% of APA regulated genes showed 3'UTR lengthening (red), while fewer than 1% showed 3'UTR shortening (green) in all comparisons between 10 sALS and 8 control samples. The cumulative number of APA events identified (n) over 80 comparisons is indicated under the bar chart. Data labels indicate number of APA events identified among all cross comparisons. * = $p<0.05$, Fisher's exact Test. UTR length changes were identified using DaPars analysis.

B. A table to show the biological processes enriched in genes showing UTR lengthening with GO analysis. The cohort of genes showing UTR shortening were not enriched in any biological processes.

C. 3'UTR lengthening seen in *UCHL1* gene in sALS (grey tracks) compared to control (green tracks).

D. The position of RBPs found uniquely in the alternative UTR of *UCHL1* are indicated by blue boxes.

4A.5 Discussion

Extended 3'UTRs have previously been identified in the brain, which are likely to harbour further regulatory elements (Miura et al. 2013). However, there have been few studies to investigate changes in 3'UTR length in neurodegeneration. The aim of this chapter was to globally assess APA alterations and consequently 3'UTR length in AD, PD and ALS.

4A.5.1 The Use of DaPars

DaPars enables assessment of poly(A) site usage in RNA-seq data from scarce patient samples. This bioinformatics method has allowed investigation of APA in numerous diseases (Masamha et al. 2014; Xia et al. 2014; B. Hu et al. 2016; Prudencio et al. 2015), however this is the first time it was used to assess changes in different types of neurodegeneration.

One limitation of the DaPars analysis is that it can only identify usage of annotated poly(A) sites in the terminal exon. Extended 3'UTRs in the brain that may utilise noncanonical, unannotated poly(A) sites would not be recognised, leaving any APA changes here unidentified. In addition, changes in upstream-APA, which would result in truncation of the transcript cannot be assessed in this manner. Furthermore, DaPars has a threshold sequencing depth, which certain datasets here did not meet, limiting the number of APA and significant APA events identified. The varying quality of different RNA-seq datasets can affect the poly(A) site predictions, therefore, DaPars cannot be used to cross-compare data from different RNA-seq datasets.

Changes in the 3'UTR length between different cell lines has been assessed retrospectively from RNA-seq data using another bioinformatics algorithm GETUTR (M. H. Kim, You, and Nam 2015), however this pipeline does not enable comparison of usage of poly(A) sites, therefore provides no insight into APA. Another method has also recently been developed to look at poly(A) site usage from existing RNA-seq data, using existing poly(A) site databases (Grassi et al. 2016). This method calculates a ratio of proximal:distal poly(A) site usage between two samples to determine a ratio of a ratio (Roar), and can also only assesses poly(A) site changes in the 3'UTR. The authors identified more APA events using Roar rather than DaPars from the same RNA-seq datasets, suggesting it is a more sensitive method to assess APA. However, the identification of these additional events may increase the

number of false positive events identified, or identify very slight APA changes that may not have a physiological effect.

4A5.2. APA in AD

Assessment of 3'UTR-APA in the two AD datasets investigated identified different cohorts of genes regulated by APA, however in each case, genes encoding proteins associated with AD pathology were shown to vary in 3'UTR length. In the first AD dataset, RNA isolated from the hippocampal region between LOAD patients and controls was investigated for APA changes. A large degree of variation in APA was observed between different patient and control comparisons, suggesting that there is either natural variation between samples, or changes that may not be due or unique to AD. Here, only genes which showed APA in at least 3 of the controls were selected for further analysis eliminating more than 80% of the identified APA events. This stringent cut off makes the APA event more likely to be changing due to AD instead of other unknown factors. Other bioinformatics analyses assessing APA in disease may not be as rigorous in their analyses which may amplify the extent of APA changes in the disease state. Although similar phenotypes are seen in different AD patients, AD is a composite disease, with varying pathologies associated to each case. Therefore, the same genes may not be affected by APA in each AD sample. This RNA-seq dataset originally investigated the transcriptome of LOAD and control samples, and identified novel lncRNAs which were proposed to contribute to AD pathology (Magistri et al. 2015). Changes in gene expression in 113 protein coding genes were identified (Magistri et al. 2015), but none of these genes were identified to be regulated by APA.

The second dataset assessed APA changes in the temporal and frontal lobe of the brain (Twine et al. 2011). While 3'UTR lengthening was observed in both brain regions, most genes showed region-specific APA events. Few genes were identified that also showed APA in the hippocampus from the previous study (Supplementary Figure 3), again suggesting the brain-region specific APA differences.

In the AD brain, genes associated with neuron structure and synapse function showed altered expression (Twine et al. 2011). This analysis identified genes associated with synaptic function to be regulated by APA. Since this dataset assesses total RNA, it is unclear if the

APA events could mediate transcript stability and therefore abundance through post-transcriptional regulation. Changing protein expression of BIN1 (Chapuis et al. 2013) and VAMP2 (Vallortigara et al. 2015) have previously been associated with AD. This analysis identifies a APA as a novel mechanism in *BIN1* and *VAMP2* gene regulation, where changes in 3'UTR length may impact protein output.

Changes in splicing have been observed with age (Tollervey et al. 2011), but there is not yet evidence that APA regulation is affected in an age-dependent manner in humans. Reduced expression of the nervous system specific RBP Nova1/Nova2 was linked to altered splicing in AD patients, but not cognitively normal aged patients (Tollervey et al. 2011). Nova2 can also modulate poly(A) site choice by binding to a YCAY cis-element which inhibits co-transcriptional usage of a proximal poly(A) site through steric hindrance (Licatalosi et al. 2008). Decreased Nova expression could may result in 3'UTR shortening in AD, but this was not observed on a global scale in any of these AD datasets. However, Nova binding sites were identified in *UBR1* and *VAMP2* (C. Zhang and Darnell 2011), which both showed 3'UTR shortening in AD. Further functional studies will be required to investigate if reduced Nova expression affects poly(A) site choice of these transcripts. RBPs are important in regulating APA, and their function has shown to be dysregulated in disease (Tian and Manley 2016). Altered availability of RBP binding sites through differing 3'UTR length could contribute to gene regulation.

Defects in RNA metabolism have been implied in AD (Bai et al. 2013), and this analysis gives an indication that APA in relevant genes may also be dysregulated. Many bioinformatics studies on APA focus on the statistical significance of events, rather than assessing the physiological relevance of these APA changes. Genes known to be directly associated with AD, *PS1, PS2, APP* and *APOE*, did not show changes in poly(A) site usage in any of the datasets, suggesting no role of APA in their regulation in the cases assessed. However, APA changes observed in physiologically relevant genes identified here, could modulate protein output or localisation of these transcripts which could contribute to AD pathology.

4A.5.3 APA in PD

There is evidence that APA occurs in PD associated genes, such as α-synuclein (Rhinn et al. 2012), however changes in APA in PD have not been assessed on a global level. Here, RNA-seq data from patient and control iPSCs differentiated to dopaminergic neurons from two different datasets was used to assess 3'UTR length changes in PD.

The first dataset explored APA changes in sPD and fPD. Between monozygotic twins, where one individual had developed PD and one had not, only two APA events were identified suggesting APA did not contribute to the pathology of PD in this case of fPD. While fPD and sPD cases often exhibit similar symptoms, the causes or pathology of the disease can vary. Many more changes in APA were seen in the sPD patient compared to the healthy control than between the twins. The healthy individual here was over 30 years younger than the twins with PD. Although a study in *C. elegans* provided evidence of 3'UTR shortening in older worms (Mangone et al. 2010), age is not known to affect APA profiles in humans.

A global change in APA was not seen, however genes identified to show altered 3'UTR length were associated with mitochondrial organisation or alterations in macromolecular subunit organisation, i.e. protein aggregation. These are two key phenotypes seen in PD, suggesting APA may be affecting genes directly related to the disease state.

Protein, but not mRNA levels, of α-synuclein were higher in the midbrain dopaminergic neurons derived from iPSCs of both twins compared to the control, suggesting a link to the N270S mutation in *GBA* (Woodard et al. 2014). Although the levels of monomeric α-synuclein were not different between the twins, increased α-synuclein aggregation in the neurite region was seen in the fPD individiual. This suggests that localisation of α-synuclein, as well as aggregation, is key to pathogenesis (Woodard et al. 2014). While, evidence of APA in α-synuclein has been described in PD to influence transcript localisation, and therefore protein localisation (Rhinn et al. 2012), here no significant differences in 3'UTR length were seen in either sPD or fPD (Supplementary Figure 4), suggesting in this case, APA does not contribute to upregulated α-synuclein expression in PD.

The second dataset assessed APA in dopaminergic neurons derived from iPSCs in a further 3 sPD patients. Far fewer APA events were identified compared to control samples here, suggesting APA changes are not causative or consequential of the PD phenotype.

However, the *CHURC1* transcript showed 3'UTR lengthening in all S-PD samples. Assessment of poly(A) site usage from total RNA-seq data does not distinguish between transcriptional or post-transcriptional APA regulation, therefore it is unclear if the *CHURC1* UTR is lengthened at the point of cleavage or stabilised in the cytoplasm. RBPs identified in the alternative UTR may have altered expression in PD and therefore could mediate the 3'UTR lengthening event, but changes in the expression of CstF-64 and NUDT21 in PD have not been verified, and will need to be investigated further.

In conclusion, these data suggest that APA may have a limited influence on the fPD and sPD phenotype, however it may regulate the expression of physiologically relevant genes that could contribute to PD pathology. Assessment of APA from post-mortem patient RNA samples, and subcellular fractionated RNA would give a greater insight into the role of APA in PD.

4A.5.3 APA in ALS

APA changes using DaPars in ALS have previously been explored where greater APA changes were observed in sALS compared to c9ALS (Prudencio et al. 2015). Although widespread APA changes were identified, the physiological relevance to ALS pathology was not investigated. Two sets of age-matched control samples from this dataset were selected and subjected to DaPars analysis. Although many APA events were identified in one sALS patient, this was considerably modest in the second sALS patient. This shows the large degree of variation between patient samples, as highlighted when assessing APA in AD and PD.

Differences in APA regulation suggests that despite similar symptoms of disease in sALS and c9ALS cases, pathology at the molecular level may be very different. This work highlighted differences in the regulation of the transcriptome in c9ALS compared to sALS patients. This discrepancy between familial and sporadic patients was also seen in the DaPars analysis in PD (Chapter 4A.3). Different regions of the brain showed different APA events, as also identified in the AD dataset (Chapter 4A.2), corroborating the finding that APA may play different roles in different regions of the brain during neurodegeneration.

The genome wide study by Prudencio and colleagues assessed transcriptome wide changes in the cerebellum and frontal cortex which are not the focal points of degeneration in

ALS, although may have compromised function (Prell and Grosskreutz 2013). To further investigate APA in ALS, a publicly available RNA-seq dataset from motor neurons in the spinal cord, which is a more physiologically relevant region for ALS, was subjected to DaPars. Here, 2.7% of genes showed significant APA changes, similar to that identified in the second sALS patient in the previous RNA-seq dataset. In addition, a significant trend to 3'UTR lengthening was observed, which was not consistent in the previous dataset. Few genes were regulated by APA in the frontal cortex, cerebellum and motor neurons from sALS patients (Supplementary Figure 5), highlighting variation the different regions of the CNS.

The 3'UTR lengthening event identified in the *UCHL1* gene is of particular relevance to ALS as its protein expression has been reduced in neurodegeneration (J. Choi et al. 2004), and loss of this enzyme contributes to motor neuron degeneration (Jara et al. 2015). The role of UCHL1 in the ubiquitin proteasome pathway makes this an important future target to study in ALS pathology. Further work is required to understand the link between 3'UTR lengthening of *UCHL1* and its protein output or localisation, particularly in motor neurons which have long dendrites.

4A.5.4 Conclusions and Future Outlook

This is the first investigation to assess APA changes in different neurodegeneration diseases from existing RNA-seq datasets. Although widespread APA changes were not observed, physiologically relevant genes associated with the nervous system were identified to show differential 3'UTR length. However, it is not possible to determine if these APA events contribute or are consequential of the neurodegenerative state.

Where possible, the analyses here have been stringent to only select genes that change in multiple patient vs control cross comparisons. This is important to account for the variability in the control samples, which can otherwise overstate the number of identified APA events. The 3'UTR length changes did not always hold true in different RNA-seq datasets, which suggests there may be a large level of individual variance which impacts APA changes. Furthermore, the sequencing depth of the RNA-seq dataset may have influenced the identification of usage of poly(A) sites which would inevitably affect if APA changes were detected.

Interestingly, in AD, PD and ALS, APA was observed in genes encoding proteins associated with the ubiquitin proteasome pathway. These three neurodegenerative diseases have common pathologies such as mitochondrial dysfunction and protein aggregation, despite exhibiting very different symptoms. Increasing evidence shows differences in RNA metabolism, including in splicing (Bai et al. 2013) in the disease state, and now APA can be added to this list.

A high importance is often placed on miRNAs in regulating gene expression. A number of miRNAs have been associated with altered expression in neurodegeneration (Supplementary Table 2) (Goodall et al. 2013), but few of these miRNAs targeted APA regulated genes identified in this analysis suggesting alternative regulation of UTR length.

All RNA-seq datasets analysed here are samples of total RNA from their sources. Consequently, any changes in APA identified cannot be separated into transcriptional or post-transcriptional APA events. Therefore, it is unclear if the changes seen are due to co-transcriptional changes during 3'end processing in the nucleus, or changes in the transcriptome appear due to alterations in post transcriptional regulation of mRNAs in the cytoplasm.

DaPars has provided an insight into APA in neurodegeneration, but 3'end sequencing of patient RNA would enable better determination of poly(A) site usage. Patient RNA samples are scarce, particularly because the affected neurons are progressively degenerated making RNA isolation from these cells problematic. However *in vitro* and *in vivo* modelling is commonly used to examine changes during neurodegeneration. The next section of this chapter explores transcriptional and post-transcriptional APA changes from 3'end RNA-seq data in an established *in vitro* model of PD.

Chapter 4B:
APA in Neurodegeneration: an *in vitro* model

4B.1. Introduction

In vitro modelling of diseases is an established method to understand the changes occurring at the molecular level in the disease state. Neurodegenerative diseases have commonly been modelled in neuroblastoma cell lines and iPSCs derived from patients and differentiated into neurons. These models can explore changes in biological pathways, changes in gene expression at the transcriptome and proteome level, and assess effects of novel drugs and treatments. Mutations in genes associated with AD, PD and ALS have commonly been used to study familial cases of the diseases. However, only in PD is there an established model in neuroblastoma cells for sporadic cases of the disease. Mechanisms of *in vitro* methods used to model neurodegeneration are outlined in Table 4.8.

Table 4.8. Methods to Model Neurodegenerative Diseases *in vitro*.

Disease	Cell modification	References
AD	Introduction of misfolded or mutated Aβ peptide. Toxic $A\beta_{1-42}$ and $A\beta_{25-35}$ synthetic peptide commonly used	(Carolindah et al. 2013)
	Derivation of iPSCs to neurons from sAD patients	(Hossini et al. 2015)
	Derivation of iPSCs from fAD patients who have mutations in associated genes *PSEN1, PSEN2, APP, MAPT, APOE*	(Mohamet, Miazga, and Ward 2014)
PD	Introduction of mutations in fPD associated genes primarily *SNCA, LRRK2, GBA*	(Bekris, Mata, and Zabetian 2010)
	Treatment with MPP+ or Rotenone which are inhibitors of Complex I that induces mitochondrial dysfunction. Model of sPD	(Ryan et al. 2014) (Sanders and Greenamyre 2014)
	Inhibition of the proteasome pathway	(Bentea, Verbruggen, and Massie 2016)
	Derivation of iPSCs to dopaminergic neurons from fPD and sPD patients	(Woodard et al. 2014)
ALS	Introduction of mutations in SOD1, FUS and TDP-43 or repeat expansion in *C9ORD72* that are associated with fALS	(Myszczynska and Ferraiuolo 2016)

4B.1.1 *In vitro* model of PD using MPP+

Numerous *in vitro* and *in vivo* models have been used in PD research. The neurotoxin 1-methyl-4-phenyl-1,2,3,6-tetrahydropyridine, better known as MPTP, has been used to model PD *in vitro and in vivo* for decades. It was first discovered to induce parkinsonian symptoms soon after administration in recreational drug users in the 1970s.

In vivo, MPTP is metabolized by monoamine oxidase B to produce the active metabolite MPP+ in glial cells (Hekkila et al. 1984) (Figure 4.10A). MPP+ itself cannot cross the blood brain barrier, but is taken up by the dopamine transporter of dopaminergic neurons. MPP+ specifically targets dopaminergic neurons, found in the substantia nigra region of the brain, in mice and nonhuman primates (Perier and Vila 2012). Dopaminergic neurons are lost during PD progression. These neurons use dopamine as a neurotransmitter and have a role in motor control, therefore their loss in PD results in tremors and muscle rigidity. They are prone to oxidative stress due to the dopamine metabolic pathway, part of which produces hydrogen peroxide.

Once in the cell, MPP+ accumulates in the mitochondria where it inhibits Complex I, the first component of the ETC (Figure 4.10B). Consequently, MPP+ inhibits OXPHOS resulting in reduced ATP production, causing energy failure and cell death. In addition, MPP+ reduces the mitochondrial membrane potential and causes increased generation of ROS, partly due to electrons which build up at Complex I (Abramov et al. 2010). There is also evidence MPP+ causes mitochondrial fragmentation *in vitro* (X. Wang et al. 2011). Interestingly, MPP+ can induce toxicity in a Complex I independent manner, as loss of Complex I activity in viable mouse midbrain neurons did not protect cells against MPP+ (W.-S. Choi et al. 2008).

Mitochondria are key to PD pathophysiology as outlined in Chapter 4.1.5c. Therefore, the mitochondrial dysfunction caused by MPP+ treatment represents a widely-used model of PD. Furthermore, mitochondrial dysfunction is a common pathology seen in neurodegenerative diseases, irrespective of inherited or sporadic causes (Yana, Wang, and Zhu 2013).

The effects of MPP+ in modelling PD, both *in vitro* and *in vivo*, have been extensively studied and phenotypes in different models are summarized in Table 4.9. Interestingly, the expression of α-synuclein, the most studied gene in PD, affects the level of MPP+ toxicity, as its depletion of reduced the neurotoxic effects of MPP+ (Ryan et al. 2014). Knockdown of α-

synuclein reduced mitochondrial fragmentation (M. Zhu, Li, and Lu 2012), reduced ROS production and reduced dopamine transporter expression on the cell surface, limiting MPP+ uptake (Fountaine et al. 2008).

Other neurotoxins have also been used to model PD. The most common of these is rotenone, also a Complex I inhibitor, which binds to the Coenzyme Q binding site of Complex I to disable the transfer of electrons from Complex I to Coenzyme Q. This inhibition of the electron flow produces free radicals, which are released into the mitochondrial matrix where ROS are generated (Subramaniam and Chesselet 2013; Sanders and Greenamyre 2014). Rotenone can passively traverse the cell membrane so its neurotoxic effects are not cell specific, however dopaminergic neurons in the brain are more sensitive to rotenone mediated Complex I inhibition (Sanders and Greenamyre 2014).

fPD has been modelled by introducing the causative genetic mutations in cell lines and animals. However, MPP+ is the most established model of sPD *in vitro* and *in vivo*, and given that mitochondrial dysfunction is also seen in fPD, MPP+ can be used to model both sPD and fPD.

Neuroblastoma cell lines are commonly used to model neurodegenerative diseases. The BE(2)-M17 cell line expresses the dopamine transporter and consequently is susceptible to MPP+ toxicity. In addition, BE(2)-M17 cells have been shown to express tyrosine hydroxylase, a key enzyme in dopamine synthesis. SH-SY5Y is another neuroblastoma cell line often used to model PD, however unlike BE(2)-M17, it does not produce dopamine under basal conditions (Ryan et al. 2014; Filograna et al. 2015).

Microarrays have been used to assess genome wide changes in gene expression upon MPP+ treatment in neuronal cell lines, showing changes in expression of genes associated with oxidative stress, neurotransmission and neuronal growth, cell cycle arrest and apoptosis (Xu et al. 2005). While there have been transcriptome wide studies on the effect of MPP+ in other dopaminergic cell lines (Krug et al. 2014), murine neuroblastoma N2A cells (Soliman 2012) and MPTP administration in mice (Pattarini et al. 2008), no deep sequencing studies have been performed in MPP+ treated BE(2)-M17 cells.

As discussed in Chapter 4A, few genes have been identified to be regulated by APA in the context of neurodegenerative disease. While DaPars analysis gave an insight of altered

poly(A) site usage in patient samples, variations in sequencing depth and lack of complete information on the sample origins make it difficult to fully assess the extent of APA regulation. Therefore, an *in vitro* model of neurodegeneration was chosen to further investigate APA changes. Given its extensive established use in modelling PD, both *in vitro* and *in vivo*, MPP+ was chosen here as the neurotoxin to model neurodegeneration in undifferentiated BE(2)-M17 cells, to assess transcriptome changes in gene expression and APA.

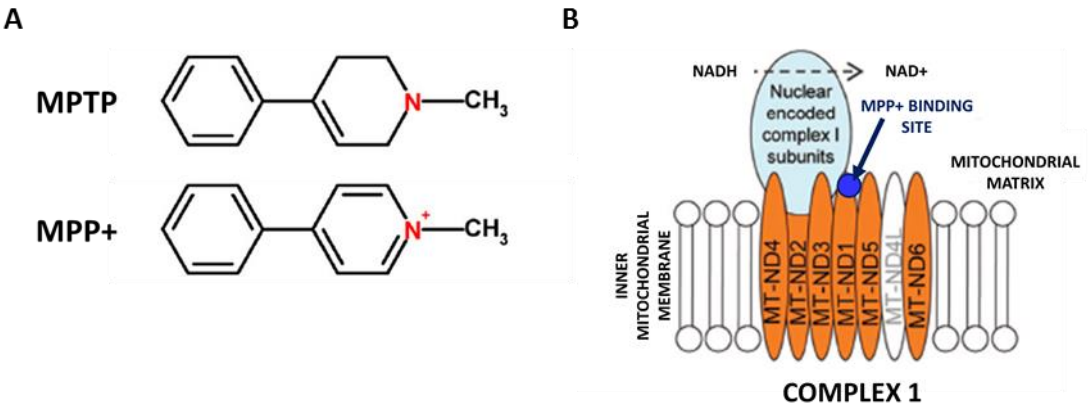


Figure 4.10 MPP+ inhibits Complex I.

A. MPTP (upper) can cross the blood brain barrier *in vivo* and is metabolized to MPP+ (lower) in glial cells. MPP+ is taken up by the dopamine receptor expressed in dopaminergic cells which are concentrated in the substantia nigra region of the brain.

B. Schematic modified from (Krug et al. 2014) showing the MPP+ binding site (blue) in Complex I in the inner mitochondrial membrane. The hydrophobic core subunits of Complex I (orange) are encoded by the mitochondrial genome.

Table 4.9. The Effects of MPP+ on Different Cellular Pathways.

Pathway	Cell line/Tissue	Phenotype described with MPP+ treatment	Reference
α-synuclein related	Mouse MPTP model; SH-SY5Y; Human midbrain cell line	Increased protein expression. Increased transcriptional upregulation and aggregation.	(Vila et al. 2000) (Kalivendi et al. 2004)(Fountaine et al. 2008)
	Substantia nigra of mice	Alternative splicing removes exon 10 producing a shorter 112 amino acid protein instead of the 140 amino acid WT protein. Overexpression of the shorter isoform induces proteasomal dysfunction and cell death.	(Kalivendi et al. 2010)
	PC12 cells SH-SY5Y cells	MPP+ treatment with α-synuclein knockdown showed reduced mitochondrial fragmentation, promoted cell survival and reduced DAT expression which reduced MPP+ uptake.	(M. Zhu, Li, and Lu 2012) (Fountaine et al. 2008)
	Rat cortical neurons	Overexpression of miR-7 and miR-153, which bind to the *SNCA* 3'UTR to downregulate its expression, reduced neurotoxicity by MPP+.	(Fragkouli and Doxakis 2014)
	SH-SY5Y Rat brain mitochondria	Aggregation of WT and A53T mutant of α-synuclein causes release of Cytochrome C to induce apoptosis.	(Parihar et al. 2008)
Induction of Apoptosis	Rat neuronal cultures; Rat nigrostriatal dopaminergic cells	Release of Cytochrome C and Apoptotic Inducible Factor (AIF) to induce caspase mediated and caspase independent apoptosis respectively.	(Lim et al. 2007) (Hung et al. 2014)
	MN9D	Upregulation of apoptotic genes identified through microarray analysis.	(J. Wang et al. 2007)
	Dopaminergic neurons derived from Human ESCs	Induces caspase 3 induction causing apoptosis. Increased cell death of Tyrosine Hydroxylase (TH) positive colonies.	(Yan et al. 2013)
	SH-SY5Y cells	Increase in p53 activity causes apoptosis.	(Kitamura et al. 1998)
	Mouse MPTP model BE(2)-M17 SH-SY5Y	Permeabilisation of lysosomal and mitochondrial membranes via upregulation of the pro-apoptotic factor BAX which is associated with neurodegeneration. Proteases leaked from lysosome to cytoplasm causing cell death.	(Bové et al. 2014)
Autophagy	Rat nigrostriatal dopaminergic cells	Induced autophagy as shown with increased LC3-II protein levels. Autophagy engulfs both damaged and healthy mitochondria, so can result in mitochondrial loss resulting in cell death.	(Hung et al. 2014) (X. Wang et al. 2011)
	BE(2)-M17	Dysregulated autophagy with increased formation of autophagosome like structures and upregulation of mTOR pathway.	(Keane et al. 2015)

		Failure of autophagic protein breakdown also observed.	
	BE(2)-M17 and Mouse MPTP model	Accumulation of autophagosomes. Reduced lysosome numbers to prevent degradation of cytoplasmic proteins.	(Dehay et al. 2010)
	BE(2)-M17	Increased lysosomal pH caused deacidification, which inhibited autophagy.	(Keane et al. 2015)
Cell Transport	Squid axoplasm	Impaired microtubule dynamics and anterograde axonal transport.	(Morfini et al. 2007)
Dopamine homeostasis	Mouse striatal slices and ventral mid-brain neuronal cultures	Depleted vesicular dopamine storage. Reduced dopamine release. Accumulation of cytosolic dopamine. Inhibition of reuptake of released dopamine by dopamine transporter.	(S. J. Choi et al. 2015)
	SH-SY5Y Rat nigrostriatal dopaminergic cells	Reduced expression of TH and enzymes associated with dopamine metabolism.	(Lee, Kim, and Lee 2011) (Hung et al. 2014)
	Mouse midbrain neurons Mouse neurons	Redistribution of dopamine from storage and secretory vesicles to the cytoplasm. Depletion of dopamine in cells reduced MPP induced cell death. Altered dopamine transporter mediated transport. Accumulation of cytosolic dopamine induced neurotoxicity	(Lotharius and O'Malley 2000) (S. J. Choi et al. 2015)
Gene Expression	Dopaminergic cells derived from human midbrain neural precursor cells	Alteration in expression of paraspeckle genes associated with increased nuclear retention of RNA. Transcriptome wide changes mediated through transcription factor ATF4.	(Krug et al. 2014)
	Mouse MPTP model	Promotes translocation of RelA, a component of NFkB, to the nucleus to suppress expression of NFkB targets.	(D. C. Choi et al. 2014).
Mitochondrial dynamics	SH-SY5Y	Mitochondrial fragmentation caused by MPP+ treatment due to DLP1 (dynamin like protein 1) dependent fragmentation.	(X. Wang et al. 2011)
	Mouse mid-brain cultures	Reduced mitochondrial trafficking and depolarization of axonal mitochondria.	(Kim-Han, Antenor-Dorsey, and O'Malley 2011)
	BE(2)-M17 and Mouse MPTP model	Accumulation of abnormal mitochondria.	(Dehay et al. 2010)
Mitochondrial dysfunction	Mouse MPP+ model	Binds Complex I at two sites to interrupt electron flow. Inhibits ATP synthesis.	(Mizuno et al. 1987)
	Rat dopaminergic cells	Reduced expression of Cytochrome C oxidase.	(Hung et al. 2014)
Mitochondrial gene expression	SH-SY5Y Mouse MPTP model	Decreased expression of *TFAM* (mitochondrial transcription factor A) mediated mitochondrial gene expression.	(Piao et al. 2012)

Mitochondrial membrane potential	SH-SY5Y BE(2)-M17	Opening of mitochondrial membrane pores dissipates mitochondrial membrane potential. Subsequent release of Cytochrome C induces apoptosis.	(Lee, Kim, and Lee 2011) (Keane et al. 2015)
Oxidative Phosphorylation	BE(2)-M17	Inhibition of Complex I reduced ATP production. Inhibition of α-ketoglutarate dehydrogenase of the Krebs cycle which further inhibits ATP production.	(Keane et al. 2015) (Banerjee et al. 2009)
	Dopaminergic cells derived from human midbrain neural precursor cells	Altered flux through the pyruvate dehydrogenase complex.	(Krug et al. 2014)
Oxidative stress	Rat nigrostriatal dopaminergic cells	Increased Heme-Oxygenase-1 protein levels and increased lipid peroxidation.	(Hung et al. 2014)
	N27 dopaminergic rat cells	Inhibition of Complex I led to build up of electrons causing ROS generation which oxidatively damages proteins and lipids.	(Zawada et al. 2011) (Liu et al., 1992)
	Mouse mid-brain cultures	ROS formation from oxidation of intracellular dopamine.	(Lotharius and O'Malley 2000)
	SH-SY5Y	MPP+ Complex I inhibition causes ROS generation causing oxidation of proteins, lipids and DNA.	(Kalivendi et al. 2003)
	Dopaminergic cells derived from human midbrain neural precursor cells	Altered methionine/cysteine metabolism suggesting increased oxidative stress.	(Krug et al. 2014)
	SH-SY5Y	Increased activation of Nitric Oxide synthase (NOS) producing nitric oxide causing stress.	(Fountaine et al. 2008)
	BE(2)-M17	Decreased GTP/ATP levels which decreased synthesis of BH4, an anti-oxidant which aids coping under oxidative stress. BH4 levels also reduced in PD patients.	(Ryan et al. 2014)
	Mouse midbrain neurons	Dopamine release from intracellular stores causes formation of hydroxyl radicals.	(Lotharius and O'Malley 2000)
Signal transduction	SH-SY5Y	Increased ERK/MAPK phosphorylation Inhibition of phosphorylation reduced MPP+ neurotoxicity.	(Gomez-Santos et al. 2002)
Ubiquitin Proteasome Pathway	SH-SY5Y	Reduced activity of the proteasome which prevents protein degradation.	(Caneda-Ferrón et al. 2008)
	MPTP Mouse Model	Altered abundance of proteins involved in ubiquitin proteasome pathway.	(X. Zhang et al. 2010)
	BE(2)-M17	Reduced protein degradation.	(Keane et al. 2015)

4B.2. Results

4B.2.1 Characterizing the MPP+ Model of PD in BE(2)-M17 cells

Different cell lines are susceptible to cellular stress by MPP+ to different extents, therefore varying concentrations of the neurotoxin are required to produce a model of PD. While some human dopaminergic cell lines, such as differentiated LUHMES, show neuronal insults at a concentration of 5 µM MPP+ for 24-72 hours (Krug et al. 2014), other studies have used concentrations up to 2 mM for shorter time points. High concentrations of MPP+ can kill cells by increasing ROS production and ATP depletion. In this study, the aim was to assess changes in APA, therefore an optimal concentration needed to be determined, where OXPHOS was significantly inhibited but the cells were still healthy enough to continue transcription. To assess the optimal concentration for BE(2)-M17 to investigate APA, the changes in oxygen consumption rate (OCR) were tested for concentrations of MPP+ between 0.05-1 mM. Undifferentiated BE(2)-M17 cells were used in line with previous MPP+ models (Ryan et al. 2014).

An optimal concentration for MPP+ was determined to be 0.5 mM, by selecting the highest concentration at which cells showed significant Complex I inhibition but were still viable to assess changes in gene expression and APA after 24 hours of treatment. Cell viability was determined by light microscopy (Figure 4.11A) and mitochondrial dysfunction was measured by changes in the OCR determined using a X96 Seahorse (Figure 4.11B). This instrument assesses the basal respiration rate, and the maximal respiratory capacity of cells by injecting the drugs oligomycin, FCCP and antimycin A at different time intervals (Chapter 2.9). Cells treated with 0.5 mM MPP+ showed a significant reduction in the OCR both at the basal level and upon addition of FCCP which shows reduction in mitochondrial respiration and OXPHOS. The FCCP injection dissipates the proton gradient and therefore provides an indication of the maximal respiratory capacity of the cells. MPP+ treated cells clearly showed a reduced maximal respiratory capacity, again indicating the cellular impact of MPP+.

Lower concentrations of MPP+ did not affect the OCR significantly and higher concentrations led to changes in cell morphology and cell death (Figure 4.11A, right). The extent of cell death was not quantified here, but a previous study showed 24-hour treatment of 0.5 mM MPP+ in BE(2)-M17 cells caused 18% cell death (X. Wang et al. 2011) which still

leaves over 80% of cells that are viable for RNA extraction. Therefore, a concentration of 0.5 mM MPP+ was selected to assess APA in this *in vitro* model of neurodegeneration.

The increased production of ROS is associated with neurodegenerative diseases. ROS oxidation of lipids, nucleic acids and proteins has been linked to exacerbating neurodegeneration. The process of OXPHOS naturally produces superoxide. MPP+ treatment has been shown to increase superoxide generation through Complex I inhibition (Zawada et al. 2011), which was linked to increased mitochondrial fragmentation. To assess superoxide production, a MitoSOX^{TM} assay was performed (Chapter 2.10) which enables detection of superoxide produced by mitochondria in live cells using a red fluorogenic dye. BE(2)-M17 cells were treated for 24 hours with 0.5 mM MPP+, after which increased superoxide levels were detected with MPP+ treatment (Figure 4.11C).

MPP+ treatment in other neuronal cell lines has previously been shown to induce (Keane et al. 2015; Cherra et al. 2010) and deregulate (Hung et al. 2014; X. Wang et al. 2011; Dehay et al. 2010) autophagy. In addition, accumulation of autophagosomes has been observed in PD patients (Poewe et al. 2017). To confirm the induction of autophagy in this *in vitro* PD model, a Cyto-ID kit assay was performed which detects the number of autophagososmes via a fluorescent green dye (Chapter 2.11). This is an indicator of autophagic flux, which is usually a measure of autophagic degradation activity. Here, 0.5 mM MPP+ treatment resulted in increased autophagosome accumulation which corresponds to increased autophagic flux compared to control cells, as detected by the level of green fluorescence (Figure 4.11D, lower panel). Induction of autophagy may be a cellular stress response to cope with oxidative stress.

These data conclude that the 0.5 mM MPP+ treatment for 24 hours in BE(2)-M17 cells is mimicking a number of physiological defects observed in PD, verifying it is an *in vitro* model of PD.

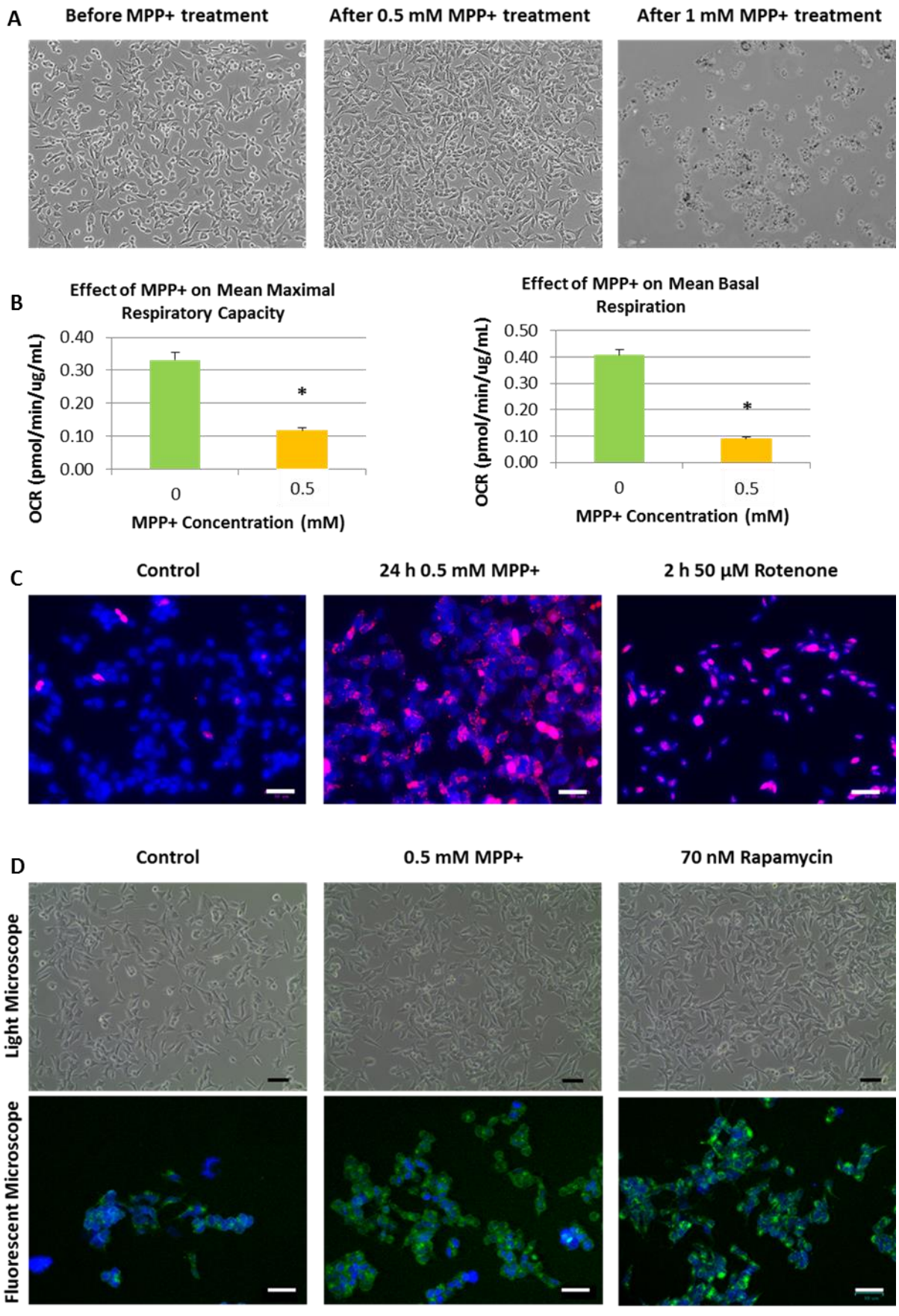

A
Before MPP+ treatment
After 0.5 mM MPP+ treatment
After 1 mM MPP+ treatment
B
Effect of MPP+ on Mean Maximal Respiratory Capacity
OCR (pmol/min/ug/mL)
0.40
0.30
0.20
0.10
0.00
*
0
0.5
MPP+ Concentration (mM)
Effect of MPP+ on Mean Basal Respiration
OCR (pmol/min/ug/mL)
0.50
0.40
0.30
0.20
0.10
0.00
*
0
0.5
MPP+ Concentration (mM)
C
Control
24 h 0.5 mM MPP+
2 h 50 µM Rotenone
D
Control
0.5 mM MPP+
70 nM Rapamycin
Light Microscope
Fluorescent Microscope

Figure 4.11. Characterizing the BE(2)-M17 MPP+ *in vitro* Model for PD.

A. Light microscope images (20 x magnification) show BE(2)-M17 cells before (left) and after 0.5 mM (middle) or 1 mM (right) MPP+ treatment for 24 hours. No morphological changes were seen in concentrations at 0.5 mM but at 1 mM cell rounding and detachment was observed to indicate significant cell death.

B. Bar charts to show that treatment of 0.5 mM MPP+ for 24 hours significantly reduces OXPHOS (T-test, * = $p<0.01$, n = 3) indicating mitochondrial dysfunction. The X96 Seahorse measured the OCR of cells to indicate the maximum mitochondrial capacity (left) and the basal respiration rate (right) which are fundamental parameters to assess mitochondrial function. Samples were normalized per µg protein, quantified using a BCA assay.

C. MitoSOX™ assay was performed to assess superoxide generation in mitochondria in untreated and MPP+ treated cells. Red fluorescence indicates level of mitochondrial superoxide production. Rotenone was used as a positive control. Scale bar = 50 µM.

D. Upper panels: No obvious changes in cell morphology with MPP+ or rapamycin treatment. Black scale bar is 500 µM. Lower panels: Green fluorescence indicates number of autophagosomes tagged using CYTO-ID® Autophagy Detection Kit. Increased induction of autophagy observed with MPP+ treatment. Rapamycin, a known inducer of autophagy, was used as a positive control. White scale bar is 50 µM. In **C** and **D**, nuclei are stained blue with Hoechst stain.

4B.2.2 MPP+ Treatment Upregulates Genes of the ER Stress Pathways

BE(2)-M17 is a commonly used cell line to model PD, however, changes in the transcriptome with MPP+ treatment have not been assessed using RNA-seq. To assess transcriptome changes in MPP+ treated cells, RNA was isolated from the cytoplasm and nuclei of the MPP+ treated and untreated cells. Libraries of two biological replicates were generated using the 3'Quant Seq Kit (Lexogen). After quality assessment on a Bioanalyzer, libraries were subjected to 3'end sequencing on the Ion Proton platform and a well-established bioinformatics pipeline was subsequently used to assess changes in gene expression and APA as described in Chapter 3.

Gene expression changes in the nucleus are likely to reflect changes in transcription. Comparison of the nuclear fractions showed 314 and 335 genes were up and downregulated respectively (Fisher's exact Test $p<0.01$, FC >2). It is more relevant to assess gene expression changes in the cytoplasm where transcripts are translated and therefore would affect the proteome. In the cytoplasm, a change in the expression of 518 genes were upregulated and 89 genes were downregulated (Fisher's exact Test $p<0.01$, FC >2) out of 12331 genes expressed in MPP+ treated compared to untreated BE(2)-M17 cells (Figure 4.12A purple and blue dots). Interestingly, only 74 genes were upregulated and 9 genes were downregulated in both the cytoplasm and the nucleus (Figure 4.12A, blue dots). This suggests that gene expression changes in MPP+ treated cells are predominantly regulated through post-transcriptional mechanisms, and that most of the nuclear transcriptome changes do not infiltrate to the cytoplasm.

Mitochondrial dysfunction caused by MPP+ is known to affect OXPHOS, which could affect the expression of glycolysis genes such as *GAPDH* to compensate for ATP production. However, this housekeeping gene showed no significant change in expression upon MPP+ treatment at the mRNA level in the sequencing data, and this was verified with RT-PCR (Figure 4.12B).

GO analysis for upregulated genes in both the nucleus and the cytoplasm showed an enrichment in genes associated ER stress (Figure 4.12C). ER stress responses have previously been associated with neurodegeneration (Reviewed in (Xiang et al. 2016; Hoozemans and Scheper 2012)), and MPP+ may induce this stress response. Upregulation of genes associated

with apoptosis were also identified in the cytoplasm, as in previous studies (J. Wang et al. 2007), despite no observed cell death.

In the nucleus, similar numbers of genes were up and downregulated, however in the cytoplasm, only 16.3% of changing genes were downregulated, and these showed no enrichments in biological pathways from GO analysis. Genes associated with mitochondrial function, translation and transport and ATP synthesis showed only a moderate downregulation (Fisher's exact Test, $p<0.01$, FC <2 but >1.3). This suggests that inhibition of OXPHOS via regulation of transcription is limited. Reduced expression of genes associated with dopamine metabolism such as tyrosine hydroxylase were observed, as in previous MPP+ models of PD (Lee, Kim, and Lee 2011; Hung et al. 2014).

These data show a cytoplasmic upregulation of genes associated with ER stress, but only a modest downregulation of genes associated with mitochondrial function in the MPP+ model of PD in BE(2)-M17 cells. Importantly, the nuclear transcriptome changes had a limited overlap with gene expression changes observed in the cytoplasm, suggesting predominantly, a post-transcriptional regulation of the transcriptome upon exposure to MPP+ in BE(2)-M17 cells.

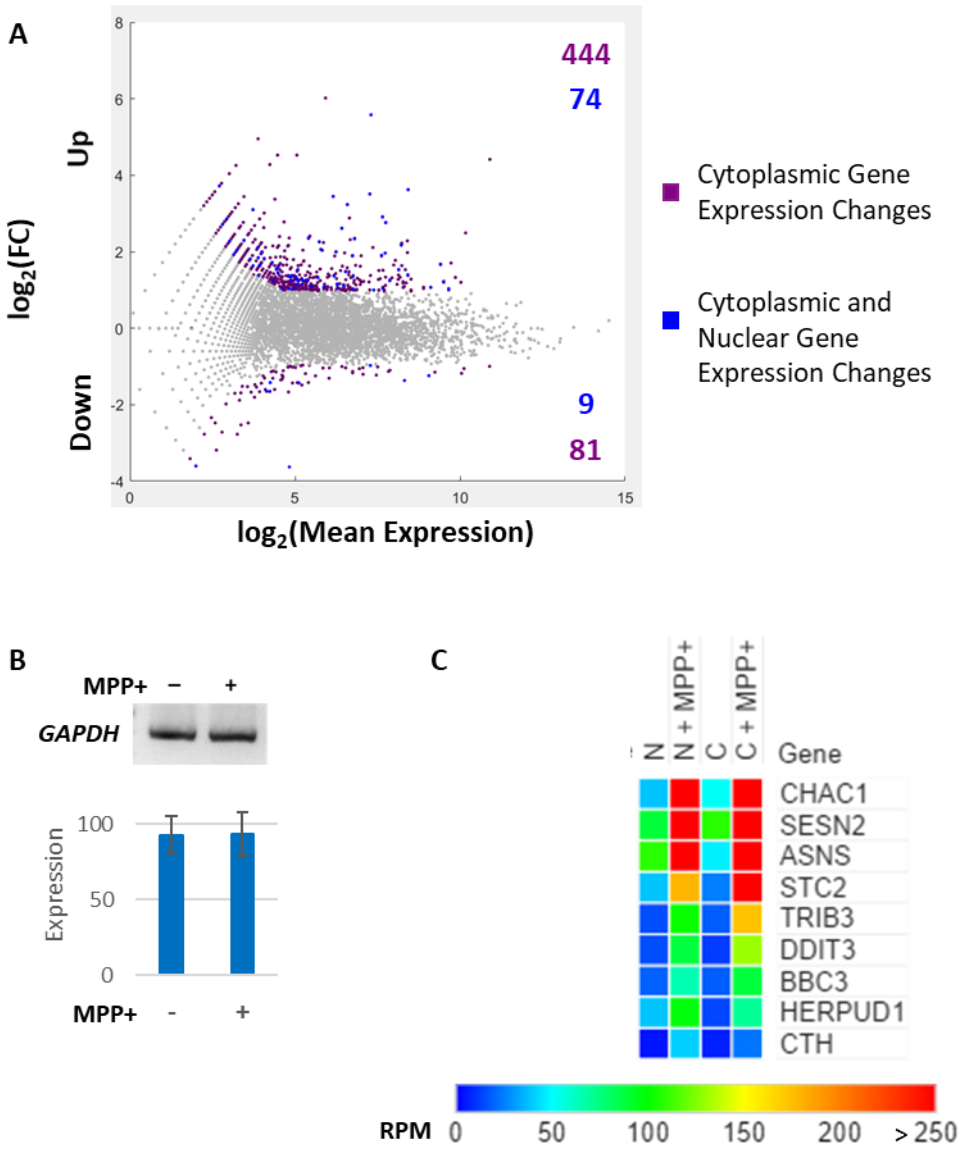


Figure 4.12. ER Stress Related Genes Upregulated with MPP+ Treatment.

A. An MA plot to show genome wide expression changes in the cytoplasm with 24 hour 0.5 mM MPP+ treatment compared to untreated BE(2)-M17 cells. A total of 525 genes showed significant expression changes (Fisher's exact Test, $p<0.01$, with a FC >2) uniquely in the cytoplasm (purple) while 83 genes were also altered in the nucleus (blue).

B. Upper panel: RT-PCR using RNA isolated from the whole cell fraction verifying constant *GAPDH* expression with MPP+ treatment. Lower panel: bar chart of quantified band intensities by ImageJ from RT-PCR. Error bars represent standard deviation, n = 3.

C. A heatmap to show genes associated with ER stress upregulated in the nucleus and cytoplasm upon MPP+ treatment. Reads per million (RPM) have been normalised to GAPDH.

4B.2.3 Protein Degradation Genes Regulated by APA in MPP+ Treated Cells

As discussed above, studies have assessed gene expression changes with MPP+ treatment, but none have assessed the role APA plays on the transcriptome in this PD model. To compare transcriptional and post-transcriptional APA regulation in MPP+ treated and untreated cells, RNA-seq reads from nuclear and cytoplasmic RNA isolates were processed through a bioinformatics pipeline (Hoque et al. 2013; Neve et al. 2016) to identify MPP+ induced APA profile changes. A total of 5933 APA events were identified in MPP+ treated compared to untreated cells in the nuclear fraction, 116 of which showed significant profile changes (Figure 4.13A). Overall, more 3'UTR lengthening than shortening events were identified, suggesting increased usage of the distal poly(A) site (Fisher's exact Test, $p<0.05$). GO analysis of genes showing 3'UTR lengthening in the nucleus were enriched in transcriptional regulation and chromatin organization while the genes showing 3'UTR shortening were not enriched in any biological pathways.

Next the APA events in the cytoplasmic fractions of MPP+ treated and untreated cells were assessed. Here, 182 statistically significant changing APA events were identified (Figure 4.13B), which only amounted to 3.13% of all APA events. This suggests that 3'UTR-APA is not affected on a global scale in this model of PD. Furthermore, unlike in the nucleus, there was no significant trend to either 3'UTR shortening or lengthening. There was a surprisingly low overlap between the genes showing APA changes in the nucleus and the cytoplasm (Figure 4.13C) indicating that many of the nuclear changes, like with gene expression, have a limited impact on the cytoplasmic transcriptome. Only 13.7% genes appeared to be both differentially expressed and regulated by APA (Figure 4.13D), suggesting APA has little effect on transcript abundance with MPP+ treatment.

GO analysis for both lengthened and shortened UTRs in the cytoplasm showed an enrichment in genes associated with protein catabolic processes. Misfolded proteins are a common pathophysiological occurrence in neurodegenerative diseases (Bendor, Logan, and Edwards 2013; Parakh and Atkin 2016). Therefore, this data suggests that genes linked to protein turnover, which is important in PD pathology, are regulated by APA in the *in vitro* MPP+ model of PD.

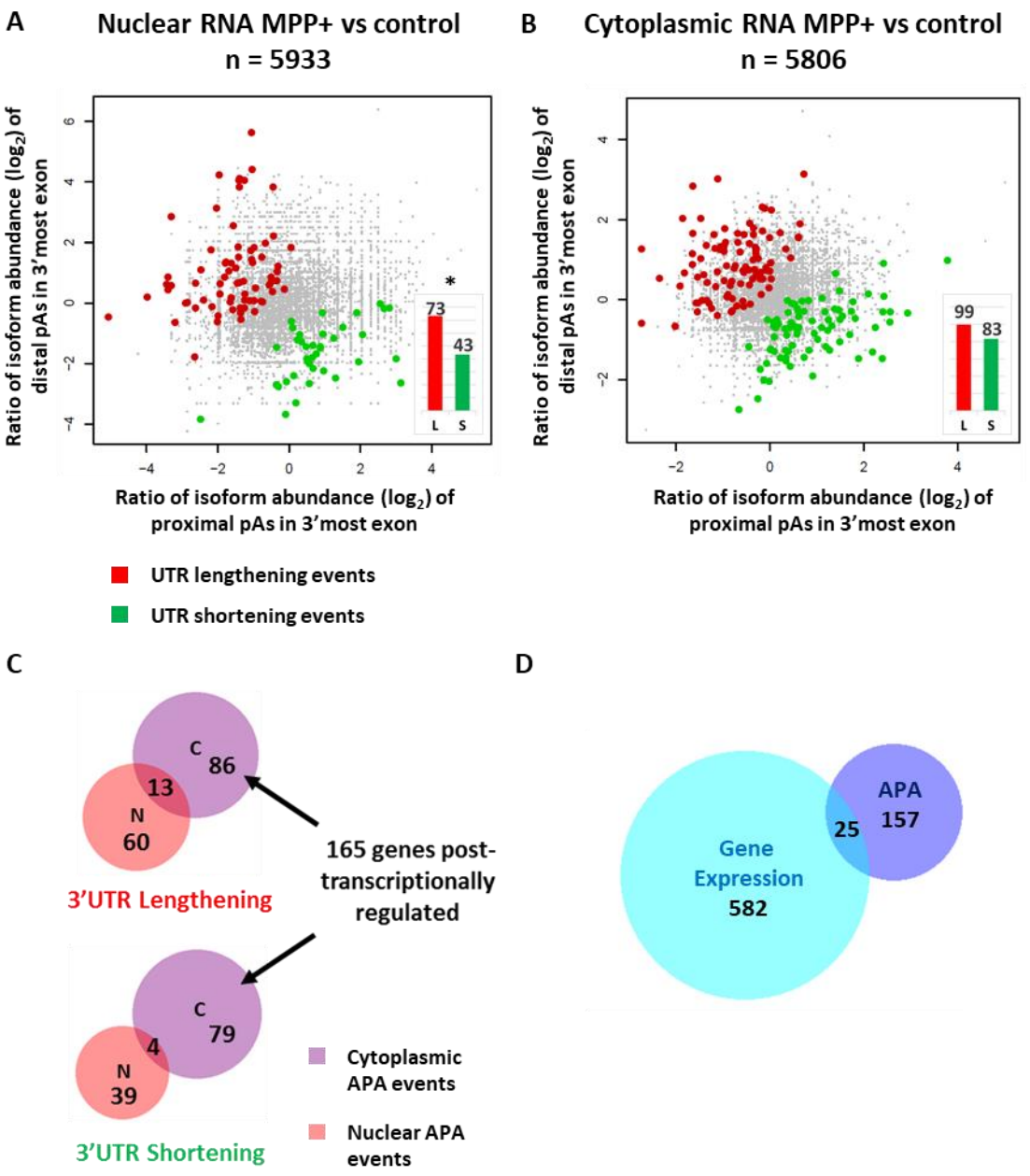


Figure 4.13. Post-transcriptional Regulation of 3'UTR APA Profiles with MPP+ Treatment.

A. Comparison of the nuclear fractions identified 116 significant APA events (Fisher's exact Test, $p<0.01$, with a minimum 5% change in APA isoform abundance) in 24 hour 0.5 mM MPP+ treated compared to untreated cells. A trend to 3'UTR lengthening (red dots and bar) compared to 3'UTR shortening (green dots and bar) (Fisher's exact Test, * = $p<0.05$) was observed with MPP+ treatment. n = number of APA events identified between the two fractions.

B. Comparison of the cytoplasmic fractions in MPP+ treated and untreated cells identified 182 significant APA events but there was no significant trend to 3'UTR lengthening or 3'UTR shortening.

C. A Venn diagram to show that few genes showed significant APA changes in both the cytoplasm (purple) and the nucleus (red).

D. A Venn diagram to show 13.7% of genes exhibiting significant APA (blue) showed significant changes in gene expression (cyan).

One gene associated with protein degradation, where significant 3'UTR shortening was observed, is *PSMB2* (Figure 4.14A). The PSMB2 protein is a component of the core 20S proteasome that degrades proteins in the ubiquitin proteasome pathway (Poewe et al. 2017). As discussed in Chapter 4.1.5a, deregulation of the ubiquitin proteasome pathway is linked to neurodegeneration. The shortening event was only observed in the cytoplasm, suggesting post transcriptional regulation (Figure 4.14A). Three poly(A) sites were used in BE(2)-M17 cells, but this analysis only assesses usage of the two most commonly used poly(A) sites. To further validate the RNA-seq data for *PSMB2*, an RT-PCR approach was employed using primers targeting the coding region (CR) and the alternative UTR (Figure 4.14B). This confirmed that the expression of *PSMB2* does not change at the overall transcript level and that the 3'UTR undergoes MPP+ dependent shortening (Figure 4.14C). A miR-505 target site has been identified in the alternative UTR of the *PSMB2* transcript (Chapter 2.24), however expression changes of this transcript have not been associated with PD or oxidative stress. To test if 3'UTR shortening impacts protein output, whole-cell protein lysate of MPP+ treated and untreated cells was subjected to western blotting. PSMB2 protein levels were significantly reduced in MPP+ treated compared to untreated cells (Figure 4.14D), suggesting the 3'UTR shortening event may impact protein output by affecting translatability.

The 3'UTR of *PSMB2* has previously been investigated because it contains inverted Alu elements, which are a type of transposable element in the SINE (short interspersed nuclear elements) family. These inverted Alu elements, found in the alternative UTR of *PSMB2* (Figure 4.14E), can hybridise and form a double-stranded RNA (dsRNA) structure in HEK293 cells (Capshew, Dusenbury, and Hundley 2012). 3'end sequencing data from the Furger Lab showed that HEK293 cell line uses the same two poly(A) sites as the BE(2)-M17 cell line (Supplementary Figure 6). The secondary structure of the 3'UTR isoforms was predicted using an RNA structure Webserver (Chapter 2.23), where the longer 3'UTR isoform showed a dsRNA duplex structure (Figure 4.14F). Reports have previously shown mRNAs containing Alu elements in the 3'UTR are nuclear retained, however Capshew and colleagues showed that the *PSMB2* transcript is efficiently exported to the cytoplasm (Capshew, Dusenbury, and Hundley 2012). Interestingly, the presence of this dsRNA duplex structure was shown to

repress translational efficiency of the longer *PSMB2* 3'UTR isoform (Capshew, Dusenbury, and Hundley 2012). Therefore, the possibility that the observed reduced expression of the PSMB2 protein may be due to post-translational regulatory mechanisms, independent of 3'UTR shortening, cannot be excluded.

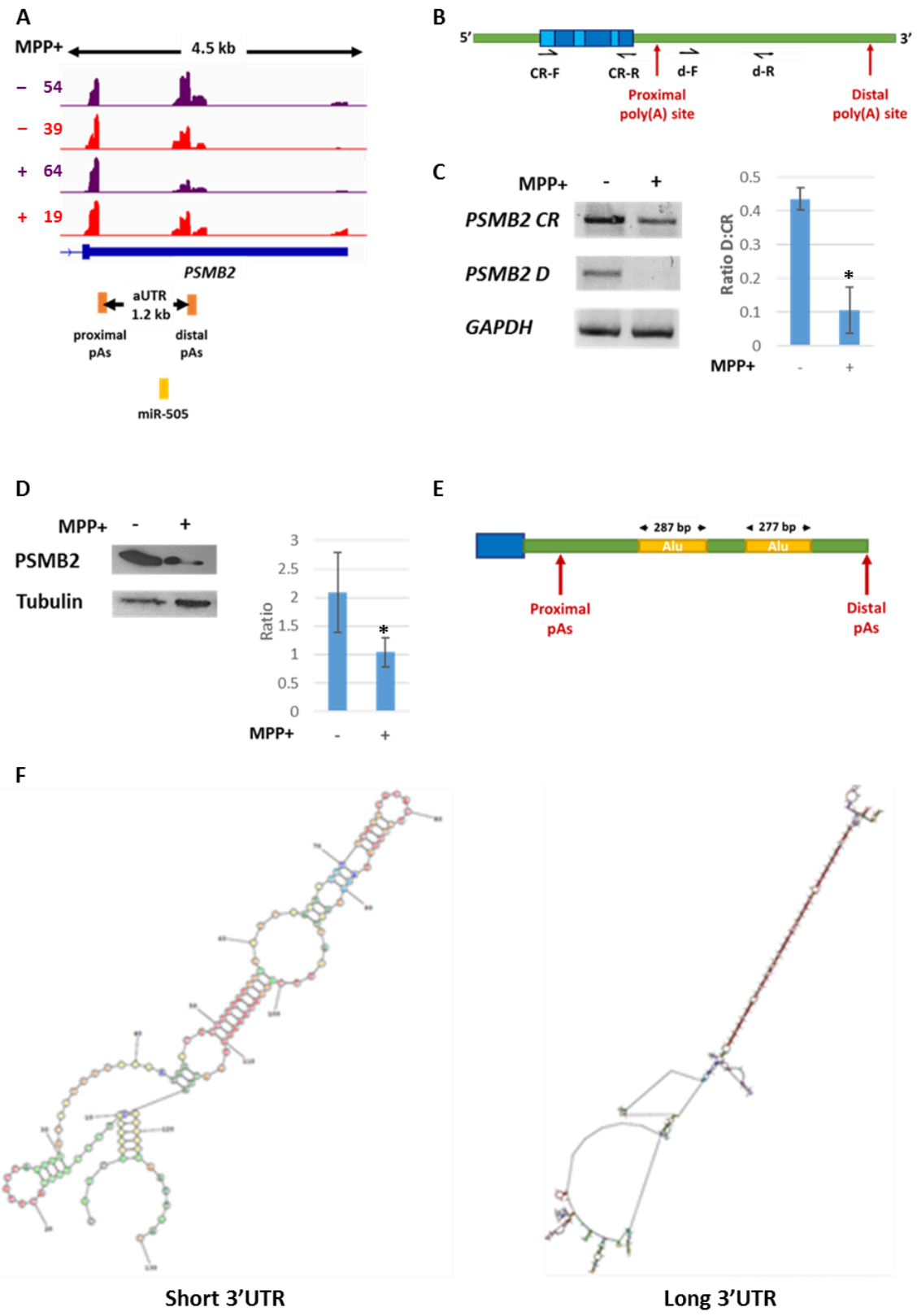

A
MPP+
4.5 kb
– 54
– 39
+ 64
+ 19
PSMB2
aUTR
1.2 kb
proximal
pAs
distal
pAs
miR-505
B
5'
3'
CR-F
CR-R
d-F
d-R
Proximal
poly(A) site
Distal
poly(A) site
C
MPP+ - +
PSMB2 CR
PSMB2 D
GAPDH
Ratio D:CR
0.5
0.4
0.3
0.2
0.1
0
*
MPP+ - +
D
MPP+ - +
PSMB2
Tubulin
Ratio
3
2.5
2
1.5
1
0.5
0
*
MPP+ - +
E
287 bp
277 bp
Alu
Alu
Proximal
pAs
Distal
pAs
F
Short 3'UTR
Long 3'UTR

Figure 4.14. 3'UTR Shortening in *PSMB2*.

A. *PSMB2* showed 3'UTR shortening in the cytoplasm (purple tracks) but not the nucleus (red tracks) upon 0.5 mM MPP+ treatment for 24 hours in BE(2)-M17 cells. Numbers on the left indicate reads per million (RPM) read numbers from sequencing data of the most abundant isoform, visualised using auto-scale on the IGV browser.

B. Schematic to show the primers used to amplify all *PSMB2* transcripts in the coding region (CR) and only the distal isoform (D).

C. Left panel: RT-PCR from cytoplasmic RNA showing representative bands of the total *PSMB2* transcript compared to the distal isoform, GAPDH used as a loading control. Right panel: quantified intensities of the bands plotted as a ratio of the distal isoform of *PSMB2* compared to the total *PSMB2* transcripts using Image J. Error bars show standard deviation, n = 3. T-test *= $p<0.01$.

D. Left panel: a representative western blot showing reduced PSMB2 expression with MPP+ treatment from protein samples isolated from whole cell fractions. Tubulin used as a protein loading control. Right panel: a bar chart showing quantified intensities of western blots showing a significant reduction in the ratio of PSMB2:Tubulin with MPP+ treatment indicating reduced PSMB2 expression. Error bars show standard deviation, n = 3. T-test *= $p<0.05$.

E. Schematic of the 3'UTR of *PSMB2* showing location of Alu elements (yellow).

F. Secondary structure predictions to highlight the distinct differences between the shorter 3'UTR (left) and longer 3'UTR (right) isoforms of *PSMB2*.

4B.2.4 Regulatory Cis-elements may Mediate Cytoplasmic APA profiles with MPP+ Treatment

Numerous miRNAs, which can post-transcriptionally regulate the transcriptome primarily through mRNA degradation, are associated with exacerbating or alleviating neurodegeneration (Supplementary Table 2). To assess the extent of miRNA mediated regulation on the cytoplasmic APA profiles with MPP+ treatment, miRNAs enriched in the alternative UTRs of APA regulated genes were investigated using miRNA enrichment analysis (Chapter 2.21), as described in Chapter 3.

Four miRNA target sites were found to be uniquely enriched in the gene alternative UTRs which showed 3'UTR shortening (Figure 4.15A). Interestingly, of these, miR-221 has previously shown to be upregulated in the cerebral cortex of PD brain samples (Tatura et al. 2016). Upregulation of miR-221 could explain a UTR shortening event, as it targets the longer isoforms for degradation. miR-221 targeted just two genes that showed 3'UTR shortening, suggesting a limited effect on global UTR landscape changes. One of these genes was *MRPS16*, which encodes a mitochondrial ribosomal protein (Figure 4.15B). Mitochondrial dysfunction is a hallmark of the MPP+ treatment, and this UTR shortening event mediated by miR-221 may affect *MRSP16* regulation thereby contributing to mitochondria related pathology.

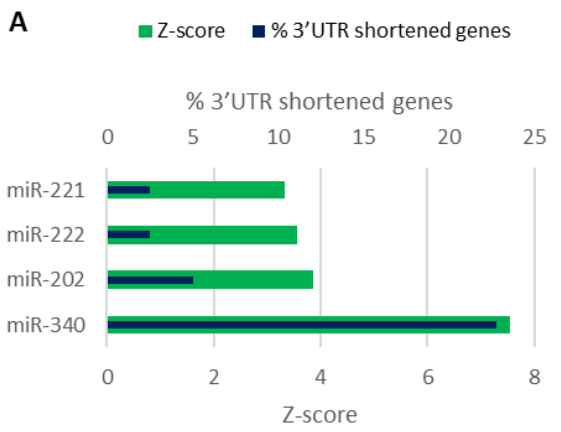
miR-340 was identified to target 22.8% of genes showing 3'UTR shortening, however expression changes with MPP+ treatment have not been verified. Targets of miR-340 included *NUCKS1*, a gene associated as a risk factor gene in PD (Satake et al. 2009), and *IDE*, which encodes an insulin degrading enzyme, that also degrades peptides, including Aβ in AD.

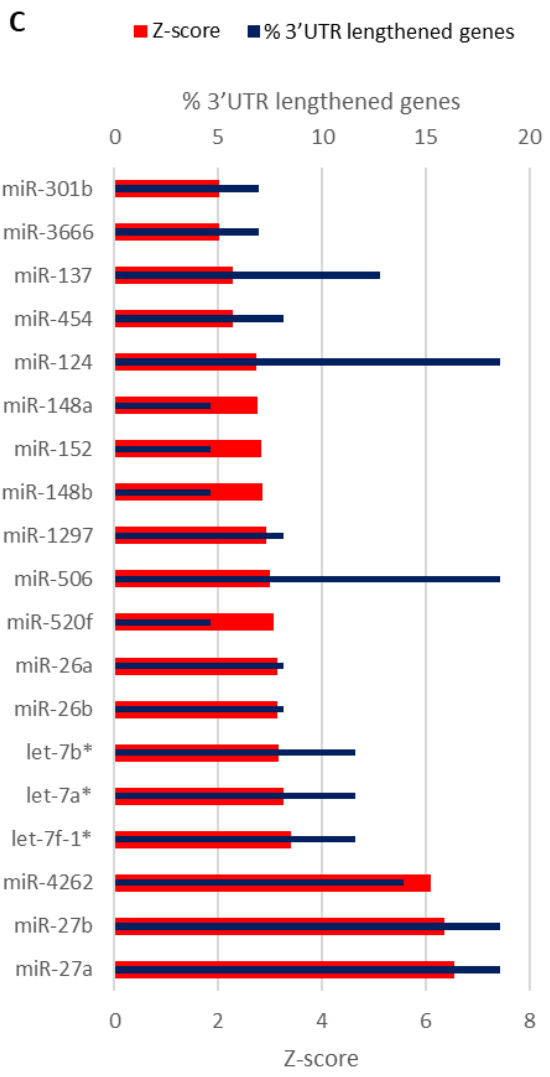
In the cohort of genes that showed 3'UTR lengthening, 19 miRNAs were uniquely enriched (Figure 4.15C). Downregulation of these miRNAs may explain the stabilisation of the longer isoforms of these genes, resulting in 3'UTR lengthening. Notable miRNAs enriched in alternative UTRs of 3'UTR lengthened genes were miR-148b and miR-124 as they have shown to be downregulated in PD or in the MPP+ model of PD (Vallelunga et al. 2014; Kanagaraj et al. 2014). A target of miR-124 that showed 3'UTR lengthening is *STMN2* (Figure 4.15D). This gene encodes a neuronal specific protein which is a regulator of microtubule dynamics and axonal transport (Shin et al. 2012). Knockdown of this protein is associated with

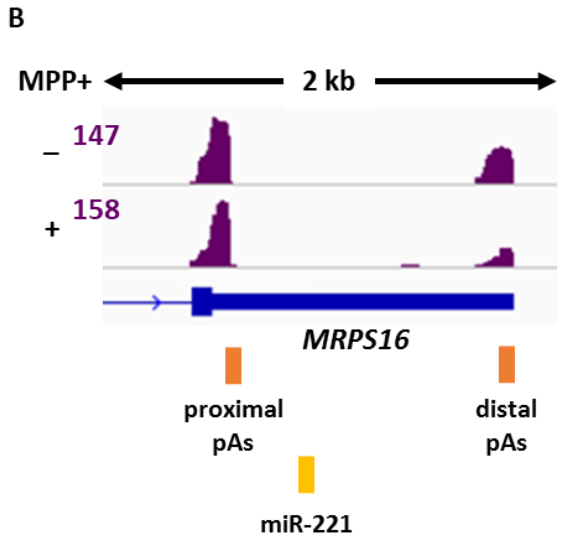
dysregulated axonal transport impairing proper mitochondrial translocation (Shin et al. 2012). Therefore, alterations in *STMN2* regulation through APA may be important in PD pathology.

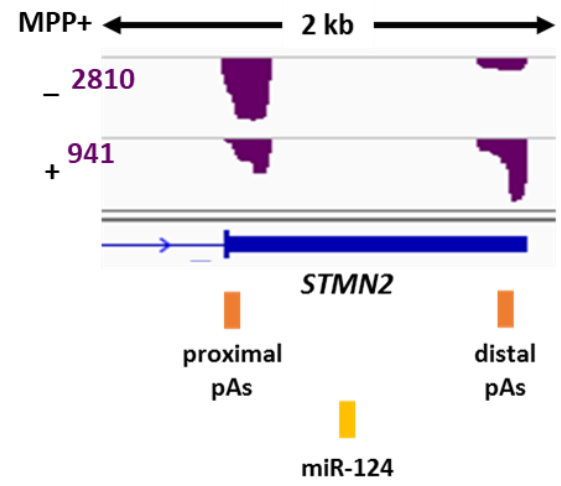
Cytoplasmic APA profiles can also be regulated by RBPs binding to the 3'UTR. The alternative UTR sequences of APA regulated genes were scanned through DREME to identify enriched motifs (Chapter 2.20). For shortened alternative UTRs, no motifs were enriched suggesting there are no RBPs globally associated with 3'UTR shortening. However, two motifs were identified in the alternative UTRs of lengthened genes (Figure 4.15E). Through TOMTOM motif analysis, the second motif, 'CGCGGAGR', was identified to be bound by LIN28 and RBM4. Although these RBPs have not been previously associated with regulating mRNA stability, they play a role in regulating translation of their target mRNAs, and thus may mediate downstream expression of genes showing 3'UTR lengthening with MPP+ treatment.

In conclusion, this analysis identifies miR-221, miR-124 and miR-148 as miRNAs that may contribute to UTR landscape changes upon MPP+ treatment. Furthermore, the identification of LIN28 in the alternative UTRs of genes that show lengthening may give an insight into how these longer transcript isoforms are stabilised. However, each of these trans-factors only affected a small cohort of APA regulated genes, suggesting multiple factors mediate the UTR landscape upon MPP+ treatment.

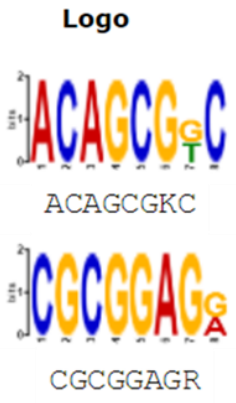








E



TOMTOM identified RBPs
YBX1; YBX2; ZC3H10; ANKHD1
ESRP2; FUS; PPRC1; HNRNPH2; SRSF1; SRSF2; RBM5; PCBP2; LIN28 RBM4; RBM8A

Figure 4.15. Global Regulation of APA through alternative UTR Cis-elements with MPP+ Treatment.

A. miRNAs identified to be enriched in genes showing 3'UTR shortening upon 24 hour 0.5 mM MPP+ treatment compared to untreated BE(2)-M17 cells.

B. *MRPS16* shows 3'UTR shortening which may be due to presence of miR-221 binding site in the alternative UTR.

C miRNAs enriched in genes showing 3'UTR lengthening upon 24 hour 0.5 mM MPP+ treatment compared to untreated BE(2)-M17 cells.

D. *STMN2* shows 3'UTR lengthening which may be due to presence of miR-124 binding site in the alternative UTR.

In **A** and **C**, Navy bars show the percentage of APA regulated genes with MPP+ treatment targeted by the corresponding miRNA. In **B** and **D** cytoplasmic tracks (purple) are shown, and the numbers on the left indicate the read numbers in RPM of the most abundant transcript isoform from sequencing data. Tracks are visualised using auto-scale settings on the IGV browser.

E. DREME analysis identified two motifs (left) enriched in the alternative UTRs of genes that showed 3'UTR lengthening. TOMTOM analysis identified RBPs found in the nucleus (red), the cytoplasm (purple) or the nucleus and the cytoplasm (blue) that bound to these motifs.

4B.2.5. Upstream-APA in *NPM1* with MPP+ Treatment Increases Abundance of Transcript Encoding Functional Protein

Upstream-APA events in MPP+ treated and untreated cells were next compared. In the nucleus, 56 upstream-APA events were identified, where an increased use of terminal exon poly(A) sites was favoured (Figure 4.16A, left). In the cytoplasm, 56 upstream-APA events were also identified, however the trend to using the poly(A) site in the terminal exon was much greater (Figure 4.16A, right). Surprisingly, just 4 genes which showed upstream-APA in the nucleus were also identified in the cytoplasm suggesting these co-transcriptional alterations in poly(A) site choice have a limited downstream impact on gene expression (Figure 4.16B).

One gene which showed upstream-APA in both the nucleus and the cytoplasm is *NPM1* (Figure 4.16C). This gene encodes a multifunctional phosphoprotein that shuttles between the nucleus and the cytoplasm. In the nucleus, it associates with mRNAs after polyadenylation and acts to regulate poly(A) tail length (Sagawa et al. 2011). The change in poly(A) site usage upon MPP+ treatment was verified by RT-PCR (Figure 4.16D).

The protein encoded by the *NPM1* gene, has two isoforms: NPM1-01, encoded by the longer transcript, and NPM1-03, encoded by the shorter transcript. With MPP+ treatment there was an increased expression of the full length *NPM-01* transcript. Both isoforms share the same N-terminal domains, however have different C-terminal exons. As shown in Figure 4.16E, *NPM1-03* encodes a shorter polypeptide, which lacks an ATP binding region and an RNA binding domain. This RNA binding activity is crucial for its association with many mRNAs to regulate the length of the poly(A) tail (Sagawa et al. 2011). Increased expression of *NPM1-01* through upstream-APA, can increase NPM1-01 protein expression which could modulate poly(A) tail regulation. Although, alterations in global poly(A) tail length have not previously been associated with neurodegeneration, the poly(A) tail is important in mRNA export. Impaired nucleocytoplasmic transport has been associated with cytoplasmic protein aggregation, as seen in neurodegenerative diseases (Woerner et al. 2015).

In conclusion, the upstream-APA event in the *NPM1* gene may result in increased functional NPM1 protein, which could mediate altered poly(A) tail length of mRNAs in response to MPP+ treatment.

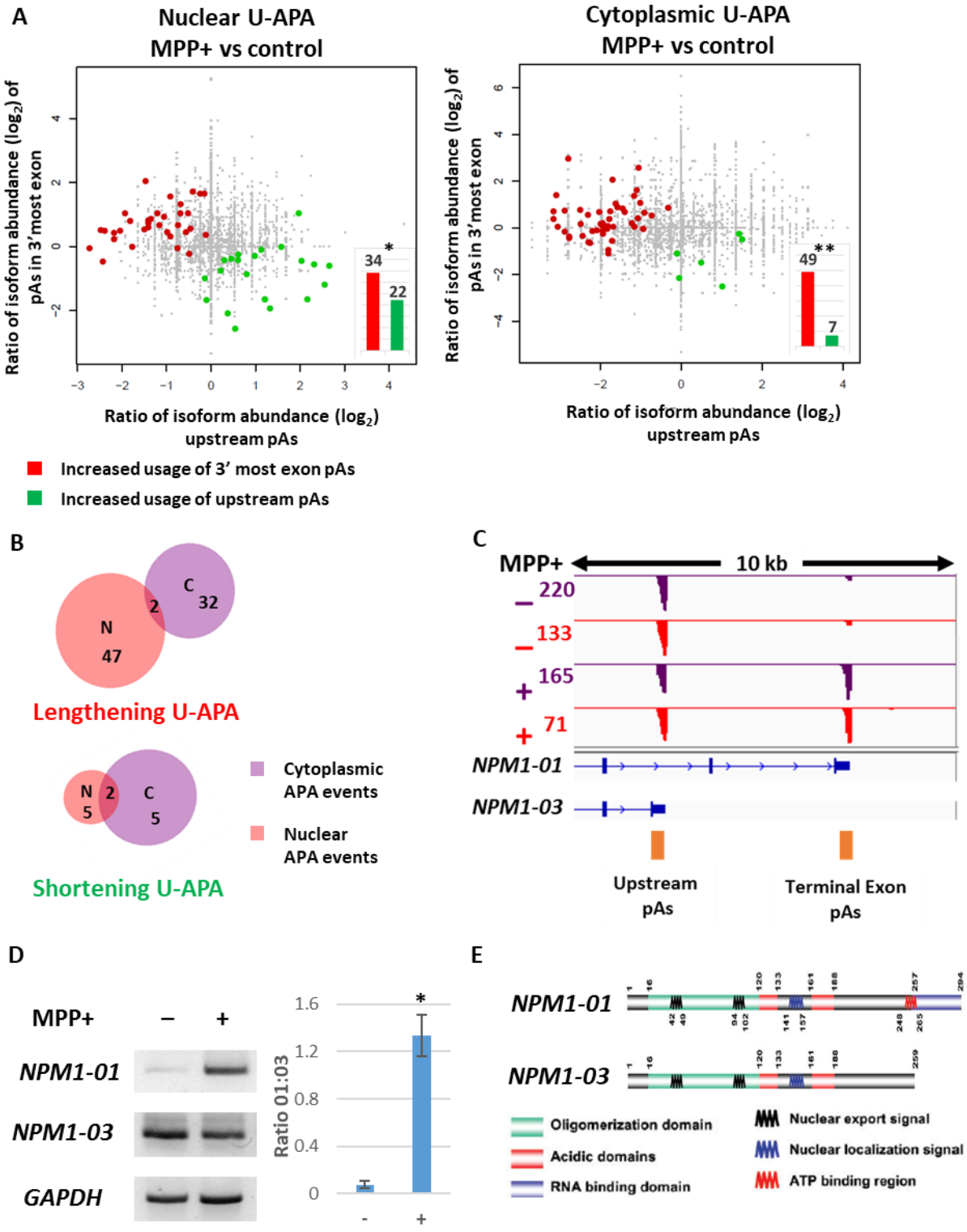

A
Nuclear U-APA
MPP+ vs control
Ratio of isoform abundance (log2) of pAs in 3'most exon
Ratio of isoform abundance (log2) upstream pAs
34
22
*
Cytoplasmic U-APA
MPP+ vs control
49
7
**
Increased usage of 3' most exon pAs
Increased usage of upstream pAs
B
C
32
2
N
47
Lengthening U-APA
N
2
5
C
5
Shortening U-APA
Cytoplasmic APA events
Nuclear APA events
C
MPP+
10 kb
220
133
165
71
NPM1-01
NPM1-03
Upstream pAs
Terminal Exon pAs
D
MPP+
–
+
NPM1-01
NPM1-03
GAPDH
Ratio 01:03
1.6
1.2
0.8
0.4
0
*
-
+
E
NPM1-01
NPM1-03
Oligomerization domain
Acidic domains
RNA binding domain
Nuclear export signal
Nuclear localization signal
ATP binding region

Figure 4.16. Upstream-APA Increases Full-length *NPM-1* Expression with MPP+ Treatment.

A. Upstream-APA events showing increased usage of poly(A) sites in the terminal exon (red bars and dots) or increased usage of an upstream poly(A) site (green bars and dots) were identified in the nuclear (left) and cytoplasmic (right) fractions upon 24 hour 0.5 mM MPP+ treatment. There was a trend to increased mRNA length in the nucleus and the cytoplasm (* $p<0.05$, ** $p<0.01$, Fisher's exact Test).

B. Venn diagrams to show the overlap in upstream-APA events between the nuclear (red) and cytoplasmic (purple) fractions.

C. A screenshot to show upstream-APA in the *NPM1* gene in both the nucleus (red tracks) and the cytoplasm (purple tracks). Numbers on the left indicate reads in RPM from sequencing data of the most abundant isoform visualised using auto-scale settings on the IGV browser.

D. Left panel: an RT-PCR of cytoplasmic RNA to verify the upstream-APA event using primers in the two different terminal exon regions. Right panel: a bar chart plotting the ratio of NPM1-01:NPM1-03, quantified by the intensities of the bands from RT-PCR using ImageJ software. Error bars show standard deviation, n = 3. T-test, * $p<0.01$.

E. Schematic to show difference in domains in the two NPM1 protein isoforms. Image modified from (Okuwaki 2008).

4B.3 Discussion

Treatment of the BE(2)-M17 cell line with MPP+ is an established *in vitro* PD model, that induces mitochondrial dysfunction, which is seen in both fPD and sPD cases. While there has been investigation of gene expression changes at the RNA and protein level, changes in APA in this *in vitro* PD model have not been investigated. Here, no global shifts in APA were identified, as was also seen in bioinformatics analyses in Chapter 4A, however physiologically relevant genes were identified that responded to MPP+ treatment by changing their APA profiles.

4B.3.1 Characterisation of MPP+ to model PD *in vitro*

MPP+ treatment in neuroblastoma cells is an established method to model PD *in vitro*. A concentration of 0.5 mM MPP+ reduced mitochondrial function, induced mitochondrial ROS production and induced autophagy, which are all characteristics observed in PD patients. *In vitro* models of neurodegeneration do not represent the complexity of the brain, and transcriptome changes during progression of the disease cannot be tracked. However, the similarities to PD at a cellular level verify the MPP+ treatment in BE(2)-M17 cells to model PD.

4B.3.2 Gene expression changes with MPP+ treatment

Genome wide analysis of gene expression in this MPP+ model showed an upregulation of genes associated with ER stress, as previously observed (Nakato et al. 2015). An upregulation in genes associated with glycolysis to increase ATP production where OXPHOS is compromised has also been observed (Krug et al. 2014), while others reported a downregulation of glycolytic genes (J. Wang et al. 2007). Although reduced OXPHOS was seen with MPP+ treatment in this study, expression of glycolysis related genes including *HK1 PFKM, PGAM* and *GAPDH* were unchanged.

Surprisingly, genes associated with mitochondrial function and ATP synthesis were only modestly downregulated, despite a significant reduction in the oxygen consumption rate of MPP+ treated cells compared to untreated cells. This could be explained by stabilization

but translational repression of these transcripts under conditions of oxidative stress, perhaps in stress granules (as discussed in Chapter 5).

The *SNCA* gene encodes α-synuclein, a protein that has been heavily associated in both fPD and sPD pathophysiology (Table 4.2) (Bisaglia et al. 2010; Spillantini et al. 1997; Polymeropoulos et al. 1997; Lundblad et al. 2012). The expression of *SNCA* in the RNA-seq data was low in BE(2)-M17 cells both with and without MPP+ treatment (Supplementary Figure 7), which identifies a potential flaw in this *in vitro* model of PD.

4B.3.3. APA changes in the MPP+ model

In the MPP+ model, the cohort of APA regulated genes showed an overrepresentation of genes associated with protein degradation, a pathway that has previously been shown to respond to MPP+ treatment *in vitro* (Caneda-Ferrón et al. 2008; Keane et al. 2015) and is impaired in neurodegeneration (Poewe et al. 2017). 3'UTR length changes in these genes may affect their final protein expression levels. Therefore, APA may make a critical contribution to combat oxidative stress generated by MPP+ exposure. Alternatively, UTR length changes may be a result of dysregulation of APA with MPP+ treatment, which may prevent effective degradation of protein aggregates, and could contribute to the neurotoxicity of MPP+.

Due to the nature of upstream-APA events, a physiological consequence is often easier to establish. In this analysis, a notable upstream-APA event was identified in the *NPM1* gene where a switch to producing more of the full-length functional transcript was observed upon MPP+ treatment. As well as its role in regulating poly(A) tail length (Sagawa et al. 2011), the full-length NPM1-01 may play a neuroprotective role, by preventing nuclear protein aggregation using its negative charge to shield aggregate-prone protein surfaces (Woerner et al. 2015). Increased NPM1-01 expression with MPP+ treatment may be a neuroprotective mechanism to combat protein aggregation, which has been observed in previous MPP+ models (Kalivendi et al. 2004; Keane et al. 2015). The role of the shorter NPM1-03 protein is not yet known, however it has been postulated to block RNA binding activity of full-length protein through heterodimerisation (Okuwaki 2008). Overall, this increased expression in *NPM1-01*, regulated by upstream-APA, may have an important protective role.

One study had previously identified *SNCA* to utilize a more distal poly(A) site in PD patient RNA isolated from the cerebral cortex, which is not directly affected in PD. This was shown to influence transcript localization and therefore direct α-synuclein towards mitochondria, contributing to disease pathology (Rhinn et al. 2012). *SNCA* has been extensively associated with PD pathogenesis, therefore a deeper insight into the molecular mechanism of its aggregation is crucial for understanding Lewy body formation in PD. 3'UTR shortening in *SNCA* was not identified in this MPP+ PD model (Supplementary Figure 7), nor in the bioinformatics analysis with DaPars (Supplementary Figure 4). This could be because *SNCA* APA changes differ in different brain regions both in healthy and disease states, therefore changes in the cerebral cortical tissue may not be present in the dopaminergic neurons of the substantia nigra.

4B.3.4 Cis-element regulation of APA in MPP+ model

miRNAs are involved in regulating the cytoplasmic APA landscape. Here 23 miRNAs were uniquely enriched in the alternative UTRs of genes showing 3'UTR shortening and lengthening, suggesting these miRNAs may enable a broad level of post-transcriptional gene regulation. Notable examples of miR-124 and miR-148b, which have previously been shown to be downregulated in MPP+ models of PD (Kanagaraj et al. 2014; Vallelunga et al. 2014) were identified in the alternative UTRs of genes showing 3'UTR lengthening which could explain the shift in APA profiles. Furthermore, upregulation of miR-124 was shown to reduce the neurotoxic effects of MPP+, by reducing apoptosis and impaired autophagy (H. Wang et al. 2016), suggesting reduced expression of this miRNA may contribute to pathogenesis. Expression changes in individual miRNAs have been investigated in the MPP+ model (D. C. Choi et al. 2014; Fragkouli and Doxakis 2014) and in PD patients (Miñones-Moyano et al. 2011; Mouradian 2012), however genome wide changes in miRNA expression have not previously been explored in the MPP+ model of PD.

Similarly, the role, or altered role, of RBPs in PD has not been extensively investigated. No RBPs with a cytoplasmic function were identified here to be globally mediating 3'UTR lengths, however individual genes may be affected by changing RBP dynamics under oxidative stress induced by MPP+.

4B.3.5 Comparison of *in silico* and *in vitro* APA analysis

In both *in silico* and *in vitro* analyses assessing APA changes in PD, genes associated with protein degradation pathways were identified, suggesting a physiological role of APA in gene regulation in PD. However, few genes were identified to be regulated by APA in the two RNA-seq datasets assessed with DaPars analysis, and in the MPP+ model (Figure 4.17A). A gene encoding a cholesterol transporter in the endosomal/lysosomal system, *NPC2*, showed 3'UTR lengthening in both treatment with MPP+, and in sPD in the second PD dataset assessed in DaPars (Figure 4.17B). Cholesterol is important in synaptic vesicle formation and proper neurotransmission, which is compromised in AD and PD. Accumulation of cholesterol in association with α-synulcein has been observed in PD (J. P. Liu et al. 2010). Furthermore, the lysosomal pathway is important in autophagy, therefore regulation of *NPC2* by APA may have a relevant function in PD.

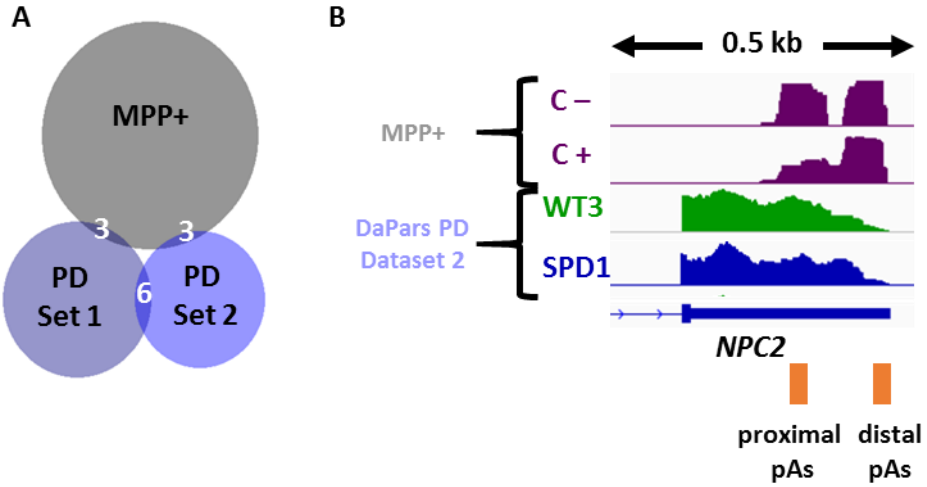


Figure 4.17. Overlap of APA Events in PD between *in silico* and *in vitro* Analysis.

A. A Venn diagram to show the overlap of APA events identified in the MPP+ *in vitro* PD model (grey) compared to the DaPars analysis (navy and blue) in Chapter 4A.3. White numbers indicate genes showing significant APA changes in different models.

B. A 3'UTR lengthening event identified in *NPC2* in the cytoplasm of MPP+ treated cells (purple tracks) and in S-PD (blue track) compared to wild type (WT, green track).

4B.3.6 Conclusions and Future Outlook

APA is an established regulator of gene expression. The results in the *in vitro* MPP+ PD model, and the *in silico* investigation in Chapter 4A highlight different genes that may be regulated by APA in PD. This may be due to variation in different patient samples and variation in sequencing depth, as discussed in Chapter 4A, but also the inherent transcriptomic differences between dopaminergic neuroblastoma cell lines and dopaminergic neurons derived from patient iPSCs. For example, two of the six genes that showed APA in both the PD RNA-seq datasets were not expressed in BE(2)-M17 cells. However, the consistent identification of physiologically relevant genes showing APA gives an insight into how this method of transcriptome regulation may contribute to or be consequential of PD pathology.

Neurodegenerative diseases are composite and different patients are affected in different ways. It is difficult to assess changes in the substantia nigra of PD patients, as this region of the brain is progressively degenerated, therefore little tissue may remain in post mortem samples for RNA-seq analysis. Future work involving the assessment of transcriptional and post-transcriptional APA changes in dopaminergic neurons derived from patient iPSCs may give deeper insights into the impact of APA regulation in PD.

Chapter 5: APA in Cellular Stress

5.1 Introduction

5.1.1 Types of Cellular Stress

Cellular stress can be induced from an environmental change, including changes in temperature, oxygen availability and exposure to toxins. This can cause a variety of pathological effects in cells such as mitochondrial dysfunction or inhibition of key metabolic pathways such as transcription and OXPHOS. To enable survival, cells have numerous adaptive response mechanisms, which are specific to the stress type. However many stresses result in translational inhibition through phosphorylation of the initiation factor eIF2α (Pakos-Zebrucka et al. 2016). Alterations in gene expression, at the level of the transcriptome and proteome, are key to modulate the changes required in the new environment. Some stresses induce a specific response through activation of transcription factors such as Hypoxia-Inducible Factor 1 (HIF-1), or Heat Shock Response Factor 1 (HSF1), but general stress response transcription factors have also been identified, for example ATF4 (Pakos-Zebrucka et al. 2016). Table 5.1 highlights a selection of stress inducers and their associated response pathways.

The formation of dynamic cytoplasmic inclusions, called stress granules, has been observed upon exposure to a number of stresses including temperature shock, arsenic, hypoxia and ER stress (Nancy Kedersha, Ivanov, and Anderson 2013). These granules consist of mRNA-protein complexes (mRNP) that aggregate with nucleating proteins, primarily TIA1/TIAR and G3BP1/2 (Matsuki et al. 2013; Kedersha, Ivanov, and Anderson 2013; Buchan and Parker 2009). The polyadenylated mRNAs are bound by RBPs that guide the transcripts to subcellular locations where the RBPs aggregate via their glycine rich domains (N Kedersha and Anderson 2002). Different RBPs contribute to stress granule formation in different stress conditions. The translation factors eIF3, eIF4E and eIF4G and ribosomal subunits are also found in stress granules (Kedersha and Anderson 2002). The role of the cytoskeleton is important in stress granule formation as inhibition of RBP transport enhances the chance of their aggregation (Decker and Parker 2012). Stress granule formation was

initially thought to be essential for translational inhibition and transcript stability in stress conditions. However, recent studies have shown translational inhibition can occur in absence of stress granules (Hofmann et al. 2012), and the mRNP interaction is more important for maintaining transcript stability (Bley et al. 2015).

Many stress conditions have been studied to understand the stress response mechanisms to adapt to the new environment, but few studies have assessed the contribution of APA to changes in regulating the transcriptome. This chapter assesses transcriptome-wide changes in cold shock and hypoxia, and further investigates APA events that occur in both stresses to identify stress-regulated APA events.

Table 5.1. *In vitro* Stress Inducers and Response Pathways.

Stress Type	Stress Inducer	Effect on Cell and Pathways induced in Response	Reference
Temperature	Heat shock	Activation of transcription factor HSF1. Upregulation of target genes, including heat shock proteins (HSPs). HSPs are molecular chaperone proteins that facilitate proper protein folding under stress conditions.	(Richter, Haslbeck, and Buchner 2010)
	Cold shock	Cell cycle arrest. Upregulation of cold shock proteins RBM3 and CIRBP to combat stress conditions. (Chapter 5.1.2) Global translational inhibition mediated by phosphorylation of eIF2α. Recent studies also suggest inhibition of translational elongation by phosphorylation of elongation factor eEF2.	(Fujita 1999; Knight et al. 2015)
Chemical	Arsenite	Induces morphological abnormalities, growth inhibition and apoptosis. Induces nitric oxide production causing oxidative stress. Linked to inducing Heat Shock Response. Formation of stress granules. Translational inhibition.	(Bernstam and Nriagu 2000)
ER stress	DTT	Reduces disulphide bond formation in proteins. Misfolded proteins accumulate in ER lumen. Initiates unfolded protein response which has 3 branches via PERK, ATF6 and IRE1. Four kinases, including ER resident kinase PERK, can phosphorylate eIF2α to inhibit cap dependent translational initiation.	(Ron and Walter 2007)
Glucose Deprivation	-	Linked to ROS production inducing oxidative stress. Studies show induction of UPR. Accumulation of aggregated proteins can induce autophagy. ATF4 mediated apoptosis observed under prolonged conditions	(Marambio et al. 2010; Iurlaro et al. 2017)
Oxidative stress	MPP+, rotenone	Inhibition of OXPHOS resulting in reduced ATP production. Increased ROS production which damaged macromolecules. Mitochondrial dysfunction can lead to Cytochrome C release inducing caspase mediated apoptosis. See Table 4.9 for more information.	(Keane et al. 2015; Krug et al. 2014; Kalivendi et al. 2003; Lim et al. 2007)
Oxygen availability	Hypoxia	Hypoxia inducible response activated (Chapter 5.1.3). Reduced ATP production from inhibition of OXPHOS. Inhibition of translation through PERK phosphorylation of eIF2α.	(Nizet and Johnson 2009)
Transcriptional inhibition	α-amanitin, Actinoymcin D	Activate DNA damage stress responses. Upregulation of transcription of a subset of genes from increased P-TEFβ activity. Accumulation of p53 to activate transcription of p53 target genes. p53 accumulation in the mitochondria causes apoptosis. Inhibition of rRNA transcription inhibits translation. Reorganisation of chromatin and nucleolus.	(Ljungman 2007; Bensaude 2011)
26 S proteasome inhibition	Bortezomib	Depletes pool of amino acids available for protein synthesis as preventing protein turnover pathway. Increased protein aggregation. Activation of autophagy.	(Pakos-Zebrucka et al. 2016)

5.1.2 Cold Shock

Temperature stress through heat shock has been studied extensively in tissue culture. The heat shock response is a well understood pathway where the heat stress causes the trimerization of the heat shock transcription factor, HSF1, which subsequently translocates to the nucleus to mediate transcriptional changes. HSF1 binds to heat shock response elements in the promoter and enhancer regions of its target genes, which include heat shock proteins (HSPs), that are molecular chaperone proteins that aid the stress response (Richter, Haslbeck, and Buchner 2010).

In contrast, there is no such defined 'cold shock response', and much of the work on cold shock has focussed on the upregulation of two cold shock proteins, RBM3 and CIRBP (Y Liu et al. 2013; Fujita 1999; Chip et al. 2011; Jackson et al. 2015; Al-Fageeh and Smales 2009; X. Zhu et al. 2016). Although there is abundant evidence that these proteins predominantly localize to the nucleus (Rzechorzek et al. 2015; Nishiyama et al. 1997). Upregulation of CIRBP and RBM3 at lower temperatures was linked to suppression of proximal poly(A) sites during transcription causing 3'UTR lengthening during cold shock in mouse embryonic fibroblasts (MEFs) (Y Liu et al. 2013). However, they can also bind and stabilize 3'UTRs in the cytoplasm. RBM3 is suggested to bind to the 60S ribosomal subunit to enhance translation by polysome formation (Dresios et al. 2005; Smart et al. 2007), as well as mediate pre-miRNA processing (Pilotte, Dupont-Versteegden, and Vanderklish 2011). CIRBP can mediate mRNA nuclear export (Morf et al. 2012), function as an RNA chaperone to facilitate translation (Gotic et al. 2016), and play a role in protein folding and transport (Fujita 1999). Despite the cytoplasmic functions of RBM3 and CIRBP, post-transcriptional regulation of mRNAs in cold shock has not been studied.

In tissue culture, cell lines are typically grown at a body temperature of 37°C. Deviations from this temperature can induce a stress response in cells (Richter, Haslbeck, and Buchner 2010; Fujita 1999). The nature of this response, as well as the ability of cells to recover from the stress, is dependent on the extent of the temperature change and the length of the induced stress.

Therapeutic hypothermia at moderate to mild temperatures (28-34°C) has been known to ameliorate brain injury and the effect of ischemia for over 20 years (Chavez et al. 2015).

Colder temperatures reduce ATP consumption, protein synthesis rates, and post-translational protein modification processing (Dresios et al. 2005; Lleonart 2010; Quintin et al. 2014) and cause stress granule formation (Hofmann et al. 2012). The exact mechanism of how cold treatment is neuroprotective is still not fully elucidated, though recent evidence suggests that upregulation of cold shock proteins, CIRBP and RBM3, may play a crucial role in protecting neurons against neurodegeneration (Peretti et al. 2015; Pilotte, Dupont-Versteegden, and Vanderklish 2011; Rzechorzek et al. 2015; Zhang et al. 2015; Chip et al. 2011; Saito et al. 2010).

Transcriptome-wide changes in moderate hypothermia have not been extensively investigated. Therefore, the impact of moderate hypothermia, at 28°C for 24 hours, on the transcriptome of BE(2)-M17 cells was investigated using the 3'end RNA-seq approach. Further, to explore if the changes in APA were consistent in the more neuronal phenotype of BE(2)-M17, cells differentiated with RA were exposed to moderate hypothermia for 24 hours. Alterations in APA in moderate hypothermia were then compared to HEK293 cells to assess the cell specific effect of cold shock response on the transcriptome.

5.1.3 Hypoxia

Hypoxia is another model of cellular stress, where widespread gene expression changes have been observed to enable cell survival. Many biological pathways are affected in low oxygen conditions, including reduced OXPHOS resulting in reduced ATP production (Fähling 2009). Consequently, a global reduction in protein synthesis is well documented during hypoxia to adapt to the new low oxygen environment, as translation is the most ATP consuming biological pathway (Fähling 2009). Low oxygen availability also affects disulphide bond formation, resulting in increased misfolded proteins. This process occurs in the ER and under low oxygen conditions, ER stress responses are activated to degrade these misfolded proteins. Phosphorylation of PERK, a resident kinase in the ER, leads to phosphorylation of eIF2α on S51 to inhibit protein synthesis. This is a branch of the unfolded protein response pathway, which combats misfolded proteins, and is induced in hypoxia (Wouters et al. 2005) and in cold shock (Tessier and Storey 2014). Although there is global translational inhibition in hypoxia (Fähling 2009), a recent study showed that ribosomes associated with the ER continue protein synthesis, providing a spatial regulation of translation in stress (Staudacher et al. 2015).

In cell culture, the normal oxygen concentration or 'normoxia' is defined as 21%, which is the concentration of oxygen in the air. A reduction in oxygen concentration in hypoxic chambers, by replacing oxygen in the air with nitrogen, to 5% is considered to be a mild hypoxic state for cell culture, while concentrations lower than 2% are considered to be hypoxic (Nizet and Johnson 2009).

One characteristic feature of hypoxia is the induced expression of the hypoxia inducible transcription factor HIF-1. HIF-1 consists of a hypoxia induced polypeptide HIF-1α and a constitutively expressed polypeptide HIF-1β. Transcription of HIF-1α is constitutive but its expression is regulated at the protein level where post-translational modifications determine the protein stability. Specifically, two proline residues on HIF-1α are hydroxylated by iron- and oxygen-dependent prolyl hydroxylases (PHDs), making the protein a target for polyubiquitination. Alternatively, oxidation of a cysteine residue or phosphorylation of certain serine or tyrosine residues can also target the protein for degradation via ubiquitin proteasome pathway mediated degradation (Reviewed in (Nizet and Johnson 2009)).

During hypoxia, HIF-1α is stabilised due to inactivation of PHDs and is subsequently translocated into the nucleus where it interacts with HIF-1β to form the functional HIF-1 transcription factor. HIF-1 binds to hypoxic response elements (HREs) typically a RCGTG target sequence, in the promoter regions of its target genes, and recruits co-transactivation factors CBP/p300 to mediate transcription. The regulation of HIF-1α during hypoxia is outlined in Figure 5.1.

HIF-1 affects the transcription of over 100 target genes involved in cell proliferation, angiogenesis, iron metabolism and cell cycle control, though the extent of the hypoxia response is cell type dependent. HIF-1 also induces NFkB activation, enabling the indirect transcription of genes required to cellular adaptation to low oxygen conditions. HIF-1 activation has also been observed in other stresses apart from oxygen deprivation including iron deprivation, cancer and bacterial infection (Nizet and Johnson 2009). Despite the extensive change in gene expression associated in hypoxia, the contribution of APA in this altered gene regulation during hypoxia has not previously been investigated.

Oxygen deprivation has been extensively studied in the context of cancerous tissues and tumours, which adapt to cell proliferation in low oxygen conditions (Bertout, Patel, and Simon 2008). Hypoxia has been studied in neuroblastoma cells in the context of cancer, although the effect of hypoxia in BE(2)-M17 cells on a genome wide scale has not previously been explored. To assess the effect of hypoxia on the transcriptome, BE(2)-M17 cells were exposed to hypoxic conditions for 24 hours, after which RNA from the cytoplasmic and nuclear fractions was sequenced and analysed to assess the impact of hypoxia on gene expression and APA.

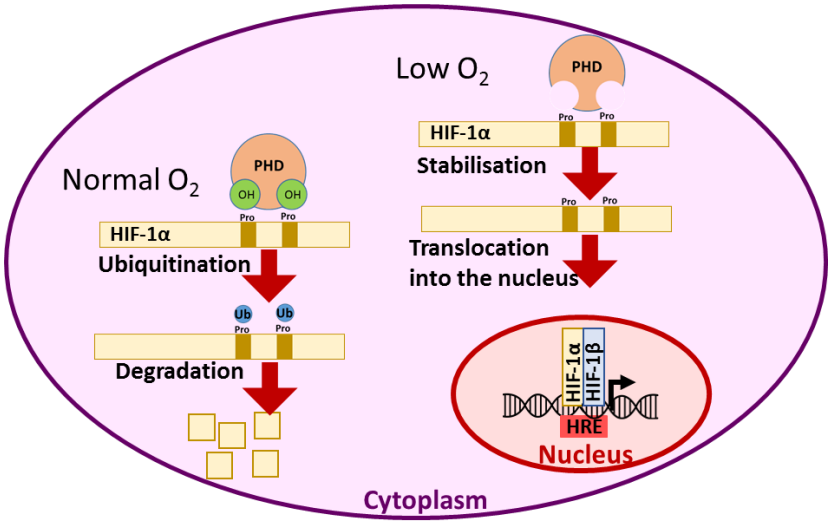


Figure 5.1. Outline of the Hypoxia Signalling Pathway.

Under normal oxygen conditions, PHD proteins (peach) are hydroxylated and therefore can hydoxylate proline (Pro) residues on the HIF-1α protein which targets it for ubiquitination and consequently degradation by the proteasome system. In low oxygen conditions, PHD proteins lose the ability to hydroxylate HIF-1α, stabilizing the protein in the cytoplasm. HIF-1α then translocates into the nucleus where it heterodimerises with HIF-1β and binds to hypoxia response elements (HRE) in the promoter regions of genes to enhance transcription of target genes. Figure modified from (Nizet and Johnson 2009).

5.1.4 Effect of Combined Stress Inducers

There is debate about whether the response to cellular stress invokes a general stress response or if it is specific to the nature of the stress. Furthermore, there is little information regarding the effect of combinatory stresses on cellular pathways. Although some stresses cause the same responses such as global inhibition of translation in both cold shock and hypoxia (Gorospe et al. 2011), no studies have explored the changing transcriptome in different stresses or how stress combinations affect this further.

There are reports that CIRBP and RBM3 are also upregulated in hypoxia (Qiang et al. 2013; Q. Zhang et al. 2017; Gorospe et al. 2011) and in UV irradiation (Wellmann et al. 2004). This suggests that these proteins may be associated with a variety of stress responses, and therefore mediate the transcriptome in different biological stresses. However the upregulation of HIF-1 targets was not seen in hypothermia suggesting that HIF-1 is specific to low oxygen (Wellmann et al. 2004).

Though cold shock itself is described as a form of cellular stress, there is growing evidence that it provides a neuroprotective role. Furthermore, the neurotoxic effects were delayed in a mouse model of PD where MPTP was administered at a lower temperature (S. J. Choi et al. 2015). Therefore, moderate hypothermia may affect the gene expression changes and APA regulation in cells simultaneously exposed to the neurotoxin MPP+, or hypoxia. To investigate this, 3'end RNA-seq was performed on BE(2)-M17 cells exposed to moderate hypothermia in combination with the neurotoxin MPP+ or hypoxia.

5.1.5 Chapter Aims

Stress responses have largely been grouped together implying that the response is similar regardless of the stress type. While this may be true with regards to certain upregulated pathways, transcriptome changes regulated by APA have not been greatly explored. This chapter investigates the impact of different stress types on APA and how this affects the stress responses. BE(2)-M17 cells were subjected to cold shock and hypoxic conditions, and the results were also compared with the effects of the neurotoxin MPP+ (discussed in Chapter 4B). This investigation found that different cellular stresses affect APA in largely different cohorts of genes in BE(2)-M17 cells, suggesting the stress response, at the level of the transcriptome, is largely specific to the nature of the stress to enable cell survival.

5.2 APA in Cold Shock

5.2.1 Cold Shock at 28°C does not Alter Cell Morphology or the Cell Cycle

The neuroblastoma BE(2)-M17 cell line was subjected to a temperature of 28°C for cold shock as it is the lowest temperature in the range for moderate hypothermia used in therapeutic hypothermia treatment. Cell morphology was shown not to vary with cold shock treatment, and there was no indication of cell death (Figure 5.2A), as observed in other cell lines (Knight et al. 2015). Culturing cells at mild-moderate hypothermic temperatures has previously shown to alter their cell cycle progression (Nishiyama et al. 1997; Lleonart 2010; Fujita 1999). As this may skew the expression pattern of many genes it was essential to establish to what extent BE(2)-M17 cell cycle progression was altered by cultivation at lower temperatures. Therefore, BE(2)-M17 cells grown at 28°C for 24 hours were subjected to FACS analysis (Chapter 2.12), which showed the same distribution of BE(2)-M17 cells in each stage of the cell cycle at both temperatures (Figure 5.2B). This suggests that exposure of BE(2)-M17 cells does not affect their progression through the cell cycle thus changes in gene expression are unlikely to be due to trapping cells in a stage of the cycle.

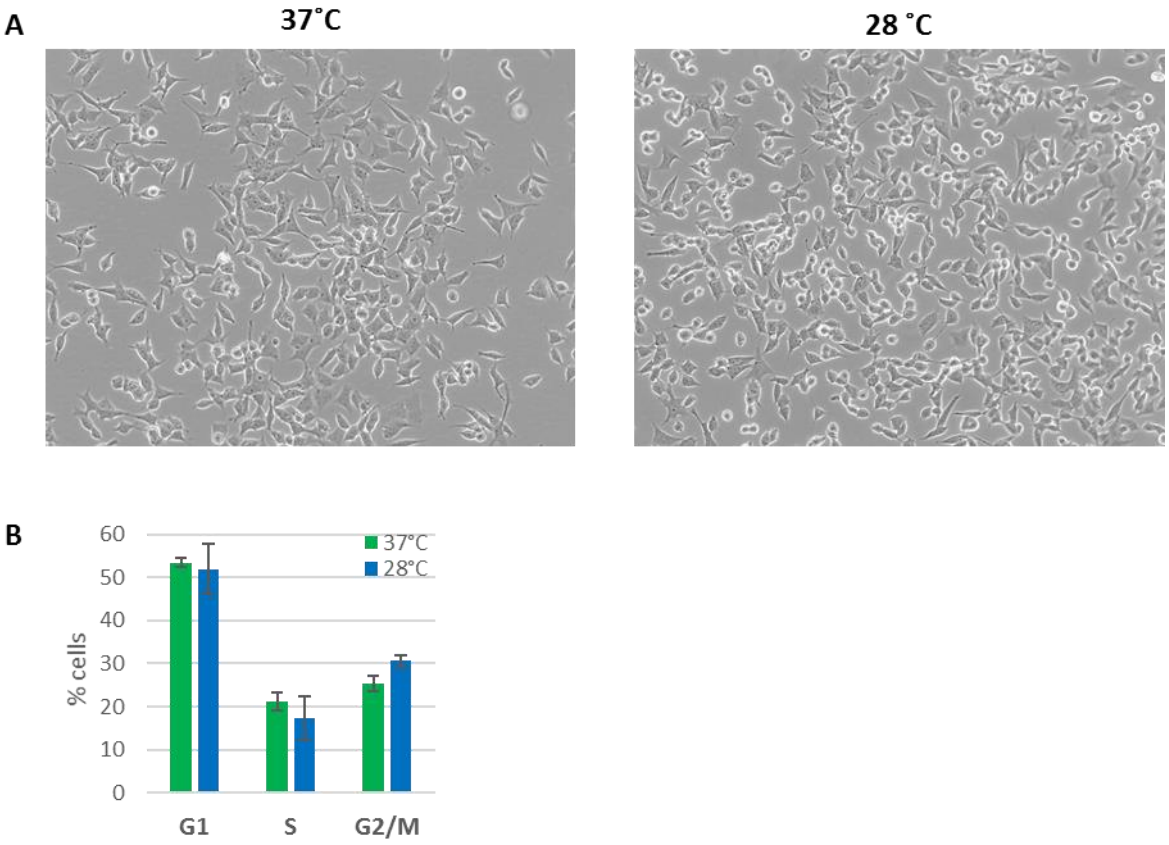


Figure 5.2. Characterisation of Cold Shock at 28°C for 24 h in BE(2)-M17 cells.

A. Light microscopy images to show no visually obvious change in cell morphology was observed with 24 h exposure to 28°C.

B. A bar chart indicating no significant change in the percentage of cells in each stage, G1, S and G2/M in the cell cycle, as quantified by FACS analysis. Error bars show standard deviation, n = 3.

5.2.2 Gene Expression Changes with Cold Shock

After confirming that moderate hypothermia did not affect progression of the cell cycle, the impact of cold shock on the cellular transcriptome was assessed. To distinguish the effects of cold shock at the co- and post-transcriptional level, RNA was separately isolated from the nuclear and cytoplasmic fractions of BE(2)-M17 cells subjected to a moderate hypothermic or normal temperature. RNA isolated from the two fractions was quality controlled by visualisation on an RNA gel before being processed using the QuantSeq library kit (Lexogen) as described in Chapter 3.2.2. The resulting libraries were quantified using a Bioanalyzer and sequenced on the Ion Proton system. Reads were analysed using an established bioinformatics pipeline (Hoque et al. 2013; Neve et al. 2016) to assess changes in gene expression and APA.

First the expression of the cold shock proteins RBM3 and CIRBP was assessed, which are highly upregulated in moderate to mild hypothermia (Fujita 1999; Lleonart 2010; Y Liu et al. 2013). Interestingly, the expression of the *RBM3* transcript does not change significantly in the nucleus (Figure 5.3A, RBM3 red column) but its cytoplasmic mRNA levels increase more than threefold upon cold exposure (Figure 5.3A RBM3 purple column). This suggests that cytoplasmic regulatory mechanisms, most likely involving increased transcript stability, are responsible for the upregulation of RBM3 transcripts during cold shock. In contrast, the expression of *CIRBP* is upregulated twofold in the nucleus suggesting upregulation at the transcriptional level, and this upregulation is also seen in the cytoplasm (Figure 5.3A CIRBP purple column). The extent of RBM3 upregulation in the cytoplasm was greater than of CIRBP, agreeing with previous reports (Rzechorzek et al. 2015). However, the increased expression of both RBM3 and CIRBP at the protein level was modest, and not statistically significant (Figure 5.3B). This contrasts with other studies which have suggested a strong upregulation of RBM3 and CIRBP mediates the regulation of numerous pathways that adapt cells to survival at lower temperatures.

Next, other genes that showed significant upregulation (Fisher's exact Test, $p<0.01$, FC >2) in the cytoplasm and nucleus during cold stress were assessed and subjected to a GO analysis. Widespread gene expression changes were observed (Figure 5.3C), and upregulated transcripts in the cytoplasm and nucleus were primarily associated with the same biological pathways including regulation of protein modification and regulation of the cell cycle. However,

few transcript abundance changes in the cytoplasm were also observed in the nucleus (Figure 5.3C, blue dots and numbers). Considering no changes in the cell cycle were observed from FACS analysis, it is surprising that genes associated with regulating the cell cycle (Figure 5.3D left panel) were upregulated in BE(2)-M17 cells cultured at 28°C. The most highly expressed genes that showed significant upregulation in moderate hypothermia included *CIRBP* and *RBM3* (Figure 5.3D right panel), which were shown not to be upregulated at the protein level. Similarly, it is possible that cell cycle regulation genes also do not show altered protein expression, explaining no change in cell cycle progression during moderate hypothermia in BE(2)-M17 cells.

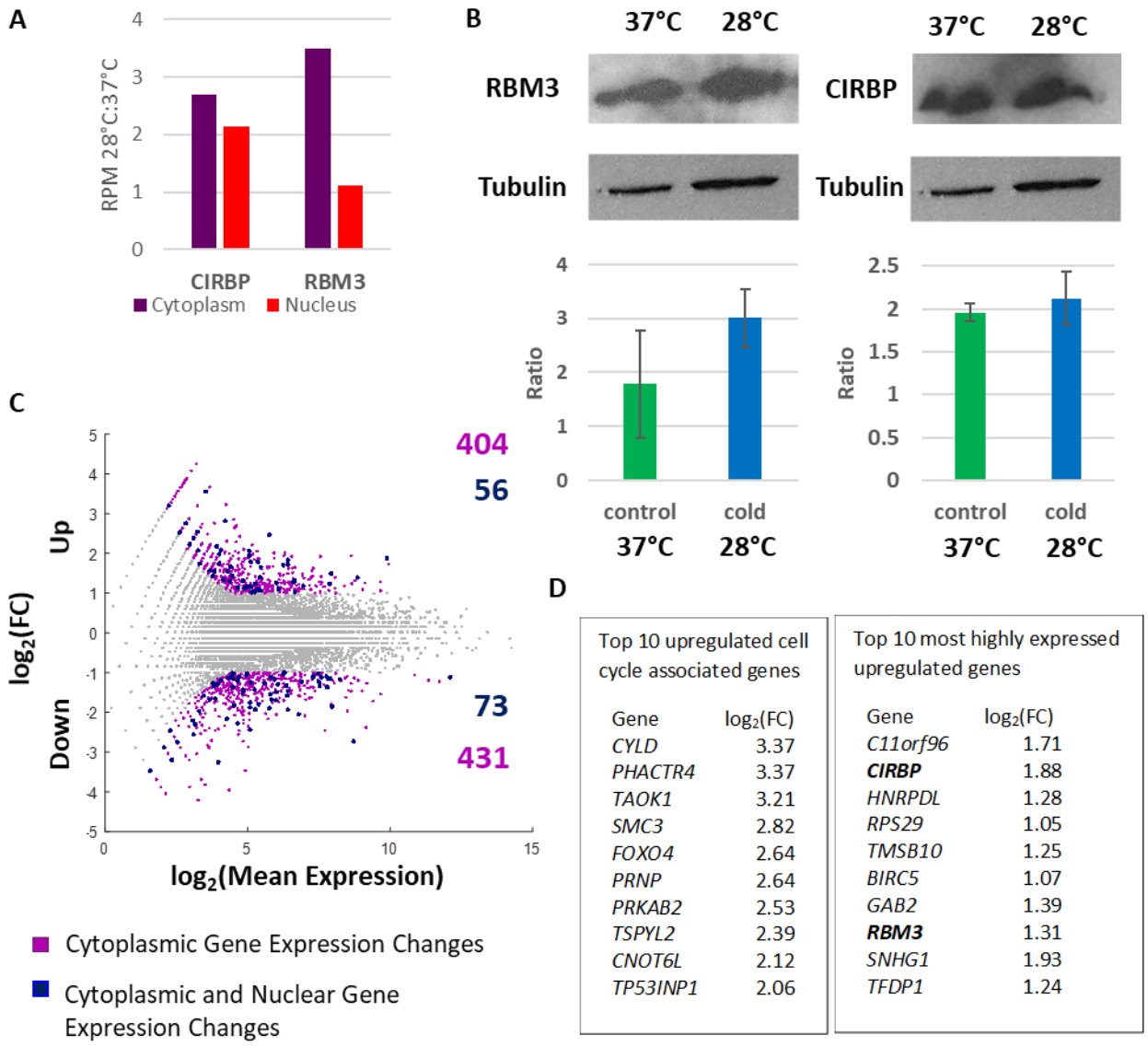


Figure 5.3. Widespread Gene Expression Changes in Cold Shock.

A. 3'end RNA-seq data showed that *RBM3* and *CIRBP* were upregulated at the transcript level in the cytoplasmic fraction (purple bars) in BE(2)-M17 cells exposed to cold shock at 28°C for 24 hours. Only CIRBP showed increased expression in the nuclear fraction (red bars). The ratio of expression in cold shock is calculated from reads per million (RPM) normalised to *TUBG1.*

B. No significant change in protein expression of RBM3 (left) and CIRBP (right) through western blotting during cold shock. Protein samples were isolated from whole cell fractions. Tubulin used as a protein loading control. The ratio is calculated by quantifying intensities of RBM3 and CIRBP and dividing by the quantified intensity of Tubulin expression. Error bars show standard deviation, n = 3.

C. MA Plot showing widespread cytoplasmic gene expression changes in cold shock. Each dot indicates a single gene. Blue dots indicate genes also differentially expressed in the nucleus; Purple dots indicate genes differentially expressed uniquely in the cytoplasm (Fisher's exact Test p <0.01, FC >2). Gene expression was normalised to *TUBG1.*

D. Table to show the most upregulated genes associated with the cell cycle (left) and most highly upregulated genes overall (right).

5.2.3 A Trend to 3'UTR Lengthening Observed in the Nuclear and Cytoplasmic Fractions

The results above indicate widespread gene expression changes in the cytoplasm during cold shock, although the underlying molecular mechanisms that control these changes are largely unknown. APA has been proposed to be a key regulatory factor to enable cell survival at hypothermic temperatures. Specifically, RBM3 and CIRBP have been implicated in modulating poly(A) site choice at the point of cleavage (Y Liu et al. 2013). Both proteins were suggested to directly suppress the usage of the proximal poly(A) site resulting in 3'UTR lengthening of the affected transcripts (Y Liu et al. 2013). However, in BE(2)-M17 cells, neither protein was significantly induced upon cold shock and is therefore unlikely to regulate APA in the same manner.

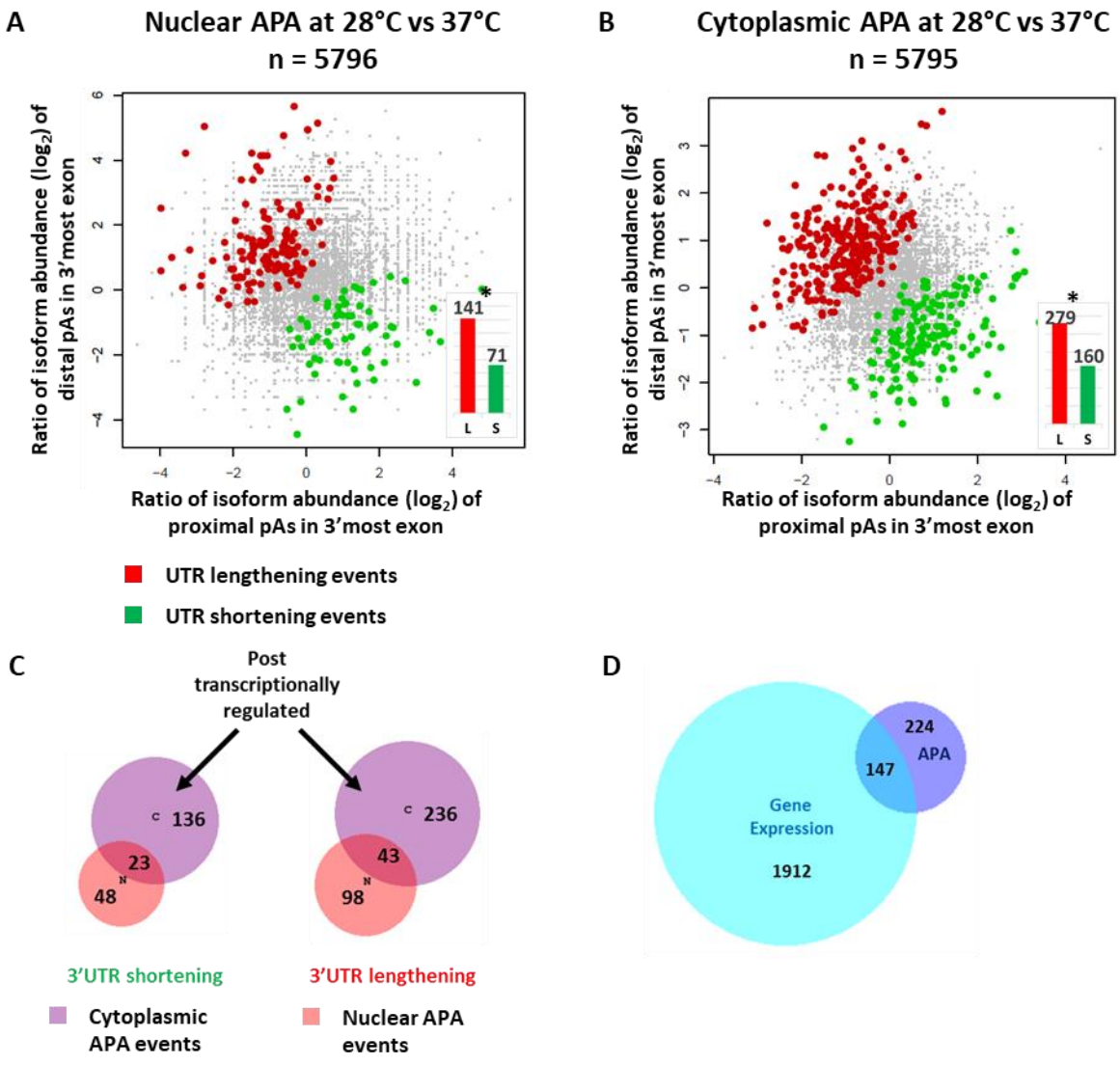
To assess APA in BE(2)-M17 cells under moderate hypothermia, reads of two biological replicates were combined and significantly changing APA events ($p<0.01$ Fisher's exact Test, with a minimum 5% change in APA isoform abundance) in the nucleus and the cytoplasm were identified separately. In the nucleus, a total of 5976 APA events were identified, 212 of which were significant (Figure 5.4A). Almost two-thirds of these (66.5%) represent an increased usage of the distal poly(A) site resulting in 3'UTR lengthening events (Figure 5.4A, red dots and red column). Conversely, 71 mRNA isoforms showed the opposite trend during cold shock, with increased usage of the proximal poly(A) site and therefore a shortening of the 3'UTR (Figure 5.4A, green dots and green column in bar chart). These changes occur in the nucleus so are likely to be either due to a change in poly(A) site usage at the point of cleavage or due to retention of APA isoforms.

Comparison of the cytoplasmic fractions of BE(2)-M17 cells grown at 28°C compared to 37°C showed twice as many significant APA events (Figure 5.4B). As seen in the nucleus, a significant trend towards 3'UTR lengthening was observed (Fisher's exact Test, $p<0.01$), however fewer than 20% of the events in the cytoplasm overlap with those in the nucleus (Figure 5.4C). This suggests that the cytoplasmic APA events may be due to post-transcriptional regulatory mechanisms that are involved in temperature dependent changes in transcript stability. Interestingly, 39.6% of the genes that show significant APA in the cytoplasm are part of the cohort that show statistically significant changes in gene expression

levels (Figure 5.4D). GO analysis showed that this overlapping cohort of genes was associated with translation and post-transcriptional gene expression (Figure 5.4E), two biological processes which are altered in cold stress conditions.

Upstream-APA changes in cold shock were also assessed. While in the nucleus, a trend to producing longer transcripts was observed, the opposite was true in the cytoplasm (Supplementary Figure 8A). In line with UTR-APA, most cytoplasmic APA changes were independent of nuclear changes emphasizing the importance of post-transcriptional regulation of these genes (Supplementary Figure 8B). The *UBE3B* transcript showed increased expression of a shorter transcript, which encodes a truncated E3 ubiquitin ligase protein that would lack ubiquitin ligase activity (Supplementary Figure 8C). This may contribute to overall protein stability through reduced protein degradation, which may be required in conditions of translational inhibition in cold shock.

These results show that there is a tendency to express APA isoforms with longer 3'UTRs in BE(2)-M17 cells exposed to moderate hypothermia, as observed in other cell types (Y Liu et al. 2013), however, most of these APA changes are due to post-transcriptional events. Given that RBM3 and CIRBP were not significantly upregulated during cold shock in BE(2)-M17 cells, these APA events are likely to be independent of these two proteins.



E

Biological Process	# Genes Present	# Genes Expected	Fold Enrichment	P-value
Translation	14	2.69	5.21	5.24E-03
Post-transcriptional Regulation of Gene Expression	14	3.26	4.3	4.72E-02

Figure 5.4. A Trend to 3'UTR Lengthening Occurs in Cold Shock in BE(2)-M17 cells.

A. and **B.** A trend to 3'UTR lengthening (red dots and columns) over 3'UTR shortening (green dots and column) was observed in both the nuclear (**A**) and the cytoplasmic (**B**) fraction in cells exposed to 24 hours at 28°C compared to control cells kept at 37°C. * = $p<0.01$, T-test. Statistically significant events (red and green dots) passed the $p<0.01$, Fisher's exact Test, with a minimum 5% change in APA isoform abundance.

C. A Venn Diagram to highlight the small proportion of genes that are regulated by APA in both the nucleus (red) and the cytoplasm (purple).

D. A Venn diagram identifying the cohort of genes that show both significant changes in APA (blue) and significant changes in Gene Expression (cyan).

E. A table to show biological pathways enriched by GO analysis in differentially expressed genes regulated by APA.

Despite the observation of a trend to 3'UTR lengthening in the cytoplasm, it is important to assess the potential physiological effect of the genes that show 3'UTR shortening. The *RAB7A* gene showed a shift to usage of the proximal poly(A) site in moderate hypothermia, but this switch was only significant in the cytoplasmic fractions (Figure 5.5A). This gene encodes a member of the Rab protein family, and is crucial in regulating vesicular transport in endocytosis, lysosome biogenesis and autophagosome maturation (Hyttinen et al. 2013). To investigate the impact of the 3'UTR shortening event on protein output, samples of whole-cell protein lysate were subjected to western blotting. This showed that the 3'UTR shortening event in cold shock correlated to an increased RAB7A protein expression (Figure 5.5B), despite global translational inhibition. RAB7A promotes autophagy, therefore its upregulation in cold shock may contribute to increased autophagy observed in temperature stress during the stress response (Das, Shravage, and Baehrecke 2012; D. Tang et al. 2016).

.

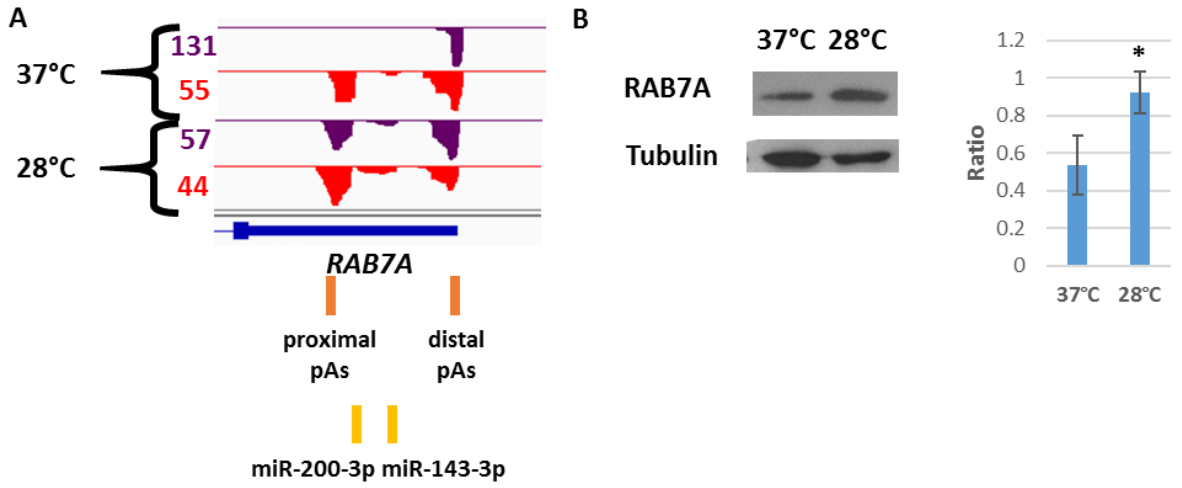


Figure 5.5. 3'UTR Shortening in *RAB7A* Correlates with Increased Protein Output in Cold Shock.

A. A screenshot to show a shift of using the distal poly(A) site at 37°C to the proximal poly(A) site at 28°C. This switch is only observed in the cytoplasm (purple tracks) and not the nucleus (red tracks). Numbers on the left indicate read numbers (in RPM) from sequencing data of the most abundant transcript isoform visualised using auto-scale settings on the IGV browser.

B. Left panel: a western blot indicating upregulation of RAB7A at 28°C using protein samples isolated from whole cell fractions. Right panel: a bar chart displaying a ratio of RAB7A:Tubulin of the band intensities quantified by ImageJ software. Error bars show standard deviation, n = 3. T-test, * $p<0.05$.

5.2.4 RBM3 and CIRBP do not widely affect APA Profile Changes in Cold Shock in BE(2)-M17 cells

The results above suggest widespread post-transcriptional APA changes. During cellular stress, RBM3 and CIRBP have been reported to translocate to the cytoplasm (Dresios et al. 2005; Gotic et al. 2016). To assess if expression of these proteins in the subcellular fractions changed during cold shock, protein from the cytoplasmic and nuclear fraction were isolated and RBM3 and CIRBP expression was assessed through western blotting (Figure 5.6A). Despite no increase in total protein expression, both RBM3 and CIRBP showed increased expression in the cytoplasm at 28°C compared to 37°C, but a decreased expression in the nucleus. This suggests that in BE(2)-M17 cells, RBM3 and CIRBP do translocate to the cytoplasm during cold shock.

RBM3 and CIRBP can bind to 3'UTRs to stabilise their target mRNAs. To identify which genes may be regulated by RBM3 and CIRBP in BE(2)-M17 cells, the APA regulated genes in the cytoplasm during cold shock were overlapped with RBM3 and CIRBP targets identified through PAR-CLIP analysis in MEFs (Y Liu et al. 2013).

Over 40% of genes showing APA changes in the cytoplasm were also targets of RBM3 (Figure 5.6B, left). However, almost half of these targets had an RBM3 binding site in the coding region (CR) and a sizeable proportion of genes had an RBM3 binding site in the intron, which of course is not present in the cytoplasm. Only 5.9% and 6.6% of UTR lengthened and shortened genes respectively were RBM3 targets. Since RBM3 bound a similar proportion of UTR lengthened and shortened genes, it is likely that RBM3 binding does not preferentially promote UTR lengthening or shortening.

CIRBP bound 10.2% of UTR lengthened and 16.9% of UTR shortened genes in the 3'UTR, but again binding to the coding region was most prevalent (Figure 5.B, right). Interestingly more UTR shortened genes were targets of CIRBP than UTR lengthened genes. This suggests CIRBP binding may destabilise longer UTR isoforms, which contradicts previous roles of CIRBP in promoting UTR lengthening (Y Liu et al. 2013).

These results suggest that RBM3 and CIRBP are localised in the cytoplasm during cold shock in BE(2)-M17 cells. Most RBM3 and CIRBP target genes are bound by these RBPs in regions which do not affect UTR length, suggesting the extent of their post-transcriptional APA regulation is limited. Both proteins have been suggested to promote UTR lengthening in cold shock, but these data suggest CIRBP binding may promote UTR shortening, while RBM3 binds UTR lengthened and shortened targets equally. This contradicts their previous proposed role in mediating UTR length, however the cytoplasmic localisation of these proteins may have alternative roles in the cold shock response.

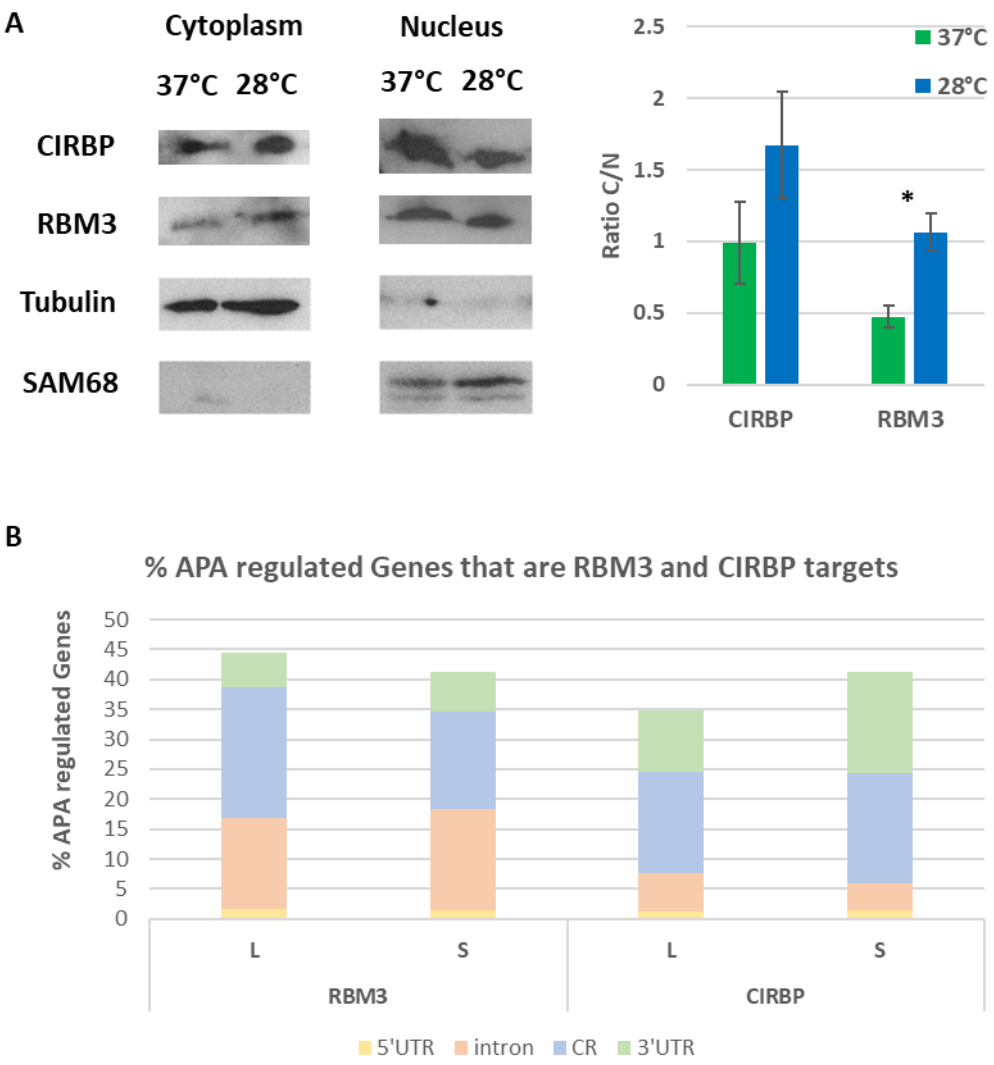


Figure 5.6. Role of RBM3 and CIRBP in Cold Shock in BE(2)-M17 cells.

A. Left panel: A western blot showing the expression of CIRBP and RBM3 in the cytoplasm (left) and nucleus (right) upon cold shock. Cytoplasmic loading control was Tubulin, and nuclear loading control was SAM68. Right panel: A bar chart to show the ratio of cytoplasmic to nuclear expression of CIRBP and RBM3. Error bars show standard deviation, n = 3. * = $p<0.05$, T-Test.

B. A bar chart to show the proportion of genes regulated by APA in the cytoplasm that have binding sites for RBM3 (left) or CIRBP (right) in the 5'UTR, intron, coding region (CR) or 3'UTR. L = Genes showing 3'UTR lengthening, S = Genes showing 3'UTR shortening.

5.2.5 Let-7 miRNA Family Associated with Cytoplasmic APA Profile Changes During Cold Shock

The above results show that although RBM3 and CIRBP may mediate cytoplasmic APA profile changes, their impact may be limited to a small cohort of genes. Therefore, other cis-elements in the alternative UTRs of the genes exhibiting APA were investigated. Altered miRNA expression has previously been observed in cold shock (Pilotte, Dupont-Versteegden, and Vanderklish 2011), therefore miRNA enrichment analysis, as described in Chapter 3.6 was performed on alternative UTRs of APA regulated genes in cold shock.

A total of 20 miRNAs were enriched in the shortened alternative UTRs while 18 were enriched in the lengthened alternative UTRs (Supplementary Figure 9). Of these 38, 11 miRNAs were members of the miRNA let-7 family. (Figure 5.7A). Mild hypothermia in neuroblastoma cells previously altered expression of the let-7 family of miRNAs (Pilotte, Dupont-Versteegden, and Vanderklish 2011). Given the enrichment of the let-7 family in the alternative UTRs of APA regulated genes, these miRNAs may contribute to the changing APA profile in the cytoplasm of BE(2)-17 cells.

To assess if post-transcriptional APA changes were due to global regulation through RBPs binding to the alternative UTRs, the cohort of genes showing 3'UTR shortening and 3'UTR lengthening were subjected to motif enrichment analysis using DREME (Chapter 2.20). No motifs were enriched in the cohort of shortened alternative UTRs suggesting there is no global regulation causing degradation of longer UTR isoforms. However, 8 motifs were enriched in the lengthened alternative UTRs (Figure 5.7B), and TOMTOM motif analysis was performed to identify RBPs which bind the corresponding motif (Figure 5.7B right column). Many of the RBPs identified were localised to the nucleus (Figure 5.7B, red RBPs) and therefore would not impact cytoplasmic APA profiles. However, cytoplasmic RBPs (Figure 5.7B, purple) and proteins that shuttle between the nucleus and the cytoplasm (Figure 5.7B, blue) were also identified.

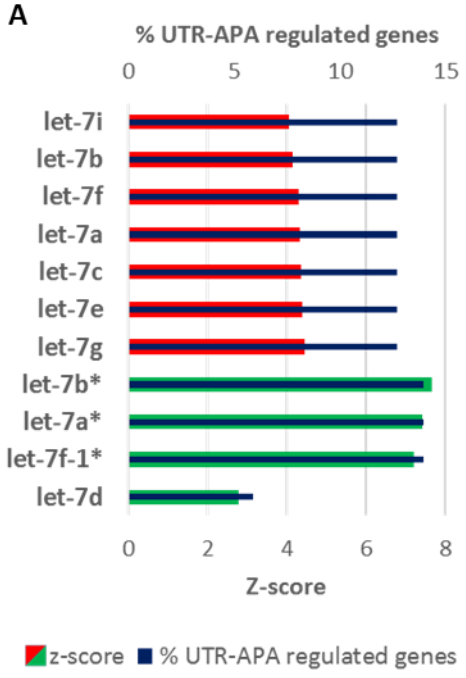
LIN28 was one RBP that binds three of the identified motifs. This protein is associated with translational inhibition of mRNAs targeted to the ER (Cho et al. 2012) as well has inhibiting let-7 miRNA family processing (F. Mayr et al. 2012). Therefore, LIN28 may mediate reduced let-7 miRNA expression which can contribute to global 3'UTR lengthening of let-7

miRNA family target mRNAs. In addition, LIN28 has been associated with stress granules (Buchan and Parker 2009). Therefore, its binding to UTRs may enable localisation of its targets to stress granules where they are stabilised and translationally repressed during cold shock.

Two cytoplasmic RBPs identified to bind these motifs were SAMD4A and G3BP2. Binding of these RBPs in the 3'UTR region contributes to translational inhibition of their target transcripts (Baez and Boccaccio 2005; Matsuki et al. 2013). Therefore, enrichment of SAMD4A and G3BP2 binding motifs in UTR lengthened genes may not explain the APA profile switch, but it can explain the importance of the 3'UTR lengthening event during cold shock, where there is global translational inhibition. G3BP2 is associated with stress granule formation (Matsuki et al. 2013), and its binding to transcripts may facilitate their localisation to these cytoplasmic inclusions where the transcripts are stabilised under stress conditions.

This section identifies the potential importance of the let-7 miRNA family on regulating APA profile changes during cold shock. The identification of LIN28 binding to three enriched motifs in UTR lengthened genes suggests this protein may be important during this temperature stress. Furthermore, binding of LIN28, along with SAM4DA and G3BP2 to the UTR region may aid translational inhibition during cold shock.

A



B

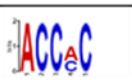
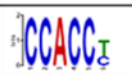
Motif	Logo	E-value	TOMTOM proteins
GASCCC		2.8e-004	PPRC1; ESRP2; FUS; SRSF9; RBM8A
CTCCRG		1.9e-003	RBM6; ESRP2; HNRNPH2; SRSF9; SRSF2; RBM5; **LIN28** SAMD4A
CGCM		9.1e-003	FUS; PPRC1; RBM4; RBM8A; **LIN28**
CMTCCAC		2.4e-002	SRSF1; HNRNPH2; SRSF9; SRSF2 RBM6; RBM28; BRUNOL6; SFPQ; PCBP2; **LIN28**; RBFOX1; G3BP2
ACCMC		1.5e-002	SRSF7; ESRP2; SFPQ; BRUNOL6; RBM45; ELAVL1
CCACCY		1.7e-002	SRSF9; HNRNPH2; SRSF1; SRSF2; DAZAP1; HNRNPK; BRUNOL6; MSI1;
CACAS		4.8e-002	RBM24; BRUNOL5; BRUNOL4; HNRNPL; CNOT4; BRUNOL6; IGF2BP3; HNRPLL
CAGMC		4.3e-002	HNRNPK; G3BP2

Figure 5.7. Let-7 Family of miRNAs may Impact UTR Landscape in Cold Shock.

A. Members of the let-7 miRNA family were enriched in the alternative UTRs of APA regulated genes showing 3'UTR lengthening (red) and 3'UTR shortening (green). Navy bars show the percentage of APA regulated genes targeted by the corresponding miRNA.

B. A table to show the motifs enriched from DREME analysis in the alternative UTRs of genes showing 3'UTR lengthening in cold shock. RBPs that bind to the motifs were identified with TOMTOM analysis and are shown in the right column. RBPs in red are localised to the nucleus, those in blue shuttle between the nucleus and the cytoplasm, and those in purple are localised to the cytoplasm. LIN28 is emphasised in bold as an RBP that interacts with three of the enriched motifs.

5.2.6. A Significant Trend to 3'UTR Lengthening in the Nucleus but not the Cytoplasm During Cold Shock in Differentiated BE(2)-M17 cells

The results above characterise a trend to 3'UTR lengthening in cold shock of BE(2)-M17 cells, but point towards an emphasis on the importance of post-transcriptional APA mediating APA profile changes. In Chapter 3, the BE(2)-M17 cell line was differentiated with retinoic acid (RA) to a more neuronal phenotype. To investigate if the APA changes observed in BE(2)-M17 cells under moderate hypothermia changed in the differentiated cellular state, BE(2)-M17 cells were treated with RA for 72 hours to induce the differentiated phenotype at 37°C and then exposed to moderate hypothermia at 24 hours at 28°C, while control cells were maintained at 37°C.

Undifferentiated and differentiated BE(2)-M17 cells have different gene expression patterns (Chapter 3.2.3). To assess how cold shock affected the gene expression signature, hierarchical clustering analysis was performed (Figure 5.8A). The dendrogram indicates that cold shock has a greater impact on gene expression than neuronal differentiation in both the cytoplasm and the nucleus, as samples cluster based on temperature rather than the differentiation state.

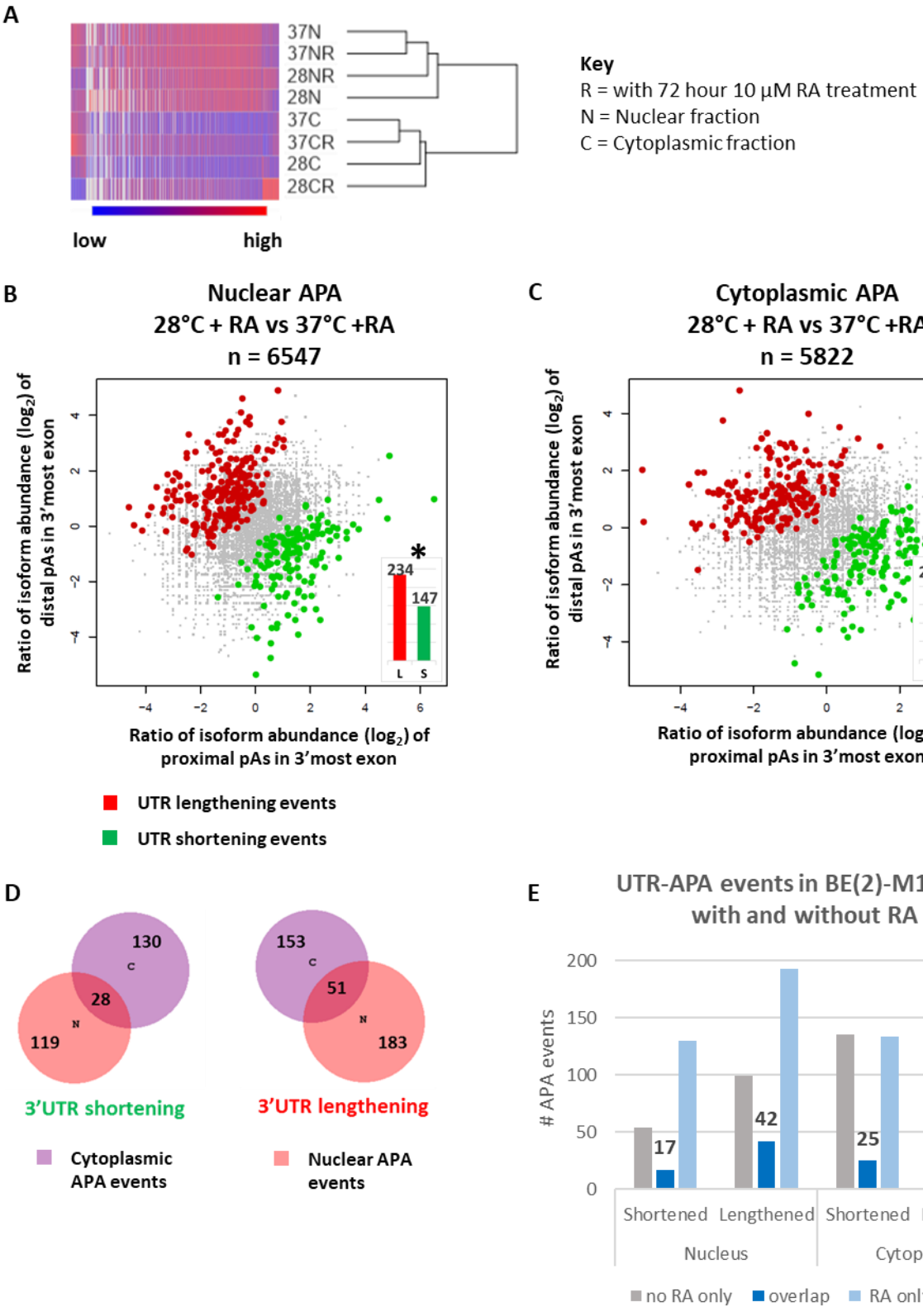
Next, to assess the impact of APA on differentiated BE(2)-M17 cells exposed to cold shock, changes in 3'UTR length were investigated as described in Chapter 5.2.3. In differentiated BE(2)-M17 cells exposed to moderate hypothermia, a total of 381 and 362 significant APA events were identified in the nuclear and cytoplasmic fractions respectively compared to differentiated cells kept at 37°C (Figure 5.8B and C). As in undifferentiated cells, a trend towards 3'UTR lengthening was observed in both the nucleus and the cytoplasm, however in the cytoplasm the extent of this shift in APA profiles was reduced and not significant (Fisher's exact Test $p<0.05$). This may be explained by some transcripts in differentiated cells already using the most distal poly(A) site (as observed in Chapter 3), and therefore do not further lengthen their UTRs during moderate hypothermia. Comparison of the APA regulated genes in the nucleus and the cytoplasm highlights that most cytoplasmic APA profile changes are from post-transcriptional APA regulation (Figure 5.8D) as also observed in undifferentiated cells. This was also observed with upstream-APA (Supplementary Figure 10A-D).

To understand which genes are regulated by APA in both cell types, the significant APA changes between undifferentiated and differentiated cells were overlaid. This showed a modest overlap (Figure 5.8D). Genes showing 3'UTR lengthening in both the nucleus and the cytoplasm of undifferentiated and differentiated cells were enriched in splicing (Supplementary Figure 10E). This suggests that APA control of these genes in cold shock is consistent in both cell types, and important in the cellular adaptation to moderate hypothermia. The other cohorts of genes showing APA in both undifferentiated and differentiated cells were not enriched in any biological processes.

As in undifferentiated BE(2)-M17, 40.4% of APA events are common to differentially expressed genes during moderate hypothermia (Figure 5.8F), suggesting APA is a considerable regulator of transcript abundance in cold shock. GO analysis identified that the overlapping genes were enriched in post-transcriptional regulation of gene expression, as identified in undifferentiated cells in cold shock, but also in RNA processing and intracellular transport (Supplementary Figure 10F).

RAB7A showed significant 3'UTR shortening in the cytoplasm of differentiated cells (Figure 5.8G) as observed in undifferentiated cells. However, 3'UTR shortening was also observed in the nucleus unlike in undifferentiated cells where alterations in the UTR length was a post-transcriptional event. Therefore, although 3'UTR shortening in *RAB7A* is observed in both undifferentiated and differentiated cells, the mechanism of this regulation may vary between the two cellular states.

Investigation into the cis-elements found in the alternative UTRs of APA regulated genes in differentiated BE(2)-M17 cells did not identify any of the same miRNAs or motifs as in undifferentiated cells. Together, these data indicate that a similar global trend to 3'UTR lengthening is present during moderate hypothermia in undifferentiated and differentiated BE(2)-M17 cells, however APA affects different genes and the mechanisms mediating the APA events differ between the two cellular states.


A
37N
37NR
28NR
28N
37C
37CR
28C
28CR
low
high
Key
R = with 72 hour 10 µM RA treatment
N = Nuclear fraction
C = Cytoplasmic fraction
B
Nuclear APA
28°C + RA vs 37°C +RA
n = 6547
Ratio of isoform abundance (log2) of distal pAs in 3'most exon
Ratio of isoform abundance (log2) of proximal pAs in 3'most exon
234
147
L
S
*
UTR lengthening events
UTR shortening events
C
Cytoplasmic APA
28°C + RA vs 37°C +RA
n = 5822
Ratio of isoform abundance (log2) of distal pAs in 3'most exon
Ratio of isoform abundance (log2) of proximal pAs in 3'most exon
204
158
L
S
D
130
C
28
N
119
3'UTR shortening
Cytoplasmic APA events
153
C
51
N
183
3'UTR lengthening
Nuclear APA events
E
UTR-APA events in BE(2)-M17 cells with and without RA
APA events
200
150
100
50
0
17
42
25
75
Shortened
Lengthened
Shortened
Lengthened
Nucleus
Cytoplasm
no RA only
overlap
RA only

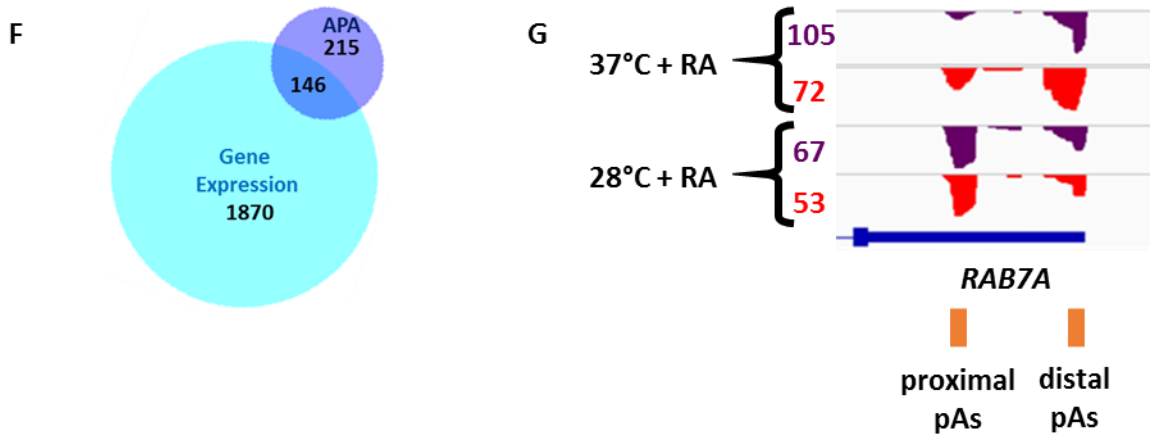


Figure 5.8. Cold shock mediated APA changes in differentiated BE(2)-M17 cells.

A. A heatmap and dendrogram to show the clustering of nuclear and cytoplasmic samples of undifferentiated and differentiated BE(2)-M17 cells in cold shock. R indicates cells treated with 10 µM RA treatment for 72 hour prior to cold shock exposure. Expression of genes from low (blue) to high (red) corresponds to relative expression.

B. and **C.** UTR-APA changes in the nucleus (**B**) and cytoplasm **(C)** showed a trend to 3'UTR lengthening (red bars and dots) compared to 3'UTR shortening (green bars and dots) during cold shock, however this was not significant in the cytoplasm (Fisher's test, * = $p<0.05$).

D. A Venn diagram to show that only 20% of cytoplasmic APA events (purple) also occur in the nucleus (red).

E. A bar chart to show the overlap in UTR-APA during cold shock between undifferentiated (grey) and differentiated (light blue) BE(2)-M17 cells. The genes exhibiting APA in both are indicated by blue bars.

F. A Venn Diagram to show that 40.4% of APA events (blue) overlap with differentially expressed transcripts (cyan).

G. A 3'UTR shortening event that was identified in undifferentiated BE(2)-M17 in the *RAB7A* transcript also holds true in differentiated cells during moderate hypothermia. The 3'UTR shortening event was statistically significant in both the cytoplasm (purple tracks) and the nucleus (red tracks). Numbers on the left indicate the read numbers (in RPM) from sequencing data of the most abundant isoform visualised on the IGV browser using the auto-scale setting.

5.2.7 Cold Shock Induces Cell Type Specific APA Changes between BE(2)-M17 and HEK293 cells

The above results show that during cold shock, different genes were regulated by APA in undifferentiated and differentiated BE(2)-M17 cells. To further explore how APA profiles are affected in cold shock in other cell lines, changes in poly(A) site usage in the HEK293 cell line were investigated.

During cold shock in HEK293 cells, a trend to 3'UTR lengthening was observed in both the nuclear and cytoplasmic fractions (Figure 5.9A and B), with over twice as many significant APA observed in the cytoplasm than in the nucleus. Similar to BE(2)-M17, most of the APA events identified in the cytoplasm were not present in the nucleus suggesting post-transcriptional regulation (Figure 5.9C).

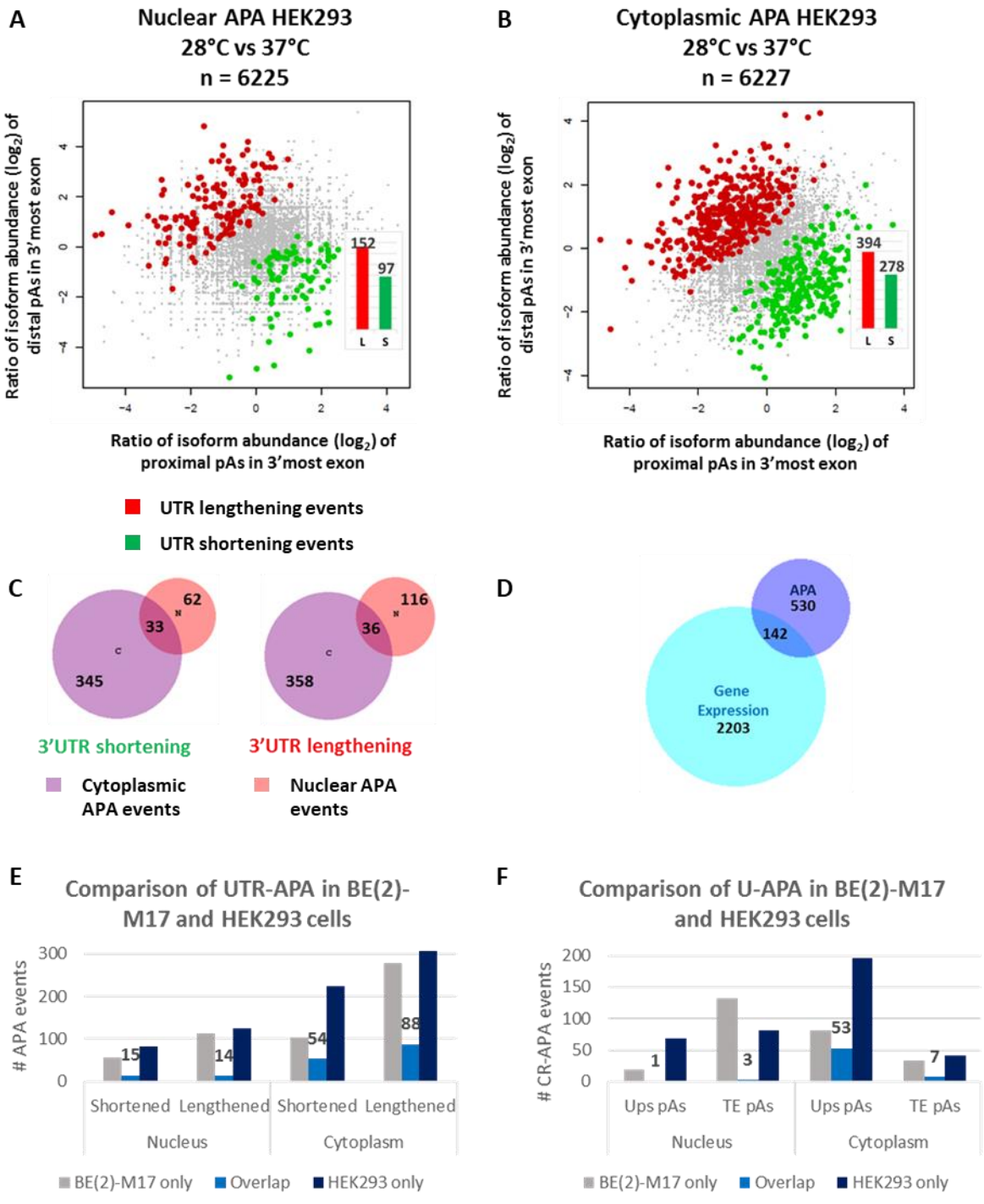
In HEK293 cells, 21.1% of genes that showed APA also exhibited differential gene expression changes (Figure 5.9D). This is significantly lower than in both undifferentiated and differentiated BE(2)-M17 cells, where the overlap was closer to 40%. This indicates that in HEK293 cells, APA plays a reduced role in altering transcript abundance during cold shock.

Overlaying the APA events seen with cold shock in BE(2)-M17 cells and HEK293 cells shows that many of these events are cell type specific, as few genes were APA regulated in moderate hypothermia in both cell lines (Figure 5.9E). In the nuclear fraction, just 11.0% and 21.1% of 3'UTR lengthened and shortened genes respectively in BE(2)-M17 cells also showed APA in HEK293 cells. While in the cytoplasm, 34.2% of 3'UTR shortening events and 24.0% 3'UTR lengthening events from BE(2)-M17 cells were also seen in HEK293 cells. This suggests that poly(A) site choice at the point of cleavage is more cell type dependent than post-transcriptional APA regulation.

To investigate cis-elements in the alternative UTRs of APA regulated genes in HEK293 cells that may mediate post-transcriptional APA, miRNA and motif enrichment analysis was performed as previously described (Chapter 2.20, 2.21). However, none of the same miRNAs or RBP motifs were identified in UTR shortened or lengthened genes. This indicates differential global regulation of the transcriptome in the two cell lines upon exposure to cold shock.

Increased usage of the upstream proximal poly(A) site is seen in the cytoplasmic fractions of both cell lines, however in HEK293 cells, upstream-APA in the cytoplasm was far more prevalent than in BE(2)-M17 cells (Supplementary Figure 11A-B). Interestingly, 53 genes showed an increased usage of an upstream poly(A) site in both BE(2)-M17 and HEK293 cells (Figure 5.9F), as exemplified by the *UBE3B* transcript (Figure 5.9G). This suggests that this upstream-APA event may be a conserved mechanism to contribute to increased protein stability during cold shock.

These results indicate a cell-type specific response at the level of APA during moderate hypothermia. This discrepancy may partly be attributed to differential gene expression, and due to different polyadenylation sites being utilized in different cell types at normal temperatures. Interestingly, in HEK293 cells, GO analysis showed APA regulated genes in the cytoplasm were associated with splicing and mRNA processing, which are the same biological processes as identified in BE(2)-M17 cells (Supplementary Figure 11C). Therefore, while the exact genes may differ, the post-transcriptional regulated changes in APA profiles may nevertheless have a similar effect on the two cell lines.


A
Nuclear APA HEK293
28°C vs 37°C
n = 6225
Ratio of isoform abundance (log2) of distal pAs in 3'most exon
Ratio of isoform abundance (log2) of proximal pAs in 3'most exon
152
97
L
S
B
Cytoplasmic APA HEK293
28°C vs 37°C
n = 6227
Ratio of isoform abundance (log2) of distal pAs in 3'most exon
Ratio of isoform abundance (log2) of proximal pAs in 3'most exon
394
278
L
S
UTR lengthening events
UTR shortening events
C
62
33
N
C
345
116
36
N
C
358
3'UTR shortening
3'UTR lengthening
Cytoplasmic APA events
Nuclear APA events
D
APA
530
142
Gene Expression
2203
E
Comparison of UTR-APA in BE(2)-M17 and HEK293 cells
APA events
300
200
100
0
15
14
54
88
Shortened
Lengthened
Shortened
Lengthened
Nucleus
Cytoplasm
BE(2)-M17 only
Overlap
HEK293 only
F
Comparison of U-APA in BE(2)-M17 and HEK293 cells
CR-APA events
200
150
100
50
0
1
3
53
7
Ups pAs
TE pAs
Ups pAs
TE pAs
Nucleus
Cytoplasm
BE(2)-M17 only
Overlap
HEK293 only

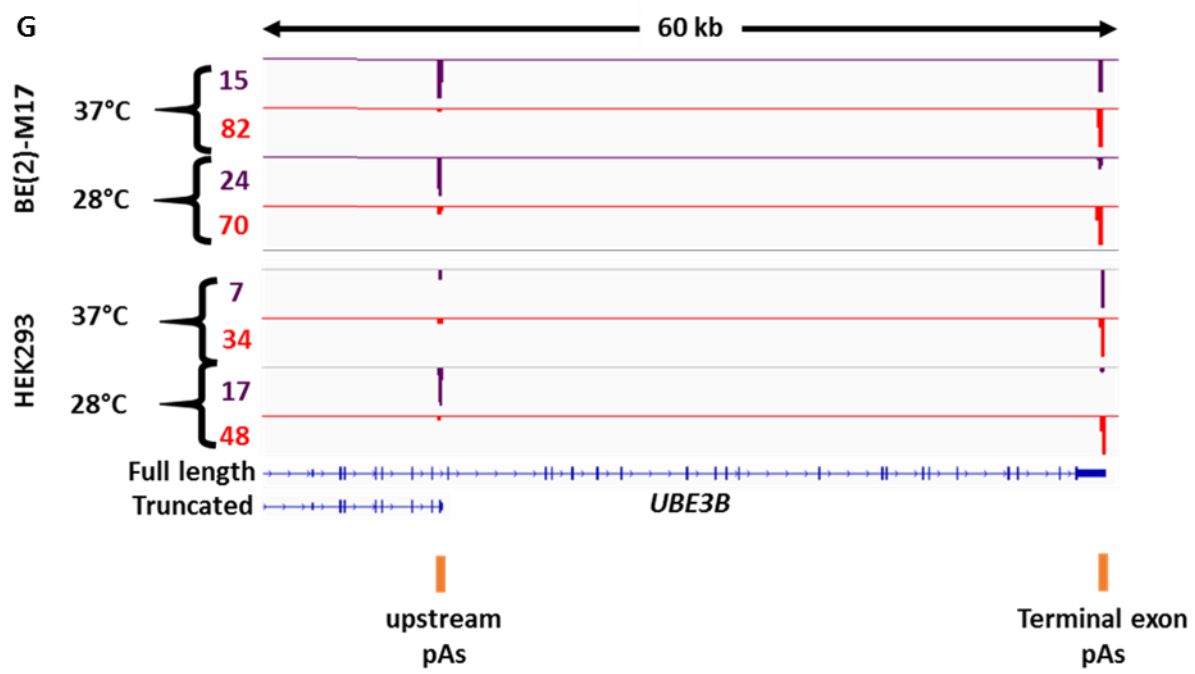


Figure 5.9. 3'UTR lengthening observed in cold shock in HEK293 cells.

A. and **B.** A trend to 3'UTR lengthening is seen in both the nucleus (**A)** and (**B**) the cytoplasm in cold shock in HEK293s as seen in BE(2)-M17 cells.

C. A Venn diagram to show low overlap between the nuclear and cytoplasmic APA events.

D. A Venn diagram to show that 21% of all APA events (blue) identified in HEK293 cells also show altered Gene Expression (cyan).

E. A bar graph highlighting the minimal overlap in genes showing 3'UTR-APA changes in BE(2)-M17 cells (grey bars) and HEK293s (navy bars). The overlapping genes are indicated by blue bars.

F. A bar graph indicating the overlap of upstream-APA regulated genes in BE(2)-M17 cells (grey) and HEK293 cells (navy). Genes that show upstream-APA in both cell lines are indicated by blue bars. Ups pAs: genes that show increased usage of the upstream poly(A) site; TE pAs: genes that show increased usage of the terminal exon poly(A) site.

G. A screenshot to show increased usage of the upstream poly(A) site in the *UBE3B* transcript was observed in the cytoplasmic fraction (purple tracks) but not in the nuclear fraction (red tracks), of HEK293 and BE(2)-M17 cells. The numbers on the left indicate read numbers (in RPM) from sequencing data of the most abundant transcript isoforms visualised on IGV Browsert using auto-scale settings.

5.3. APA in Hypoxia

5.3.1. Characterisation of Hypoxia in BE(2)-M17

An oxygen concentration of 2% has been used to mimic hypoxic conditions in cell culture (Chi et al. 2006). Hypoxia treatment for 24 hours in colorectal cancer cells has previously shown no effect on cell proliferation or apoptosis (Memon et al. 2016). To assess transcriptome changes in BE(2)-M17 cells under hypoxia, cells were grown at 37°C with 2% oxygen for 24 hours. As observed in other cell lines, no obvious changes in cell morphology were seen (Figure 5.10A).

Hypoxic conditions mediate gene expression changes through the hypoxia-inducible transcription factor HIF-1. HIF-1 expression is regulated post-translationally, as described in Chapter 5.1.3. To confirm HIF-1 mediated changes in BE(2)-M17 cells exposed to hypoxia, expression of *HIF1A* and the known HIF-1 target *VEGFA* were verified with RT-PCR. As expected, *HIF1A* did not show a significant increase in expression, however *VEGFA* showed significant upregulation through RT-PCR analysis (Figure 5.10B). *VEGFA* is upregulated in tumours, and induces proliferation of vascular endothelial cells. Therefore, it is interesting that this gene is upregulated with hypoxia in this neuroblastoma cell line, despite not having an obvious function.

To assess hypoxia induced changes on gene expression on a genome-wide scale, nuclear and cytoplasmic RNA from hypoxia treated and untreated cells were subject to RNA-seq, and reads were analysed through a bioinformatics pipeline as described in Chapter 3.2.2. Upon exposure to hypoxia 452 and 479 genes showed statistically significant (Fisher's exact Test, $p<0.01$, FC >2) upregulation and downregulation respectively in the nucleus (Figure 5.10C, left panel). HIF-1 can influence transcription of over 100 genes (Weidemann and Johnson 2008), but this magnitude of change, suggests additional transcription factors are contributing to gene expression changes.

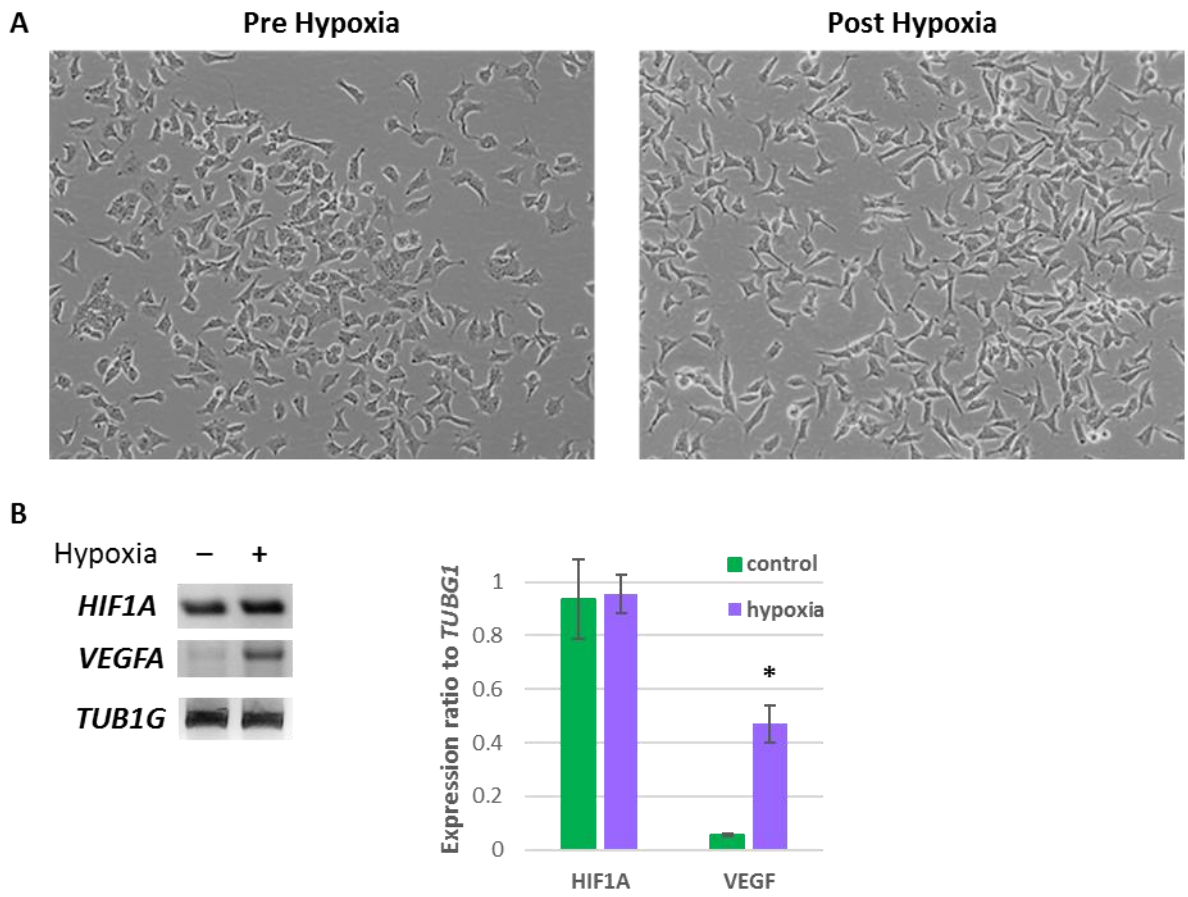
Over 1500 genes showed altered expression in hypoxia in the cytoplasmic fraction, with 563 upregulated and 992 downregulated (Figure 5.10C, middle panel). From these, 484 and 873 were uniquely up- or downregulated only in the cytoplasm and not the nucleus suggesting

alternative factors are mediating transcript abundance in the cytoplasm (Figure 5.10C, right panel).

Through GO analysis, upregulated genes in the nucleus were identified to be associated with the 'cellular response to hypoxia', while downregulated genes were associated with RNA catabolism and with the cell cycle (Figure 5.10D, upper panel). Downregulation of genes associated with RNA degradation may contribute to increased RNA stability in hypoxic conditions as has been previously observed (Gardner 2008).

Genes that were downregulated only in the cytoplasm were associated with mitochondrial translation and mitochondrial respiratory chain assembly. This may suggest reduced ATP synthesis, as would be expected in low oxygen conditions when there is a shift from OXPHOS to anaerobic glycolysis (Figure 5.10D, lower panel). Notably, these genes are downregulated post-transcriptionally and not through transcriptional activity. Upregulated genes were associated with cellular stress and hypoxic response (Figure 5.10D, lower panel). This suggests that the abundance of an additional cohort of transcripts encoding proteins associated with stress are regulated only in the cytoplasm.

Together these results show that HIF-1 inducible genes were indeed upregulated in hypoxic conditions in BE(2)-M17 cells, but a large proportion of gene expression changes in the cytoplasm were not through changes in transcription, but rather changes in nuclear export or cytoplasmic stability. Upregulation of genes associated with glucose metabolism in hypoxia and downregulation of genes associated with the cell cycle was observed as in previous studies (Weigand et al. 2012).


A
Pre Hypoxia
Post Hypoxia
B
Hypoxia – +
HIF1A
VEGFA
TUB1G
Expression ratio to TUBG1
control
hypoxia
*
HIF1A
VEGF
C
Nucleus
452
476
Up
Down
Log2(FC)
log2(Mean Expression)
Cytoplasm
484
79
119
873
Changes in Gene Expression in Hypoxia
Number of Genes
79
119
UP
DOWN
N only
overlap
C only

D

	Nucleus GO biological process	# Genes present	# Genes Expected	Fold Enrichment	P-value
UP	Glycolytic Process	9	1.13	7.95	2.48E-02
	mRNA splicing, via spliceosome	32	8.25	3.88	1.48E-06
	Response to Hypoxia	32	12.85	2.49	3.35E-02
	Nuclear-transcribed mRNA catabolic process, Nonsense-mediated Decay	13	2.67	4.86	3.70E-02
DOWN	RNA processing	50	19.49	2.56	1.69E-05
	Cell Cycle	63	29.76	2.12	1.81E-04

	Cytoplasm GO biological process	# Genes present	# Genes Expected	Fold Enrichment	P-value
UP	Canonical Glycolysis	9	1	9	9.24E-03
	mRNA splicing, via spliceosome	49	10.93	4.48	9.99E-14
	Cellular Response to Hypoxia	23	7	3.28	9.91E-03
	Cellular Response to Decreased Oxygen levels	23	7.27	3.16	1.84E-02
	Cell Cycle Process	74	38.4	1.93	8.25E-04
DOWN	Mitochondrial Respiratory Chain Complex I Assembly	15	3.6	4.17	4.71E-02
	Mitochondrial Translation	21	6.05	3.47	1.28E-02
	Translation	74	22.2	3.33	1.13E-14
	Cellular Respiration	27	9.36	2.88	1.48E-02

Figure 5.10. Gene Expression Signature of Hypoxia in BE(2)-M17 cells.

A. No visually obvious change in cell morphology observed with 2% oxygen incubation for 24 hours.

B. Left panel: a representative RT-PCR using RNA isolated from the whole cell fraction to show no significant increase in expression of *HIF1A* at mRNA level but large increase in HIF-1 target gene *VEGFA* upon hypoxia in the cytoplasmic fractions of BE(2)-M17 cells. Right panel: A bar chart to show quantified intensities of bands using ImageJ software, showing the ratio of change in expression of *HIF1A* and *VEGFA* normalised to *TUBG1*. Error bars show standard deviation, n = 3. T-test * = $p<0.01$.

C. MA plot to show the number of genes differentially expressed during 24 hour hypoxia treatment in BE(2)-M17 cells. Left panel: differentially expressed genes in the nucleus are indicated by red dots. Middle panel: differentially expressed genes only in the cytoplasm are represented by purple dots, while those that are also altered in the nucleus are indicated by blue dots. Right panel: a bar chart to highlight the low overlap (blue) of gene expression changes in the nucleus (red) and cytoplasm (purple). Statistically differentially expressed genes are defined by Fisher's exact Test, $p<0.01$, $FC>2$.

D. A table to show a selection of enriched biological pathways identified through GO Analysis of genes showing differential expression in the nucleus (upper panel) and uniquely in the cytoplasm (lower panel).

5.3.2 Hypoxia does not Mediate a Shift to either 3'UTR Lengthening or 3'UTR Shortening

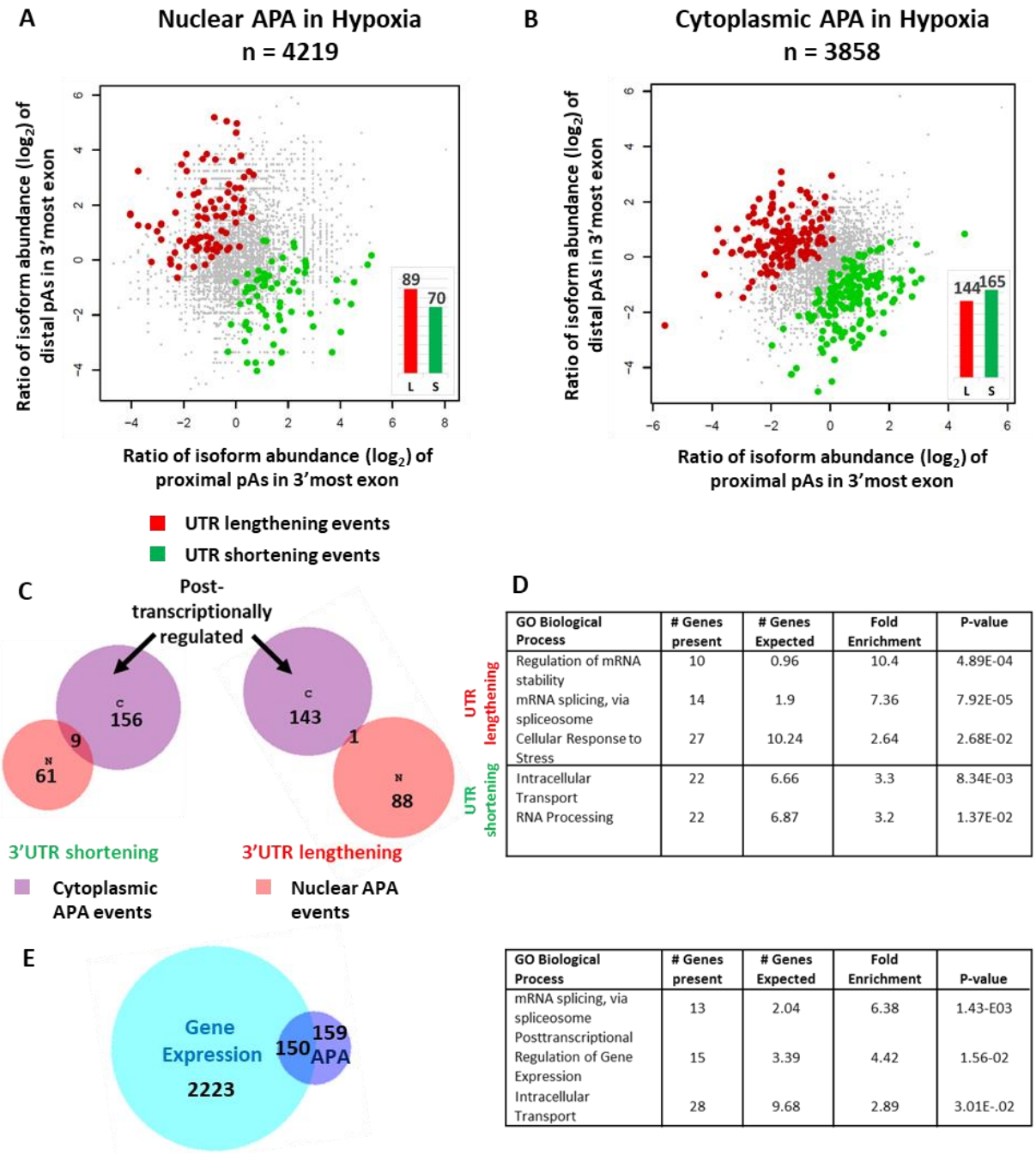
Widespread gene expression changes were observed during hypoxia in BE(2)-M17 cells, though the majority of changes in the cytoplasm represented post-transcriptional changes. Although widespread gene expression changes have been reported in hypoxia, the changes in the transcriptome at the level of APA have not been assessed. To address this, significantly changing APA events ($p<0.01$ Fisher's exact Test, with a minimum 5% change in APA isoform abundance) between cells grown at normoxia or hypoxia (2% oxygen), were identified separately in the nucleus and cytoplasm.

In the nucleus, 159 statistically significant APA events were identified, 56% of which increased usage of a distal poly(A) site (Figure 5.11A, red dots and bars). However, unlike cold shock, this did not show a statistically significant trend to 3'UTR lengthening. During hypoxia, 309 statistically significant APA events were identified in the cytoplasm (Figure 5.11B), but only 10 of these were also identified in the nucleus (Figure 5.11C). As observed with cold shock, most of the cytoplasmic APA events appear to be regulated in a post-transcriptional manner, however unlike cold shock, there was no statistical trend to 3'UTR shortening or lengthening. This result indicates that the nature of the cellular stress can have very different implications on the transcriptome at the level of APA. However, through GO analysis, genes showing 3'UTR lengthening in the cytoplasm were enriched in genes associated with splicing and cellular response to stress (Figure 5.11D), as also seen in cold shock. This indicates similarities in the cohorts of genes subjected to APA in general stress conditions.

Interestingly, 48.5% of genes exhibiting significant APA also showed statistically significant changes in gene expression (Figure 5.11E, left panel), suggesting APA may be important in mediating transcriptome changes during hypoxia. The overlap of genes was enriched in genes associated with splicing and regulation of gene expression (Figure 5.11E, right panel), which are affected during the hypoxic response.

These results show that that APA regulation is distinctly different in hypoxia compared to moderate hypothermia, as no trend to 3'UTR lengthening was observed. Significant APA during hypoxic conditions was observed in a cohort of physiologically relevant genes including genes associated with RNA processing and stress responses. This suggests that

APA is important for transcriptome changes in the hypoxic response. Interestingly almost 50% of genes regulated by APA also showed differential expression, highlighting the novel regulation of this cohort of genes during hypoxia. Comparison of APA regulation in hypoxia and moderate hypothermia is further explored in Chapter 5.4.



GO Biological Process	# Genes present	# Genes Expected	Fold Enrichment	P-value
Regulation of mRNA stability	10	0.96	10.4	4.89E-04
mRNA splicing, via spliceosome	14	1.9	7.36	7.92E-05
Cellular Response to Stress	27	10.24	2.64	2.68E-02
Intracellular Transport	22	6.66	3.3	8.34E-03
RNA Processing	22	6.87	3.2	1.37E-02

GO Biological Process	# Genes present	# Genes Expected	Fold Enrichment	P-value
mRNA splicing, via spliceosome	13	2.04	6.38	1.43-E03
Posttranscriptional Regulation of Gene Expression	15	3.39	4.42	1.56-02
Intracellular Transport	28	9.68	2.89	3.01E-.02

Figure 5.11. Greater extent of post-transcriptional APA regulation in hypoxia.

A. and **B.** Statistically significant APA events ($p<0.01$ Fisher's exact Test, with a minimum 5% change in APA isoform abundance) identified in BE(2)-M17 during 24 hour hypoxia exposure compared to normoxia in the nucleus (**A**) and cytoplasm (**B**). Red dots and bars: 3'UTR lengthening events; Green dots and bars: 3'UTR shortening events.

C. A Venn diagram to show the limited overlap of APA events between the nuclear (red) and cytoplasmic (purple) fractions.

D. A table highlighting biological pathways associated with the genes regulated by APA in hypoxia.

E. Left panel: a Venn diagram to show that 48.5% of genes exhibiting APA (blue) also show changes in gene expression (cyan) under low oxygen conditions. Right panel: a table to show biological pathways associated with the genes regulated by APA that show differential expression in hypoxia.

5.3.3 Cis-elements in alternative UTRs may Mediate Cytoplasmic APA profiles

To understand the global regulatory mechanisms of post-transcriptional APA changes during hypoxia, cis-elements in the alternative UTR of the genes exhibiting APA in the cytoplasm were investigated. Motif enrichment analysis using DREME (Chapter 2.20) identified no statistically significant motifs in either the cohort of genes showing 3'UTR shortening or 3'UTR lengthening in hypoxia. This suggests that there are no RBPs that globally regulate APA profile changes in hypoxia.

Extensive changes in miRNA expression have been identified during hypoxia which contribute to the cellular response and physiological cellular state (Supplementary Table 4) (Nallamshetty, Chan, and Loscalzo 2013; Kulshreshtha et al. 2008; Kulshreshtha et al. 2006). To investigate if miRNAs are involved in regulating APA profiles in BE(2)-M17 cells subjected to hypoxia, the alternative UTRs of genes exhibiting only cytoplasmic APA were subjected to an miRNA target site enrichment analysis, as previously described (Chapter 2.21). From this, 7 miRNAs were enriched in the alternative UTRs of genes showing 3'UTR shortening (Figure 5.12A), while 21 miRNAs were enriched in the alternative UTRs of genes showing 3'UTR lengthening (Figure 5.12B).

Downregulation of an miRNA during hypoxia that targets the alternative UTR region of a gene may result in stabilization of the longer transcript isoform. miR-19a, which has shown altered expression in hypoxia (Kulshreshtha et al. 2008) targets 13 genes that show 3'UTR lengthening during hypoxic stress in BE(2)-M17. One of the miR-19a target genes that shows 3'UTR lengthening during hypoxia is *IREB2* (Figure 5.12C). This gene encodes an RBP that binds iron responsive elements in the 5'- and 3'UTRs of its target mRNAs to mediate their translation. IREB2 was shown to regulate translation of the *HIF2A* transcript (Sanchez et al. 2007). Downregulation of miR-19a could contribute to the stabilisation of the longer *IREB2* transcript which may affect its protein expression during hypoxia, mediating the expression of *HIF2A*. However, other miRNAs are also found in the *IREB2* alternative UTR (Figure 5.12C, yellow boxes) which could modulate the 3'UTR lengthening event, although it is unclear if their expression is altered in hypoxia. The expression change of miR-19a during hypoxic treatment of BE(2)-M17 cells should be further investigated to verify the mechanism of this UTR lengthening event.

This section gives an insight into which miRNAs may be globally regulating the cytopasmic transcriptome under hypoxia stress conditions. The changing expression of these miRNAs during hypoxia in BE(2)-M17 cells would need to be validated to understand the extend of miRNA mediated regulation in hypoxia.

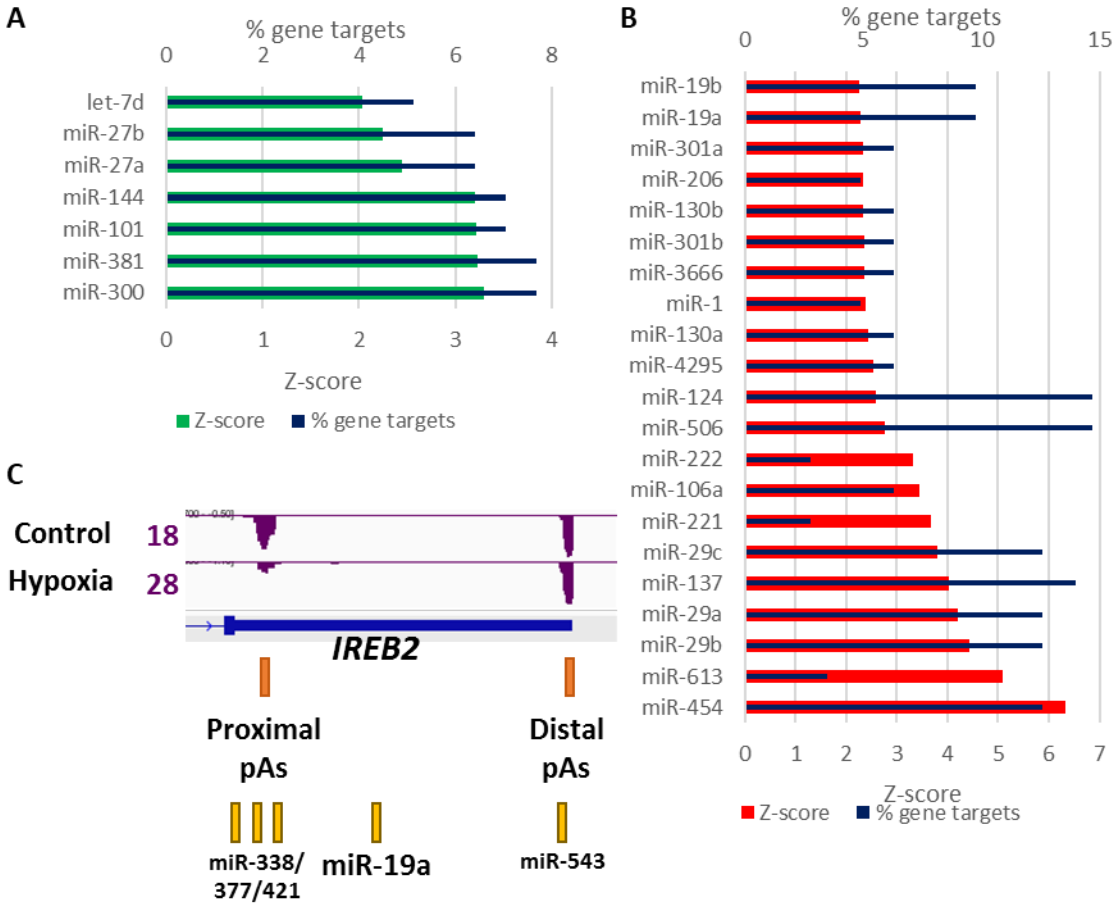


Figure 5.12. The role of miRNAs in mediating the UTR landscape during hypoxia.

A. and **B.** The miRNAs enriched through z-score analysis in the cohort of genes showing 3'UTR shortening (**A**) and 3'UTR lengthening (**B**) are shown in green and red bars respectively. Navy bars indicate the percentage of gene targets of the corresponding miRNA in the cohort of shortened or lengthened genes.

C. 3'UTR lengthening observed in the *IREB2* gene which may be attributed to the downregulation of miR-19a in hypoxia. Other miRNA target sites in the *IREB2* UTR are indicated yellow boxes. Purple tracks represent cytoplasmic reads identified through 3'end RNA-seq. The numbers onf the left indicate the read numbers in reads per million (RPM) from sequencing data of the most abundant transcript isoform. Tracks are visualised on the IGV Browser using auto-scale settings.

5.4. APA in Combined Stresses

5.4.1 Moderate Hypothermia Reduces Impact of Differential Gene Expression Induced by MPP+ and Hypoxia

Different stress conditions induce various responses to adapt to the new environment and enable cell survival. The last two sections of this chapter characterised transcriptome changes in BE(2)-M17 cells in cold shock and low oxygen conditions. The above results show that the general APA trends and cohorts of genes affected during moderate hypothermia and hypoxia are very different, suggesting stress specific responses.

To identify genes showing altered expression in general stress conditions, differentially expressed genes in moderate hypothermia, hypoxia, and stress induced by the neurotoxin MPP+ were compared to unstressed cells. This comparison identified very few genes that were differentially expressed in all three stress conditions (Figure 5.13A, white numbers).

Reports have suggested that hypothermia can have a neuroprotective role and therefore ameliorate neurotoxic insults (Peretti et al. 2015; Pilotte, Dupont-Versteegden, and Vanderklish 2011; Rzechorzek et al. 2015; Zhang et al. 2015; Chip et al. 2011; Saito et al. 2010), however global transcriptome changes upon cold shock and other stresses have not been investigated. Therefore, cells were exposed to moderate hypothermic conditions and low oxygen or MPP+ treatment to assess how the abundance of transcripts changed under multiple stress conditions.

First, hierarchical clustering of gene expression using reads per million from sequencing data in each of the stress conditions was done to assess the global impact of combined stresses. In the nucleus, cold shock and cold shock with MPP+ treatment clustered together showing the most similar expression pattern (Figure 5.13B, upper panel). Gene expression under hypoxia was distinctly different from the other stresses and remarkably, most different between hypoxia at the two temperatures, suggesting a unique transcriptional response at 28°C compared to 37°C in low oxygen conditions.

In the cytoplasm, cold shock, cold shock with MPP+ and MPP+ treatment clustered in a similar manner to the nucleus (Figure 5.13B, lower panel). However, cold shock with hypoxia was more like hypoxia at 37°C and clustered closer to untreated cells than other cold

shock profiles, suggesting this combination of stresses has a more similar transcriptome profile to control cells.

Together, these results show that the transcriptome profiles in different stresses cluster differentially in the cytoplasm and the nucleus, and that the hypoxia signature at both temperatures is distinctly different to MPP+ and cold shock in both subcellular fractions.

Next, the genes that were differentially expressed upon exposure to hypoxia or MPP+ at control (37°C) and cold (28°C) temperatures were compared. With both hypoxia and MPP+ treatment, exposure to moderate hypothermia significantly reduced the number of genes that were differentially expressed in the nucleus ($p < 0.01$, Fisher's exact Test) (green and blue bars, Figure 5.13C). This may suggest that moderate hypothermia reduces the extent of transcriptomic changes when cells are exposed to additional stresses. However, this did not hold true in the cytoplasm, suggesting that the combination of cellular stress affects the nuclear and cytoplasmic transcriptome differently.

To identify stress response genes that are induced specifically in hypoxia and MPP+, overlaps between differentially expressed genes with hypoxia or MPP+ exposure at the two temperatures, 28°C and 37°C were assessed. Comparison of cells exposed to hypoxia showed a greater overlap of genes differentially expressed between the two temperatures than with MPP+ treatment (yellow bars, Figure 5.13C). In both the nucleus and the cytoplasm, the genes upregulated at both temperatures were associated with the 'cellular response to hypoxia', and several of these genes were targets of the transcription factor HIF-1. This indicates that the hypoxic response via HIF-1 is not affected in moderate hypothermia.

Only 7 genes show altered gene expression with MPP+ treatment at both temperatures in the nucleus (Right panel, yellow bars, Figure 5.13C). This suggests that transcriptional changes with MPP+ treatment are distinctly different at the two temperatures. In the cytoplasm, 32% of genes upregulated at 28°C with MPP+ treatment were also upregulated at 37°C. These 34 genes were not enriched in any biological pathways from GO analysis. With MPP+ treatment at 37°C, upregulated genes were enriched in apoptotic genes suggesting preparation for cell death, and downregulated genes were associated with mitochondrial biogenesis and OXPHOS due to mitochondrial dysfunction (Chapter 4B). However, neither of these pathways was identified with MPP+ exposure at 28°C, suggesting that cold shock may

have prevented upregulation of apoptotic genes and mitochondria were not as severely affected by the MPP+ treatment.

This data suggests that moderate hypothermia can reduce the extent of transcriptional changes upon exposure to other stresses in BE(2)-M17 cells. This could play a protective role at the transcriptional level by mediating which mRNAs are expressed to affect the cellular response. However, genes induced by the transcription factor HIF-1 were still induced in hypoxia at 28°C.

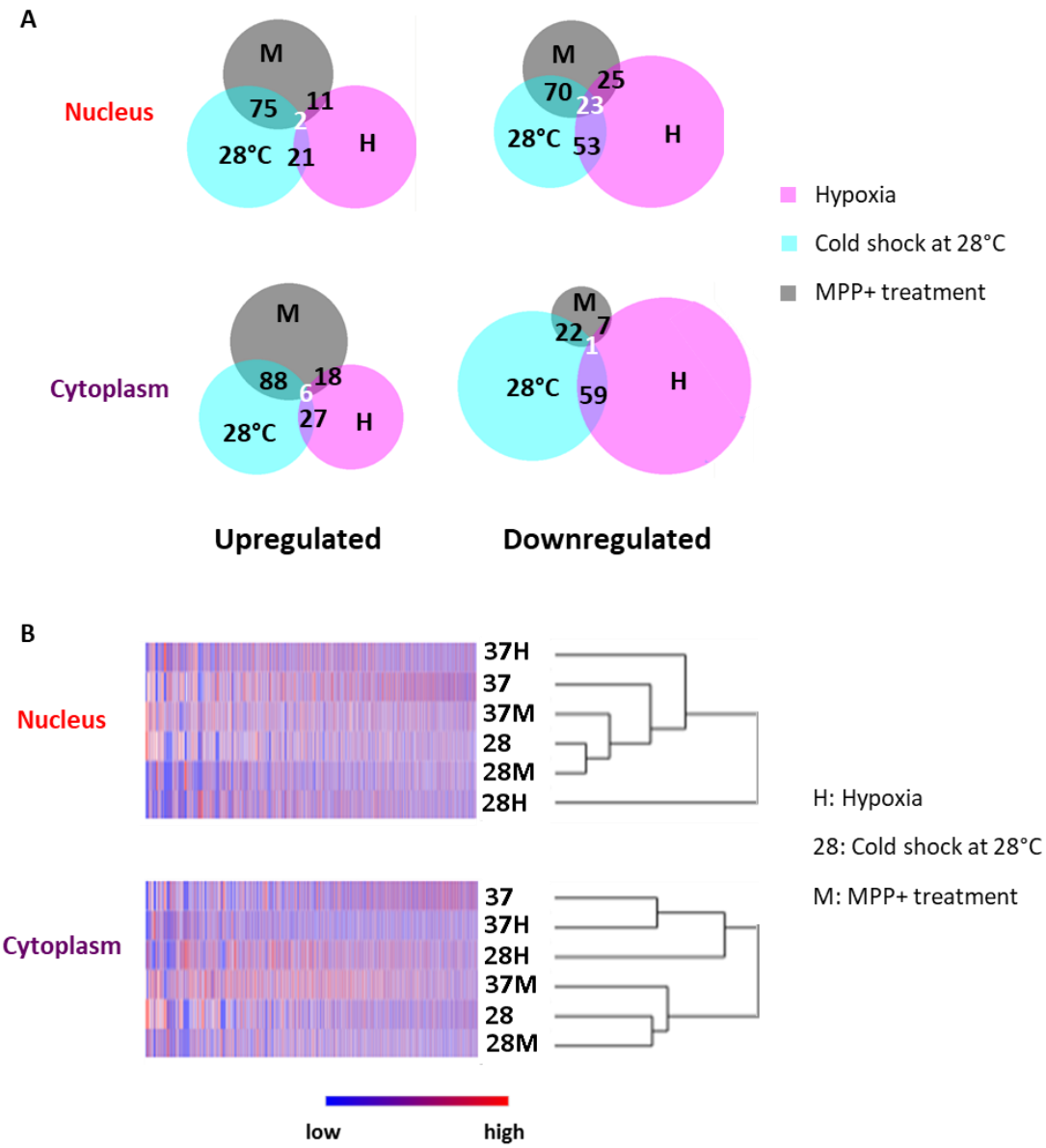

A
Nucleus
M
75
11
2
28°C
21
H
M
70
25
23
28°C
53
H
Hypoxia
Cold shock at 28°C
MPP+ treatment
Cytoplasm
M
88
18
6
28°C
27
H
M
22
7
1
28°C
59
H
Upregulated
Downregulated
B
Nucleus
37H
37
37M
28
28M
28H
H: Hypoxia
28: Cold shock at 28°C
M: MPP+ treatment
Cytoplasm
37
37H
28H
37M
28
28M
low
high
C
Genes Differentially Expressed under exposure to MPP+ or Hypoxia at different temperatures
Number of Genes
800
700
600
500
400
300
200
100
0
37°C only
Overlap
28°C only
96
48
91
42
4
3
34
3
UP
DOWN
UP
DOWN
UP
DOWN
UP
DOWN
Nucleus
Cytoplasm
Nucleus
Cytoplasm
Hypoxia
MPP+

Figure 5.13. Differential Gene Expression in BE(2)-M17 cells Exposed to MPP+ or Hypoxia at Different Temperatures.

A. Venn diagrams to show the number of genes upregulated (left) and downregulated (right) in the nucleus (upper) and cytoplasm (lower) in stress conditions compared to control cells. MPP+ (M, grey); cold shock (28°C, cyan); Hypoxia (H, pink). Cells were exposed to different types of stress for 24 hours. The number of genes differentially expressed in two stress conditions are indicated in black numbers, while white numbers show the number of genes differentially expressed in all three stress conditions.

B. A heatmap (left) and dendrogram (right) to show hierarchical clustering of the gene expression signatures with MPP+ (M) Hypoxia (H), Cold (28) or a combination and untreated BE(2)-M17 cells in the nucleus (upper) and the cytoplasm (lower). Relative gene expression is shown by the blue (low) to red (high) scale.

C. A bar chart to show the number of genes differentially expressed in Hypoxia (left) or MPP+ (right) at 37°C (green bars) or 28°C (blue bars). Asterisks indicate where significantly fewer genes were differentially expressed at the colder temperature (Fisher's exact Test, * = $p<0.01$). The genes which were differentially expressed at both temperatures are indicated by yellow bars.

5.4.2 Different Cohorts of Genes are Regulated by APA under Different Stress Conditions

The previous sections assessed genome wide transcript expression changes under different stress conditions. To investigate which genes are regulated by APA in different stress conditions, the UTR-APA regulated genes were overlapped. As shown in Figure 5.14A, there was a greater overlap in APA regulated genes in the cytoplasm (Figure 5.14A, lower panel) than APA regulated genes in the nucleus (Figure 5.14A, upper panel). This suggests that post-transcriptional APA regulation is more similar between the different stress responses, than transcriptional APA regulation.

Cold shock showed a trend to 3'UTR lengthening in the cytoplasm and nucleus but exposure of cells to both MPP+ and hypoxia did not exhibit a trend to either 3'UTR lengthening or shortening. To assess if there was a significant shift in UTR length with combined stresses, poly(A) site usage in cells exposed to cold shock **and** MPP+ or hypoxia were compared to cells exposed to either cold shock **or** MPP+ or hypoxia.

APA events that were specific to hypoxia or MPP+ were investigated by overlapping the cohorts of genes showing significant UTR-APA with hypoxia or MPP+ exposure at both temperatures. In hypoxia, fewer than 8% of genes that were regulated by APA at 37°C were also regulated by APA at 28°C (Figure 5.14B left panel). This indicates that APA events at the two different temperatures are independent of the low oxygen state, but more likely to be due to a temperature shift. The same observation was made in cells exposed to MPP+ at different temperatures (Figure 5.14B right panel).

In the cytoplasm of cells exposed to hypoxia, there were more significant APA events at 28°C than 37°C (Figure 5.14B, blue bars compared to green bars), suggesting that cold shock has a larger impact on APA shifts than the other two stresses. This was observed in both the nucleus and the cytoplasm of MPP+ treated cells (Figure 5.14B, right)

These data suggest that cold shock has greater impact on APA than the other two stresses, and that APA changes due to cold shock override those induced by hypoxia or MPP+.

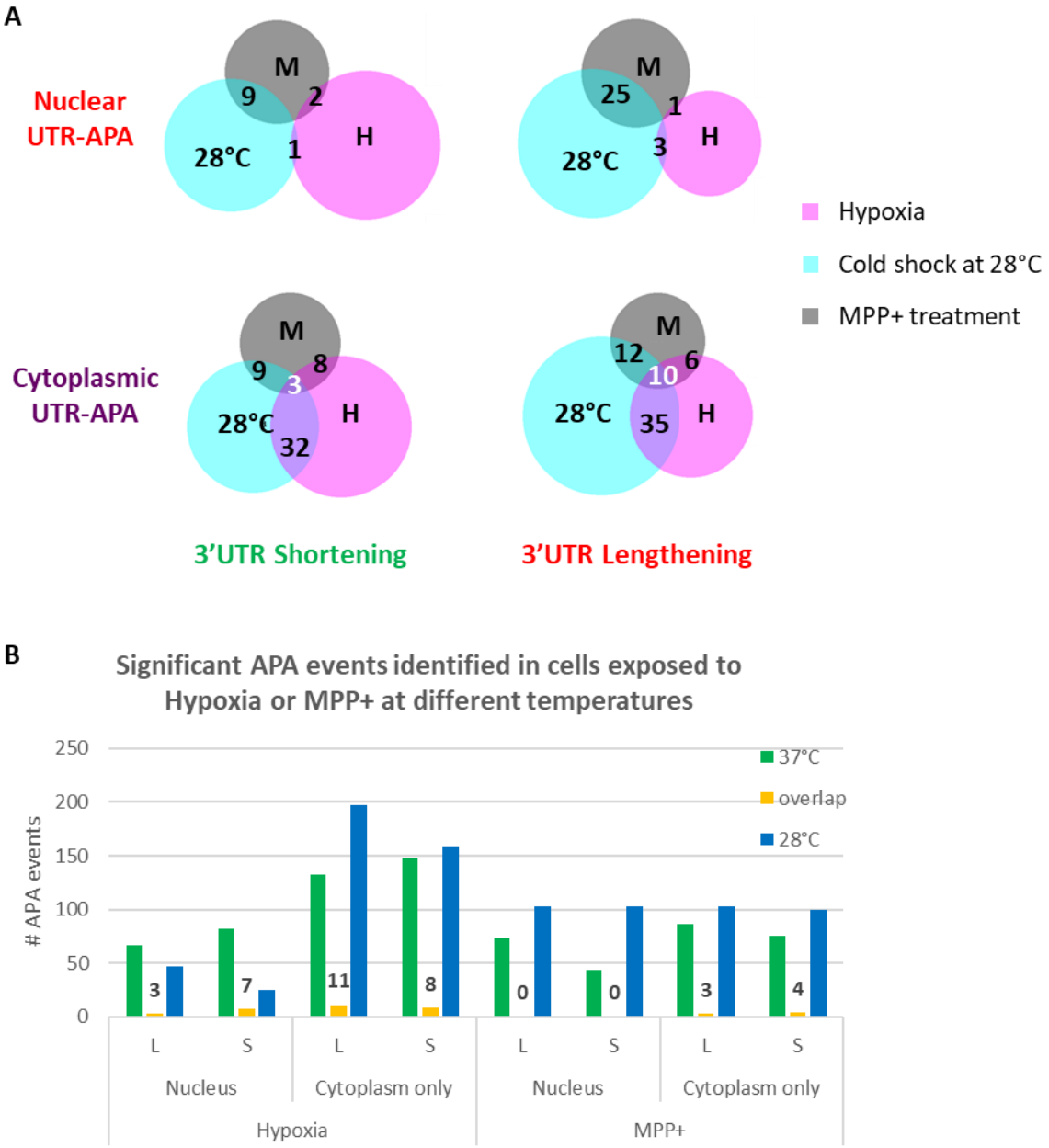


Figure 5.14. Differential APA Regulation in BE(2)-M17 cells exposed to MPP+ or Hypoxia at Different Temperatures.

A. Venn diagrams to show overlap in 3'UTR shortening (left) and lengthening (right) events in cold shock (28°C, cyan), MPP+ treatment (M, grey) or Hypoxia (H, pink) compared to control cells. Cells were exposed to stress for 24 hours. The number of commonly regulated APA genes are shown in black numbers, whereas white numbers indicate APA events occurring in all three stress conditions.

B. A bar chart to show significant APA changes in hypoxia (left) and MPP+ treatment (right) at 37°C (green bars) or 28°C (blue bars). The genes which were regulated by APA at both temperatures are indicated by yellow bars. L indicates 3'UTR lengthening events, S indicates 3'UTR shortening events.

To investigate if moderate hypothermia has the same impact of 3'UTR lengthening in combination with other stresses, UTR-APA events in BE(2)-M17 cells exposed to either MPP+ or hypoxia at 28°C or 37°C were compared. A significant trend to 3'UTR lengthening was observed in the cytoplasmic fractions with both hypoxia and MPP+ at 28°C compared to 37°C (Figure 5.15A). However, the trend to lengthening was less significant in the nuclear fraction with hypoxia, and not present with MPP+. This suggests that post-transcriptional APA regulatory mechanisms in cold shock persist in the presence of other stresses to stabilize longer UTRs in the cytoplasm.

The UTR-APA events that were specific to cold shock were identified by overlapping the APA regulated genes in cold shock with hypoxia or MPP+ treatment compared to cells exposed to hypoxia or MPP+ at 37°C (Figure 5.19B). Notably, there is a greater overlap of APA regulated genes between cold shock and cold shock with MPP+ treatment compared to cold shock and cold shock with hypoxia (Figure 5.19B grey and cyan circles). This suggests that hypoxia has a distinctly different impact on APA at lower temperatures than MPP+.

The *RRM2* gene shows 3'UTR lengthening at 28°C in every stress condition (Figure 5.15C). This gene encodes a protein associated with DNA synthesis and cell proliferation. Translational inhibition is observed in cold shock, and this 3'UTR lengthening event may facilitate translational repression of this transcript during stress conditions.

These data therefore suggest that although the general trend of 3'UTR lengthening in the cytoplasm persists in moderate hypothermia in combination with other stresses, the actual genes that are regulated are unique in each combined stress. This may be due to changing concentrations of cleavage factors in the nucleus or altered expression of RBPs and miRNAs in the cytoplasm to influence transcriptional and post-transcriptional APA regulation respectively.

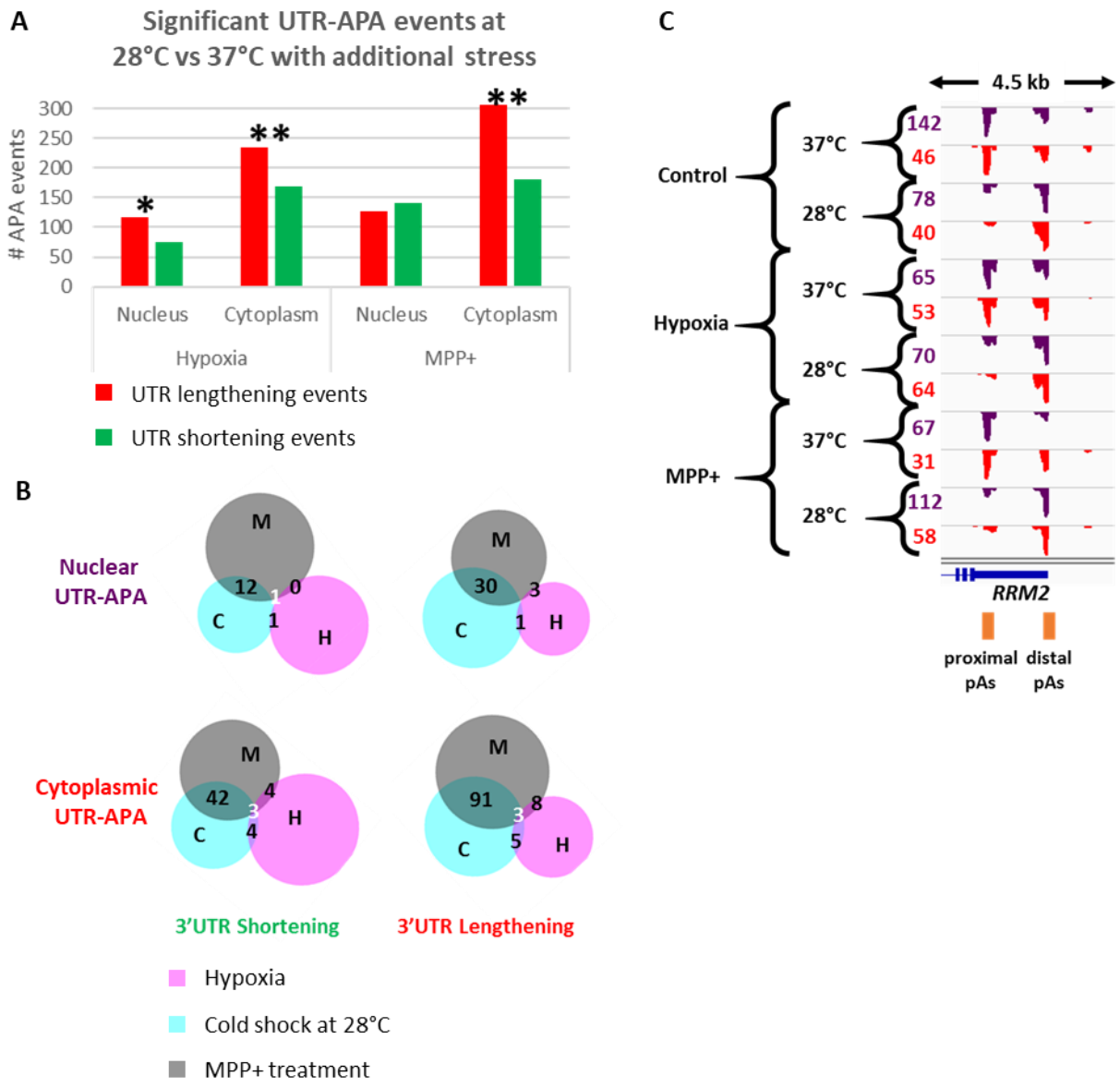


Figure 5.15. Stress Specific APA Changes at 28°C Compared to 37°C.

A. A bar chart to show the number of 3'UTR lengthening (red) and 3'UTR shortening (green) events in hypoxia (left) or MPP+ (right) treated cells at 28°C compared to exposure of these stresses at 37°C. BE(2)-M17 cells were exposed to hypoxia or MPP+ stress for 24 hours. Asterisks indicate a significant trend to 3'UTR lengthening at the colder temperature (Fisher's exact Test, * = $p<0.05$; ** = $p<0.01$).

B. Venn diagrams to show the number of genes showing 3'UTR shortening (left) and lengthening (right) in the nucleus (upper) and cytoplasm (lower) in stress conditions at 28°C compared to 37°C. Cold shock + MPP+ (M, grey); Cold shock + hypoxia (H, pink); Only cold shock (C, cyan). The number of genes showing APA in two stress conditions are indicated in black numbers, while white numbers show the number of genes differentially expressed in all three stress conditions.

C. 3'UTR lengthening observed in *RRM2* in all stresses at 28°C compared to 37°C in the cytoplasm (purple tracks) but not the nucleus (red tracks). The numbers indicate read numbers (in RPM) from sequencing data of the most abundant isoform visualised on the IGV browser using auto-scale settings.

5.4.3 The Extent of 3'UTR Shortening of *ELAVL1* is Correlated with the Level of Increased Protein Expression

The ubiquitously expressed RBP ELAVL1, also known as HuR, is a member of the Hu family of proteins that shuttle between the nucleus and cytoplasm. Many studies have suggested the function of ELAVL1 is primarily nuclear, mediating RNA processing during splicing and APA (Mansfield and Keene 2012; H. Zhu et al. 2007). However, in the cytoplasm, ELAVL1, and the other Hu proteins, bind to ARE regions in 3'UTRs of their target mRNAs to stabilize them and mediate their cytoplasmic transport (Gorospe et al. 2011).

The *ELAVL1* gene showed 3'UTR shortening in BE(2)-M17 in response to hypoxia and all types of cold shock, but not in response to only MPP+ (Figure 5.16A). However, the APA profile of the 3'UTR varied in a stress type manner. In control and MPP+ treated cells at 37°C, the most distal poly(A) site is used in both the nucleus and the cytoplasm. However, at 37°C in hypoxia, a switch to usage of the middle or proximal poly(A) site constitutes a significant 3'UTR shortening event compared to control cells. This change is observed in the nucleus as well as the cytoplasm suggesting change in poly(A) site usage at the point of cleavage, perhaps mediated through autoregulation by ELAVL1 (Dai, Zhang, and Makeyev 2012).

In cold shock, 3'UTR shortening in the *ELAVL1* transcript is observed in all three conditions, but at 28°C and 28°C with MPP+ treatment, the longer isoform is still present, and a complete switch in APA profile to usage of the proximal poly(A) site is only observed in cells exposed to cold shock and hypoxia. Furthermore, the 3'UTR shortening during cold shock event is not significant in the nuclear fraction suggesting changes in the *ELAVL1* mRNA UTR length are a post-transcriptional phenomenon in cold shock. Therefore, although 3'UTR shortening was identified in different stresses, the regulatory mechanism behind this switch is different under cold shock conditions in hypoxia than at 37°C.

The longer *ELAVL1* isoform is known to have a reduced protein output (Mansfield and Keene 2012). This correlation between increased expression of the shorter isoform and increased protein expression was verified in the hypoxia and cold shock with western blotting (Figure 5.16B). This showed that the upregulation of ELAVL1 was greater in hypoxia, where

there was no presence of the longer *ELAVL1* mRNA, compared to in cold shock, suggesting that the abundance of the longer isoform can limit the upregulation of ELAVL1 protein.

This highlights the fact that different regulatory pathways are in place in the different stress conditions, although hypoxia and cold shock both inevitably result in increased presence of the more stable *ELAVL1* transcript which produces more protein.

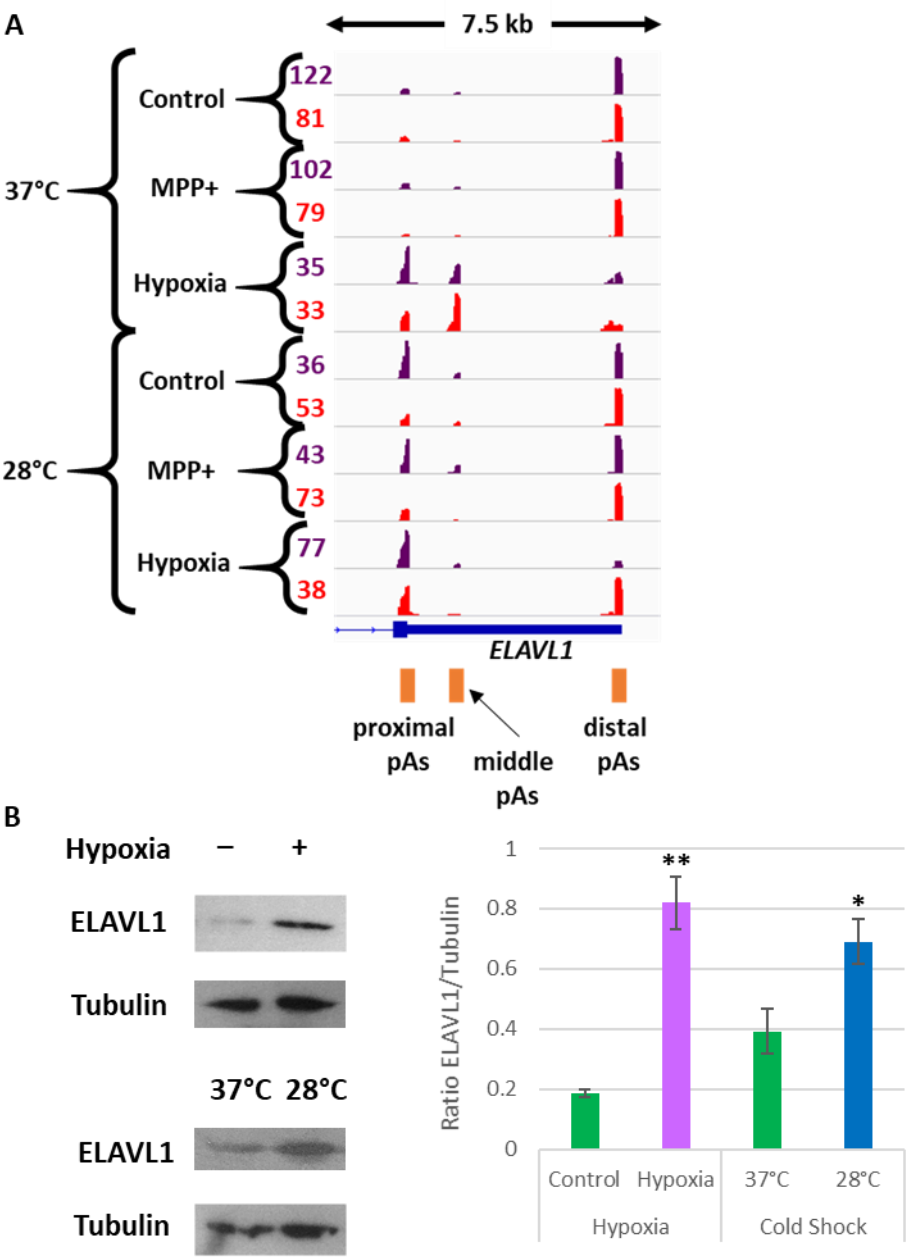


Figure 5.16. Regulation of *ELAVL1* by APA correlates with Protein Output in Different Stress Conditions.

A. A screenshot to show 3'UTR shortening of *ELAVL1* in hypoxia but not MPP+, and in cold shock with additional stresses. The 3'UTR shortening event in hypoxia at 37°C is also present in the nucleus (red tracks) but in cold shock it is only present in the cytoplasm (purple tracks). Numbers indicate read numbers (in RPM) from sequencing data. Tracks are visualised on the IGV browser using auto-scale settings.

B. Left panel: A western blot to show the upregulation of ELAVL1 protein was greater in hypoxia (upper panel) than in cold shock (lower panel). Tubulin used as a protein loading control. Right panel: Quantification of western blot using band intensities quantified by ImageJ software. Error bars indicate standard deviation, n = 3. T-test, * = $p<0.05$; ** = $p<0.01$.

5.5 Discussion

Transcriptome changes in stress conditions have been explored in the context of alternative splicing changes (Yamamoto et al. 2016) but this is the first study to experimentally investigate into how APA differs in different stress conditions through RNA-seq in the same cell line.

APA changes in different biological states have been investigated using publicly available microarray datasets (Wenchao Hu, Liu, and Yan 2014), which emphasized a role of RBPs in maintaining different APA profiles in different conditions including cold shock and hypoxia. Investigation into the changing APA profiles observed here suggested a greater impact of post-transcriptional regulation in mediating the UTR landscape, which may well be a result of changing RBP expression during stress conditions.

Previous studies have suggested APA is affected in the same manner in different stress conditions (Hollerer et al. 2016). This investigation into the impact of stress on APA in the BE(2)-M17 cell line shows that distinctly different genes are affected in different stress conditions at both the level of gene expression and APA.

5.5.1 APA in Cold Shock

The cold shock response is not as established as that of heat shock, however distinct phenotypes are associated with this temperature stress. This study investigated transcriptome changes through gene expression and APA in cold shock of the BE(2)-M17 cell line.

Cold shock and Gene expression

Inhibition of the cell cycle has been observed in cold shock (Nishiyama et al. 1997), however FACS analysis did not show any significant changes in the cell cycle of BE(2)-M17 cells subjected to cold shock, suggesting transcriptome changes were not due to cell cycle arrest. Extensive changes in gene expression were seen in both undifferentiated and differentiated BE(2)-M17 cells during cold shock. Despite the modest overlap of genes affected, the different cohorts of genes affected in the two cellular states were enriched in the same biological processes including translation and RNA processing. A similar result was observed comparing gene expression changes between the BE(2)-M17 and HEK293 cell lines. This indicates that despite variance in differential individual gene expression in cold shock in the three cell types, there is a similar overall effect on transcript abundance by moderate hypothermia.

Cold shock and APA

Alternative splicing in cold shock and in mammalian hibernation has been reported (Tessier and Storey 2014; Stieler et al. 2011), however widespread APA changes in cold shock have only been investigated in one study. Cold shock in MEFs showed widespread changes in APA, with a trend to 3'UTR lengthening attributed to the upregulation of RBM3 and CIRBP which repress usage of the proximal poly(A) site, thus regulating transcriptional APA (Y Liu et al. 2013). Neither of these RBPs were significantly upregulated in either BE(2)-M17 (Figure 5.3B) or HEK293 cells (Supplementary Figure 12), yet widespread APA changes, with a trend to 3'UTR lengthening were observed with cold shock. Further, RBM3 and CIRBP were depleted from the nucleus during cold shock, therefore it is unlikely they could suppress proximal poly(A) sites during 3'end processing to induce 3'UTR lengthening. Importantly, in this thesis, APA profile changes in the nucleus and cytoplasm were assessed separately in cold

shock conditions to investigate transcriptional and post-transcriptional APA profile changes for the first time.

A trend to 3'UTR lengthening in moderate hypothermia was observed in both the nuclear and cytoplasmic fractions of undifferentiated and differentiated BE(2)-M17 cells and HEK293s. However, most APA profile changes in the cytoplasm were due to regulation by post-transcriptional, not transcriptional APA mechanisms. Furthermore, APA changing genes in the two cell lines showed little overlap, although the cohorts of genes showing APA were associated with the same biological processes including mRNA splicing. This suggests that APA mediated regulation affects different genes, but the same pathways in different cell lines.

The let-7 family of miRNAs was enriched in the alternative UTRs of genes showing 3'UTR lengthening in cold shock in BE(2)-M17 cells. Downregulation of these miRNAs could mediate this 3'UTR lengthening event, however expression changes of miRNAs in cold shock in BE(2)-M17 cells would need to be verified. LIN28 was identified as an RBP which may bind and stabilize long UTR isoforms keeping them translationally repressed. LIN28 has also been shown to suppress let-7 miRNA biogenesis (F. Mayr et al. 2012). Therefore, this RBP may be important in directly and indirectly mediating APA profile changes. LIN28, and G3BP2, which may also bind to 3'UTR lengthened genes, are associated with stress granules. The 3'UTR lengthening events may enable exposure of LIN28/G3BP2 binding sites which enable the target transcripts to accumulate in stress granules where they remain translationally suppressed but stable. LIN28 has also been observed in P-bodies, which suggests binding of this RBP could guide transcripts to NMD mediated degradation. Therefore, regulation by LIN28 may contribute to the 40% of genes that showed both changes in APA and transcript abundance.

Although a trend to 3'UTR lengthening was observed, the genes showing 3'UTR shortening were associated with splicing in both BE(2)-M17 and HEK293 cells. The regulation of these cytoplasmic 3'UTR shortening events is still unclear as no global regulators were identified to bind to the alternative UTRs of these genes which may cause nuclear retention or cytoplasmic degradation of the longer transcript isoforms.

Comparison of APA events in undifferentiated and differentiated cells showed few overlapping events, however, physiologically relevant APA changes such as in *RAB7A* held true in both cellular states of BE(2)-M17 cells during moderate hypothermia. RAB7A promotes

autophagy, which may be protective under stress conditions (Das, Shravage, and Baehrecke 2012; D. Tang et al. 2016; Pan et al. 2009). Interestingly, the regulatory mechanisms of these APA events may differ, since in differentiated cells, *RAB7A* showed altered APA in the nucleus and the cytoplasm suggesting altered poly(A) site choice at the point of cleavage, while in undifferentiated cells, the APA event was post-transcriptional.

Global upstream-APA changes during cold shock were also assessed. In both BE(2)-M17 cells and HEK293 cells, the *UBE3B* transcript showed an increased usage of the upstream proximal poly(A) site during cold shock. This shorter isoform encodes a truncated protein which lacks the domain required for E3 ubiquitin ligase activity. This may be an example of an APA event that enables increased protein stability through inhibition of the ubiquitin proteasome pathway.

Conclusion

In conclusion, this work shows that a significant shift to 3'UTR lengthening is observed during moderate hypothermia in both undifferentiated and differentiated BE(2)-M17 cells, and in HEK293 cells, although the affected genes and regulatory mechanisms behind APA changes are very much cell type dependent. The 3'UTR lengthening observed may contribute to accumulation of transcripts in stress granules or P-bodies where they are translationally repressed.

5.5.2 APA in Hypoxia

Widespread gene expression changes have been associated with hypoxia, however there is little understanding on the role APA may play in transcriptome changes upon exposure to low oxygen conditions. This work highlights that although there are no global changes in APA, almost 50% of significant APA events are found in genes that are also differentially expressed, suggesting APA is an important regulator of transcript stability in low oxygen conditions.

Hypoxic Stress Conditions

Hypoxia has primarily been studied in the context of tumour biology in cancer, however hypoxia is also associated with other cardiovascular, haematological and pulmonary disorders as well as neurodegeneration (Zlokovic 2011). There is controversy about the way hypoxia is defined in cell culture to be less than 2% oxygen, as for many cells in the body this is closer to the physiological oxygen concentration. While the blood can have an oxygen concentration of 12%, it can be as low as 0.5% in the brain (Ivanovic 2009). Indeed, primary cell lines have been shown to grow better in so called hypoxic conditions as they are physiologically closer to *in vivo* conditions (Ivanovic 2009). However, cell lines such as BE(2)-M17 have been cultured at 21% oxygen for decades and have consequently adapted to growing in this environment. A reduction of oxygen to 2% therefore does mimic a hypoxic environment, which was shown here to induce transcriptional effects mediated by hypoxia inducible factors such as HIF-1 to increase expression of their target genes.

Hypoxia and Gene Expression

During hypoxia, increased expression of HIF-1 target genes and genes associated with glycolysis was observed, to enable a shift away from OXPHOS for ATP production, as previously identified in hypoxia systems (Weidemann and Johnson 2008). Genes encoding proliferation proteins were repressed at the mRNA level in hypoxic conditions in BE(2)-M17 cells, as previously reported (Chi et al. 2006; Jögi et al. 2004).

It is important to note that upregulation of all HIF-1 targets at the transcript level does not mean that these mRNAs will be translated. Increased expression of *VEGF* was detected in hypoxic conditions in BE(2)-M17, however it is unlikely its encoded protein, which

induces proliferation of vascular endothelial cells, plays an important role in the stress response to hypoxia in this neuroblastoma cell line. A previous study reported that only 30% of genes upregulated by the hypoxic response at the mRNA level, were engaged with active ribosomes and therefore were able to be upregulated at the protein level (Staudacher et al. 2015). Genome wide proteome studies would be required to assess differential protein expression of genes in this hypoxic model.

Hypoxia and APA

In low oxygen conditions, global inhibition of transcription, and modified Pol II function through post-translational modifications have been suggested (Gorospe et al. 2011). However, the changing UTR landscape has not been investigated on a genome-wide scale.

The changes in APA profiles in the cytoplasm were predominantly due to post-transcriptional regulatory mechanisms, though the full extent of this is still unclear. Among the biological pathways that were enriched in the cohorts that showed APA, were genes associated with RNA processing and splicing. Alternative splicing has been linked to hypoxic conditions including through the action of HIF-1 itself, which mediates exon skipping of upregulated genes, and exon inclusion of downregulated genes in hypoxia (Sena et al. 2014). A recent study assessing the effect of hypoxia on splicing showed the cohort of genes subjected to alternative splicing in hypoxia were associated with DNA repair pathways, the cell cycle and RNA splicing (Memon et al. 2016). Together this suggests the transcripts encoding these proteins are alternatively processed through both alternative splicing and APA in hypoxia.

Global Regulation of UTR Length in Hypoxia

Assessment of the alternative UTRs from genes that showed altered cytoplasmic APA profiles did not yield motif enrichment suggesting there is no global regulation through RBPs binding to a specific motif. However, this cannot rule out the possibility that RBPs mediate transcriptome changes via APA on an individual transcript basis. A plethora of RBPs including, hnRNPs, ELAVL1, PTB, CIRBP and RBM3, have been associated to affect mRNA stability and translation in hypoxia (Gorospe et al. 2011), which may influence the UTR landscape.

The role of miRNAs in mediating a cellular response to hypoxia has been well studied (Kulshreshtha et al. 2006; Kulshreshtha et al. 2008; Gorospe et al. 2011), however there have not been any studies assessing changes in miRNA expression in neuroblastoma cell lines exposed to low oxygen conditions. Considering the miRNA signature in hypoxia is cell type dependent, and specific to the context of the low oxygen condition (Nallamshetty, Chan, and Loscalzo 2013; Kulshreshtha et al. 2008), it is not possible to assume miRNAs that show altered expression in other systems would be altered in BE(2)-M17 exposed to 2% oxygen for 24 hours. Here, miRNAs that were enriched in the alternative UTRs of genes exhibiting altered cytoplasmic APA were identified, giving an insight into mechanisms of global regulation of the transcriptome in hypoxic conditions. However, miRNA expression changes would have to be verified through small RNA-seq or microarray analysis.

Conclusion

In conclusion, these results show widespread gene expression changes in hypoxia, including in almost 50% of transcripts regulated by APA. The data suggest that cytoplasmic UTR-APA changes are predominantly altered through post-transcriptional regulatory mechanisms, although global regulation by RBPs was not identified. A low oxygen stress environment had a distinctly different effect on APA compared to moderate hypothermia, suggesting stress specific responses affect the transcriptome at the level of APA in distinctly different ways.

5.5.3 APA in Combined stresses

Generic stress responses have been observed with different stresses such as a global reduction in protein synthesis, but there has been no previous investigation into the effect of different cellular stresses on APA on a global scale. This section investigated the changes induced by moderate hypothermia, hypoxia and mitochondrial dysfunction, and combinations of these stresses, on the transcriptome at the level of transcript abundance (gene expression) and APA. Few genes were identified to be regulated by APA in different stresses suggesting stress specific APA mediated regulation.

Differential Gene Expression in Different Stress Conditions

Many groups have investigated gene expression changes with exposure to cold shock (Al-Fageeh and Smales 2009), MPP+ treatment (Krug et al. 2014; J. Wang et al. 2007) and hypoxia (Weigand et al. 2012), however this is the first study to investigate these three stresses, and combinations of these stresses, in the same cell line. These results showed that that different cohorts of genes were differentially expressed in the different stress conditions. The hypoxic nuclear expression signature was distinctly different from that of the other stresses, which may be attributed to altered transcriptional upregulation by HIF-1. However, this distinct hypoxic gene expression signature was not observed in the cytoplasm suggesting many changes in transcript abundance through transcription are retained in the nucleus or these transcripts are degraded upon export into the cytoplasm. Notably, the cytoplasmic transcriptome profile in hypoxia at both 37°C and 28°C is more like untreated cells than cold shock or MPP+. These differential expression changes are especially interesting, given that MPP+ and hypoxia are both forms of oxidative stress.

Moderate hypothermia has been proposed to have a neuroprotective role. One study observed a reduced uptake of MPP+ in mice striatal and cortex slices during moderate hypothermia (S. J. Choi et al. 2015). In moderate hypothermia combined with MPP+ or hypoxia in BE(2)-M17 cells, generally fewer genes showed differential expression, and the changing genes were not enriched in the stress response related pathways identified by differentially expressed genes with MPP+ or hypoxia treatment at 37°C. This can suggest that

the lower temperature reduces differential gene expression in stress conditions, which could be an aspect of its protective role.

APA in Different Stress Conditions

A trend to 3'UTR lengthening was observed in moderate hypothermia, but no significant trends to 3'UTR lengthening or shortening were identified in hypoxia or with MPP+ treatment. The results here showed that few genes were regulated by APA in all three stresses, suggesting stress specific APA changes.

Previous studies assessing the effect of stress on APA have assumed that different stresses have the same effect on the length of 3'UTRs (Hollerer et al. 2016). This report also suggested little overlap between genes subjected to APA regulation and mRNA abundance in stress conditions (Hollerer et al. 2016), however in both hypoxia and cold shock approximately half of the APA regulated genes showed altered gene expression.

When assessing APA in different stresses, cold shock induced the greatest number of significant 3'UTR-APA events. This was also true in the case of upstream-APA events (Supplementary Figure 13). Interestingly, when cells were exposed to hypoxia or MPP+ at a lower temperature, more significantly changing APA events were identified than at 37°C in the cytoplasm of cells exposed to hypoxia or MPP+, and in the nucleus of MPP+ treated cells. In addition, the trend to 3'UTR lengthening was observed in cold shock of cells exposed to hypoxia and MPP+ compared to cells stressed at 37°C. This novel finding suggests that temperature changes have a greater effect on global APA regulation than hypoxia or MPP+ treatment. Notably although the same trend to 3'UTR lengthening was observed, the overlap of APA regulated genes was modest. This indicates that the same global mechanisms cause 3'UTR lengthening in hypothermia regardless of other stresses, but these changes are not gene specific.

Global translational inhibition is an established response to hypothermic conditions and has also been observed in hypoxia (Wouters et al. 2005). The binding of RBPs to lengthened 3'UTRs may contribute to global translational repression in stress conditions. 3'UTR lengthening may expose RBP binding sites for proteins like LIN28 and RBM8A in the alternative UTR. These RBPs were identified to bind to enriched motifs in 3'UTR lengthened

genes in both cold shock and cells exposed to the neurotoxin MPP+ (Chapter 4B). LIN28 is associated with stress granules (Gorospe et al. 2011), and could bind and recruit its targets to these cytoplasmic inclusions during stress conditions. Further analysis into the localisation of the APA regulated genes would give a better understanding into the physiological relevance, of 3'UTR lengthening observed in hypothermia.

ELAVL1 Expression correlates with APA changes in Specific Stress Conditions

The mechanism behind the significantly changing APA events in the different stress conditions is unclear. As observed in the individual stresses, most of the APA events identified in the cytoplasm were not present in the nucleus (Supplementary Figure 14), suggesting these are regulated through post-transcriptional APA. Changing expression of RBPs and miRNAs could contribute to changes in cytoplasmic mRNA stability.

In hypoxia, ELAVL1 has been shown to accumulate in the cytoplasm (Blanco et al. 2015; Osera et al. 2015) where it has been suggested to play a protective role by stabilizing mRNAs. Here, ELAVL1 protein expression was significantly upregulated upon exposure to hypoxia and moderately upregulated in cold shock, which corresponded to 3'UTR shortening at the transcriptional level. With MPP+, ELAVL1 was not regulated by APA and showed no increase in protein expression. The 3'UTR shortening event in the *ELAVL1* transcript correlating to increased ELAVL1 protein expression has previously been characterised (Mansfield and Keene 2012), but this is the first time that the APA event is associated with hypoxia and cold shock as a mechanism to increase ELAVL1 expression during stress conditions.

Interestingly, the mechanism of 3'UTR shortening in the *ELAVL1* transcript appears to be temperature dependent. In hypoxia at 37°C, the APA change is seen both in the nucleus and in the cytoplasm. However, at 28°C, in all conditions of stress assessed, a 3'UTR shortening event is identified only in the cytoplasm suggesting post-transcriptional regulation.

While reports of increased ELAVL1 in cold shock have not previously been observed, interestingly, during heat shock ELAVL1 was shown to be ubiquitinated and targeted for proteasome mediated degradation in different cell lines (Abdelmohsen et al. 2009). This highlights a distinctly different response between the two temperature stresses.

ELAVL1 has been proposed to play a role in protection against stress, as knockdown of ELAVL1 has shown increased cell vulnerability in a number of stress conditions (Rhee et al. 2010; Skliris et al. 2014; Osera et al. 2015; Blanco et al. 2015). While there is global translational inhibition in both cold shock and hypoxia, ELAVL1 may aid the stabilization of transcripts and perhaps enable translation of the transcripts required to adapt to the stress condition. ELAVL1 can also accumulate in stress granules (Buchan and Parker 2009), therefore its upregulation may enable increased localisation of its target transcripts to stress granules for storage. In hypoxia, ELAVL1 has been associated with stabilizing and increasing translation of the *HIF1A* transcript (Galbán et al. 2008) to increase expression of hypoxia induced genes by HIF-1. In addition, it has been shown to increase stability of HIF-1 targets such as *VEGFA* (Osera et al. 2015).

ELAVL1 is extensively regulated by post-translational modifications (Grammatikakis, Abdelmohsen, and Gorospe 2016) enabling a quick response to different cellular conditions. However in BE(2)-M17 the increased expression of ELAVL1 protein suggests the post-translational modification is not sufficient to mediate the stress response. Previous studies have postulated that post-translational modifications of ELAVL1, primarily increased phosphorylation, are associated with its cytoplasmic translocation in hypoxia (Grammatikakis, Abdelmohsen, and Gorospe 2016).

In conclusion, this is the first time that the UTR shortening in the ELAVL1 transcript has been associated to the increase in ELAVL1 expression in stress conditions. As well as chemical stresses, ELAVL1 expression was increased both at the mRNA and protein level with mechanical stress in HUVEC cells (Rhee et al. 2010). It would be interesting to investigate if APA regulates ELAVL1 expression in further stress types. Given the role of ELAVL1 in stabilizing transcripts, it would also be interesting to assess the UTR landscape in ELAVL1 depleted cells subjected to stress.

5.5.4 Role of RBM3 and CIRBP in Stress

The induction of the unfolded protein response has been linked to the neuroprotective role of cold shock (Rzechorzek et al. 2015), however other studies suggest neuroprotection is a direct result of upregulation of RBM3 (Peretti et al. 2015; Bastide et al. 2017; Chip et al. 2011) or CIRBP (Saito et al. 2010). In this study, BE(2)-M17 cells were exposed to the lower end of the moderate to mild hypothermic range at 28°C for 24 hours. At this temperature, there was no significant increase in RBM3 or CIRBP expression in both undifferentiated and differentiated BE(2)-M17 cells, and in HEK293 cells. Many studies investigated moderate hypothermia at a higher temperature of 32°C (Y Liu et al. 2013; Nishiyama et al. 1997; Gotic et al. 2016; Bastide et al. 2017), however RBM3 and CIRBP were not significantly upregulated at this temperature in BE(2)-M17 (Supplementary Figure 15) or HEK293 cells (Supplementary Figure 12).

However, in moderate hypothermia, localisation of both RBPs to the cytoplasm was observed in BE(2)-M17 cells, as previously reported in stress (Dresios et al. 2005; Gotic et al. 2016). Under cold shock conditions, RBM3 and CIRBP may bind alternative UTRs to stabilise transcripts in the cytoplasm contributing to the trend of 3'UTR lengthening. However, fewer than 50% of genes regulated by APA in cold shock in BE(2)-M17 cells were targets of RBM3 or CIRBP, indicating other RBPs are clearly involved in mediating UTR length.

Both RBM3 and CIRBP were upregulated or differentially localised in other stresses including hypoxia and neurotoxin mediated stress (X. Zhu, Buhrer, and Wellmann 2016; Zhou et al. 2014; Qiang et al. 2013). Interestingly, an upregulation of RBM3 was observed in hypoxia and MPP+ exposure, whereas CIRBP was significantly upregulated only in hypoxic conditions of BE(2)-M17 cells, but showed no change with MPP+ treatment (Supplementary Figure 16). Altered expression of these proteins has been observed in other cells in low oxygen conditions (Q. Zhang et al. 2017; Wellmann et al. 2004; Chip et al. 2011). CIRBP also binds 3'UTRs of genes upregulated in heat shock (Gotic et al. 2016) where it downregulates translation of its target transcripts (De Leeuw et al. 2007), suggesting this protein has different functions in different stress conditions. Together these results suggest that RBM3 and CIRBP are not universal cold shock proteins, and their upregulation is cell type and stress specific.

5.5.5 Conclusions and Further Work

This chapter investigated changes in gene expression and APA in different stress conditions, and found stress specific transcriptome changes with regards to transcript abundance and APA regulation. A general trend to increased 3'UTR lengthening or shortening in different stresses was not evident, however, moderate hypothermia induced 3'UTR lengthening regardless of exposure to additional stresses. Cold shock and hypoxia have been associated with similar global stress responses such as translational inhibition, however the results here suggest that regulation of the transcriptome differs in these two stress types, both through transcript abundance and APA regulation. In addition, in all stress conditions, cytoplasmic APA profiles were predominantly mediated through post-transcriptional regulation, as previously suggested (Hollerer et al. 2016).

It is important to remember that APA does have natural biological variation, so not all identified significant APA events may be a direct function of the stressful environment. However, an enrichment in genes associated with stress responses suggest that these genes do not randomly show APA changes, but in fact are targeted for APA mediated regulation. In future, APA changes in a further range of stresses, such as inhibiting different pathways such as transcription and translation, and even mechanical stress could be investigated to assess changes in the UTR landscape in the stress response.

In this study, simultaneous exposure to moderate hypothermia and oxidative stress suggested a neuroprotective role through altered transcriptional regulation. Fewer stress response genes were differentially expressed with MPP+ treatment and hypoxia suggesting moderate hypothermia reduces the toxicity of these two stresses. The neuroprotective role of moderate hypothermia has been extensively described in the literature(Rzechorzek et al. 2015; Choi et al. 2015; Stieler et al. 2011; Rzechorzek et al. 2016; Yenari and Han 2012), however, this finding suggests a novel role of moderate hypothermia in neuroprotection through transcriptional regulation. An optimal temperature for neuroprotection would need to be characterised as overcooling has shown to be damaging in cell culture (Neutelings et al. 2013), and in piglet brains (Alonso-Alconada et al. 2015)

Pre-conditioning cells or animals at lower temperatures before exposure to neurotoxins has previously shown a neuroprotective role (Peretti et al. 2015). Future work could include pre-conditioning cells at lower temperatures before exposure to stress to understand how transcriptional regulation could mediate neuroprotection.

Exposure of cells to hypoxia is a known reversible adaptation to the low oxygen environment (Wouters et al. 2005) and reintroducing cells to normal oxygen conditions has been shown to reverse the stress response. It would be interesting to investigate if this reversible switch is also true in terms of changing APA profiles, to understand how removal of the stress conditions could impact the UTR landscape.

During cold shock, both BE(2)-M17 and HEK-293 cells showed a shift to 3'UTR lengthening, although cell type specific changes were observed. Investigation of the cold shock response in a broader range of cell types would aid investigation of understanding the general mechanisms determining APA profile changes at reduced temperatures.

This study investigated APA profile and gene expression changes in BE(2)-M17 cells after 24 hour exposure to different stress conditions. Altering the length of time of the stress exposure could be done in future experiments to assess the time it takes to induce transcriptome wide changes through gene expression and APA regulation.

It is well documented that stress granules, neuronal granules and P-bodies store mRNAs to inhibit their translation during stress (Hofmann et al. 2012; Anderson and Kedersha 2006). The translocation of mRNAs to these 'subcytoplasmic domains' is highly dependent on binding of RBPs to the 3'UTRs to enable their localisation. Therefore, altered 3'UTRs through APA in the stress response can increase presence of RBP binding sites and mediate transcript localisation to stress granules or P-bodies. Assessing changes in mRNA localisation of transcripts shown to be regulated by APA here would enable a better understanding on the impact of the APA event. Furthermore, assessing UTR length changes in stress with depletion of RBPs known to recruit to stress granules, such as ELAVL1 or LIN28, would help understand reasons for APA profile changes in stress conditions.

In conclusion, this chapter has identified stress specific transcriptome changes in cold shock and hypoxia through altered regulation of gene expression and APA. Most of the APA changes identified in the cytoplasm were not present in the nucleus, suggesting they are

mediated by post-transcriptional regulatory mechanisms. Further investigations into altered expressions of RBPs or miRNAs would give a deeper insight into the mechanisms behind the changing cytoplasmic UTR landscape.

Chapter 6: Discussion

6.1 Introduction

Over 70% of human protein-coding genes have multiple poly(A) sites (Derti et al. 2012). The alterations in usage of poly(A) sites under different conditions have been extensively investigated with a great focus on changes in cancer (C. Mayr and Bartel 2009; Xia et al. 2014; Morris et al. 2012) and development (Zhe Ji et al. 2009; Hoque et al. 2013; Ulitsky et al. 2012).

This thesis explored the changes in transcriptional and post-transcriptional APA regulation in the neuroblastoma cell line BE(2)-M17 during differentiation and stress conditions. This is the first time such an extensive investigation of APA has been performed in a single cell line. This thesis also investigated the role of APA in the neurodegenerative diseases AD, PD and ALS using a bioinformatics approach. The key findings of this project were:

- In BE(2)-M17 cells, transcriptome changes upon environmental changes were different in the nucleus and the cytoplasm.
- The cytoplasmic UTR landscape is predominantly regulated by post-transcriptional APA rather than changes in poly(A) site usage at the point of cleavage.
- Identification of physiologically relevant genes that show APA in different environments can contribute to phenotypic changes in the changing cellular state.
- Changing APA profiles in cellular stress are dependent on the stress inducer with cold shock having the greatest impact on UTR length.
- Identification of APA regulation in key genes in neurodegeneration may contribute to or be consequential of disease pathology.

This chapter will discuss the importance of these findings and outline future work to answer remaining questions regarding the importance of APA in a changing environment and in neurodegeneration.

6.2 The Importance of Subcellular Fractionation to Investigate APA

Studies investigating differences in APA profiles in different areas of the cell are becoming more commonplace (Neve et al. 2016; Taliaferro et al. 2016) but most studies focus on changes in total RNA APA profiles. APA is regulated through transcriptional and post-transcriptional APA mechanisms, which cannot be distinguished by assessing whole-cell RNA. This can distort the understanding behind APA profile changes, as explored in Chapter 3, where the trend to 3'UTR lengthening was far greater in the cytoplasm than in the nucleus highlighting the importance of post-transcriptional APA regulation.

In the cytoplasm a trend to 3'UTR shortening was observed in the BE(2)-M17 cell line (Chapter 3.2.5) as in other cell lines (Neve et al. 2016). This suggests that longer UTR isoforms are generally less stable in the cytoplasm than their shorter UTR counterparts. Alternatively, it suggests that longer UTR isoforms are more likely to be nuclear retained. One limitation to separating nuclear and cytoplasmic RNA to investigate APA changes, is that it is not possible to distinguish between these two fates. Furthermore, nuclear APA profile changes from altered poly(A) site choice or differential transcript export cannot be differentiated. Methods that monitor the transcriptome over time may give a deeper insight into mRNA stability, such as done by Spies and colleagues (Spies, Burge, and Bartel 2013). However, the subcellular fractionation method highlights differential changes in the UTR landscape of the nucleus and cytoplasm in changing environments.

Upstream-APA profile changes have been investigated to a lesser extent than UTR-APA changes, despite their clear impact on the coding potential of the transcript. This thesis investigated upstream-APA changes in different conditions and identified important physiological changes where the upstream-APA event may contribute to the changing cellular state. As with UTR-APA changes, few upstream-APA changes in the cytoplasm were also observed in the nuclear fraction suggesting post-transcriptional regulatory events also dominate control of upstream-APA changes.

This thesis employed a 3'end RNA sequencing method to assess APA profile changes in BE(2)-M17 cells exposed to different conditions. Biological replicates were performed on cells passaged separately. Many studies use only technical replicates which does not give an insight into how different populations of cells behave under the same conditions. Single cell

RNA-seq determined APA profile heterogeneity even within a population of mouse embryonic stem cells (Velten et al. 2015). Therefore, biological replicates are critical to verify APA changes are true in the changing environment and not a result of biological variation. Investigating the impact of environmental changes on nuclear and cytoplasmic APA profiles in individual cells would be interesting, however further technicalities need to be overcome before RNA from the nucleus and the cytoplasm of a single cell can be isolated.

6.3 Post-Transcriptional APA Regulation in Changing Cellular States

This is the first study to extensively investigate transcriptome changes under different cellular states in the BE(2)-M17 neuroblastoma cell line. In all cases, the number of APA regulated genes was modest. However, genes were investigated on an individual basis to understand the physiological relevance of the altered UTR length, focussing on the importance of the APA change rather than bioinformatic trends.

Many studies have emphasised the importance of altered poly(A) site usage during 3'end processing in different environments (Batra, Manchanda, and Swanson 2015; Z Ji et al. 2011; W. Li et al. 2016; Y Liu et al. 2013) although modulation of UTR length through a combination of poly(A) site usage and post-transcriptional regulation has been postulated (Zhe Ji and Tian 2009). With each treatment, a disparity in APA changes between the nuclear and cytoplasmic transcriptome was observed, even though nuclear and cytoplasmic RNA samples were isolated from the same cells. This observation questions the extent of the downstream impact of poly(A) site choice during 3'end processing, and gives an unprecedented emphasis on the role of post-transcriptional regulation of the transcriptome.

Post-transcriptional regulation is broadly thought to be a mechanism to fine-tune gene expression while changes in transcript abundance have been primarily thought to be a result of changing transcriptional activity (Schwanhausser et al. 2011). However, in this study, there was a substantial overlap between the genes showing altered expression and altered APA regulation, particularly in the stress environments.

Over 60% of human genes have miRNA binding sites (Friedman et al. 2009), however recent studies suggest that the regulation of the transcriptome by miRNAs has been overstated (A. R. Gruber et al. 2014). The ability of a miRNA to bind to its target depends not just on

its complementary seed region, but also on secondary structure of mRNAs and the binding of other RBPs which could mask the miRNA binding site (Ameres, Martinez, and Schroeder 2007). In this thesis, miRNAs were investigated from a bioinformatics perspective assessing the enrichment of miRNA target sites in cohorts of APA regulated genes. While this analysis gives an insight into how miRNAs might affect the UTR landscape further investigation into the changing expression of miRNAs in different cellular states should be investigated genome wide through miRNA microarray analysis or small RNA-seq.

Changes in RBP expression could largely impact the UTR landscape, as binding to the 3'UTR can mediate transcript stability along with translatability and localisation, as demonstrated by individual RBP examples (Batra et al. 2014; Taliaferro et al. 2016). The role of RBPs in modulating UTR length was also bioinformatically assessed in this study through motif enrichment analysis to identify enriched RBP binding sites. RBPs with potentially important roles in different cellular states were identified, however further analysis into changing RBP expression profiles at the protein level will give a better understanding into how RBP binding can have a downstream impact on gene expression.

A subset of lncRNAs can also be processed by cleavage and polyadenylation at the 3'end (Hoque et al. 2013). In this thesis, few lncRNAs showed significant APA changes in changing environments of BE(2)-M17 cells, though the same trends, such as transcript lengthening in differentiation were identified (Supplementary Figure 17). The impact of APA changes in lncRNAs, which are often nuclear retained, is not well characterised. Further investigation into this may provide novel insights into the effect of APA in lncRNAs which may contribute to a variety of regulatory pathways.

6.4 Importance of APA in Neurodegeneration

The CNS has the highest level of mRNA diversity, which occurs from increased alternative splicing and APA (Miura et al. 2014). This thesis provides the first study to comprehensively assess 3'UTR lengths in different datasets of patient samples from the three most common sporadic neurodegenerative diseases: AD, PD and ALS.

The analysis of 3'UTR lengths with DaPars analysis suggests that APA is differentially regulated in the three diseases, with PD showing very few APA changes compared to ALS and

AD. However, limitations of this bioinformatics analysis, including the sequencing depth of the RNA-seq data, can largely influence the output thereby skewing the results. An important finding from these analyses is that APA profile changes are specific to different regions of the CNS. This is especially notable in neurodegeneration where only specific regions of the CNS are affected.

An established *in vitro* model of PD, which compromises mitochondrial function, was used to assess APA profile changes and the regulatory mechanism through either transcriptional or post-transcriptional APA. Together these data identified genes that are associated with the pathways affected in neurodegeneration, where differential APA regulation could contribute to disease pathology.

Given the discrepancy in the cytoplasmic and nuclear transcriptomes in BE(2)-M17 cells, it will be interesting to assess if transcriptome changes observed in neurodegeneration arise from altered co- or post-transcriptional regulation. This may be particularly important in fALS, where transcriptional changes are heavily implied by mutations in the RBPs TARDBP and FUS, that are important in mRNA processing. Isolating sufficient RNA from affected neurons is difficult as these cells are progressively degenerated. However, further work could involve investigating transcriptional and post-transcriptional APA changes in the associated neurons derived from iPSCs of patients and healthy individuals.

Studies that have assessed APA from patient RNA in the past have combined the APA changes from different patients and different controls (Prudencio et al. 2015). Not all changes in UTR length will be present in all patients, therefore combining the data in this manner overstates the number of APA events. In this thesis, where possible, APA events were only considered to be linked to neurodegeneration if they were observed in multiple patients compared to multiple control samples. This stringent analysis identifies fewer significant APA events, however, accounts for biological variation in the transcriptome between different individuals, which should be considered in future studies assessing APA in disease samples.

In conclusion, the number of genes that are differentially regulated by APA in neurodegeneration may be modest, however the identification of physiologically relevant genes in AD, PD and ALS, suggests APA may be a novel regulator of gene expression during disease progression. Future work should investigate the impact of these identified APA events on

downstream gene expression, and assess if the APA profile changes are causative or consequential of the neurodegenerative state.

6.5 Conclusions and Future Outlook

This work has given a novel insight into the changing APA profiles in different cellular states of the BE(2)-M17 cell line and in neurodegeneration. Numerous global studies investigating APA have assessed changes in whole-cell RNA (Sandberg et al. 2008; C. Mayr and Bartel 2009; Y Liu et al. 2013; Derti et al. 2012), which does not provide the same detail behind changing APA profiles as investigated here.

Many studies that look at genome-wide APA claim 'global changes' are identified in different cell conditions. However, the term "global changes" is poorly defined in the literature, and often only a small proportion of the transcriptome is affected. For example, Jenal and colleagues claimed global 3'UTR shortening with knockdown of PABPN1 because 90% of the APA changes are shortening whereas 10% show 3'UTR lengthening (Jenal et al. 2012). However, all the changing APA events in this study account for less than 10% of all genes that can be regulated by APA. Thus, can this be considered 'global 3'UTR shortening'? Furthermore, studies often focus on bioinformatics correlations such 3'UTR lengthening in differentiation or 3'UTR shortening in cancer without investigating APA changes on a gene by gene basis to understand the impact of APA regulation (Nick J. Proudfoot 2011). Arguably the impact of APA on downstream expression and its physiological relevance is more important than the number of APA events, and should be emphasized in future work in the field.

This thesis considers differences in subcellular APA profile changes and assesses the impact on downstream gene expression of identified APA events. Although the number of APA changes was often modest, changes in UTR length of physiologically relevant genes were identified through both *in vitro* and *in silico* analysis. Future work should investigate the expression changes of miRNAs and RBPs to understand their contribution in regulating the cytoplasmic UTR landscape.

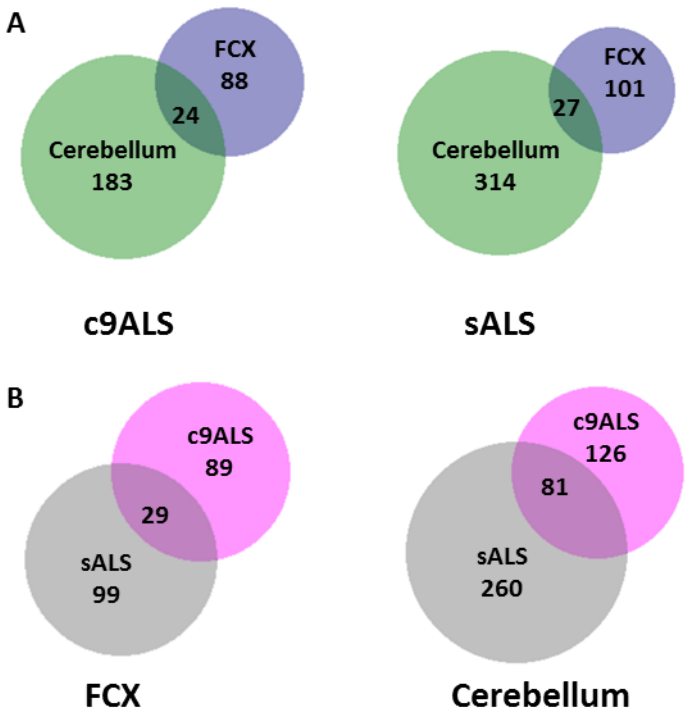
Chapter 7: Supplementary Data

7.1 Supplementary Figures

Motif	Logo	E-value	TOMTOM Proteins
GCACGTR		6.5e-003	PPRC1; SNRPA; FUS; RBM4L RBM8A; FXR2
CTCCCGY		8.3e-003	SRSF1; HNRNPH2; RBM5; SRSF9; SRSF2; SRSF9; RBM6; SRSF10; PPRC1; RBM8A; RBM4 PCBP2; LIN28A; SAMD4A
CGKGGACC		2.8e-002	SRSF1; ESPR2; SRSF7; LIN28A; RBM8A; RBM45; FMR1; SAMD4A

Supplementary Figure 1. Enriched motifs in the alternative UTR sequences of genes showing 3'UTR lengthening in RA mediated differentiation of BE(2)-M17 cells.

The proteins in the fourth column indicate RBPs identified to bind to the corresponding motifs using TOMTOM analysis. Red indicates nuclear RBPs, blue indicates RBPs that shuttle between the nucleus and the cytoplasm, purple indicates cytoplasmic RBPs.



Supplementary Figure 2. Comparison of APA in different regions of the brain and in sALS compared to c9ALS in Set 2.

A. Venn diagrams to show the overlap of APA events between the frontal cortex (FCX) (blue) and the cerebellum (green) in c9ALS and sALS patients in Set 2.

B. Venn diagrams to show the overlap of APA events between sALS (grey) and c9ALS (purple) in the frontal cortex (FCX) and the cerebellum in Set 2.

A



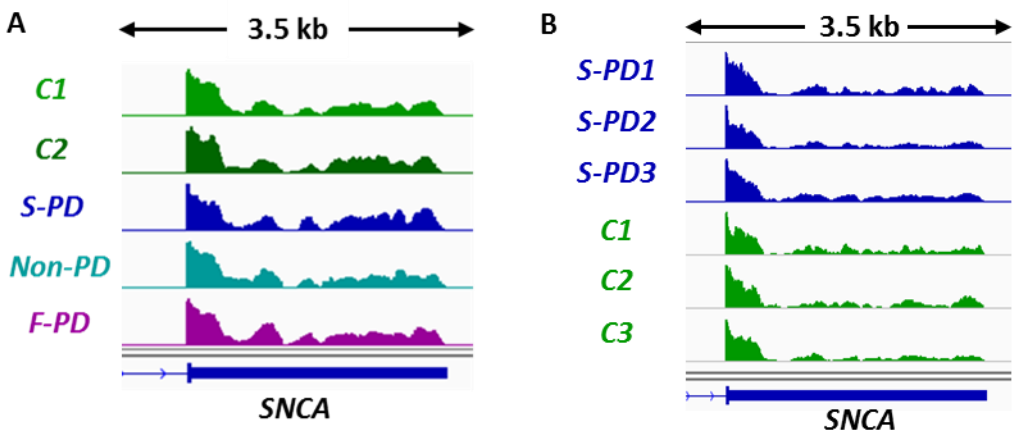
B

3'UTR lengthening	3'UTR shortening	Differential APA regulation
ATPV1E1	MOBP	ARL2
HSP90AB1		CAMK2B
NPDC1		EEF2
PFKP		ENO2
PINK1		GABARAPL2
PRKCB		GOT1
SARS		HPCAL1
SNCB		NPTN
TTYH1		RAB11B
WDR13		TMEM59L

Supplementary Figure 3. A comparison of APA events from the two AD datasets assessed.

A. A Venn Diagram to show the overlap of genes regulated by APA in the hippocampus from AD Dataset 1 (teal) and different brain regions from AD Dataset 2 (blue).

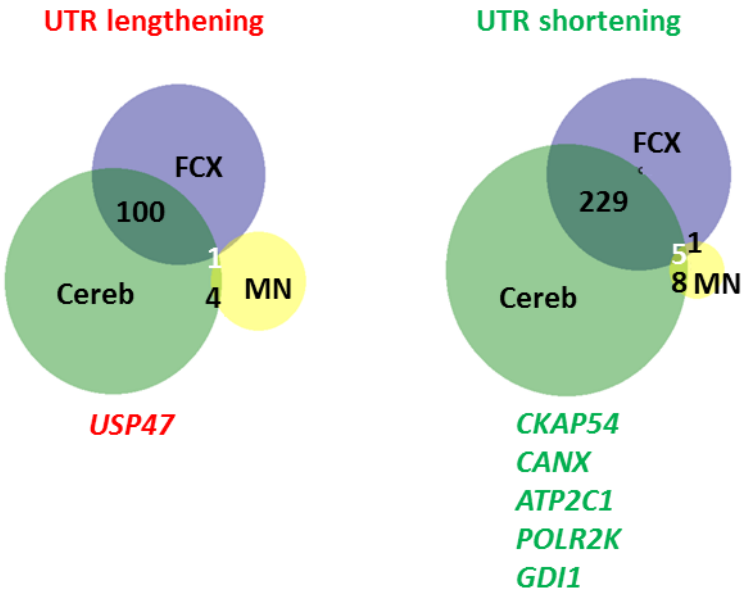
B. A table to show the genes showing 3'UTR lengthening, 3'UTR shortening or differential APA regulation between the two datasets.



Supplementary Figure 4. *SNCA* does not show significant APA in dopaminergic neurons derived from iPSCs from PD patients and healthy individuals in either dataset investigated in this study.

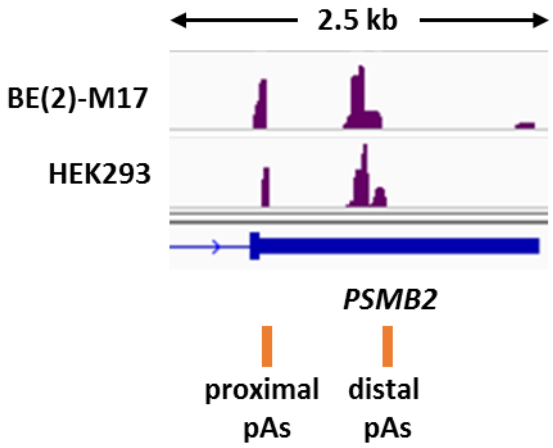
A. C1 and C2 tracks (green) are healthy controls, S-PD is the sporadic PD patient (blue), Non-PD is the twin with the *GBA* mutation who did not develop PD (teal), F-PD is the twin with the *GBA* mutation which did develop familial PD (purple).

B. Three sporadic PD patients (S-PD) are shown by blue tracks, three healthy individual control samples are shown by green tracks.



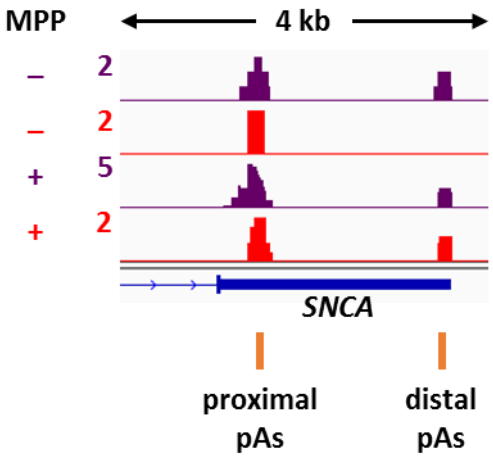
Supplementary Figure 5. Comparison of APA events in ALS in different regions of the brain.

Venn Diagrams to show the overlap of APA regulated genes in different regions of the CNS in sALS patients from DaPars analysis. FCX: Frontal Cortex, blue; Cereb: Cerebellum, green; MN: Motor Neurons, yellow. Black numbers indicate number of APA regulated genes between two regions. White numbers indicate the number of APA regulated genes in all three regions. These genes are listed below the Venn Diagrams.



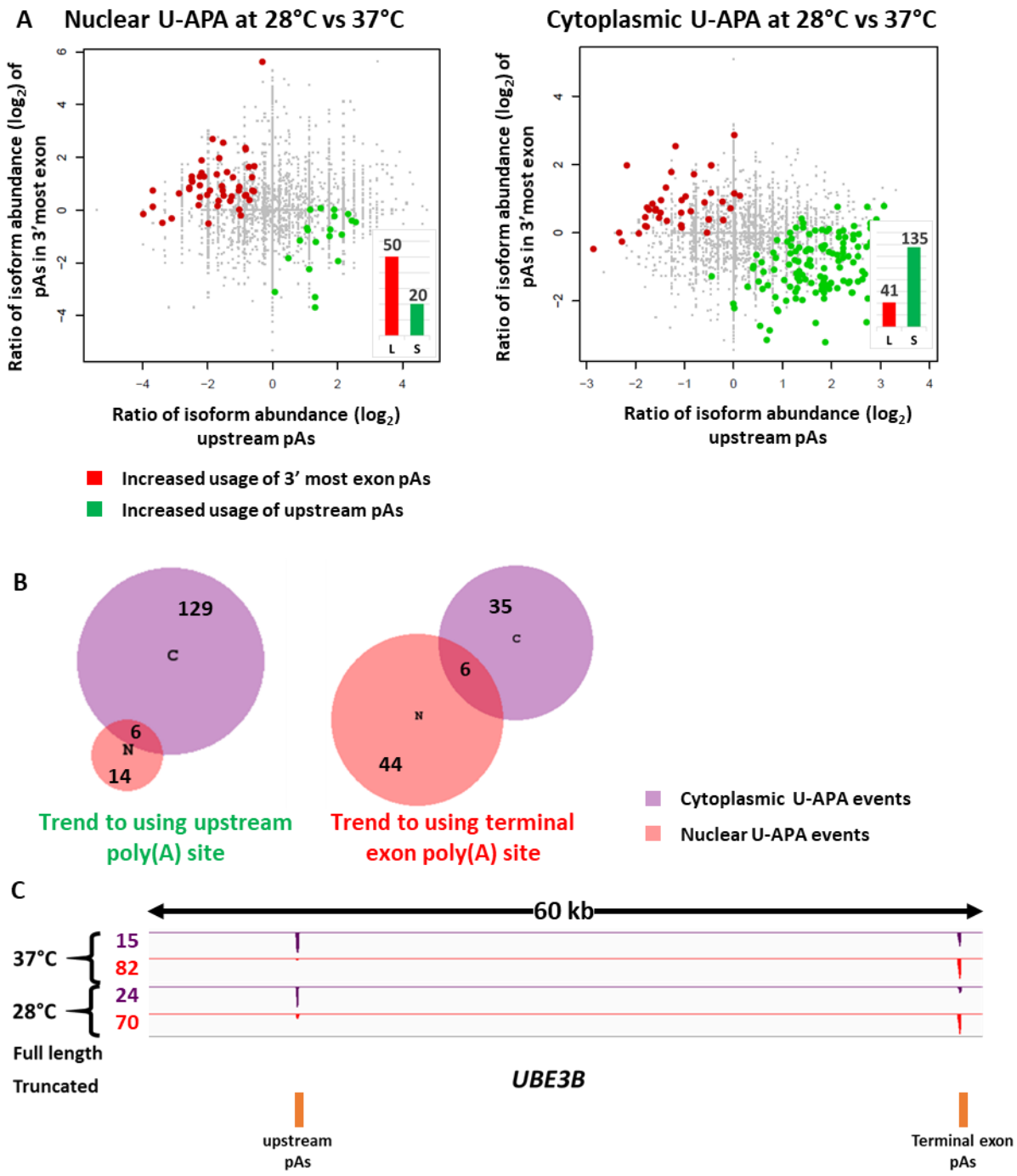
Supplementary Figure 6. Poly(A) sites in *PSMB2*.

HEK293s use the same poly(A) sites in *PSMB2* as in BE(2)-M17 cells. Cytoplasmic tracks shown for the two cell lines. Orange boxes indicate poly(A) sites.



Supplementary Figure 7. Low expression of *SNCA* in BE(2)-M17 cells.

A screenshot to show reads at the 3'end of *SNCA* in BE(2)-M17 cells with and without MPP+ treatment. Although two poly(A) sites were detected, read numbers (RPM) from sequencing data (indicated on the left of the tracks) were too low to assess significant APA changes.

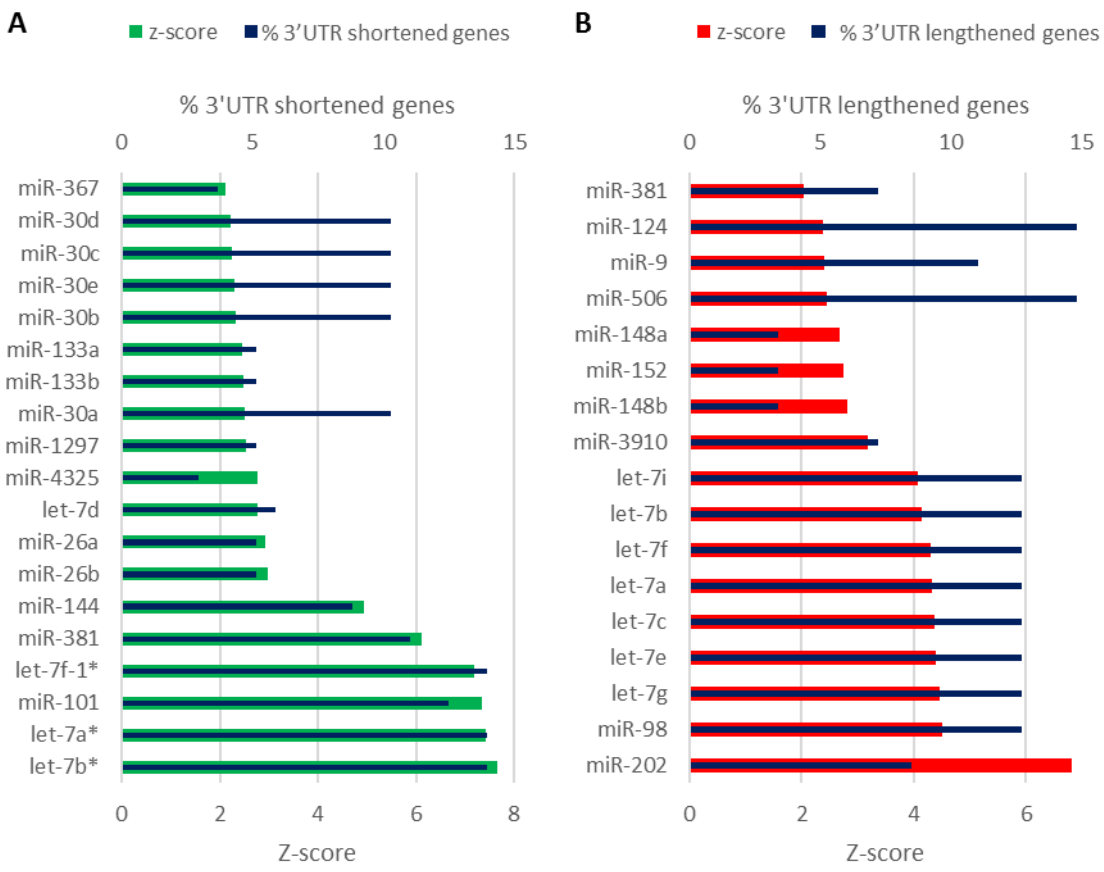


Supplementary Figure 8. Upstream-APA in cold shock.

A. Different trends to using upstream (green dots) or terminal exon (red dots) poly(A) sites in the nucleus (left) and the cytoplasm (right)

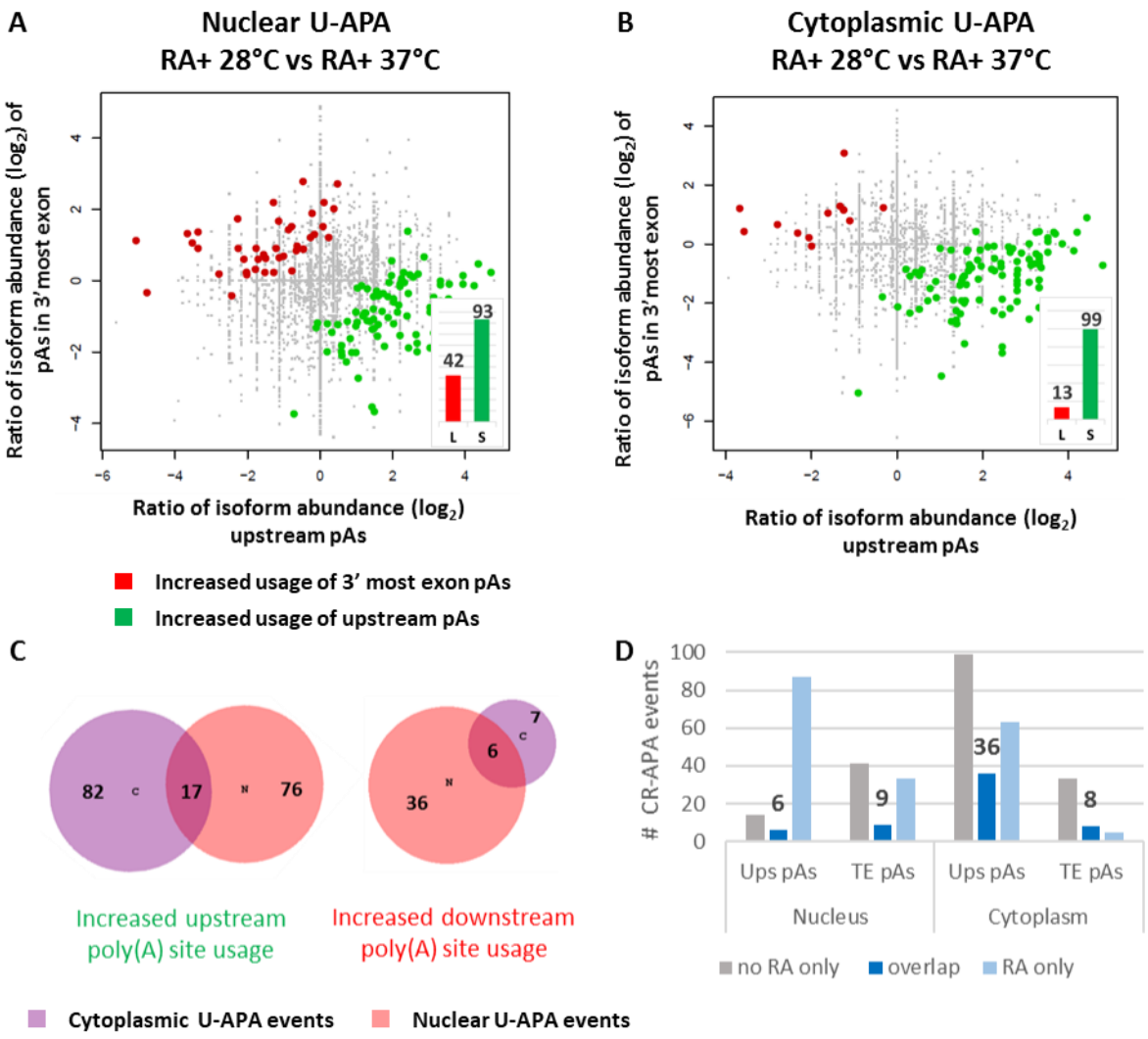
B. Only 12% and 30% of upstream-APA changes in the nucleus (red) for increased downstream or upstream poly(A) site usage respectively were observed in the cytoplasm (purple).

C. Increased expression of a shorter isoform of the *UBE3B* transcript in the cytoplasm (purple tracks) but not the nucleus (red tracks) was seen in cold shock which encodes a truncated and dysfunctional E3 ubiquitin ligase. Numbers on the left of the tracks indicate read numbers from sequencing data in reads per million (RPM).



Supplementary Figure 9. miRNA enrichment in alternative UTRs of APA regulated genes in cold shock.

Bar charts to show the z-score enrichment and the proportion of genes targeted by miRNAs (navy bars) in genes showing 3'UTR shortening (**A**) and 3'UTR lengthening (**B**) in cold shock.



E

Biological Process	# Genes Present	# Genes Expected	Fold Enrichment	P-value
mRNA splicing via spliceosome	9	1.03	8.78	7.67E-03
temination of Pol II transcription	5	0.25	20	4.81E-02
mRNA processing	11	1.64	6.72	6.02E-03

F

Biological Process	# Genes Present	# Genes Expected	Fold Enrichment	P-value
Post-transcriptional regulation of gene expression	15	3.44	4.37	1.83E-02
RNA processing	22	6.33	3.47	3.35E-03
Intracellular Transport	27	9.81	2.75	1.32E-02
Mitosis	12	1.91	6.28	5.14E-03

Supplementary Figure 10. Upstream-APA in differentiated BE(2)-M17 cells exposed to cold shock.

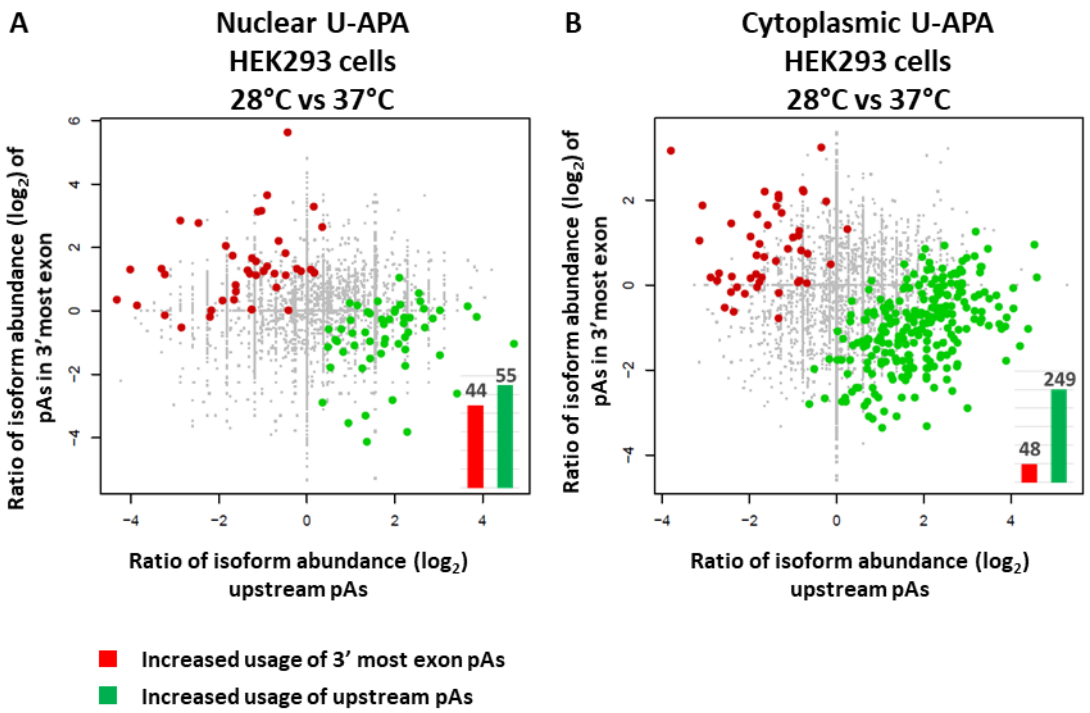
A. and **B.** A trend to using upstream poly(A) sites (green dots) compared to poly(A) sites in the terminal exon (red dots) in both the nucleus (**A**) and the cytoplasm (**B**) in differentiated BE(2)-M17 cells exposed to cold shock at 28°C for 24 hours.

C. Venn diagrams to show the overlap of upstream-APA events in the nucleus and the cytoplasm.

D. A bar chart to show the overlap of upstream-APA events in undifferentiated cells (grey) and differentiated cells (light blue). The number of genes regulated by upstream-APA in both cell states are shown by blue bars.

E. A table to show enriched biological processes by GO in the cohort of genes that show 3'UTR lengthening in the nucleus and the cytoplasm in undifferentiated and differentiated BE(2)-M17 cells exposed to cold shock.

F. A table to show enriched biological processes by GO in the cohort of genes that were differentially expressed and regulated by APA in BE(2)-M17 cells differentiated with RA exposed to cold shock.



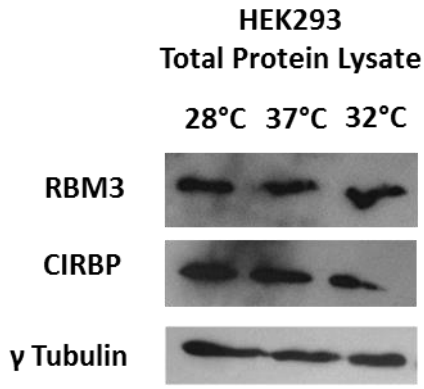
C

Cell Line	Biological Process	# Genes Present	# Genes Expected	Fold Enrichment	P-value
BE(2)-M17	Translation	13	2.5	5.19	1.34E-02
	Intracellular Transport	26	8.65	3.01	3.61E-03
	mRNA splicing via spliceosome	19	3.29	5.77	1.24E-05
	Cellular Response to Stress	42	17.72	2.37	1.43E-03
HEK293	mRNA splicing via spliceosome	21	3.85	5.46	4.81E-06
	intracellular Transport	36	11.44	3.15	1.44E-05
	mRNA 3'end processing	10	1.45	6.88	2.35E-02
	Translation	27	7.44	3.63	1.26E-04

Supplementary Figure 11. Upstream-APA in HEK293 cells exposed to cold shock

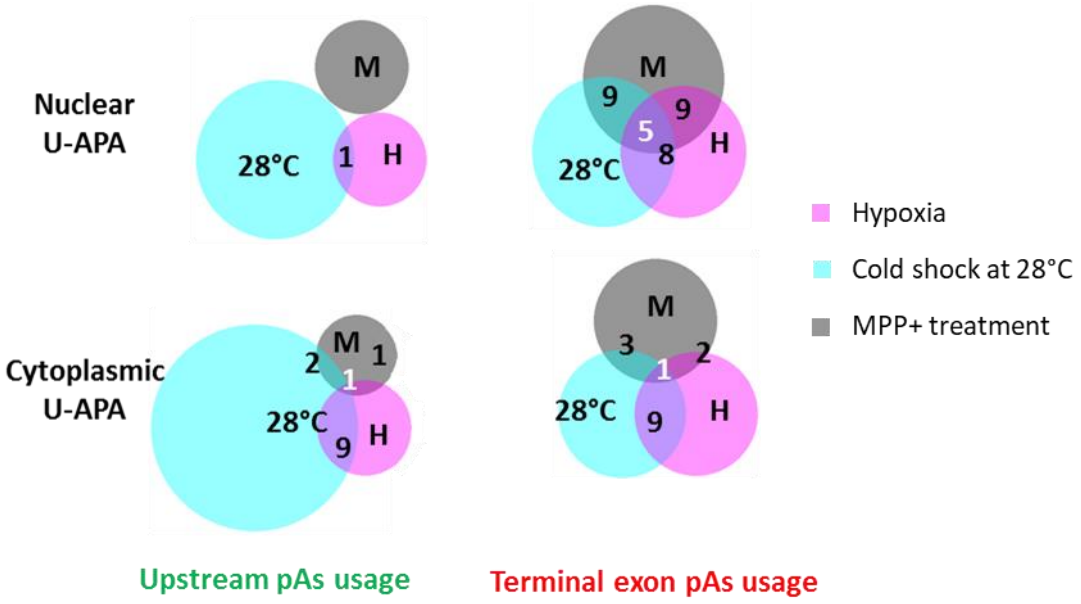
A. and **B.** Upstream-APA events in the nucleus (**A**) and the cytoplasm (**B**). A trend to using an upstream poly(A) site in cold shock was observed in the cytoplasm but not the nucleus in HEK293 cells. Red dots and bars are upstream-APA events where there is a shift to using the terminal exon poly(A) site; Green dots and bars are upstream-APA events where there is a shift to using an upstream poly(A) site.

C. A table to show enriched biological processes by GO in APA regulated genes upon cold shock exposure in BE(2)-M17 and HEK293 cells.



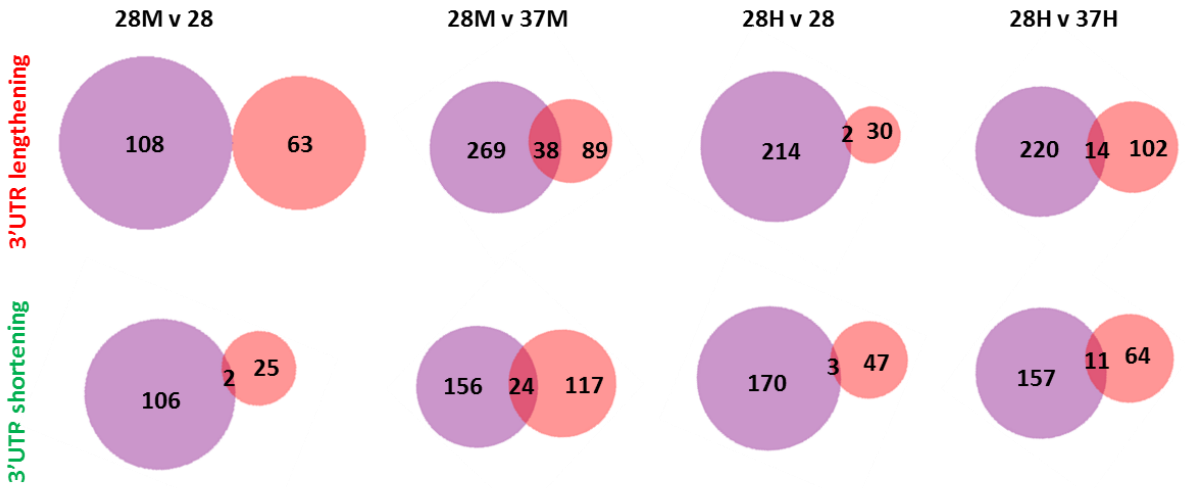
Supplementary Figure 12. RBM3 and CIRBP expression in HEK293 cells

A western blot to show RBM3 and CIRBP expression in HEK293 cells at 37°C and two cold shock temperatures, 28°C and 32°C. Protein samples isolated from whole cell lysate. Tubulin used as a protein loading control.



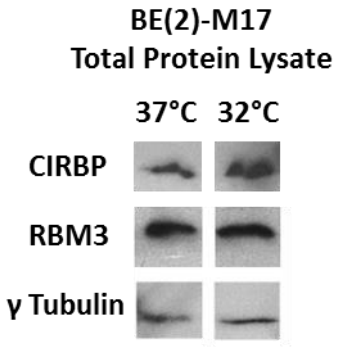
Supplementary Figure 13. Upstream-APA in different stresses

Venn diagrams to show the overlap of genes regulated by upstream-APA in different stresses in the nucleus (upper) and the cytoplasm (lower). Cold shock (28°C, cyan), hypoxia (H, pink) and MPP+ (M, grey). The number of genes regulated by upstream-APA in two stresses are indicated by black numbers, while white numbers show the number of genes regulated by upstream-APA in all three stresses.



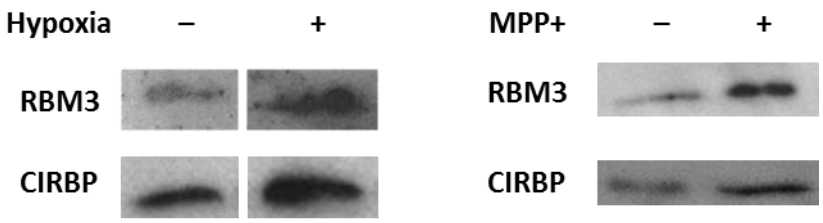
Supplementary Figure 14. Little overlap of UTR-APA events in the cytoplasm and nucleus in combined stresses.

Venn diagrams to show the overlap of UTR-APA regulated events in the nucleus (red) and the cytoplasm (purple). Numbers indicate number of APA regulated genes. Stress comparisons shown above Venn Diagrams e.g. 28M v 28: APA events identified in cells exposed to MPP+ at 28°C compared to cells exposed to 28°C. M: MPP+; H: hypoxia.



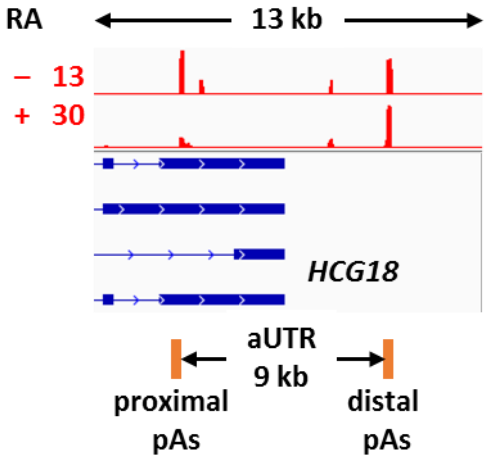
Supplementary Figure 15. RBM3 and CIRBP expression at 32°C.

A western blot to show the expression of CIRBP and RBM3 at 32°C compared to 37°C in protein samples isolated from whole cell lysate from BE(2)-M17 cells. Tubulin used as a protein loading control.



Supplementary Figure 16. Expression of RBM3 and CIRBP in other stresses.

A western blot of protein samples isolated from the whole cell fraction to show the expression of RBM3 and CIRBP in hypoxia (left) and MPP+ (right). BE(2)-M17 cells were stressed for 24 hours before protein extraction.



Supplementary Figure 17. 3'UTR lengthening in lncRNAs during RA mediated differentiation.

A screenshot of the lncRNA *HCG18* which showed 3'UTR lengthening in the nucleus during RA differentiation in BE(2)-M17 cells. The red tracks show reads in the nuclear fractions. Read numbers are shown on the left in RPM from sequencing data.

7.2 Supplementary Tables

Supplementary Table 1. RNA-seq methods to investigate APA

Method	Outline	Reference
3'-seq	Total RNA reverse transcribed with oligodT primer containing a U. Second strand synthesis. Nick introduced at the Uridine, and nick translation used to shift the nick 50-75 bases away from the 3'end. Created blunt end at the position of the nick and ligated a second sequencing adaptor. 10 PCR cycles, and gel purification to generate library for sequencing.	(Lianoglou et al. 2013)
3'READS	3' Region Extraction And Deep Sequencing. Uses a CU_5T_{45} oligo primer to capture poly(A)+ RNA which prevents priming to internal A streches. RNaseH digestion of the poly(A) tail degrades all RNA not bound to the oligo primer. 3' and 5' adaptor ligation, reverse transcription and PCR generates library for deep sequencing.	(Hoque et al. 2013)
3P-Seq	Poly(A) fragments from total RNA isolated using a biotinylated primer that binds to streptavidin. Reverse transcription fills in the poly(A) tail. RNaseH cleaves the poly(A) tail resulting in the 3'end remaining which is used for library generation.	(Jan et al. 2011)
A-seq	Isolate poly(A)+ RNA using oligo$(dT)_{25}$ magnetic beads. Fragment RNA using RNase. Phosphorylate 5'end and ligate 5' adaptor. Reverse transcribe the bead captured 3'end with split oligo dT primer. Size select on denaturing gel and amplify with PCR to produce library.	(Martin et al. 2012)
Poly(A)-seq	Oligo(dT) primer used to anneal to poly(A)+ RNA in reverse transcription reaction. RNA template degraded with RNaseH and DNA purified using PCR purification kit. A random primer was used for second strand synthesis. Sample was amplified by PCR and library was purified using magnetic beads.	(Derti et al. 2012)
PAS-seq	Poly(A)+ RNAs are fragmented to 60-200 nucleotides and reverse transcribed using a SMART adaptor to reduce internal priming. Double nucleotide anchored oligo(dT) primer used to ensure reverse transcription starts at poly(A) junctions. Upon reaching the 5'end of the RNA template, untemplated deoxycytodines are added to the 3'ends of cDNAs. The cDNA therefore has linkers on both ends. cDNAs are size selected and amplified to generate library for sequencing.	(Shepard et al. 2011)
PAT-seq	Enables identification of both poly(A) site choice and also poly(A) tail length. Poly(A) tail extension with Klenow and dNTPs using annealed anchor-oligo as a template. Limited digest by RNase T1. Collect 3' fragments on streptavidin magnetic beads. Reverse transcribe bead bound anchor sequences. Size select 120-300 bases on a denaturing gel and amplify with PCR to produce library.	(Harrison et al. 2015)

Supplementary Table 2. miRNAs associated in neurodegeneration
(Reviewed in (Goodall et al. 2013))

	miRNA	**Change in disease**	**Model/Sample**	**Gene targets**	**Biological effect**
AD	miR-106a/b	DOWN	Human AD temporal cortex; cerebral cortex in mouse model of AD	*APP* *ABCA1*	Increased APP expression and Increased Aβ production
	miR-107	DOWN	Human AD temporal cortex	*BACE1* *ADAM10*	Increased BACE1 which increases Aβ production
	miR-124a	DOWN	Human AD temporal cortex	*BACE1* *PTBP1*	increased BACE1 expression which increased Ab production
	miR-132	DOWN	Human AD hippocampus, cerebellum and medial frontal gyrus	*SIRT1* *AChE* *PTEN* *FOXO3a* *P300*	Increased expression of AD associated genes Target genes associated with AD and have a role in neural apoptosis
	miR-132-3p	DOWN	LOAD brain areas in 3 cohorts of patients	*FOXO1a*	Increased expression of the transcription factor FOXO1A
	miR-146a	UP	AD hippocampus and temporal cortex	*IRAK1* *CFH* *TRAF6* *TSPAN12*	Targets NFkB and TSPAN12 to potentially impact Aβ production
	miR-153	DOWN	Cerebral cortex of AD mouse model Human AD frontal cortex	*APP* *APLP2*	Impacts Aβ production (Long, Ray, and Lahiri 2012)
	miR-181c	DOWN	Human temporal cortex and patient serum	*SIRT1*	Affects Tau metabolism
	miR-29a/b	DOWN	Human AD temporal cortex, cerebellum	*BACE1*	Increases Aβ production. miRNA linked to modulation of microglial activation and ageing in the brain
	miR-29c	UP	AD mouse model	*BACE1*	Increases Ab production
	miR-34a	UP	Human AD hippocampus, cerebellum Cerebral cortex of AD mouse model	*BCL2* *SIRT1* *TAU*	Could increase apoptotic cell death Impacts tau metabolism miR-34a targets the longer 3'UTR of *TAU* (Dickson et al. 2013)
	miR-9	DOWN	Human AD brain tissue	*NFH* *SIRT1*	Increases plaque and tangle formation
	miR-135a	DOWN	Transgenic AD mouse model; Cerebrospinal fluid of AD patients	*BACE1*	Increased Ab production (C. G. Liu et al. 2014)
	miR-200b	DOWN	Transgenic AD mouse model; Cerebrospinal fluid of AD patients	*APP*	Increased APP increased Ab production (C. G. Liu et al. 2014)
	miR-429	DOWN	Transgenic AD mouse model; Cerebrospinal fluid of AD patients	*APP*	Increased APP increased Ab production (C. G. Liu et al. 2014)
	miR-23b	DOWN	Lower expression level detected in AD patient cortex than control sample		[Wang et al., 2008 – Journal of Neuroscience. Paper in Mendeley]

	miRNA	**Change in disease**	**Model/Sample**	**Gene targets**	**Biological effect**
PD	Let-7	DOWN	*C. elegans* model of PD		Increased expression of E2F1 and DP TF which led to dopaminergic neuronal cell death
	miR-106a -3p	UP	Post-mortem sample from substantia nigra of PD patient		Chaperone mediated autophagy
	miR-133b	DOWN	PD patient midbrain	*PITX3*	Negatively regulates TF PITX3 which alters transcriptome in function of midbrain
	miR-153	-	-	*SNCA*	Interacts with *SNCA* in cell culture
	miR-184-3p	DOWN	Drosophila model of PD	-	Increased dopaminergic neuronal cell death via increased expression of E2F1 and DP TFs
	miR-205	DOWN	PD cerebral cortex tissue	*LRRK2*	Increased LRRK2 expression associated with PD
	miR-21-3p	UP	Post-mortem sample from substantia nigra of PD patient		Alters autophagy pathway
	miR-224	UP	Post-mortem sample from substantia nigra of PD patient	*LAMP2A*	Alters autophagy pathway
	miR-26b	UP	Post-mortem sample from substantia nigra of PD patient	*HSC70*	Alters autophagy pathway
	miR-301b	UP	Post-mortem sample from substantia nigra of PD patient		Alters autophagy pathway
	miR-373-3p	UP	Post-mortem sample from substantia nigra of PD patient	*LAMP2A*	Alters autophagy pathway
	miR-64/65	DOWN	*C.elegans* model of PD	-	unknown
	miR-7	-	Cell culture models of PD	*SNCA*	miRNA known to suppress SNCA mediated toxicity
	miR-124	DOWN	MPTP mouse model; MPP+ treatment in MN9D cells	-	Affects neuronal function
	miR-34b/c	DOWN	PD frontal cortex and substantia nigra	-	Associated with altered mitochondrial function and oxidative stress
ALS	miR-124a	DOWN	Spinal cord from SOD1 ALS mouse model	*EAAT2/ GLT1*	Increased expression of glutamate transport protein. increased glutamate associated with ALS
	miR-206	UP	Muscle from ALS patients ALS mouse model	-	Affects nerve-muscle communication
	miR-338-3p	UP	Human ALS frontal cortex and ALS leukocytes	-	Alters neurotransmitter signalling pathways
	miR-155	UP	SOD1 mouse model Human Spinal cord of fALS and sALS patients	Many targets including *JARID2 CSF1R*	Targets include microglial specific genes, whose protein expression was impacted with upregulation of miR-155 in ALS. Knockdown of miR-155 reversed >70% of the dyregulated proteins in the spinal cord of SOD1 mice (Butovsky et al. 2015)
	117 other miRNAs show altered expression				Extent of altered regulation still unknown (Butovsky et al. 2015)

Supplementary Table 3. Read depth in RNA-seq datasets used in DaPars

* Where biological replicates were available, the mean sequencing depth is given, as combined Bedgraph files were processed through DaPars

Disease	Dataset	Single/Paired end	Read Length	Sample	Sequencing Depth
AD	Hippocampi of LOAD v CTRL	Single	99	LOAD1	187,514,717
				LOAD2	180,318,237
				LOAD3	178,521,597
				LOAD4	188,604,801
				CTRL1	177,108,169
				CTRL2	173,894,719
				CTRL3	164,772,379
				CTRL4	170,053,030
	Temporal Lobe v Frontal Lobe v Whole Brain	Single	36	TL-AD	14,227,702
				FL-AD	15,228,832
				W-AD	14,720,816
				TL-C	15,256,752
				FL-C	15,772,947
				W-C	13,442,077
PD	Midbrain dopaminergic neurons derived from iPSCs from fPD v sPD and Control	Single	101	C1*	34,828,525
				C2*	32,836,787
				s-PD*	26,453,734
				F-PD*	33,794,095
				Non-F-PD*	30,948,770
	Derived midbrain dopaminergic neurons from iPSCs from sPD v control	Single	50	S-PD1*	51,050,112
				S-PD2*	54,799,948
				S-PD3*	50,887,494
				C1*	49,375,529
				C2*	51,633,314
				C3*	49,688,949
ALS	Frontal Cortex and Cerebellum from c9ALS v sALS v control	Paired	202	C9ALS1 FCX	34,434,015
				C9ALS1 Cereb	49,990,019
				C9ALS2 FCX	46,591,566
				C9ALS2 Cereb	49,276,759
				sALS1 FCX	65,999,560
				sALS1 Cereb	48,931,471
				sALS2 FCX	33,496,410
				sALS2 Cereb	43,032,909
				C1 FCX	45,174,455
				C1 Cereb	42,097,505
				C2 FCX	42,402,353
				C2 Cereb	50,038,325
	Lumbar spinal cord motor neurons from sALS v control	Paired	50	sALS1	26,241,715
				sALS2	29,643,723
				sALS3	30,508,179
				sALS4	30,899,786
				sALS5	31,944,963
				sALS6	32,710,741
				sALS7	32,978,331
				sALS8	34,575,411
				sALS9	34,754,975
				sALS10	36,101,437
				C1	21,117,915
				C2	22,359,173
				C3	22,359,173
				C4	30,222,648
				C5	30,616,734
				C6	35,390,202
				C7	35,702,384
				C8	36,089,192

Supplementary Table 4. miRNA expression changes in Hypoxia.
Reviewed in (Nallamshetty, Chan, and Loscalzo 2013; Kulshreshtha et al. 2008; Kulshreshtha et al. 2006).

miRNA	**Change in Hypoxia**	**Target Genes**	**Effects**	**Other information**
miR-21	UP	*CDC25A*	Cell cycle arrest	*In silico* prediction.
miR-23	UP	*BID, BINP3L, CCNH, CASP7, CCND2*	Deregulates expression of apoptotic and cell cycle genes to induce cell cycle arrest and apoptosis.	*In silico* prediction of apoptosis related genes.
miR-26	UP	*PAR-4* *BAK1* *CCNE1* *CDK6*	Deregulates expression of apoptotic and cell cycle genes to induce cell cycle arrest and apoptosis.	Promoter of this miRNA has HRE which is bound by HIF Experimentally shown to be upregulated.
miR-103	UP	*PCDC10* *CDC25A* *CCND2* *CDK6*	Deregulates expression of apoptotic and cell cycle genes to induce cell cycle arrest and apoptosis.	Experimentally shown to be upregulated. HIF overexpression induced expression of this miRNA.
miR-155	UP	*HIF1A*	Fine tuning expression of *HIF1A* transcript.	Has a functional HRE in promoter region.
miR-146	UP	*TRAF6*, *IRAK1*	Repress NFkB signalling to reduce inflammatory responses.	
miR-210	UP	*VEGF* *GPD1L* Iron-sulphur cluster assembly and COX proteins *E2F3* RAD52 RAD23B	Fine-tuning of *VEGF* expression. Degrades *GPD1L* to stabilize HIF-1α. Represses mitochondrial respiration. Associated with cell cycle arrest Restrict DNA repair responses.	Promoter of miRNA gene has HRE. Experimentally shown to be upregulated. HIF overexpression induced expression of this miRNA. Expression induced by p53 in the absence of HIF.
miR-107	UP	*PCDC10* *CDC25A* *CCND2* *CDK6*	Deregulates expression of apoptotic and cell cycle genes to induce cell cycle arrest and apoptosis.	*In silico* prediction.
miR-424	UP	*CUL2*	Degrades *CUL2* transcript which stabilizes HIF1A.	
miR-373	UP	*RAD23B*	This gene is involved in nucleotide excision repair – alteration of its expression will modulate DNA repair during hypoxic stress.	
miR-181a/b/c	UP	*PAR-4* *PCDC10* *TNFA*	Decreased TNFα limits inflammatory pathways and apoptosis in hypoxic neurons.	Promoter of this miRNA has HRE which is bound by HIF. Experimentally confirmed.
miR-15b	DOWN	*BCL2*	Increased *BCL2* (anti-apoptotic gene) to prevent cell death.	Experimentally confirmed target.
miR-16	DOWN	*BCL2* *VEGF*	VEGF key in hypoxic response – would increase expression level.	*BCL2* Experimentally confirmed target.
miR-199a	DOWN	*HIF1A*	Stabilizes *HIF1A* transcript.	
miR-320	DOWN	*VEGF*	VEGF key in hypoxic response – would increase expression level.	
miR-20	DOWN	*VEGF* *HIF1A*	VEGF key in hypoxic response – would increase expression level Stabilizes *HIF1A* transcript	

Chapter 8: References

Abdelmohsen, Kotb, Subramanya Srikantan, Xiaoling Yang, Ashish Lal, Hyeon Ho Kim, Yuki Kuwano, Stefanie Galban, et al. 2009. "Ubiquitin-Mediated Proteolysis of HuR by Heat Shock." *The EMBO Journal* 28 (9): 1271–82. doi:10.1038/emboj.2009.67.

Abemayor, E., and N. Sidell. 1989. "Human Neuroblastoma Cell Lines as Models for the in Vitro Study of Neoplastic and Neuronal Cell Differentiation." *Environmental Health Perspectives* 80: 3–15. doi:10.1289/ehp.89803.

Abramov, Andrey Y., Tora K. Smulders-Srinivasan, Denise M. Kirby, Rebeca Acin-Perez, José Antonio Enriquez, Robert N. Lightowlers, Michael R. Duchen, and Douglass M. Turnbull. 2010. "Mechanism of Neurodegeneration of Neurons with Mitochondrial DNA Mutations." *Brain* 133 (3): 797–807. doi:10.1093/brain/awq015.

Absalon, S., D. M. Kochanek, V. Raghavan, and A. M. Krichevsky. 2013. "MiR-26b, Upregulated in Alzheimer's Disease, Activates Cell Cycle Entry, Tau-Phosphorylation, and Apoptosis in Postmitotic Neurons." *Journal of Neuroscience* 33 (37): 14645–59. doi:10.1523/JNEUROSCI.1327-13.2013.

Al-Fageeh, Mohamed B, and C Mark Smales. 2009. "Cold-Inducible RNA Binding Protein (CIRP) Expression Is Modulated by Alternative mRNAs." *RNA (New York, N.Y.)* 15 (6): 1164–76. doi:10.1261/rna.1179109.

Alkan, S A, K Martincic, and C Milcarek. 2006. "The hnRNPs F and H2 Bind to Similar Sequences to Influence Gene Expression." *Biochem J* 393 (Pt 1): 361–71. doi:BJ20050538 [pii]\n10.1042/BJ20050538.

Alonso-Alconada, Daniel, Kevin D. Broad, Alan Bainbridge, Manigandan Chandrasekaran, Stuart D. Faulkner, Áron Kerenyi, Jane Hassell, et al. 2015. "Brain Cell Death Is Reduced with Cooling by 3.5??C to 5??C but Increased with Cooling by 8.5??C in a Piglet Asphyxia Model." *Stroke* 46 (1): 275–78. doi:10.1161/STROKEAHA.114.007330.

Ameres, Stefan Ludwig, Javier Martinez, and Renée Schroeder. 2007. "Molecular Basis for Target RNA Recognition and Cleavage by Human RISC." *Cell* 130 (1): 101–12. doi:10.1016/j.cell.2007.04.037.

An, Juan Ji, Kusumika Gharami, Guey Ying Liao, Newton H. Woo, Anthony G. Lau, Filip Vanevski, Enrique R. Torre, et al. 2008. "Distinct Role of Long 3' UTR BDNF mRNA in Spine Morphology and Synaptic Plasticity in Hippocampal Neurons." *Cell* 134 (1): 175–87. doi:10.1016/j.cell.2008.05.045.

Anderson, Paul, and Nancy Kedersha. 2006. "RNA Granules." *Journal of Cell Biology* 172 (6): 803–8. doi:10.1083/jcb.200512082.

Andreassi, Catia, and Antonella Riccio. 2009. "To Localize or Not to Localize: mRNA Fate Is in 3???UTR Ends." *Trends in Cell Biology* 19 (9): 465–74. doi:10.1016/j.tcb.2009.06.001.

Andres, Devon, Brian M Keyser, John Petrali, Betty Benton, Kyle S Hubbard, Patrick M McNutt, and Radharaman Ray. 2013. "Morphological and Functional Differentiation in BE(2)-M17 Human Neuroblastoma Cells by Treatment with Trans-Retinoic Acid." *BMC Neuroscience* 14 (January): 49. doi:10.1186/1471-2202-14-49.

Ara, Takeshi, Fabrice Lopez, William Ritchie, Philippe Benech, and Daniel Gautheret. 2006. "Conservation of Alternative Polyadenylation Patterns in Mammalian Genes." *BMC Genomics* 7: 189. doi:10.1186/1471-2164-7-189.

Au, Ka Wing, Cecy Y C Kou, Anthony Y H Woo, Stephen S C Chim, Kwok Pui Fung, Christopher H K Cheng, Mary M Y Waye, and Stephen K W Tsui. 2006. "Calcyclin Binding Protein Promotes DNA Synthesis and Differentiation in Rat Neonatal Cardiomyocytes." *Journal of*

Cellular Biochemistry 98 (3): 555–66. doi:10.1002/jcb.20710.

Baez, María V., and Graciela L. Boccaccio. 2005. "Mammalian Smaug Is a Translational Repressor That Forms Cytoplasmic Foci Similar to Stress Granules." *Journal of Biological Chemistry* 280 (52): 43131–40. doi:10.1074/jbc.M508374200.

Bagga, P S, G K Arhin, and J Wilusz. 1998. "DSEF-1 Is a Member of the hnRNP H Family of RNA-Binding Proteins and Stimulates Pre-mRNA Cleavage and Polyadenylation in Vitro." *Nucleic Acids Research* 26 (23): 5343–50. doi:gkb833 [pii].

Bai, Bing, Chadwick M Hales, Ping-chung Chen, Yair Gozal, Eric B Dammer, and Jason J Fritz. 2013. "U1 Small Nuclear Ribonucleoprotein Complex and RNA Splicing Alterations in Alzheimer ' S Disease." *Proceedings of the National Academy of Sciences of the United States of America* 110 (41): 16562–67. doi:10.1073/pnas.1310249110/-/DCSupplemental.www.pnas.org/cgi/doi/10.1073/pnas.1310249110.

Bailey, Timothy L. 2011. "DREME: Motif Discovery in Transcription Factor ChIP-Seq Data." *Bioinformatics* 27 (12): 1653–59. doi:10.1093/bioinformatics/btr261.

Banerjee, Rebecca, Anatoly a Starkov, M Flint Beal, and Bobby Thomas. 2009. "Mitochondrial Dysfunction in the Limelight of Parkinson's Disease Pathogenesis." *New York* 1792 (7): 651–63. doi:10.1016/j.bbadis.2008.11.007.Mitochondrial.

Bao, Jianqiang, Kristoffer Vitting-Seerup, Johannes Waage, Chong Tang, Ying Ge, Bo T. Porse, and Wei Yan. 2016. "UPF2-Dependent Nonsense-Mediated mRNA Decay Pathway Is Essential for Spermatogenesis by Selectively Eliminating Longer 3'UTR Transcripts." *PLoS Genetics* 12 (5): 1–24. doi:10.1371/journal.pgen.1005863.

Bartel, David P. 2009. "MicroRNAs: Target Recognition and Regulatory Functions." *Cell* 136 (2): 215–33. doi:10.1016/j.cell.2009.01.002.

Bastide, Amandine, Diego Peretti, John R.P. Knight, Stefano Grosso, Ruth V. Spriggs, Xavier Pichon, Thomas Sbarrato, et al. 2017. "RTN3 Is a Novel Cold-Induced Protein and Mediates Neuroprotective Effects of RBM3." *Current Biology* 27 (5). Elsevier Ltd.: 638–50. doi:10.1016/j.cub.2017.01.047.

Batra, Ranjan, Konstantinos Charizanis, Mini Manchanda, Apoorva Mohan, Moyi Li, Dustin J. Finn, Marianne Goodwin, et al. 2014. "Loss of MBNL Leads to Disruption of Developmentally Regulated Alternative Polyadenylation in RNA-Mediated Disease." *Molecular Cell* 56 (2). Elsevier Inc.: 311–22. doi:10.1016/j.molcel.2014.08.027.

Batra, Ranjan, Kasey Hutt, Anthony Vu, Stuart J Rabin, Michael W Baughn, Ryan T Libby, Shawn Hoon, John Ravits, and Gene W Yeo. 2016. "Gene Expression Signatures of Sporadic ALS Motor Neuron Populations." *bioRxiv*, 38448. doi:10.1101/038448.

Batra, Ranjan, Mini Manchanda, and Maurice S Swanson. 2015. "Global Insights into Alternative Polyadenylation Regulation." *RNA Biology* 12 (6): 597–602. doi:10.1080/15476286.2015.1040974.

Bava, Felice-Alessio, Carolina Eliscovich, Pedro G Ferreira, Belen Miñana, Claudia Ben-Dov, Roderic Guigó, Juan Valcárcel, and Raúl Méndez. 2013. "CPEB1 Coordinates Alternative 3'-UTR Formation with Translational Regulation." *Nature* 495 (7439): 121–25. doi:10.1038/nature11901.

Beaudoing, E., and D. Gautheret. 2001. "Identification of Alternate Polyadenylation Sites and Analysis of Their Tissue Distribution Using EST Data." *Genome Research* 11 (9): 1520–26. doi:10.1101/gr.190501.

Bekris, Lynn, Ignacio Mata, and Cyrus Zabetian. 2010. "The Genetics of Parkinson's Disease." *National Institute of Health* 23 (4): 228–42. doi:10.1177/0891988710383572.The.

Bendor, Jacob, Todd Logan, and Robert H Edwards. 2013. "The Function of α-Synuclein." *Neuron* 79 (6): 1–43. doi:10.1016/j.neuron.2013.09.004.The.

Bennett, C. L., M. E. Brunkow, F. Ramsdell, K. C. O'Briant, Q. Zhu, R. L. Fuleihan, A. O. Shigeoka, H. D. Ochs, and P. F. Chance. 2001. "A Rare Polyadenylation Signal Mutation of the FOXP3 Gene (AAUAAA???AAUGAA) Leads to the IPEX Syndrome." *Immunogenetics* 53 (6): 435–39.

doi:10.1007/s002510100358.

Bensaude, Olivier. 2011. “Inhibiting Eukaryotic Transcription: Which Compound to Choose? How to Evaluate Its Activity?” *Transcription* 2 (3): 103–8. doi:10.4161/trns.2.3.16172.

Bentea, Eduard, Lise Verbruggen, and Ann Massie. 2016. “The Proteasome Inhibition Model of Parkinson’s Disease.” *Journal of Parkinson’s Disease* Preprint (Preprint): 1–33. doi:10.3233/JPD-160921.

Bentley, David L. 2014. “Coupling mRNA Processing with Transcription in Time and Space.” *Nature Reviews Genetics* 15 (3): 163–75. doi:10.1016/j.immuni.2010.12.017.Two-stage.

Berkovits, Binyamin D, and Christine Mayr. 2015. “Alternative 3’ UTRs Act as Scaffolds to Regulate Membrane Protein Localization.” *Nature* 522 (7556): 363–67. doi:10.1038/nature14321.

Bernstam, Luda, and Jerome Nriagu. 2000. “Molecular Aspects of Arsenic Stress.” *Journal of Toxicology and Environmental Health, Part BOnline) Journal ASPECTS OF ARSENIC STRESS Journal of Toxicology and Environmental Health, Part B* 3 (4): 1093–7404. doi:10.1080/109374000436355.

Bertout, Jessica A, Shetal A Patel, and M Celeste Simon. 2008. “The Impact of O2 Availability on Human Cancer.” *Nature Reviews. Cancer* 8 (12): 967–75. doi:10.1038/nrc2540.

Beveridge, Natalie J., Paul A. Tooney, Adam P. Carroll, Nham Tran, and Murray J. Cairns. 2009. “Down-Regulation of miR-17 Family Expression in Response to Retinoic Acid Induced Neuronal Differentiation.” *Cellular Signalling* 21 (12). Elsevier Inc.: 1837–45. doi:10.1016/j.cellsig.2009.07.019.

Bisaglia, Marco, Elisa Greggio, Dragan Maric, David W Miller, Mark R Cookson, and Luigi Bubacco. 2010. “Alpha-Synuclein Overexpression Increases Dopamine Toxicity in BE2-M17 Cells.” *BMC Neuroscience* 11 (January): 41. doi:10.1186/1471-2202-11-41.

Blake, J. A., K. R. Christie, M. E. Dolan, H. J. Drabkin, D. P. Hill, L. Ni, D. Sitnikov, et al. 2015. “Gene Ontology Consortium: Going Forward.” *Nucleic Acids Research* 43 (D1): D1049–56. doi:10.1093/nar/gku1179.

Blanco, F F, M Jimbo, J Wulfkuhle, I Gallagher, J Deng, L Enyenihi, N Meisner-Kober, et al. 2015. “The mRNA-Binding Protein HuR Promotes Hypoxia-Induced Chemoresistance through Posttranscriptional Regulation of the Proto-Oncogene PIM1 in Pancreatic Cancer Cells.” *Oncogene* 35 (19). Nature Publishing Group: 2529–41. doi:10.1038/onc.2015.325.

Bley, Nadine, Marcell Lederer, Birgit Pfalz, Claudia Reinke, Tommy Fuchs, Markus Glaß, Birgit Möller, and Stefan Hüttelmaier. 2015. “Stress Granules Are Dispensable for mRNA Stabilization during Cellular Stress.” *Nucleic Acids Research* 43 (4). doi:10.1093/nar/gku1275.

Blokhuis, Anna M., Ewout J N Groen, Max Koppers, Leonard H. Van Den Berg, and R. Jeroen Pasterkamp. 2013. “Protein Aggregation in Amyotrophic Lateral Sclerosis.” *Acta Neuropathologica* 125 (6): 777–94. doi:10.1007/s00401-013-1125-6.

Bogaerts, V., J. Theuns, and C. Van Broeckhoven. 2008. “Genetic Findings in Parkinson’s Disease and Translation into Treatment: A Leading Role for Mitochondria?” *Genes, Brain and Behavior* 7 (2): 129–51. doi:10.1111/j.1601-183X.2007.00342.x.

Bonifati, Vincenzo, Patrizia Rizzu, Marijke J van Baren, Onno Schaap, Guido J Breedveld, Elmar Krieger, Marieke C J Dekker, et al. 2003. “Mutations in the DJ-1 Gene Associated with Autosomal Recessive Early-Onset Parkinsonism.” *Science (New York, N.Y.)* 299 (5604): 256–59. doi:10.1126/science.1077209.

Bové, Jordi, Marta Martínez-Vicente, Benjamin Dehay, Celine Perier, Ariadna Recasens, Agnes Bombrun, Bruno Antonsson, and Miquel Vila. 2014. “BAX Channel Activity Mediates Lysosomal Disruption Linked to Parkinson Disease.” *Autophagy* 10 (5): 889–900. doi:10.4161/auto.28286.

Braak, E, and H Braak. 1995. “Staging of Alzheimer â€™ S Disease-Related Neurofibrillary Changes.” *Neurobiology of Aging* 16 (3): 271–78. doi:10.1007/s00401-006-0127-z.

Buchan, J. Ross, and Roy Parker. 2009. “Eukaryotic Stress Granules: The Ins and Outs of Translation.” *Molecular Cell* 36 (6). Elsevier Ltd: 932–41. doi:10.1016/j.molcel.2009.11.020.

Butovsky, Oleg, Mark P. Jedrychowski, Ron Cialic, Susanne Krasemann, Gopal Murugaiyan, Zain Fanek, David J. Greco, et al. 2015. “Targeting miR-155 Restores Abnormal Microglia and Attenuates Disease in SOD1 Mice.” *Annals of Neurology* 77 (1): 675–99. doi:10.1016/j.pmr.2014.05.001.Functional.

Caneda-Ferrón, Begoña, Luigi A. De Girolamo, Teresa Costa, Katy E. Beck, Robert Layfield, and E. Ellen Billett. 2008. “Assessment of the Direct and Indirect Effects of MPP+ and Dopamine on the Human Proteasome: Implications for Parkinson’s Disease Aetiology.” *Journal of Neurochemistry* 105 (1): 225–38. doi:10.1111/j.1471-4159.2007.05130.x.

Capshew, Claire R., Kristen L. Dusenbury, and Heather A. Hundley. 2012. “Inverted Alu dsRNA Structures Do Not Affect Localization but Can Alter Translation Efficiency of Human mRNAs Independent of RNA Editing.” *Nucleic Acids Research* 40 (17): 8637–45. doi:10.1093/nar/gks590.

Carolindah, M.N., R. Rosli, A. Adam, and N. Nordin. 2013. “An Overview of in Vitro Research Models for Alzheimer’S Disease (Ad).” *Regenerative Research* 2 (2): 8–13. http://www.regres.tesma.org.my/pdf/RR-040613-001 R1 (2).pdf.

Castelo-Branco, Pedro, Andre Furger, Matthew Wollerton, Christopher Smith, Alexandra Moreira, and Nick Proudfoot. 2004. “Polypyrimidine Tract Binding Protein Modulates Efficiency of Polyadenylation.” *Molecular and Cellular Biology* 24 (10): 4174–83. doi:10.1128/MCB.24.10.4174.

Cawley, Simon, Stefan Bekiranov, Huck H. Ng, Philipp Kapranov, Edward A. Sekinger, Dione Kampa, Antonio Piccolboni, et al. 2004. “Unbiased Mapping of Transcription Factor Binding Sites along Human Chromosomes 21 and 22 Points to Widespread Regulation of Noncoding RNAs.” *Cell* 116 (4): 499–509. doi:10.1016/S0092-8674(04)00127-8.

Chang, Hyeshik, Jaechul Lim, Minju Ha, and V. Narry Kim. 2014. “TAIL-Seq: Genome-Wide Determination of poly(A) Tail Length and 3’ End Modifications.” *Molecular Cell* 53 (6). Elsevier Inc.: 1044–52. doi:10.1016/j.molcel.2014.02.007.

Chapuis, J, F Hansmannel, M Gistelinck, a Mounier, C Van Cauwenberghe, K V Kolen, F Geller, et al. 2013. “Increased Expression of BIN1 Mediates Alzheimer Genetic Risk by Modulating Tau Pathology.” *Molecular Psychiatry* 18 (11): 1225–34. doi:10.1038/mp.2013.1.

Chavez, L. O., M. Leon, S. Einav, and J. Varon. 2015. “Inside the Cold Heart: A Review of Therapeutic Hypothermia Cardioprotection.” *European Heart Journal: Acute Cardiovascular Care*, no. 1000460758. doi:10.1177/2048872615624242.

Chen, Chyi-Ying A, Nianhua Xu, and Ann-Bin Shyu. 2002. “Highly Selective Actions of HuR in Antagonizing AU-Rich Element-Mediated mRNA Destabilization.” *Molecular and Cellular Biology* 22 (20): 7268–78. doi:10.1128/MCB.22.20.7268–7278.2002.

Chen, Sheng, Pavani Sayana, Xiaojie Zhang, and Weidong Le. 2013. “Genetics of Amyotrophic Lateral Sclerosis: An Update.” *Molecular Neurodegeneration* 8 (1): 28. doi:10.1186/1750-1326-8-28.

Chen, Xiong, Ping Mo, Xiaohua Li, Peichan Zheng, Lina Zhao, Zengfu Xue, Gui Ren, Guohong Han, Xin Wang, and Daiming Fan. 2011. “CacyBP/SIP Protein Promotes Proliferation and G1/S Transition of Human Pancreatic Cancer Cells.” *Molecular Carcinogenesis* 50 (10): 804–10. doi:10.1002/mc.20737.

Cherra, Salvatore J., Scott M. Kulich, Guy Uechi, Manimalha Balasubramani, John Mountzouris, Billy W. Day, and Charleen T. Chu. 2010. “Regulation of the Autophagy Protein LC3 by Phosphorylation.” *Journal of Cell Biology* 190 (4): 533–39. doi:10.1083/jcb.201002108.

Cheung, Zelda H., and Nancy Y. Ip. 2011. “Autophagy Deregulation in Neurodegenerative Diseases - Recent Advances and Future Perspectives.” *Journal of Neurochemistry* 118 (3): 317–25. doi:10.1111/j.1471-4159.2011.07314.x.

Chi, Jen-Tsan, Zhen Wang, Dimitry S A Nuyten, Edwin H Rodriguez, Marci E Schaner, Ali Salim, Yun Wang, et al. 2006. “Gene Expression Programs in Response to Hypoxia: Cell Type Specificity and Prognostic Significance in Human Cancers.” *PLoS Medicine* 3 (3): e47. doi:10.1371/journal.pmed.0030047.

Chiba-Falek, Ornit, Grisel J. Lopez, and Robert L. Nussbaum. 2006. “Levels of Alpha-Synuclein mRNA in Sporadic Parkinson Disease Patients.” *Movement Disorders* 21 (10): 1703–8. doi:10.1002/mds.21007.

Chip, Sophorn, Andrea Zelmer, Omolara O. Ogunshola, Ursula Felderhoff-Mueser, Cordula Nitsch, Christoph Bührer, and Sven Wellmann. 2011. “The RNA-Binding Protein RBM3 Is Involved in Hypothermia Induced Neuroprotection.” *Neurobiology of Disease* 43 (2). Elsevier Inc.: 388–96. doi:10.1016/j.nbd.2011.04.010.

Cho, Jun, Hyeshik Chang, S. Chul Kwon, Baekgyu Kim, Yoosik Kim, Junho Choe, Minju Ha, Yoon Ki Kim, and V. Narry Kim. 2012. “LIN28A Is a Suppressor of ER-Associated Translation in Embryonic Stem Cells.” *Cell* 151 (4). Elsevier Inc.: 765–77. doi:10.1016/j.cell.2012.10.019.

Choi, Doo Chul, Yoon-Jee Chae, Savan Kabaria, Amrita Datta Chaudhuri, Mohit Raja Jain, Hong Li, M Maral Mouradian, and Eunsung Junn. 2014. “MicroRNA-7 Protects against 1-Methyl-4-Phenylpyridinium-Induced Cell Death by Targeting RelA.” *The Journal of Neuroscience : The Official Journal of the Society for Neuroscience* 34 (38): 12725–37. doi:10.1523/JNEUROSCI.0985-14.2014.

Choi, Joungil, Allan I. Levey, Susan T. Weintraub, Howard D. Rees, Marla Gearing, Lih Shen Chin, and Lian Li. 2004. “Oxidative Modifications and Down-Regulation of Ubiquitin Carboxyl-Terminal Hydrolase L1 Associated with Idiopathic Parkinson’s and Alzheimer’s Diseases.” *Journal of Biological Chemistry* 279 (13): 13256–64. doi:10.1074/jbc.M314124200.

Choi, Se Joon, Anne Panhelainen, Yvonne Schmitz, Kristin E. Larsen, Ellen Kanter, Min Wu, David Sulzer, and Eugene V. Mosharov. 2015. “Changes in Neuronal Dopamine Homeostasis Following 1-Methyl-4-Phenylpyridinium (MPP+) Exposure.” *Journal of Biological Chemistry* 290 (11): 6799–6809. doi:10.1074/jbc.M114.631556.

Choi, Won-Seok, Shane E Kruse, Richard D Palmiter, and Zhengui Xia. 2008. “Mitochondrial Complex I Inhibition Is Not Required for Dopaminergic Neuron Death Induced by Rotenone, MPP+, or Paraquat.” *Proceedings of the National Academy of Sciences of the United States of America* 105 (39): 15136–41. doi:10.1073/pnas.0807581105.

Ciavardelli, D, E Silvestri, a Del Viscovo, M Bomba, D De Gregorio, M Moreno, C Di Ilio, F Goglia, L M T Canzoniero, and S L Sensi. 2010. “Alterations of Brain and Cerebellar Proteomes Linked to Aβand Tau Pathology in a Female Triple-Transgenic Murine Model of Alzheimer’s Disease.” *Cell Death & Disease* 1 (10). Nature Publishing Group: e90. doi:10.1038/cddis.2010.68.

Crawford, Eric K, Jeffery E Ensor, Indira Kalvakolanu, and Jeffrey D Hasday. 1997. “The Role of 3 â€™ Poly (A) Tail Metabolism in Tumor Necrosis Factor- Alpha Regulation.” *Metabolism Clinical And Experimental* 272 (34): 21120–27.

Curinha, Ana, Sandra Oliveira Braz, Isabel Pereira-Castro, Andrea Cruz, and Alexandra Moreira. 2014. “Implications of Polyadenylation in Health and Disease.” *Nucleus (Austin, Tex.)* 5 (6): 508–19. doi:10.4161/nucl.36360.

Dai, Weijun, Gen Zhang, and Eugene V. Makeyev. 2012. “RNA-Binding Protein HuR Autoregulates Its Expression by Promoting Alternative Polyadenylation Site Usage.” *Nucleic Acids Research* 40 (2): 787–800. doi:10.1093/nar/gkr783.

Das, Gautam, Bhupendra V. Shravage, and Eric H. Baehrecke. 2012. “Regulation and Function of Autophagy during Cell Survival and.” *Cold Spring Harbor Laboratory Press* 4 (6): 22661635. doi:10.1101/cshperspect.a008813.Regulation.

Datta, Prasun K, Joseph F Bonner, Christopher J Haas, and Itzhak Fischer. 2013. “Neuronal Cell Culture.” *Neuronal Cell Culture: Methods and Protocols* 1078: 35–44. doi:10.1007/978-1-62703-

640-5.

de Klerk, Eleonora, and Peter A C 't Hoen. 2015. "Alternative mRNA Transcription, Processing, and Translation: Insights from RNA Sequencing." *Trends in Genetics* 31 (3). Elsevier Ltd: 128–39. doi:10.1016/j.tig.2015.01.001.

De Klerk, Eleonora, Andrea Venema, S. Yahya Anvar, Jelle J. Goeman, OuHua Hu, Capucine Trollet, George Dickson, et al. 2012. "Poly(A) Binding Protein Nuclear 1 Levels Affect Alternative Polyadenylation." *Nucleic Acids Research* 40 (18): 9089–9101. doi:10.1093/nar/gks655.

De Leeuw, Frederic, Tong Zhang, Corinne Wauquier, Georges Huez, Véronique Kruys, and Cyril Gueydan. 2007. "The Cold-Inducible RNA-Binding Protein Migrates from the Nucleus to Cytoplasmic Stress Granules by a Methylation-Dependent Mechanism and Acts as a Translational Repressor." *Experimental Cell Research* 313 (20): 4130–44. doi:10.1016/j.yexcr.2007.09.017.

Decker, Carolyn J, and Roy Parker. 2012. "P-Bodies and Stress Granules: Possible Roles in the Control of Translation and mRNA Degradation." *Cold Spring Harbor Perspectives in Biology*.

Dehay, Benjamin, Jordi Bové, Natalia Rodríguez-Muela, Celine Perier, Ariadna Recasens, Patricia Boya, and Miquel Vila. 2010. "Pathogenic Lysosomal Depletion in Parkinson's Disease." *The Journal of Neuroscience : The Official Journal of the Society for Neuroscience* 30 (37): 12535–44. doi:10.1523/JNEUROSCI.1920-10.2010.

Demaria, Christine T., and Gary Brewer. 1996. "AUF1 Binding Affinity to A+U-Rich Elements Correlates with Rapid mRNA Degradation." *Journal of Biological Chemistry* 271 (21): 12179–84. doi:10.1074/jbc.271.21.12179.

Dennissen, F. J A, N. Kholod, and F. W. van Leeuwen. 2012. "The Ubiquitin Proteasome System in Neurodegenerative Diseases: Culprit, Accomplice or Victim?" *Progress in Neurobiology* 96 (2). Elsevier Ltd: 190–207. doi:10.1016/j.pneurobio.2012.01.003.

Derti, Adnan, Philip Garrett-Engele, Kenzie D. MacIsaac, Richard C. Stevens, Shreedharan Sriram, Ronghua Chen, Carol A. Rohl, Jason M. Johnson, and Tomas Babak. 2012. "A Quantitative Atlas of Polyadenylation in Five Mammals." *Genome Research* 22 (6): 1173–83. doi:10.1101/gr.132563.111.

Desideri, Enrico, and L. Miguel Martins. 2012. "Mitochondrial Stress Signalling: HTRA2 and Parkinson's Disease." *International Journal of Cell Biology* 2012. doi:10.1155/2012/607929.

Di Giammartino, Dafne C., Kensei Nishida, and James L. Manley. 2011. "Mechanisms and Consequences of Alternative Polyadenylation." *Molecular Cell* 43 (6): 853–66. doi:10.1016/j.molcel.2011.08.017.Mechanisms.

Dickson, John R., Carla Kruse, Daniel R. Montagna, Bente Finsen, and Michael S. Wolfe. 2013. "Alternative Polyadenylation and miR-34 Family Members Regulate Tau Expression." *Journal of Neurochemistry* 127 (6): 739–49. doi:10.1111/jnc.12437.

Ding, Chunming, and Charles R Cantor. 2004. "Quantitative Analysis of Nucleic Acids--the Last Few Years of Progress." *Journal of Biochemistry and Molecular Biology* 37 (1): 1–10. doi:<ARTICLE_ID IdType=doi> [pii].

Djebali, Sarah, Carrie A. Davis, Angelika Merkel, and Thomas R. Gingeras. 2012. "Landscape of Transcription in Human Cells." *Nature* 489 (7414): 101–8. doi:10.1038/nature11233.Landscape.

Dominski, Zbigniew, and William F. Marzluff. 2007. "Formation of the 3' End of Histone mRNA: Getting Closer to the End." *Gene* 396 (2): 373–90. doi:10.1016/j.gene.2007.04.021.

Dresios, John, Armaz Aschrafi, Geoffrey C Owens, Peter W Vanderklish, Gerald M Edelman, and Vincent P Mauro. 2005. "Cold Stress-Induced Protein Rbm3 Binds 60S Ribosomal Subunits, Alters microRNA Levels, and Enhances Global Protein Synthesis." *Proceedings of the National Academy of Sciences of the United States of America* 102 (6): 1865–70. doi:10.1073/pnas.0409764102.

Dumitriu, Alexandra, Javad Golji, Adam T Labadorf, Benbo Gao, Thomas G Beach, Richard H

Myers, Kenneth A Longo, and Jeanne C Latourelle. 2016. “Integrative Analyses of Proteomics and RNA Transcriptomics Implicate Mitochondrial Processes, Protein Folding Pathways and GWAS Loci in Parkinson Disease.” *BMC Medical Genomics* 9. BMC Medical Genomics: 5. doi:10.1186/s12920-016-0164-y.

Eliscovich, Carolina, and Robert H Singer. 2017. “RNP Transport in Cell Biology: The Long and Winding Road.” *Current Opinion in Cell Biology* 45. Elsevier Ltd: 38–46. doi:10.1016/j.ceb.2017.02.008.

Elkon, Ran, Jarno Drost, Gijs van Haaften, Mathias Jenal, Mariette Schrier, Joachim a F Oude Vrielink, and Reuven Agami. 2012. “E2F Mediates Enhanced Alternative Polyadenylation in Proliferation.” *Genome Biology* 13 (7): R59. doi:10.1186/gb-2012-13-7-r59.

Eréndira Avendaño-Vázquez, S., Ashish Dhir, Sara Bembich, Emanuele Buratti, Nicholas Proudfoot, and Francisco E. Baralle. 2012. “Autoregulation of TDP-43 mRNA Levels Involves Interplay between Transcription, Splicing, and Alternative polyA Site Selection.” *Genes and Development* 26 (15): 1679–84. doi:10.1101/gad.194829.112.

Fabian, Marc Robert, Nahum Sonenberg, and Witold Filipowicz. 2010. “Regulation of mRNA Translation and Stability by microRNAs.” *Annual Review of Biochemistry* 79: 351–79. doi:10.1146/annurev-biochem-060308-103103.

Fähling, Michael. 2009. “Surviving Hypoxia by Modulation of mRNA Translation Rate.” *Journal of Cellular and Molecular Medicine* 13 (9 A): 2770–79. doi:10.1111/j.1582-4934.2009.00875.x.

Filograna, Roberta, Laura Civiero, Vanni Ferrari, Gaia Codolo, Elisa Greggio, Luigi Bubacco, Mariano Beltramini, and Marco Bisaglia. 2015. “Analysis of the Catecholaminergic Phenotype in Human SH-SY5Y and BE(2)-M17 Neuroblastoma Cell Lines upon Differentiation.” *PLoS ONE* 10 (8): 1–18. doi:10.1371/journal.pone.0136769.

Filosto, Massimiliano, Mauro Scarpelli, Maria Sofia Cotelli, Valentina Vielmi, Alice Todeschini, Valeria Gregorelli, Paola Tonin, Giuliano Tomelleri, and Alessandro Padovani. 2011. “The Role of Mitochondria in Neurodegenerative Diseases.” *Journal of Neurology* 258 (10): 1763–74. doi:10.1007/s00415-011-6104-z.

Flavell, Steven W., Tae Kyung Kim, Jesse M. Gray, David A. Harmin, Martin Hemberg, Elizabeth J. Hong, Eirene Markenscoff-Papadimitriou, Daniel M. Bear, and Michael E. Greenberg. 2008. “Genome-Wide Analysis of MEF2 Transcriptional Program Reveals Synaptic Target Genes and Neuronal Activity-Dependent Polyadenylation Site Selection.” *Neuron* 60 (6). Elsevier Ltd: 1022–38. doi:10.1016/j.neuron.2008.11.029.

Fountaine, T M, L L Venda, N Warrick, H C Christian, P Brundin, K M Channon, and R Wade-Martins. 2008. “The Effect of Alpha-Synuclein Knockdown on MPP plus Toxicity in Models of Human Neurons.” *European Journal of Neuroscience* 28 (12): 2459–73. doi:10.1111/j.1460-9568.2008.06527.x.The.

Fragkouli, Apostolia, and Epaminondas Doxakis. 2014. “miR-7 and miR-153 Protect Neurons against MPP(+)-Induced Cell Death via Upregulation of mTOR Pathway.” *Frontiers in Cellular Neuroscience* 8 (July): 182. doi:10.3389/fncel.2014.00182.

Friedman, Robin C., Kyle Kai How Farh, Christopher B. Burge, and David P. Bartel. 2009. “Most Mammalian mRNAs Are Conserved Targets of microRNAs.” *Genome Research* 19 (1): 92–105. doi:10.1101/gr.082701.108.

Fu, Yonggui, Yu Sun, Yuxin Li, Jie Li, Xingqiang Rao, Chong Chen, and Anlong Xu. 2011. “Differential Genome-Wide Profiling of Tandem 3’ UTRs among Human Breast Cancer and Normal Cells by High-Throughput Sequencing.” *Genome Research* 21: 741–47. doi:10.1101/gr.115295.110.21.

Fujita, Jun. 1999. “Cold Shock Response in Mammalian Cells.” *Journal of Molecular Microbiology and Biotechnology* 1 (2): 243–55.

Gaidatzis, Dimos, Erik van Nimwegen, Jean Hausser, and Mihaela Zavolan. 2007. “Inference of

miRNA Targets Using Evolutionary Conservation and Pathway Analysis." *BMC Bioinformatics* 8: 69. doi:10.1186/1471-2105-8-69.

Galbán, Stefanie, Yuki Kuwano, Rudolf Pullmann, Jennifer L Martindale, Hyeon Ho Kim, Ashish Lal, Kotb Abdelmohsen, et al. 2008. "RNA-Binding Proteins HuR and PTB Promote the Translation of Hypoxia-Inducible Factor 1alpha." *Molecular and Cellular Biology* 28 (1): 93–107. doi:10.1128/MCB.00973-07.

Gardner, Lawrence B. 2008. "Hypoxic Inhibition of Nonsense-Mediated RNA Decay Regulates Gene Expression and the Integrated Stress Response." *Molecular and Cellular Biology* 28 (11): 3729–41. doi:10.1128/MCB.02284-07.

Garland, Patrick, Shmma Quraishe, Pim French, and Vincent O'Connor. 2008. "Expression of the MAST Family of Serine/threonine Kinases." *Brain Research* 1195: 12–19. doi:10.1016/j.brainres.2007.12.027.

Gaynes, John A., Hideo Otsuna, Douglas S. Campbell, John P. Manfredi, Edward M. Levine, and Chi Bin Chien. 2015. "The RNA Binding Protein Igf2bp1 Is Required for Zebrafish RGC Axon Outgrowth in Vivo." *PLoS ONE* 10 (9): 1–20. doi:10.1371/journal.pone.0134751.

Ge, Zhiyun, Bao Lin Quek, Karen L. Beemon, and J. Robert Hogg. 2016. "Polypyrimidine Tract Binding Protein 1 Protects mRNAs from Recognition by the Nonsense-Mediated mRNA Decay Pathway." *eLife* 5 (JANUARY2016): 1–25. doi:10.7554/eLife.11155.001.

Geisberg, Joseph V., Zarmik Moqtaderi, Xiaochun Fan, Fatih Ozsolak, and Kevin Struhl. 2014. "Global Analysis of mRNA Isoform Half-Lives Reveals Stabilizing and Destabilizing Elements in Yeast." *Cell* 156 (4). Elsevier Inc.: 812–24. doi:10.1016/j.cell.2013.12.026.

Gennarino, Vincenzo A., Callison E. Alcott, Chun An Chen, Arindam Chaudhury, Madelyn A. Gillentine, Jill A. Rosenfeld, Sumit Parikh, et al. 2015. "NUDT21-Spanning CNVs Lead to Neuropsychiatric Disease and Altered MeCP2 Abundance via Alternative Polyadenylation." *eLife* 4: 1–13. doi:10.7554/eLife.10782.

Goedert, M., C. M. Wischik, R. A. Crowther, J. E. Walker, and A. Klug. 1988. "Cloning and Sequencing of the cDNA Encoding a Core Protein of the Paired Helical Filament of Alzheimer Disease: Identification as the Microtubule-Associated Protein Tau." *Proceedings of the National Academy of Sciences* 85 (11): 4051–55. doi:10.1073/pnas.85.11.4051.

Goldberg, a L. 2000. "Probing the Proteasome Pathway." *Nature Biotechnology* 18 (5): 494–96. doi:10.1038/75349.

Gomez-Santos, C, I Ferrer, J Reiriz, F Vinals, M Barrachina, and S Ambrosio. 2002. "MPP+ Increases Alpha-Synuclein Expression and ERK/MAP-Kinase Phosphorylation in Human Neuroblastoma SH-SY5Y Cells." *Brain Research* 935 (1–2): 32–39. doi:S0006899302024228 [pii].

Goodall, Emily F, Paul R Heath, Oliver Bandmann, Janine Kirby, and Pamela J Shaw. 2013. "Neuronal Dark Matter: The Emerging Role of microRNAs in Neurodegeneration." *Frontiers in Cellular Neuroscience* 7 (October): 178. doi:10.3389/fncel.2013.00178.

Gorospe, Myriam, Kumiko Tominaga, Xue Wu, Michael Fähling, and Mircea Ivan. 2011. "Post-Transcriptional Control of the Hypoxic Response by RNA-Binding Proteins and MicroRNAs." *Frontiers in Molecular Neuroscience* 4 (July): 7. doi:10.3389/fnmol.2011.00007.

Goss, Dixie J., and Frida E. Kleimann. 2013. "Poly(A) Binding Proteins - Are They All Created Equal?" *Wiley Interdisciplinary Reviews: RNA* 4 (2): 167–79. doi:10.1002/wrna.1151.Poly(A).

Gotic, Ivana, Saeed Omidi, Fabienne Fleury-Olela, Nacho Molina, Felix Naef, and Ueli Schibler. 2016. "Temperature Regulates Splicing Efficiency of the Cold-Inducible RNA-Binding Protein Gene Cirbp." *Genes and Development* 30 (17): 2005–17. doi:10.1101/gad.287094.116.

Graber, Joel H., Fathima I. Nazeer, Pei Chun Yeh, Jason N. Kuehner, Sneha Borikar, Derick Hoskinson, and Claire L. Moore. 2013. "DNA Damage Induces Targeted, Genome-Wide Variation of poly(A) Sites in Budding Yeast." *Genome Research* 23 (10): 1690–1703. doi:10.1101/gr.144964.112.

Grammatikakis, Ioannis, Kotb Abdelmohsen, and Myriam Gorospe. 2016. “Posttranslational Control of HuR Function.” *Wiley Interdisciplinary Reviews: RNA* 8 (February): 1–11. doi:10.1002/wrna.1372.

Grassi, Elena, Elisa Mariella, Antonio Lembo, Ivan Molineris, and Paolo Provero. 2016. “Roar: Detecting Alternative Polyadenylation with Standard mRNA Sequencing Libraries.” *BMC Bioinformatics* 17. BMC Bioinformatics: 1–9. doi:10.1186/s12859-016-1254-8.

Gruber, A R, G Martin, P Muller, A Schmidt, A J Gruber, R Gumienny, N Mittal, et al. 2014. “Global 3’ UTR Shortening Has a Limited Effect on Protein Abundance in Proliferating T Cells.” *Nat Commun* 5: 5465. doi:10.1038/ncomms6465.

Gruber, Andreas J., Ralf Schmidt, Andreas R. Gruber, Georges Martin, Souvik Ghosh, Manuel Belmadani, Walter Keller, and Mihaela Zavolan. 2016. “A Comprehensive Analysis of 3’ End Sequencing Data Sets Reveals Novel Polyadenylation Signals and the Repressive Role of Heterogeneous Ribonucleoprotein C on Cleavage and Polyadenylation.” *Genome Research* 26 (8): 1145–59. doi:10.1101/gr.202432.115.

Grzybowska, Ewa A. 2012. “Human Intronless Genes: Functional Groups, Associated Diseases, Evolution, and mRNA Processing in Absence of Splicing.” *Biochemical and Biophysical Research Communications* 424 (1). Elsevier Inc.: 1–6. doi:10.1016/j.bbrc.2012.06.092.

Gunderson, Samuel I, Maria Polycarpou-Schwarz, and Iain W Mattaj. 1998. “U1 snRNP Inhibits Pre-mRNA Polyadenylation through a Direct Interaction between U1 70K and Poly(A) Polymerase.” *Molecular Cell* 1 (2): 255–64. doi:10.1016/S1097-2765(00)80026-X.

Gupta, Ishaan, Sandra Clauder-Munster, Bernd Klaus, Aino I Järvelin, Raeka S Aiyar, Vladimir Benes, Stefan Wilkening, Wolfgang Huber, Vicent Pelechano, and Lars M Steinmetz. 2014. “Alternative Polyadenylation Diversifies Post-Transcriptional Regulation by Selective RNA – Protein Interactions.” *Molecular Systems Biology* 10 (719): 1–11.

Gupta, Shobhit, John A Stamatoyannopoulos, Timothy L Bailey, and William Stafford Noble. 2007. “Quantifying Similarity between Motifs.” *Genome Biology* 8 (2): R24. doi:10.1186/gb-2007-8-2-r24.

Hall-Pogar, Tyra, Haibo Zhang, Bin Tian, and Carol S. Lutz. 2005. “Alternative Polyadenylation of Cyclooxygenase-2.” *Nucleic Acids Research* 33 (8): 2565–79. doi:10.1093/nar/gki544.

Han, Tina W., Masato Kato, Shanhai Xie, Leeju C. Wu, Hamid Mirzaei, Jimin Pei, Min Chen, et al. 2012. “Cell-Free Formation of RNA Granules: Bound RNAs Identify Features and Components of Cellular Assemblies.” *Cell* 149 (4). Elsevier Inc.: 768–79. doi:10.1016/j.cell.2012.04.016.

Harrison, Paul F, David R Powell, Jennifer L Clancy, Thomas Preiss, Peter R Boag, Ana N A Traven, Torsten Seemann, and Traude H Beilharz. 2015. “PAT-Seq : A Method to Study the Integration of 3’ -UTR Dynamics with Gene Expression in the Eukaryotic Transcriptome.” *Rna* 21 (8): 1502–10. doi:10.1261/rna.048355.114.

Hekkila, Richard E., Lawrence Manzino, Felicitas S. Cabbat, and Roger C. Duvoisin. 1984. “Protection against the Dopaminergic Neurotoxicity of 1-Methyl-4-Phenyl-1,2,5,6-Tetrahydropyridine by Monoamine Oxidase Inhibitors.” *Nature* 308 (22): 339.

Hoffman, Yonit, Debora Rosa Bublik, Alejandro P. Ugalde, Ran Elkon, Tammy Biniashvili, Reuven Agami, Moshe Oren, and Yitzhak Pilpel. 2016. “3’UTR Shortening Potentiates MicroRNA-Based Repression of Pro-Differentiation Genes in Proliferating Human Cells.” *PLoS Genetics* 12 (2): 1–15. doi:10.1371/journal.pgen.1005879.

Hofmann, Sarah, Valeria Cherkasova, Peter Bankhead, Bernd Bukau, and Georg Stoecklin. 2012. “Translation Suppression Promotes Stress Granule Formation and Cell Survival in Response to Cold Shock.” *Molecular Biology of the Cell* 23 (19): 3786–3800. doi:10.1091/mbc.E12-04-0296.

Hogg, J. Robert, and Stephen P. Goff. 2010. “Upf1 Senses 3’UTR Length to Potentiate mRNA Decay.” *Cell* 143 (3). Elsevier Inc.: 379–89. doi:10.1016/j.cell.2010.10.005.

Hollerer, Ina, Tomaz Curk, Bettina Haase, Vladimir Benes, Christian Hauer, Gabriele Neu-Yilik,

Madhuri Bhuvanagiri, Matthias W Hentze, and Andreas E Kulozik. 2016. “The Differential Expression of Alternatively Polyadenylated Transcripts Is a Common Stress-Induced Response Mechanism That Modulates Mammalian mRNA Expression in a Quantitative and Qualitative Fashion.” *RNA (New York, N.Y.)* 22 (9): 1441–53. doi:10.1261/rna.055657.115.

Hoozemans, Jeroen J M, and Wiep Scheper. 2012. “Endoplasmic Reticulum: The Unfolded Protein Response Is Tangled in Neurodegeneration.” *International Journal of Biochemistry and Cell Biology* 44 (8). Elsevier Ltd: 1295–98. doi:10.1016/j.biocel.2012.04.023.

Hoque, Mainul, Zhe Ji, Dinghai Zheng, Wenting Luo, Wencheng Li, Bei You, Ji Yeon Park, Ghassan Yehia, and Bin Tian. 2013. “Analysis of Alternative Cleavage and Polyadenylation by 3’ Region Extraction and Deep Sequencing.” *Nature Methods* 10 (2): 133–39. doi:10.1038/nmeth.2288.

Hossini, Amir M, Matthias Megges, Alessandro Prigione, Bjoern Lichtner, Mohammad R Toliat, Wasco Wruck, Friederike Schröter, et al. 2015. “Induced Pluripotent Stem Cell-Derived Neuronal Cells from a Sporadic Alzheimer’s Disease Donor as a Model for Investigating AD-Associated Gene Regulatory Networks.” *BMC Genomics* 16 (1): 84. doi:10.1186/s12864-015-1262-5.

Hu, Benxia, Xin Li, Yongxia Huo, Yafen Yu, Qiuping Zhang, Guijun Chen, Yaping Zhang, Nigel W. Fraser, Dongdong Wu, and Jumin Zhou. 2016. “Cellular Responses to HSV-1 Infection Are Linked to Specific Types of Alterations in the Host Transcriptome.” *Scientific Reports* 6 (May). Nature Publishing Group: 28075. doi:10.1038/srep28075.

Hu, Wenchao, Yuting Liu, and Jun Yan. 2014. “Microarray Meta-Analysis of RNA-Binding Protein Functions in Alternative Polyadenylation.” *PLoS ONE* 9 (3). doi:10.1371/journal.pone.0090774.

Hu, Wenyan, Shengguo Li, Ji Yeon Park, Sridhar Boppana, Ting Ni, Miaoxin Li, Jun Zhu, Bin Tian, Zhi Xie, and Mengqing Xiang. 2017. “Dynamic Landscape of Alternative Polyadenylation during Retinal Development.” *Cellular and Molecular Life Sciences* 74 (9). Springer International Publishing: 1721–39. doi:10.1007/s00018-016-2429-1.

Huang, Huan, Jiao Chen, Hongde Liu, and Xiao Sun. 2013. “The Nucleosome Regulates the Usage of Polyadenylation Sites in the Human Genome.” *BMC Genomics* 14 (1): 912. doi:10.1186/1471-2164-14-912.

Hung, Kai Chih, Hui Ju Huang, Ming Wei Lin, Yen Ping Lei, and Anya Maan Yuh Lin. 2014. “Roles of Autophagy in MPP+-Induced Neurotoxicity in Vivo: The Involvement of Mitochondria and ??-Synuclein Aggregation.” *PLoS ONE* 9 (3): 1–9. doi:10.1371/journal.pone.0091074.

Hwang, Hun Way, Christopher Y. Park, Hani Goodarzi, John J. Fak, Aldo Mele, Michael J. Moore, Yuhki Saito, and Robert B. Darnell. 2016. “PAPERCLIP Identifies MicroRNA Targets and a Role of CstF64/64tau in Promoting Non-Canonical poly(A) Site Usage.” Journal Article. *Cell Reports* 15 (2): 423–35. doi:10.1016/j.celrep.2016.03.023.

Hyttinen, Juha M T, Minna Niittykoski, Antero Salminen, and Kai Kaarniranta. 2013. “Maturation of Autophagosomes and Endosomes: A Key Role for Rab7.” *Biochimica et Biophysica Acta - Molecular Cell Research* 1833 (3). Elsevier B.V.: 503–10. doi:10.1016/j.bbamcr.2012.11.018.

Itoh, Kie, Ken Nakamura, Miho Iijima, and Hiromi Sesaki. 2013. “Mitochondrial Dynamics in Neurodegeneration.” *Trends in Cell Biology* 23 (2): 64–71. doi:10.1016/j.tcb.2012.10.006.

Iurlaro, Raffaella, Franziska Püschel, Clara Lucía León-Annicchiarico, Hazel O’Connor, Seamus J. Martin, Daniel Palou-Gramón, Estefanía Lucendo, and Cristina Muñoz-Pinedo. 2017. “Glucose Deprivation Induces ATF4-Mediated Apoptosis through TRAIL Death Receptors.” *Molecular and Cellular Biology*, no. February: MCB.00479-16. doi:10.1128/MCB.00479-16.

Ivanovic, Zoran. 2009. “Hypoxia or in Situ Normoxia: The Stem Cell Paradigm.” *Journal of Cellular Physiology* 219 (2): 271–75. doi:10.1002/jcp.21690.

Jackson, T. C., M. D. Manole, S. E. Kotermanski, E. K. Jackson, R. S B Clark, and P. M. Kochanek. 2015. “Cold Stress Protein RBM3 Responds to Temperature Change in an Ultra-Sensitive Manner in Young Neurons.” *Neuroscience* 305. IBRO: 268–78.

doi:10.1016/j.neuroscience.2015.08.012.

Jan, Calvin H., Robin C. Friedman, J. Graham Ruby, and David P. Bartel. 2011. "Formation, Regulation and Evolution of Caenorhabditis Elegans 3'UTRs." *Nature* 469 (7328). Nature Publishing Group: 97–101. doi:10.1038/nature09616.

Jara, Javier H., Bariş Genç, Gregory A. Cox, Martha C. Bohn, Raymond P. Roos, Jeffrey D. Macklis, Emel Ulupinar, and P. Hande Özdinler. 2015. "Corticospinal Motor Neurons Are Susceptible to Increased ER Stress and Display Profound Degeneration in the Absence of UCHL1 Function." *Cerebral Cortex* 25 (11): 4259–72. doi:10.1093/cercor/bhu318.

Jenal, Mathias, Ran Elkon, Fabricio Loayza-Puch, Gijs Van Haaften, Uwe K??hn, Fiona M. Menzies, Joachim A F Oude Vrielink, et al. 2012. "The poly(A)-Binding Protein Nuclear 1 Suppresses Alternative Cleavage and Polyadenylation Sites." *Cell* 149 (3): 538–53. doi:10.1016/j.cell.2012.03.022.

Ji, X, J Wan, M Vishnu, Y Xing, and S A Liebhaber. 2013. "alphaCP Poly(C) Binding Proteins Act as Global Regulators of Alternative Polyadenylation." *Mol Cell Biol* 33 (13): 2560–73. doi:10.1128/MCB.01380-12.

Ji, Z, W Luo, W Li, M Hoque, Z Pan, Y Zhao, and B Tian. 2011. "Transcriptional Activity Regulates Alternative Cleavage and Polyadenylation." *Mol Syst Biol* 7 (534). Nature Publishing Group: 534. doi:10.1038/msb.2011.69.

Ji, Zhe, Ju Youn Lee, Zhenhua Pan, Bingjun Jiang, and Bin Tian. 2009. "Progressive Lengthening of 3' Untranslated Regions of mRNAs by Alternative Polyadenylation during Mouse Embryonic Development." *Proceedings of the National Academy of Sciences* 106 (23): 9535–9535. doi:10.1073/pnas.0905246106.

Ji, Zhe, W Luo, Wenghen Li, Mainul Hoque, Z Pan, Y Zhao, and Bin Tian. 2011. "Transcriptional Activity Regulates Alternative Cleavage and Polyadenylation." *Mol Syst Biol* 7 (534). Nature Publishing Group: 534. doi:10.1038/msb.2011.69.

Ji, Zhe, and Bin Tian. 2009. "Reprogramming of 3' Untranslated Regions of mRNAs by Alternative Polyadenylation in Generation of Pluripotent Stem Cells from Different Cell Types." *PloS One* 4 (12): e8419. doi:10.1371/journal.pone.0008419.

Jia, Xin, Shaochun Yuan, Yao Wang, Yonggui Fu, Yong Ge, Yutong Ge, Xihong Lan, et al. 2017. "The Role of Alternative Polyadenylation in the Antiviral Innate Immune Response." *Nature Communications* 8. Nature Publishing Group: 14605. doi:10.1038/ncomms14605.

Jin, Seok Min, and Richard J. Youle. 2013. "The Accumulation of Misfolded Proteins in the Mitochondrial Matrix Is Sensed by PINK1 to Induce PARK2/Parkin-Mediated Mitophagy of Polarized Mitochondria." *Autophagy* 9 (11): 1750–57. doi:10.4161/auto.26122.

Jögi, Annika, Johan Vallon-Christersson, Linda Holmquist, Håkan Axelson, Åke˚ Borg, and Sven Påhlman. 2004. "Human Neuroblastoma Cells Exposed to Hypoxia: Induction of Genes Associated with Growth, Survival, and Aggressive Behavior." *Experimental Cell Research* 295 (2): 469–87. doi:10.1016/j.yexcr.2004.01.013.

Kaida, Daisuke, Michael G Berg, Ihab Younis, Mumtaz Kasim, Larry N Singh, Lili Wan, and Gideon Dreyfuss. 2010. "U1 snRNP Protects Pre-mRNAs from Premature Cleavage and Polyadenylation." *Nature* 468 (7324). Nature Publishing Group: 664–68. doi:10.1038/nature09479.

Kalivendi, Shasi V., Sonya Cunningham, Srigiridhar Kotamraju, Joy Joseph, Cecilia J. Hillard, and B. Kalyanaraman. 2004. "Alpha-Synuclein up-Regulation and Aggregation during MPP +-Induced Apoptosis in Neuroblastoma Cells." *Journal of Biological Chemistry* 279 (15): 15240–47. doi:10.1074/jbc.M312497200.

Kalivendi, Shasi V., Deepthi Yedlapudi, Cecilia J. Hillard, and B. Kalyanaraman. 2010. "Oxidants Induce Alternative Splicing of Alpha-Synuclein: Implications for Parkinson's Disease." *Free Radical Biology and Medicine* 48 (3). Elsevier B.V.: 377–83.

doi:10.1016/j.freeradbiomed.2009.10.045.

Kalivendi, Shasi V, Srigiridhar Kotamraju, Sonya Cunningham, Tiesong Shang, Cecilia J Hillard, and B Kalyanaraman. 2003. "1-Methyl-4-Phenylpyridinium (MPP+)-Induced Apoptosis and Mitochondrial Oxidant Generation: Role of Transferrin-Receptor-Dependent Iron and Hydrogen Peroxide." *Biochemical Journal* 371: 151–64.

Kanagaraj, N., H. Beiping, S. T. Dheen, and S. S W Tay. 2014. "Downregulation of miR-124 in MPTP-Treated Mouse Model of Parkinson's Disease and MPP Iodide-Treated MN9D Cells Modulates the Expression of the calpain/cdk5 Pathway Proteins." *Neuroscience* 272. IBRO: 167–79. doi:10.1016/j.neuroscience.2014.04.039.

Kapeli, Katannya, Gabriel A Pratt, Anthony Q Vu, Kasey R Hutt, Fernando J Martinez, Balaji Sundararaman, Ranjan Batra, et al. 2016. "Distinct and Shared Functions of ALS-Associated Proteins TDP-43, FUS and TAF15 Revealed by Multisystem Analyses." *Nature Communications* 7. Nature Publishing Group: 12143. doi:10.1038/ncomms12143.

Katz, Yarden, Eric T Wang, Edoardo M Airoldi, and Christopher B Burge. 2010. "Analysis and Design of RNA Sequencing Experiments for Identifying Isoform Regulation." *Nature Methods* 7 (12): 1009–15. doi:10.1038/nmeth.1528.

Keane, Harriet, Brent J Ryan, Brendan Jackson, Alan Whitmore, and Richard Wade-Martins. 2015. "Protein-Protein Interaction Networks Identify Targets Which Rescue the MPP+ Cellular Model of Parkinson's Disease." *Scientific Reports* 5. Nature Publishing Group: 17004. doi:10.1038/srep17004.

Kedersha, N, and P Anderson. 2002. "Stress Granules: Sites of mRNA Triage That Regulate mRNA Stability and Translatability." *Biochemical Society Transactions* 30 (Pt 6): 963–69. doi:10.1042/BST0300963.

Kedersha, Nancy, Pavel Ivanov, and Paul Anderson. 2013. "Stress Granules and Cell Signaling: More than Just a Passing Phase?" *Trends in Biochemical Sciences* 38 (10). Elsevier Ltd: 494–506. doi:10.1016/j.tibs.2013.07.004.

Kenny, Phillip J, Hongjun Zhou, Miri Kim, Geena Skariah, Radhika S Khetani, Jenny Drnevich, Mary Luz Arcila, Kenneth S Kosik, and Stephanie Ceman. 2014. "MOV10 and FMRP Regulate AGO2 Association with microRNA Recognition Elements." *Cell Reports* 9 (5): 1729–41. doi:10.1016/j.celrep.2014.10.054.MOV10.

Kim-Han, Jeong Sook, Jo Ann Antenor-Dorsey, and Karen L. O'Malley. 2011. "The Parkinsonian Mimetic, MPP+ , Specifically Impairs Mitochondrial Transport in Dopamine Axons." *Journal of Neuroscience* 31 (9): 7212–21. doi:10.1038/jid.2014.371.

Kim, Jongpil, Keiichi Inoue, Jennifer Ishii, William B Vanti, Sergey V Voronov, Elizabeth Murchison, Gregory Hannon, and Asa Abeliovich. 2007. "A MicroRNA Feedback Circuit in Midbrain Dopamine Neurons." *Science (New York, N.Y.)* 317 (5842): 1220–24. doi:10.1126/science.1140481.

Kim, Jungsu, Jacob M. Basak, and David M. Holtzman. 2009. "The Role of Apolipoprotein E in Alzheimer's Disease." *Neuron* 63 (3). Elsevier Inc.: 287–303. doi:10.1016/j.neuron.2009.06.026.

Kim, Min Hyeok, Bo Hyun You, and Jin Wu Nam. 2015. "Global Estimation of the 3' Untranslated Region Landscape Using RNA Sequencing." *Methods* 83. Elsevier Inc.: 111–17. doi:10.1016/j.ymeth.2015.04.011.

Kim, S N, S G Kim, S D Park, Y S Cho-Chung, and S H Hong. 2000. "Participation of Type II Protein Kinase A in the Retinoic Acid-Induced Growth Inhibition of SH-SY5Y Human Neuroblastoma Cells." *Journal of Cellular Physiology* 182 (3): 421–28. doi:10.1002/(SICI)1097-4652(200003)182:3<421::AID-JCP13>3.0.CO;2-2.

Kitamura, Y, T Kosaka, J I Kakimura, Y Matsuoka, Y Kohno, Y Nomura, and T Taniguchi. 1998. "Protective Effects of the Antiparkinsonian Drugs Talipexole and Pramipexole against 1-Methyl-4-Phenylpyridinium-Induced Apoptotic Death in Human Neuroblastoma SH-SY5Y Cells."

Molecular Pharmacology 54 (6): 1046–54. doi:10.1124/mol.54.6.1046.

Knight, John Rp P, Amandine Bastide, Anne Roobol, Jo Roobol, Thomas John Jackson, Wahyu Utami, David A Barrett, C Mark Smales, and Anne E Willis. 2015. "Eukaryotic Elongation Factor 2 Kinase Regulates the Cold Stress Response by Slowing Translation Elongation." *The Biochemical Journal* 465 (2): 227–38. doi:10.1042/BJ20141014.

Koyama, Akihide, Akihiro Sugai, Taisuke Kato, Tomohiko Ishihara, Atsushi Shiga, Yasuko Toyoshima, Misaki Koyama, et al. 2016. "Increased Cytoplasmic TARDBP mRNA in Affected Spinal Motor Neurons in ALS Caused by Abnormal Autoregulation of TDP-43." *Nucleic Acids Research* 44 (12): 5820–36. doi:10.1093/nar/gkw499.

Kraynik, Stephen M., Andrew Gabanic, Sarah R. Anthony, Melissa Kelley, Waltke R. Paulding, Anne Roessler, Michael McGuinness, and Michael Tranter. 2015. "The Stress-Induced Heat Shock Protein 70.3 Expression Is Regulated by a Dual-Component Mechanism Involving Alternative Polyadenylation and HuR." *Biochimica et Biophysica Acta - Gene Regulatory Mechanisms* 1849 (6). Elsevier B.V.: 688–96. doi:10.1016/j.bbagrm.2015.02.004.

Krug, A. K., Simon Gutbier, L. Zhao, D. Pöltl, C. Kullmann, V. Ivanova, S. Förster, et al. 2014. "Transcriptional and Metabolic Adaptation of Human Neurons to the Mitochondrial Toxicant MPP(+)." *Cell Death & Disease* 5: e1222. doi:10.1038/cddis.2014.166.

Kulshreshtha, R., M. Ferracin, S. E. Wojcik, R. Garzon, H. Alder, F. J. Agosto-Perez, R. Davuluri, et al. 2006. "A MicroRNA Signature of Hypoxia." *Molecular and Cellular Biology* 27 (5): 1859–67. doi:10.1128/MCB.01395-06.

Kulshreshtha, R, R V Davuluri, G a Calin, and M Ivan. 2008. "A microRNA Component of the Hypoxic Response." *Cell Death and Differentiation* 15 (4): 667–71. doi:10.1038/sj.cdd.4402310.

Lackford, Brad, Chengguo Yao, Georgette M. Charles, Lingjie Weng, Xiaofeng Zheng, Eun A. Choi, Xiaohui Xie, et al. 2014. "Fip1 Regulates mRNA Alternative Polyadenylation to Promote Stem Cell Self-Renewal." *EMBO Journal* 33 (8): 878–89. doi:10.1002/embj.201386537.

Lau, Pierre, Koen Bossers, Rekin's Janky, Evgenia Salta, Carlo Sala Frigerio, Shahar Barbash, Roy Rothman, et al. 2013. "Alteration of the microRNA Network during the Progression of Alzheimer's Disease." *EMBO Molecular Medicine* 5 (10): 1613–34. doi:10.1002/emmm.201201974.

Lee, Dae Hee, Cuk Seong Kim, and Yong J. Lee. 2011. "Astaxanthin Protects against MPTP/MPP+-Induced Mitochondrial Dysfunction and ROS Production in Vivo and in Vitro." *Food and Chemical Toxicology* 49 (1). Elsevier Ltd: 271–80. doi:10.1016/j.fct.2010.10.029.

Legendre, Matthieu, William Ritchie, Fabrice Lopez, and Daniel Gautheret. 2006. "Differential Repression of Alternative Transcripts: A Screen for miRNA Targets." *PLoS Computational Biology* 2 (5): 333–42. doi:10.1371/journal.pcbi.0020043.

Lejeune, Fabrice, and Lynne E. Maquat. 2005. "Mechanistic Links between Nonsense-Mediated mRNA Decay and Pre-mRNA Splicing in Mammalian Cells." *Current Opinion in Cell Biology* 17 (3): 309–15. doi:10.1016/j.ceb.2005.03.002.

Levine, Beth, Noboru Mizushima, and Herbert W Virgin. 2011. "Autophagy in Immunity and Inflammation." *Nature* 469 (7330): 323–35. doi:10.1038/nature09782.

Lewis, Joe D, and Elisa Izaurralde. 1997. "The Role of the Cap Structure in RNA Processing and Nuclear Export." *European Journal of Biochemistry* 247 (2): 461–69. doi:10.1111/j.1432-1033.1997.00461.x.

Li, Wencheng, Ji Yeon Park, Dinghai Zheng, Mainul Hoque, Ghassan Yehia, and Bin Tian. 2016. "Alternative Cleavage and Polyadenylation in Spermatogenesis Connects Chromatin Regulation with Post-Transcriptional Control." *BMC Biol* 14. BMC Biology: 6. doi:10.1186/s12915-016-0229-6.

Li, Wencheng, Bei You, Mainul Hoque, Dinghai Zheng, Wenting Luo, Zhe Ji, Ji Yeon Park, et al. 2015. "Systematic Profiling of Poly(A)+ Transcripts Modulated by Core 3' End Processing and

Splicing Factors Reveals Regulatory Rules of Alternative Cleavage and Polyadenylation." *PLoS Genetics* 11 (4): 1–28. doi:10.1371/journal.pgen.1005166.

Li, Zhonghan, and Tariq M. Rana. 2014. "Therapeutic Targeting of microRNAs: Current Status and Future Challenges." *Nature Reviews Drug Discovery* 13 (8). Nature Publishing Group: 622–38. doi:10.1038/nrd4359.

Lianoglou, Steve, Vidur Garg, Julie L. Yang, Christina S. Leslie, and Christine Mayr. 2013. "Ubiquitously Transcribed Genes Use Alternative Polyadenylation to Achieve Tissue-Specific Expression." *Genes and Development* 27 (21): 2380–96. doi:10.1101/gad.229328.113.

Liaw, Hao Han, Chen Ching Lin, Hsueh Fen Juan, and Hsuan Cheng Huang. 2013. "Differential MicroRNA Regulation Correlates with Alternative Polyadenylation Pattern between Breast Cancer and Normal Cells." *PLoS ONE* 8 (2): e56958. doi:10.1371/journal.pone.0056958.

Licatalosi, Donny D, and Robert B Darnell. 2010. "RNA Processing and Its Regulation: Global Insights into Biological Networks." *Nature Reviews. Genetics* 11 (1). Nature Publishing Group: 75–87. doi:10.1038/nrg2673.

Licatalosi, Donny D, Aldo Mele, John J Fak, Jernej Ule, Melis Kayikci, Sung Wook Chi, Tyson a Clark, et al. 2008. "HITS-CLIP Yields Genome-Wide Insights into Brain Alternative RNA Processing." *Nature* 456 (November): 464–69. doi:10.1038/nature07488.

Lim, Maria L R, Linda D Mercer, Phillip Nagley, and Philip M Beart. 2007. "Rotenone and MPP+ Preferentially Redistribute Apoptosis-Inducing Factor in Apoptotic Dopamine Neurons." *Neuroreport* 18 (4): 307–12. doi:10.1097/WNR.0b013e32801b3ca6.

Liu, Chen Geng, Jin Ling Wang, Lei Li, Li Xiang Xue, Yue Qi Zhang, and Pei Chang Wang. 2014. "MicroRNA-135a and -200b, Potential Biomarkers for Alzheimer's Disease, Regulate ?? Secretase and Amyloid Precursor Protein." *Brain Research* 1583 (1). Elsevier: 55–64. doi:10.1016/j.brainres.2014.04.026.

Liu, Jun Ping, Ying Tang, Shufeng Zhou, Ban Hock Toh, Catriona McLean, and He Li. 2010. "Cholesterol Involvement in the Pathogenesis of Neurodegenerative Diseases." *Molecular and Cellular Neuroscience* 43 (1). Elsevier Inc.: 33–42. doi:10.1016/j.mcn.2009.07.013.

Liu, Y, W Hu, Y Murakawa, J Yin, G Wang, M Landthaler, and J Yan. 2013. "Cold-Induced RNA-Binding Proteins Regulate Circadian Gene Expression by Controlling Alternative Polyadenylation." *Sci Rep* 3: 2054. doi:10.1038/srep02054.

Liu, Yichin, Lara Fallon, Hilal A. Lashuel, Zhihua Liu, and Peter Lansbury. 2002. "The UCH-L1 Gene Encodes Two Opposing Enzymatic Activities That Affect a-Synuclein Degradation and Parkinson's Disease Susceptibility." *Cell* 111: 209–18. doi:S0092867402010127 [pii].

Ljungman, Mats. 2007. "The Transcription Stress Response." *Cell Cycle* 6 (18): 2252–57. doi:10.4161/cc.6.18.4751.

Lleonart, M. E. 2010. "A New Generation of Proto-Oncogenes: Cold-Inducible RNA Binding Proteins." *Biochimica et Biophysica Acta - Reviews on Cancer* 1805 (1). Elsevier B.V.: 43–52. doi:10.1016/j.bbcan.2009.11.001.

Long, J. M., B. Ray, and D. K. Lahiri. 2012. "MicroRNA-153 Physiologically Inhibits Expression of Amyloid- Precursor Protein in Cultured Human Fetal Brain Cells and Is Dysregulated in a Subset of Alzheimer Disease Patients." *Journal of Biological Chemistry* 287 (37): 31298–310. doi:10.1074/jbc.M112.366336.

Lotharius, Julie, and Karen L. O'Malley. 2000. "The Parkinsonism-Inducing Drug 1-Methyl-4-Phenylpyridinium Triggers Intracellular Dopamine Oxidation: A Novel Mechanism of Toxicity." *Journal of Biological Chemistry* 275 (49): 38581–88. doi:10.1074/jbc.M005385200.

Loya, a D I, Lilach Pnueli, Yahav Yosefzon, Y D O Wexler, and Michal Ziv-ukelson. 2008. "The 3' -UTR Mediates the Cellular Localization of an mRNA Encoding a Short Plasma Membrane Protein." *Spring* 14: 1352–65. doi:10.1261/rna.867208.4.

Lukiw, Walter J. 2007. "Micro-RNA Speciation in Fetal, Adult and Alzheimer's Disease

Hippocampus." *Neuroreport* 18 (3): 297–300. doi:10.1097/WNR.0b013e3280148e8b.

Lukiw, Walter J., and Nicolas G. Bazan. 1997. "Cyclooxygenase 2 RNA Message Abundance, Stability, and Hypervariability in Sporadic Alzheimer Neocortex." *Journal of Neuroscience Research* 50 (6): 937–45. doi:10.1002/(SICI)1097-4547(19971215)50:6<937::AID-JNR4>3.0.CO;2-E.

Lundblad, Martin, Mickael Decressac, Bengt Mattsson, and Anders Björklund. 2012. "Impaired Neurotransmission Caused by Overexpression of α-Synuclein in Nigral Dopamine Neurons." *Proceedings of the National Academy of Sciences of the United States of America* 109 (9): 3213–19. doi:10.1073/pnas.1200575109.

Luo, Wenting, Zhe Ji, Zhenhua Pan, Bei You, Mainul Hoque, Wencheng Li, Samuel I. Gunderson, and Bin Tian. 2013. "The Conserved Intronic Cleavage and Polyadenylation Site of CstF-77 Gene Imparts Control of 3′ End Processing Activity through Feedback Autoregulation and by U1 snRNP." *PLoS Genetics* 9 (7): 1–14. doi:10.1371/journal.pgen.1003613.

MacDonald, Clinton C., and K. Wyatt McMahon. 2010. "Tissue-Specific Mechanisms of Alternative Polyadenylation: Testis, Brain, and beyond." *Wiley Interdisciplinary Reviews: RNA* 1 (3): 494–501. doi:10.1002/wrna.29.

Maden, M. 2007. "Retinoic Acid in the Development, Regeneration and Maintenance of the Nervous System." *Nature Reviews. Neuroscience* 8 (10): 755–65. doi:10.1038/nrn2212.

Magistri, Marco, Dmitry Velmeshev, Madina Makhmutova, and Mohammad Ali Faghihi. 2015. "Transcriptomics Profiling of Alzheimer's Disease Reveal Neurovascular Defects, Altered Amyloid-β Homeostasis, and Deregulated Expression of Long Noncoding RNAs." *Journal of Alzheimer's Disease* 48 (3): 647–65. doi:10.3233/JAD-150398.

Makeyev, Eugene V., Jiangwen Zhang, Monica A. Carrasco, and Tom Maniatis. 2007. "The MicroRNA miR-124 Promotes Neuronal Differentiation by Triggering Brain-Specific Alternative Pre-mRNA Splicing." *Molecular Cell* 27 (3): 435–48. doi:10.1016/j.molcel.2007.07.015.The.

Mandel, Corey R, Syuzo Kaneko, Hailong Zhang, Damara Gebauer, Vasupradha Vethantham, James L Manley, and Liang Tong. 2006. "Polyadenylation Factor CPSF-73 Is the Pre-mRNA 3'-end-Processing Endonuclease." *Nature* 444 (7121): 953–56. doi:10.1038/nature05363.

Mangone, M., A. P. Manoharan, D. Thierry-Mieg, J. Thierry-Mieg, T. Han, S. D. Mackowiak, E. Mis, et al. 2010. "The Landscape of C. Elegans 3'UTRs." *Science* 329 (5990): 432–35. doi:10.1126/science.1191244.

Mansfield, Kyle D., and Jack D. Keene. 2012. "Neuron-Specific ELAV/Hu Proteins Suppress HuR mRNA during Neuronal Differentiation by Alternative Polyadenylation." *Nucleic Acids Research* 40 (6): 2734–46. doi:10.1093/nar/gkr1114.

Marambio, Paola, Barbra Toro, Carlos Sanhueza, Rodrigo Troncoso, Valentina Parra, Hugo Verdejo, Lorena García, et al. 2010. "Glucose Deprivation Causes Oxidative Stress and Stimulates Aggresome Formation and Autophagy in Cultured Cardiac Myocytes." *Biochimica et Biophysica Acta - Molecular Basis of Disease* 1802 (6). Elsevier B.V.: 509–18. doi:10.1016/j.bbadis.2010.02.002.

Marc, Philippe, Antoine Margeot, Frédéric Devaux, Corrine Blugeon, Marisol Corral-Debrinski, and Claude Jacq. 2002. "Genome-Wide Analysis of mRNAs Targeted to Yeast Mitochondria." *EMBO Reports* 3 (2): 159–64. doi:10.1093/embo-reports/kvf025.

Martin, Georges, Andreas R. Gruber, Walter Keller, and Mihaela Zavolan. 2012. "Genome-Wide Analysis of Pre-mRNA 3' End Processing Reveals a Decisive Role of Human Cleavage Factor I in the Regulation of 3' UTR Length." *Cell Reports* 1 (6). The Authors: 753–63. doi:10.1016/j.celrep.2012.05.003.

Martinez, Fernando J., Gabriel A. Pratt, Eric L. Van Nostrand, Ranjan Batra, Stephanie C. Huelga, Katannya Kapeli, Peter Freese, et al. 2016. "Protein-RNA Networks Regulated by Normal and ALS-Associated Mutant HNRNPA2B1 in the Nervous System." *Neuron* 92 (4). Elsevier Inc.:

780–95. doi:10.1016/j.neuron.2016.09.050.

Martins, Rute, Daniela Proença, Bruno Silva, Cristina Barbosa, Ana Luísa Silva, Paula Faustino, and Luísa Romão. 2012. "Alternative Polyadenylation and Nonsense-Mediated Decay Coordinately Regulate the Human HFE mRNA Levels." *PLoS ONE* 7 (4): 1–12. doi:10.1371/journal.pone.0035461.

Masamha, Chioniso, Zheng Xia, Jingxuan Yang, Todd R. Albrecht, Min Li, Ann-Bin Shyu, Wei Li, and Eric J. Wagner. 2014. "CFIm25 Links Alternative Polyadenylation to Glioblastoma Tumour Suppression." *Nature* 509 (7505). Nature Publishing Group: 412–16. doi:10.1038/nature13261.

Masuda, Akio, Jun ichi Takeda, and Kinji Ohno. 2016. "FUS-Mediated Regulation of Alternative RNA Processing in Neurons: Insights from Global Transcriptome Analysis." *Wiley Interdisciplinary Reviews: RNA* 7 (3): 330–40. doi:10.1002/wrna.1338.

Masuda, Akio, Jun ichi Takeda, Tatsuya Okuno, Takaaki Okamoto, Bisei Ohkawara, Mikako Ito, Shinsuke Ishigaki, Gen Sobue, and Kinji Ohno. 2015. "Position-Specific Binding of FUS to Nascent RNA Regulates mRNA Length." *Genes & Development* 29 (10): 1045–57. doi:10.1101/gad.255737.114.

Matoulkova, Eva, Eva Michalova, Borivoj Vojtesek, and Roman Hrstka. 2012. "The Role of the 3' Untranslated Region in Post-Transcriptional Regulation of Protein Expression in Mammalian Cells." *RNA Biology* 9 (5): 563–76. doi:10.4161/rna.20231.

Matsuki, Hideaki, Masahiko Takahashi, Masaya Higuchi, Grace N. Makokha, Masayasu Oie, and Masahiro Fujii. 2013. "Both G3BP1 and G3BP2 Contribute to Stress Granule Formation." *Genes to Cells* 18 (2): 135–46. doi:10.1111/gtc.12023.

Mayr, Christine. 2016. "Evolution and Biological Roles of Alternative 3'UTRs." *Trends in Cell Biology* 26 (3). Elsevier Ltd: 227–37. doi:10.1016/j.tcb.2015.10.012.

Mayr, Christine, and David P. Bartel. 2009. "Widespread Shortening of 3'UTRs by Alternative Cleavage and Polyadenylation Activates Oncogenes in Cancer Cells." *Cell* 138 (4). Elsevier Ltd: 673–84. doi:10.1016/j.cell.2009.06.016.

Mayr, Florian, Anja Schütz, Nadine Döge, and Udo Heinemann. 2012. "The Lin28 Cold-Shock Domain Remodels Pre-Let-7 microRNA." *Nucleic Acids Research* 40 (15): 7492–7506. doi:10.1093/nar/gks355.

Mayr, and Bartel. 2010. "Roesser Paper 2." *Cell* 138 (4). doi:10.1016/j.cell.2009.06.016.Widespread.

Mbella, E G, S Bertrand, G Huez, and J N Octave. 2000. "A GG Nucleotide Sequence of the 3' Untranslated Region of Amyloid Precursor Protein mRNA Plays a Key Role in the Regulation of Translation and the Binding of Proteins." *Mol Cell Biol* 20 (13): 4572–79. http://www.ncbi.nlm.nih.gov/pubmed/10848584.

McCracken, Susan, Nova Fong, Emanuel Rosonina, Krassimir Yankulov, Greg Brothers, David Siderovski, Andrew Hessel, Stephen Foster, Stewart Shuman, and David L. Bentley. 1997. "5'-Capping Enzymes Are Targeted to Pre-mRNA by Binding to the Phosphorylated Carboxy-Terminal Domain of RNA Polymerase II." *Genes and Development* 11 (24): 3306–18. doi:10.1101/gad.11.24.3306.

McKinnon, Chris, and Sarah J Tabrizi. 2014. "The Ubiquitin-Proteasome System in Neurodegeneration." *Antioxidants & Redox Signaling* 0 (0): 1–20. doi:10.1089/ars.2013.5802.

Memon, Danish, Keren Dawson, Christopher SF Smowton, Wei Xing, Caroline Dive, and Crispin J Miller. 2016. "Hypoxia-Driven Splicing into Noncoding Isoforms Regulates the DNA Damage Response." *Npj Genomic Medicine* 1 (January): 16020. doi:10.1038/npjgenmed.2016.20.

Metcalf, Daniel J., Moisés García-Arencibia, Warren E. Hochfeld, and David C. Rubinsztein. 2012. "Autophagy and Misfolded Proteins in Neurodegeneration." *Experimental Neurology* 238 (1). Elsevier Inc.: 22–28. doi:10.1016/j.expneurol.2010.11.003.

Miñones-Moyano, Elena, Sílvia Porta, Georgia Escaramís, Raquel Rabionet, Susana Iraola, Birgit Kagerbauer, Yolanda Espinosa-Parrilla, Isidre Ferrer, Xavier Estivill, and Eulàlia Martí. 2011.

"MicroRNA Profiling of Parkinson's Disease Brains Identifies Early Downregulation of miR-34b/c Which Modulate Mitochondrial Function." *Human Molecular Genetics* 20 (15): 3067–78. doi:10.1093/hmg/ddr210.

Mitra, Aparna, Jack W Rostas, Donna L Dyess, Lalita a Shevde, and Rajeev S Samant. 2012. "Micro-RNA-632 Downregulates DNAJB6 in Breast Cancer." *Laboratory Investigation* 92 (9). Nature Publishing Group: 1310–17. doi:10.1038/labinvest.2012.87.

Miura, Pedro, Piero Sanfilippo, Sol Shenker, and Eric C. Lai. 2014. "Alternative Polyadenylation in the Nervous System: To What Lengths Will 3′ UTR Extensions Take Us?" *BioEssays* 36 (8): 766–77. doi:10.1002/bies.201300174.Alternative.

Miura, Pedro, Sol Shenker, Celia Andreu-Agullo, Jakub O. Westholm, and Eric C. Lai. 2013. "Widespread and Extensive Lengthening of 3'UTRs in the Mammalian Brain." *Genome Research* 23 (5): 812–25. doi:10.1101/gr.146886.112.

Mizuno, Yoshikuni, Keiji Suzuki, Nobuhito Sone, and Tomohiko Saitoh. 1987. "Inhibition of ATP Synthesis by 1-Methyl-4-Phenylpyridinium Ion (MPP+) in Isolated Mitochondria from Mouse Brains." *Neuroscience Letters* 81 (1–2): 204–8. doi:10.1016/0304-3940(87)90366-1.

Mohamet, Lisa, Natalie J Miazga, and Christopher M Ward. 2014. "Familial Alzheimer's Disease Modelling Using Induced Pluripotent Stem Cell Technology." *World Journal of Stem Cells* 6 (2): 239–47. doi:10.4252/wjsc.v6.i2.239.

Morf, Jörg, Guillaume Rey, Kim Schneider, Markus Stratmann, Jun Fujita, Felix Naef, and Ueli Schibler. 2012. "Cold-Inducible RNA-Binding Protein Modulates Circadian Gene Expression Posttranscriptionally." *Science* 338 (6105): 379–83.

Morfini, G, G Pigino, K Opalach, Y Serulle, J E Moreira, M Sugimori, R R Llinás, and S T Brady. 2007. "1-Methyl-4-Phenylpyridinium Affects Fast Axonal Transport by Activation of Caspase and Protein Kinase C." *Proceedings of the National Academy of Sciences of the United States of America* 104: 2442–47. doi:10.1073/pnas.0611231104.

Morris, Adam R., Arnold Bos, Begoña Diosdado, Koos Rooijers, Ran Elkon, Anne S. Bolijn, Beatriz Carvalho, Gerrit A. Meijer, and Reuven Agami. 2012. "Alternative Cleavage and Polyadenylation during Colorectal Cancer Development." *Clinical Cancer Research* 18 (19): 5256–66. doi:10.1158/1078-0432.CCR-12-0543.

Mouradian, M. Maral. 2012. "MicroRNAs in Parkinson's Disease." *Neurobiology of Disease* 46 (2). Elsevier Inc.: 279–84. doi:10.1016/j.nbd.2011.12.046.

Müller-McNicoll, Michaela, Valentina Botti, Antonio M. de Jesus Domingues, Holger Brandl, Oliver D. Schwich, Michaela C. Steiner, Tomaz Curk, Ina Poser, Kathi Zarnack, and Karla M. Neugebauer. 2016. "SR Proteins Are NXF1 Adaptors That Link Alternative RNA Processing to mRNA Export." *Genes and Development* 30 (5): 553–66. doi:10.1101/gad.276477.115.

Myszczynska, Monika, and Laura Ferraiuolo. 2016. "New In Vitro Models to Study Amyotrophic Lateral Sclerosis." *Brain Pathology* 26: 258–65.

Nagaike, Takashi, and James L. Manley. 2011. "Transcriptional Activators Enhance Polyadenylation of mRNA Precursors." *RNA Biology* 8 (6): 964–67. doi:10.4161/rna.8.6.17210.

Naganuma, Takao, Shinichi Nakagawa, Akie Tanigawa, Yasnory F Sasaki, Naoki Goshima, and Tetsuro Hirose. 2012. "Alternative 3'-end Processing of Long Noncoding RNA Initiates Construction of Nuclear Paraspeckles." *The EMBO Journal* 31 (20). Nature Publishing Group: 4020–34. doi:10.1038/emboj.2012.251.

Nakamura, Ken, Venu M. Nemani, Farnaz Azarbal, Gaia Skibinski, Jon M. Levy, Kiyoshi Egami, Larissa Munishkina, et al. 2011. "Direct Membrane Association Drives Mitochondrial Fission by the Parkinson Disease-Associated Protein α-Synuclein." *Journal of Biological Chemistry* 286 (23): 20710–26. doi:10.1074/jbc.M110.213538.

Nakato, Ryosuke, Yu Ohkubo, Akari Konishi, Mari Shibata, Yuki Kaneko, Takao Iwawaki, Tomohiro Nakamura, Stuart a. Lipton, and Takashi Uehara. 2015. "Regulation of the Unfolded Protein

Response via S-Nitrosylation of Sensors of Endoplasmic Reticulum Stress." *Scientific Reports* 5 (October). Nature Publishing Group: 14812. doi:10.1038/srep14812.

Nallamshetty, Shriram, Stephen Y. Chan, and Joseph Loscalzo. 2013. "Hypoxia: A Master Regulator of microRNA Biogenesis and Activity." *Free Radic Biol Med* 64: 20–30. doi:10.1038/jid.2014.371.

Nam, Jin Wu, Olivia S. Rissland, David Koppstein, Cei Abreu-Goodger, CalvinH Jan, Vikram Agarwal, Muhammed A. Yildirim, Antony Rodriguez, and David P. Bartel. 2014. "Global Analyses of the Effect of Different Cellular Contexts on microRNA Targeting." *Molecular Cell* 53 (6). Elsevier Inc.: 1031–43. doi:10.1016/j.molcel.2014.02.013.

Neutelings, Thibaut, Charles A. Lambert, Betty V. Nusgens, and Alain C. Colige. 2013. "Effects of Mild Cold Shock (25??C) Followed by Warming Up at 37??C on the Cellular Stress Response." *PLoS ONE* 8 (7). doi:10.1371/journal.pone.0069687.

Neve, Jonathan, Kaspar Burger, Wencheng Li, Mainul Hoque, Radhika Patel, Bin Tian, Monika Gullerova, and Andre Furger. 2016. "Subcellular RNA Profiling Links Splicing and Nuclear DICER1 to Alternative Cleavage and Polyadenylation." *Genome Research* 26 (1): 24–35. doi:10.1101/gr.193995.115.

Neve, Jonathan, Radhika Patel, Zhiqiao Wang, Alastair Louey, and André Martin Furger. 2017. "New Dawn for the poly(A) Site: Ending the Message Expands Gene Regulation." *RNA Biology* 6286 (May): 0. doi:10.1080/15476286.2017.1306171.

Nilsen, Timothy W, and Brenton R Graveley. 2010. "Expansion of the Eukaryotic Proteome by Alternative Splicing." *Nature* 463 (7280): 457–63. doi:10.1038/nature08909.

Nishiyama, Hiroyuki, Katsuhiko Itoh, Yoshiyuki Kaneko, Masamichi Kishishita, Osamu Yoshida, and Jun Fujita. 1997. "A Glycine-Rich RNA-Binding Protein Mediating Cold-Inducible Suppression of Mammalian Cell Growth." *Journal of Cell Biology* 137 (4): 899–908. doi:10.1083/jcb.137.4.899.

Niu, Ying-lin, Ya-jun Li, Jing-bo Wang, Yuan-yuan Lu, Zhen-xiong Liu, Shan-shan Feng, and Jian-guo Hu. 2016. "CacyBP/SIP Nuclear Translocation Regulates p27Kip1 Stability in Gastric Cancer Cells." *World Journal of Gastroenterology* 22 (15): 3992–4001. doi:10.3748/wjg.v22.i15.3992.

Nizet, Victor, and Randall Johnson. 2009. "Interdependence of Hypoxic and Innate Immune Responses." *Nature Reviews Immunology* 9 (9): 609–17. doi:10.1016/j.immuni.2010.12.017.Two-stage.

Nunes, N.M., W. Li, B. Tian, and A. Furger. 2010. "A Functional Human Poly(A) Site Requires Only a Potent DSE and an A-Rich Upstream Sequence." *EMBO Journal* 29 (9): 1523–36. doi:10.1038/emboj.2010.42.

O'Brien, Rj, and Pc Wong. 2011. "Amyloid Precursor Protein Processing and Alzheimer's Disease." *Annual Review of Neuroscience* 1987: 185–204. doi:10.1146/annurev-neuro-061010-113613.Amyloid.

Okuwaki, Mitsuru. 2008. "The Structure and Functions of NPM1/Nucleophsmin/B23, a Multifunctional Nucleolar Acidic Protein." *Journal of Biochemistry* 143 (4): 441–48. doi:10.1093/jb/mvm222.

Osaka, Hitoshi, Yu Lai Wang, Koji Takada, Shuichi Takizawa, Rieko Setsuie, Hang Li, Yae Sato, et al. 2003. "Ubiquitin Carboxy-Terminal Hydrolase L1 Binds to and Stabilizes Monoubiquitin in Neuron." *Human Molecular Genetics* 12 (16): 1945–58. doi:10.1093/hmg/ddg211.

Osera, Cecilia, Jennifer L Martindale, Marialaura Amadio, Jiyoung Kim, Xiaoling Yang, and Christopher A Moad. 2015. "Induction of VEGFA mRNA Translation by CoCl 2 Mediated by HuR." *RNA Biology* 6286 (September): 0–10. doi:10.1080/15476286.2015.1085276.

Pakos-Zebrucka, Karolina, Izabela Koryga, Katarzyna Mnich, Mila Ljujic, Afshin Samali, and Adrienne M Gorman. 2016. "The Integrated Stress Response." *EMBO Reports* 17 (10): 1374–95. doi:10.15252/embr.201642195.

Pan, T., P. Rawal, Y. Wu, W. Xie, J. Jankovic, and W. Le. 2009. “Rapamycin Protects against Rotenone-Induced Apoptosis through Autophagy Induction.” *Neuroscience* 164 (2). Elsevier Inc.: 541–51. doi:10.1016/j.neuroscience.2009.08.014.

Parakh, Sonam, and Julie D. Atkin. 2016. “Protein Folding Alterations in Amyotrophic Lateral Sclerosis.” *Brain Research* 1648. Elsevier: 633–49. doi:10.1016/j.brainres.2016.04.010.

Parihar, M. S., A. Parihar, M. Fujita, M. Hashimoto, and P. Ghafourifar. 2008. “Mitochondrial Association of Alpha-Synuclein Causes Oxidative Stress.” *Cellular and Molecular Life Sciences* 65 (7–8): 1272–84. doi:10.1007/s00018-008-7589-1.

Pattarini, R., Y. Rong, C. Qu, and J. I. Morgan. 2008. “Distinct Mechanisms of 1-Methyl-4-Phenyl-1,2,3,6-Tetrahydropyrimidine Resistance Revealed by Transcriptome Mapping in Mouse Striatum.” *Neuroscience* 155 (4): 1174–94. doi:10.1016/j.neuroscience.2008.06.064.

Peretti, Diego, Amandine Bastide, Helois Radford, Nicholas Verity, Colin Molloy, Maria Guerra Martin, Julie A Moreno, et al. 2015. “RBM3 Mediates Structural Plasticity and Protective Effects of Cooling in Neurodegeneration.” *Nature* 518 (7538). Nature Publishing Group: 236–39. doi:10.1038/nature14142.

Perier, Celine, and Miquel Vila. 2012. “Mitochondrial Biology and Parkinson’s Disease.” *Cold Spring Harbor Perspectives in Biology* 4.

Piao, Ying, Hyo Geun Kim, Myung Sook Oh, and Youngmi Kim Pak. 2012. “Overexpression of TFAM, NRF-1 and Myr-AKT Protects the MPP +-Induced Mitochondrial Dysfunctions in Neuronal Cells.” *Biochimica et Biophysica Acta - General Subjects* 1820 (5). Elsevier B.V.: 577–85. doi:10.1016/j.bbagen.2011.08.007.

Pilotte, Julie, Esther E. Dupont-Versteegden, and Peter W. Vanderklish. 2011. “Widespread Regulation of miRNA Biogenesis at the Dicer Step by the Cold-Inducible RNA-Binding Protein, RBM3.” *PLoS ONE* 6 (12). doi:10.1371/journal.pone.0028446.

Pinto, Pedro A B, Telmo Henriques, Marta O Freitas, Torcato Martins, Rita G Domingues, Paulina S Wyrzykowska, Paula A Coelho, et al. 2011. “RNA Polymerase II Kinetics in Polo Polyadenylation Signal Selection.” *The EMBO Journal* 30 (12). Nature Publishing Group: 2431–44. doi:10.1038/emboj.2011.156.

Pirson, Marc, and Bernard Knoops. 2015. “Expression of Peroxiredoxins and Thioredoxins in the Mouse Spinal Cord during Embryonic Development.” *Journal of Comparative Neurology* 523 (17): 2599–2617. doi:10.1002/cne.23807.

Poewe, Werner, Klaus Seppi, Caroline M. Tanner, Glenda M. Halliday, Patrik Brundin, Jens Volkmann, Anette-Eleonore Schrag, and Anthony E. Lang. 2017. “Parkinson Disease.” *Nature Reviews Disease Primers* 3: 17013. doi:10.1038/nrdp.2017.13.

Polymeropoulos, Mihael H, Christian Lavedan, Elisabeth Leroy, Susan E Ide, Anindya Dehejia, Amalia Dutra, Brian Pike, et al. 1997. “Mutation in the α-Synuclein Gene Identified in Families with Parkinson’s Disease.” *Science* 276 (June): 2045–47. doi:10.1126/science.276.5321.2045.

Power, John H T, Sana Asad, Tim K. Chataway, Fariba Chegini, James Manavis, James A. Temlett, Poul H. Jensen, Peter C. Blumbergs, and Wei Ping Gai. 2008. “Peroxiredoxin 6 in Human Brain: Molecular Forms, Cellular Distribution and Association with Alzheimer’s Disease Pathology.” *Acta Neuropathologica* 115 (6): 611–22. doi:10.1007/s00401-008-0373-3.

Prell, Tino, and Julian Grosskreutz. 2013. “The Involvement of the Cerebellum in Amyotrophic Lateral Sclerosis.” *Amyotrophic Lateral Sclerosis & Frontotemporal Degeneration* 14 (7–8): 507–15. doi:10.3109/21678421.2013.812661.

Proudfoot, N J, a Furger, and M J Dye. 2002. “Integrating rnRNA Processing with Transcription.” *Cell* 108: 501–512 ST–Integrating rnRNA processing with tr. doi:10.1016/S0092-8674(02)00617-7.

Proudfoot, Nick J. 2011. “Ending the Message: Poly(A) Signals Then and Now.” *Genes and Development* 25 (17): 1770–82. doi:10.1101/gad.17268411.

Prudencio, Mercedes, Veronique V Belzil, Ranjan Batra, Christian A Ross, Tania F Gendron, Luc J

Pregent, Melissa E Murray, et al. 2015. “Distinct Brain Transcriptome Profiles in C9orf72-Associated and Sporadic ALS.” *Nature Neuroscience* 18 (8): 1175–82. doi:10.1038/nn.4065.

Qiang, Xiaoling, Weng-Lang Yang, Rongqian Wu, Mian Zhou, Asha Jacob, Weifeng Dong, Michael Kuncewitch, et al. 2013. “Cold-Inducible RNA-Binding Protein (CIRP) Triggers Inflammatory Responses in Hemorrhagic Shock and Sepsis.” *Nature Medicine* 19 (11). Nature Publishing Group: 1489–95. doi:10.1038/nm.3368.

Quintin, J., Qing Ma, Zhiquan Zhang, Brian M. Barnes, and Mihai V. Podgoreanu. 2014. “Organ Protective Mechanisms Common to Extremes of Physiology: A Window through Hibernation Biology.” *Integrative and Comparative Biology* 54 (3): 497–515. doi:10.1093/icb/icu047.

Rhee, Won Jong, Chih-Wen Ni, Zhilan Zheng, Kyunghwa Chang, Hanjoong Jo, and Gang Bao. 2010. “HuR Regulates the Expression of Stress-Sensitive Genes and Mediates Inflammatory Response in Human Umbilical Vein Endothelial Cells.” *Proceedings of the National Academy of Sciences of the United States of America* 107 (15): 6858–63. doi:10.1073/pnas.1000444107.

Rhinn, Herve, Liang Qiang, Toru Yamashita, David Rhee, Ari Zolin, William Vanti, and Asa Abeliovich. 2012. “Alternative α-Synuclein Transcript Usage as a Convergent Mechanism in Parkinson’s Disease Pathology.” *Nature Communications* 3. Nature Publishing Group: 1084. doi:10.1038/ncomms2032.

Richter, Klaus, Martin Haslbeck, and Johannes Buchner. 2010. “The Heat Shock Response: Life on the Verge of Death.” *Molecular Cell* 40 (2). Elsevier Inc.: 253–66. doi:10.1016/j.molcel.2010.10.006.

Ristic, Gorica, Wei-Ling Tsou, and Sokol V Todi. 2014. “An Optimal Ubiquitin-Proteasome Pathway in the Nervous System: The Role of Deubiquitinating Enzymes.” *Frontiers in Molecular Neuroscience* 7 (August): 72. doi:10.3389/fnmol.2014.00072.

Rogelj, Boris, Laura E. Easton, Gireesh K. Bogu, Lawrence W. Stanton, Gregor Rot, Tomaž Curk, Blaž Zupan, et al. 2012. “Widespread Binding of FUS along Nascent RNA Regulates Alternative Splicing in the Brain.” *Scientific Reports* 2: 1–10. doi:10.1038/srep00603.

Ron, D, and P Walter. 2007. “Signal Integration in the Endoplasmic Reticulum Unfolded Protein Response.” *Nature reviews.Molecular Cell Biology* 8 (7): 519–29. doi:10.1038/nrm2199.

Rosinska, Sara, Wieslawa Lesniak, and Anna Filipek. 2016. “Distinct Effect of CacyBP/SIP on the ERK1/2-CREB-BDNF Pathway in Undifferentiated and Differentiated Neuroblastoma NB2a Cells.” *Neurochemistry International* 97: 65–72. doi:10.1016/j.neuint.2016.05.002.

Roush, Sarah, and Frank J. Slack. 2008. “The Let-7 Family of microRNAs.” *Trends in Cell Biology* 18 (10): 505–16. doi:10.1016/j.tcb.2008.07.007.

Ryan, Brent J., Lara L. Lourenço-Venda, Mark J. Crabtree, Ashley B. Hale, Keith M. Channon, and Richard Wade-Martins. 2014. “Synuclein and Mitochondrial Bioenergetics Regulate Tetrahydrobiopterin Levels in a Human Dopaminergic Model of Parkinson Disease.” *Free Radical Biology and Medicine* 67 (0): 58–68. doi:10.1016/j.freeradbiomed.2013.10.008.

Rzechorzek, Nina M., Peter Connick, Matthew R. Livesey, Shyamanga Borooah, Rickie Patani, Karen Burr, David Story, David J A Wyllie, Giles E. Hardingham, and Siddharthan Chandran. 2016. “Hypothermic Preconditioning Reverses Tau Ontogenesis in Human Cortical Neurons and Is Mimicked by Protein Phosphatase 2A Inhibition.” *EBioMedicine* 3. The Authors: 141–54. doi:10.1016/j.ebiom.2015.12.010.

Rzechorzek, Nina Marie, Peter Connick, Rickie Patani, Bhuvaneish Thangaraj Selvaraj, and Siddharthan Chandran. 2015. “Hypothermic Preconditioning of Human Cortical Neurons Requires Proteostatic Priming.” *EBioMedicine* 2 (6). Elsevier B.V.: 528–35. doi:10.1016/j.ebiom.2015.04.004.

Sagawa, F, H Ibrahim, A L Morrison, C J Wilusz, and J Wilusz. 2011. “Nucleophosmin Deposition during mRNA 3’ End Processing Influences poly(A) Tail Length.” *Embo J* 30 (19). Nature Publishing Group: 3994–4005. doi:10.1038/emboj.2011.272\remboj2011272 [pii].

Saito, Kosuke, Noboru Fukuda, Taro Matsumoto, Yuji Iribe, Akiko Tsunemi, Tomohiko Kazama, Chikako Yoshida-Noro, and Nariyuki Hayashi. 2010. “Moderate Low Temperature Preserves the Stemness of Neural Stem Cells and Suppresses Apoptosis of the Cells via Activation of the Cold-Inducible RNA Binding Protein.” *Brain Research* 1358. Elsevier B.V.: 20–29. doi:10.1016/j.brainres.2010.08.048.

Saldi, Tassa, Michael A. Cortazar, Ryan M. Sheridan, and David L. Bentley. 2016. “Coupling of RNA Polymerase II Transcription Elongation with Pre-mRNA Splicing.” *Journal of Molecular Biology* 428 (12). Elsevier Ltd: 2623–35. doi:10.1016/j.jmb.2016.04.017.

Sanchez, Mayka, Bruno Galy, Martina U Muckenthaler, and Matthias W Hentze. 2007. “Iron-Regulatory Proteins Limit Hypoxia-Inducible Factor-2alpha Expression in Iron Deficiency.” *Nature Structural & Molecular Biology* 14 (5): 420–26. doi:10.1038/nsmb1222.

Sandberg, Rickard, Joel R Neilson, Arup Sarma, Phillip a Sharp, and Christopher B Burge. 2008. “Proliferating Cells Express mRNAs with Shortened 3’ UTRs and Fewer microRNA Target Sites.” *Science* 320 (5883): 1643–47. doi:10.1126/science.1155390.Proliferating.

Sanders, Laurie H, and J Timothy Greenamyre. 2014. “Oxidative Damage to Macromolecules in Human PD and the Rotenone Model.” *Free Radic Biol Med* 62: 111–20. doi:10.1016/j.freeradbiomed.2013.01.003.Oxidative.

Satake, Wataru, Yuko Nakabayashi, Ikuko Mizuta, Yushi Hirota, Chiyomi Ito, Michiaki Kubo, Takahisa Kawaguchi, et al. 2009. “Genome-Wide Association Study Identifies Common Variants at Four Loci as Genetic Risk Factors for Parkinson’s Disease.” *Nature Genetics* 41 (12). Nature Publishing Group: 1303–7. doi:10.1038/ng.485.

Schneider, Gabriela, Krzysztof Nieznanski, Jolanta Jozwiak, Lukasz P. Slomnicki, Maria J. Redowicz, and Anna Filipek. 2010. “Tubulin Binding Protein, CacyBP/SIP, Induces Actin Polymerization and May Link Actin and Tubulin Cytoskeletons.” *Biochimica et Biophysica Acta - Molecular Cell Research* 1803 (11). Elsevier B.V.: 1308–17. doi:10.1016/j.bbamcr.2010.07.003.

Schneider, Gabriela, Krzysztof Nieznanski, Ewa Kilanczyk, Paweł Bieganowski, Jacek Kuznicki, and Anna Filipek. 2007. “CacyBP/SIP Interacts with Tubulin in Neuroblastoma NB2a Cells and Induces Formation of Globular Tubulin Assemblies.” *Biochimica et Biophysica Acta - Molecular Cell Research* 1773 (11): 1628–36. doi:10.1016/j.bbamcr.2007.07.013.

Schönemann, Lars, Uwe Kühn, Georges Martin, Peter Schäfer, Andreas R. Gruber, Walter Keller, Mihaela Zavolan, and Elmar Wahle. 2014. “Reconstitution of CPSF Active in Polyadenylation: Recognition of the Polyadenylation Signal by WDR33.” *Genes and Development* 28 (21): 2381–93. doi:10.1101/gad.250985.114.

Schwanhausser, Bjorn, Dorothea Busse, Na Li, Gunnar Dittmar, Johannes Schuchhardt, Jana Wolf, Wei Chen, and Matthias Selbach. 2011. “Global Quantification of Mammalian Gene Expression Control.” *Nature* 473: 337–42. doi:10.1038/nature10098.

Schwartz, Jacob C., Christopher C. Ebmeier, Elaine R. Podell, Joseph Heimiller, Dylan J. Taatjes, and Thomas R. Cech. 2012. “FUS Binds the CTD of RNA Polymerase II and Regulates Its Phosphorylation at Ser2.” *Genes and Development* 26 (24): 2690–95. doi:10.1101/gad.204602.112.

Sempere, Lorenzo F, Sarah Freemantle, Ian Pitha-Rowe, Eric Moss, Ethan Dmitrovsky, and Victor Ambros. 2004. “Expression Profiling of Mammalian microRNAs Uncovers a Subset of Brain-Expressed microRNAs with Possible Roles in Murine and Human Neuronal Differentiation.” *Genome Biology* 5 (3): R13. doi:10.1186/gb-2004-5-3-r13.

Sena, Johnny a, Liyi Wang, Lynn E Heasley, and Cheng-Jun Hu. 2014. “Hypoxia Regulates Alternative Splicing of HIF and Non-HIF Target Genes.” *Molecular Cancer Research : MCR*, 1233–44. doi:10.1158/1541-7786.MCR-14-0149.

Shankarling, Ganesh S., and Clinton C. MacDonald. 2013. “Polyadenylation Site-Specific Differences in the Activity of the Neuronal βCstF-64 Protein in PC-12 Cells.” *Gene* 529 (2): 220–27.

doi:10.1111/jnc.12437.Alternative.

Shepard, Peter J, Eun-A Choi, Jente Lu, Lisa A Flanagan, Klemens J Hertel, and Yongsheng Shi. 2011. "Complex and Dynamic Landscape of RNA Polyadenylation Revealed by PAS-Seq." *RNA (New York, N.Y.)* 17 (4): 761–72. doi:10.1261/rna.2581711.

Shi, Hengliang, Yong Gao, Yuan Tang, Yuxuan Wu, Hui Gong, Jin Du, Bao Zheng, Jinxia Hu, Qiong Shi, and Rutong Yu. 2014. "CacyBP/SIP Protein Is Important for the Proliferation of Human Glioma Cells." *IUBMB Life* 66 (4): 286–91. doi:10.1002/iub.1263.

Shi, Yongsheng. 2012. "Alternative Polyadenylation: New Insights from Global Analyses." *Rna* 18 (12): 2105–17. doi:10.1261/rna.035899.112.

Shi, Yongsheng, Dafne Campigli, Di Giammartino, Derek Taylor, Ali Sarkeshik, J Rice, John R Yates Iii, Joachim Frank, and James L Manley. 2009. "Molecular Architecture of the Human Pre-mRNA 3' Processing Complex." *Mol Cell* 33 (3): 365–76. doi:10.1016/j.molcel.2008.12.028.Molecular.

Shin, Jung Eun, Bradley R. Miller, Elisabetta Babetto, Yongcheol Cho, Yo Sasaki, Shehzad Qayum, Emilie V Russler, Valeria Cavalli, Jeffrey Milbrandt, and Aaron DiAntonio. 2012. "SCG10 Is a JNK Target in the Axonal Degeneration Pathway." *Proceedings of the National Academy of Sciences of the United States of America* 109 (52): E3696-705. doi:10.1073/pnas.1216204109.

Sidransky, Ellen, and Grisel Lopez. 2012. "The Link between the GBA Gene and Parkinsonism." *The Lancet Neurology* 11 (11): 986–98. doi:10.1016/S1474-4422(12)70190-4.

Skliris, a, O Papadaki, P Kafasla, I Karakasiliotis, O Hazapis, M Reczko, S Grammenoudi, J Bauer, and D L Kontoyiannis. 2014. "Neuroprotection Requires the Functions of the RNA-Binding Protein HuR." *Cell Death and Differentiation* 22 (5). Nature Publishing Group: 1–16. doi:10.1038/cdd.2014.158.

Smart, Fiona, Armaz Aschrafi, Annette Atkins, Geoffrey C. Owens, Julie Pilotte, Bruce A. Cunningham, and Peter W. Vanderklish. 2007. "Two Isoforms of the Cold-Inducible mRNA-Binding Protein RBM3 Localize to Dendrites and Promote Translation." *Journal of Neurochemistry* 101 (5): 1367–79. doi:10.1111/j.1471-4159.2007.04521.x.

Smibert, Peter, Pedro Miura, Jakub O Westholm, Sol Shenker, Gemma May, Michael O Duff, Dayu Zhang, et al. 2012. "Global Patterns of Tissue-Specific Alternative Polyadenylation in Drosophila." *Cell Reports* 1 (3): 277–89. doi:10.1016/j.celrep.2012.01.001.Global.

Soliman, Mazzio and. 2012. "Whole Genome Expression Profile in Neuroblastoma Cells Exposed to 1-Methyl-4-Phenylpyridine." *NeuroToxicology* 35 (5): 1156–69. doi:10.1016/j.pestbp.2011.02.012.Investigations.

Spies, Noah, Christopher B. Burge, and David P. Bartel. 2013. "3′ UTR-Isoform Choice Has Limited Influence on the Stability and Translational Efficiency of Most mRNAs in Mouse Fibroblasts." *Genome Research* 23 (12): 2078–90. doi:10.1101/gr.156919.113.

Spies, Noah, Cydney B. Nielsen, Richard A. Padgett, and Christopher B. Burge. 2009. "Biased Chromatin Signatures around Polyadenylation Sites and Exons." *Molecular Cell* 36 (2): 245–54. doi:10.1016/j.molcel.2009.10.008.Biased.

Spillantini, M G, M L Schmidt, V M Lee, J Q Trojanowski, R Jakes, and M Goedert. 1997. "Alpha-Synuclein in Lewy Bodies." *Nature* 388 (6645): 839–40. doi:10.1038/42166.

Sreedharan, Jemeen, Ian P. Blair, Vineeta B. Tripathi, Xun Hu, Caroline Vance, Boris Rogelj, Steven Ackerley, et al. 2008. "TDP-43 Mutations in Familial and Sporadic Amyotrophic Lateral Sclerosis." *Science* 319 (March): 1668–72. doi:10.1126/science.1206034.

Stallings, Raymond L, Niamh H Foley, Isabella M Bray, Sudipto Das, and Patrick G Buckley. 2011. "MicroRNA and DNA Methylation Alterations Mediating Retinoic Acid Induced Neuroblastoma Cell Differentiation." *Seminars in Cancer Biology* 21 (4): 283–90. doi:10.1097/OPX.0b013e3182540562.The.

Staudacher, Jonas J., Isabel S. Naarmann-De Vries, Stefanie J. Ujvari, Bertram Klinger, Mumtaz

Kasim, Edgar Benko, Antje Ostareck-Lederer, et al. 2015. “Hypoxia-Induced Gene Expression Results from Selective mRNA Partitioning to the Endoplasmic Reticulum.” *Nucleic Acids Research* 43 (6): 3219–36. doi:10.1093/nar/gkv167.

Stieler, Jens T., Torsten Bullmann, Franziska Kohl, Oøivind Tøien, Martina K. Brückner, Wolfgang Härtig, Brian M. Barnes, and Thomas Arendt. 2011. “The Physiological Link between Metabolic Rate Depression and Tau Phosphorylation in Mammalian Hibernation.” *PLoS ONE* 6 (1). doi:10.1371/journal.pone.0014530.

Subramaniam, Sudhakar Raja, and Marie-Francoise Chesselet. 2013. “Mitochondrial Dysfunction and Oxidative Stress in Parkinson’s Disease.” *Prog. Neurobiol* 0: 17–32. doi:10.1016/j.pneurobio.2013.04.004.Mitochondrial.

Takagaki, Yoshio, Rebecca L. Seipelt, Martha L. Peterson, and James L. Manley. 1996. “The Polyadenylation Factor CstF-64 Regulates Alternative Processing of IgM Heavy Chain Pre-mRNA during B Cell Differentiation.” *Cell* 87 (5): 941–52. doi:10.1016/S0092-8674(00)82000-0.

Taliaferro, J. Matthew, Marina Vidaki, Ruan Oliveira, Sara Olson, Lijun Zhan, Tanvi Saxena, Eric T. Wang, et al. 2016. “Distal Alternative Last Exons Localize mRNAs to Neural Projections.” *Molecular Cell* 61 (6). Elsevier Inc.: 821–33. doi:10.1016/j.molcel.2016.01.020.

Tan, Meng Shan, Jin Tai Yu, and Lan Tan. 2013. “Bridging Integrator 1 (BIN1): Form, Function, and Alzheimer’s Disease.” *Trends in Molecular Medicine* 19 (10). Elsevier Ltd: 594–603. doi:10.1016/j.molmed.2013.06.004.

Tang, Dang, Cheng Wang, Yongjun Gao, Jun Pu, Jiang Long, and Wei Xu. 2016. “Deep Hypothermia-Enhanced Autophagy Protects PC12 Cells against Oxygen Glucose Deprivation via a Mitochondrial Pathway.” *Neuroscience Letters* 632. Elsevier Ireland Ltd: 79–85. doi:10.1016/j.neulet.2016.08.049.

Tang, Fu Lei, Wei Liu, Jin-Xia Hu, Joanna Ruth Erion, Ye Jian, Lin Mei, and Wen-Cheng Xiong. 2015. “VPS35 Deficiency or Mutation Causes Dopaminergic Neuronal Loss by Impairing Mitochondrial Fusion and Function.” *Cell Reports* 12 (10): 1631–43. doi:10.1001/jamasurg.2014.1086.Feasibility.

Tatura, R, T Kraus, A Giese, T Arzberger, M Buchholz, G Hoglinger, and U Muller. 2016. “Parkinson’s Disease: SNCA-, PARK2-, and LRRK2- Targeting microRNAs Elevated in Cingulate Gyrus.” *Parkinsonism Relat Disord* 33. doi:10.1016/j.parkreldis.2016.09.028.

Tessier, Shannon N., and Kenneth B. Storey. 2014. “To Be or Not to Be: The Regulation of mRNA Fate as a Survival Strategy during Mammalian Hibernation.” *Cell Stress and Chaperones* 19 (6): 763–76. doi:10.1007/s12192-014-0512-9.

Tian, Bin, Jun Hu, Haibo Zhang, and Carol S. Lutz. 2005. “A Large-Scale Analysis of mRNA Polyadenylation of Human and Mouse Genes.” *Nucleic Acids Research* 33 (1): 201–12. doi:10.1093/nar/gki158.

Tian, Bin, and James L. Manley. 2013. “Alternative Cleavage and Polyadenylation: The Long and Short of It.” *Trends in Biochemical Sciences* 38 (6). Elsevier Ltd: 312–20. doi:10.1016/j.tibs.2013.03.005.

———. 2016. “Alternative Polyadenylation of mRNA Precursors.” *Nature Reviews Molecular Cell Biology* 18 (1): 18–30. doi:10.1038/nrm.2016.116.

Tollervey, James R, Zhen Wang, Tibor Hortobagyi, Joshua T Witten, Kathi Zarnack, Melis Kayikci, Tyson A. Clark, et al. 2011. “Analysis of Alternative Splicing Associated with Aging and Neurodegeneration in the Human Brain.” *Genome Research*, no. 21: 1572–82. doi:10.1101/gr.122226.111.1572.

Topolska-Woš, Agnieszka M., Walter J. Chazin, and Anna Filipek. 2016. “CacyBP/SIP - Structure and Variety of Functions.” *Biochimica et Biophysica Acta - General Subjects* 1860 (1): 79–85. doi:10.1016/j.bbagen.2015.10.012.

Tranter, Michael, Robert N. Helsley, Waltke R. Paulding, Michael McGuinness, Cole Brokamp,

Lauren Haar, Yong Liu, Xiaoping Ren, and W. Keith Jones. 2011. "Coordinated Post-Transcriptional Regulation of Hsp70.3 Gene Expression by microRNA and Alternative Polyadenylation." *Journal of Biological Chemistry* 286 (34): 29828–37. doi:10.1074/jbc.M111.221796.

Twine, Natalie A., Karolina Janitz, Marc R. Wilkins, and Michal Janitz. 2011. "Whole Transcriptome Sequencing Reveals Gene Expression and Splicing Differences in Brain Regions Affected by Alzheimer's Disease." *PLoS ONE* 6 (1). doi:10.1371/journal.pone.0016266.

Udagawa, Tsuyoshi, Yusuke Fujioka, Motoki Tanaka, Daiyu Honda, Satoshi Yokoi, Yuichi Riku, Daisuke Ibi, et al. 2015. "FUS Regulates AMPA Receptor Function and FTLD/ALS-Associated Behaviour via GluA1 mRNA Stabilization." *Nature Communications* 6 (May). Nature Publishing Group: 7098. doi:10.1038/ncomms8098.

Ulitsky, Igor, Alena Shkumatava, Calvin H. Jan, Alexander O. Subtelny, David Koppstein, George W. Bell, Hazel Sive, and David P. Bartel. 2012. "Extensive Alternative Polyadenylation during Zebrafish Development." *Genome Research* 22 (10): 2054–66. doi:10.1101/gr.139733.112.

Vallelunga, Annamaria, Marco Ragusa, Stefania Di Mauro, Tommaso Iannitti, Manuela Pilleri, Roberta Biundo, Luca Weis, et al. 2014. "Identification of Circulating microRNAs for the Differential Diagnosis of Parkinson's Disease and Multiple System Atrophy." *Frontiers in Cellular Neuroscience* 8 (June): 156. doi:10.3389/fncel.2014.00156.

Vallortigara, Julie, David Whitfield, William Quelch, Amani Alghamdi, David Howlett, Tibor Hortob??gyi, Mary Johnson, et al. 2015. "Decreased Levels of VAMP2 and Monomeric Alpha-Synuclein Correlate with Duration of Dementia." *Journal of Alzheimer's Disease* 50 (1): 101–10. doi:10.3233/JAD-150707.

Velten, Lars, Simon Anders, Aleksandra Pekowska, Aino I Järvelin, Wolfgang Huber, Vicent Pelechano, and Lars M Steinmetz. 2015. "Single-Cell Polyadenylation Site Mapping Reveals 3' Isoform Choice Variability." *Molecular Systems Biology* 11 (6): 812. doi:10.15252/msb.20156198.

Vila, Miquel, Slobodanka Vukosavic, Venice Jackson-Lewis, Michael Neystat, Michael Jakowec, and Serge Przedborski. 2000. "α-Synuclein up-Regulation in Substantia Nigra Dopaminergic Neurons Following Administration of the Parkinsonian Toxin MPTP." *Journal of Neurochemistry* 74 (2): 721–29. doi:10.1046/j.1471-4159.2000.740721.x.

Wächter, Kristin, Marcel Köhn, Nadine Stöhr, and Stefan Hüttelmaier. 2013. "Subcellular Localization and RNP Formation of IGF2BPs (IGF2 mRNA-Binding Proteins) Is Modulated by Distinct RNA-Binding Domains." *Biological Chemistry* 394 (8): 1077–90. doi:10.1515/hsz-2013-0111.

Wahle, Elmar. 1991. "A Novel poly(A)-Binding Protein Acts as a Specificity Factor in the Second Phase of Messenger RNA Polyadenylation." *Cell* 67 (3): 640. doi:10.1016/0092-8674(91)90537-9.

Wang, Gang, Jing Pan, and Sheng-Di Chen. 2012. "Kinases and Kinase Signaling Pathways: Potential Therapeutic Targets in Parkinson's Disease." *Progress in Neurobiology* 98 (2). Elsevier Ltd: 207–21. doi:10.1016/j.pneurobio.2012.06.003.

Wang, Huiqing, Yongyi Ye, Zhiyuan Zhu, Liqian Mo, Chunnan Lin, Qifu Wang, Haoyuan Wang, et al. 2016. "MiR-124 Regulates Apoptosis and Autophagy Process in MPTP Model of Parkinson's Disease by Targeting to Bim." *Brain Pathology* 26 (2): 167–76. doi:10.1111/bpa.12267.

Wang, Jianyong, Zengjun Xu, Hong Fang, Helen M. Duhart, Tucker A. Patterson, and Syed F. Ali. 2007. "Gene Expression Profiling of MPP+-Treated MN9D Cells: A Mechanism of Toxicity Study." *NeuroToxicology* 28 (5 SPEC. ISS.): 979–87. doi:10.1016/j.neuro.2007.02.013.

Wang, Ningju, Qingyong Ma, Yinna Wang, Gang Ma, and Huihong Zhai. 2010. "CacyBP/SIP Expression Is Involved in the Clinical Progression of Breast Cancer." *World Journal of Surgery* 34 (11): 2545–52. doi:10.1007/s00268-010-0690-2.

Wang, Xinglong, Bo Su, Wanhong Liu, Xiaohua He, Yuan Gao, Rudy J. Castellani, George Perry, Mark A. Smith, and Xiongwei Zhu. 2011. "DLP1-Dependent Mitochondrial Fragmentation

Mediates 1-Methyl-4-Phenylpyridinium Toxicity in Neurons: Iimplications for PD." *Aging Cell* 10 (5): 887–93. doi:10.1016/j.pestbp.2011.02.012.Investigations.

Wang, Yanbo, Luxiao Chen, Zhenyu Wu, Minghai Wang, Fangfang Jin, Nan Wang, Xiuting Hu, et al. 2016. "miR-124-3p Functions as a Tumor Suppressor in Breast Cancer by Targeting CBL." *BMC Cancer* 16 (1). BMC Cancer: 826. doi:10.1186/s12885-016-2862-4.

Wehrspaun, Claudia C., Chris P. Ponting, and Ana C. Marques. 2014. "Brain-Expressed 3'UTR Extensions Strengthen miRNA Cross-Talk between Ion Channel/transporter Encoding mRNAs." *Frontiers in Genetics* 5 (FEB): 1–11. doi:10.3389/fgene.2014.00041.

Weidemann, A, and R S Johnson. 2008. "Biology of HIF-1α." *Cell Death and Differentiation* 15 (4): 621–27. doi:10.1038/cdd.2008.12.

Weigand, Julia E., Jes Niels Boeckel, Pascal Gellert, and Stefanie Dimmeler. 2012. "Hypoxia-Induced Alternative Splicing in Endothelial Cells." *PLoS ONE* 7 (8). doi:10.1371/journal.pone.0042697.

Weill, L, E Belloc, F A Bava, and R Mendez. 2012. "Translational Control by Changes in poly(A) Tail Length: Recycling mRNAs." *Nat Struct Mol Biol* 19 (6): 577–85. doi:10.1038/nsmb.2311.

Wellmann, Sven, Christoph Bührer, Eva Moderegger, Andrea Zelmer, Renate Kirschner, Petra Koehne, Jun Fujita, and Karl Seeger. 2004. "Oxygen-Regulated Expression of the RNA-Binding Proteins RBM3 and CIRP by a HIF-1-Independent Mechanism." *Journal of Cell Science* 117 (Pt 9): 1785–94. doi:10.1242/jcs.01026.

Woerner, Andreas C., Frédéric Frottin, Daniel Hornburg, Li R. Feng, Felix Meissner, Maria Patra, Jörg Tatzelt, et al. 2015. "Cytoplasmic Protein Aggregates Interfere with Nucleo-Cytoplasmic Transport of Protein and RNA." *Science* 17 (6269): 1–8. doi:10.1126/science.aad2033.

Wong, J. 2013. "Altered Expression of RNA Splicing Proteins in Alzheimer's Disease Patients: Evidence from Two Microarray Studies." *Dement Geriatr Cogn Dis Extra* 3 (1): 74–85. doi:10.1159/000348406.

Wood, Andrew J, Reiner Schulz, Kathryn Woodfine, Katarzyna Koltowska, Colin V Beechey, Jo Peters, Deborah Bourc, and Rebecca J Oakey. 2008. "Regulation of Alternative Polyadenylation by Genomic Imprinting," 1141–46. doi:10.1101/gad.473408.products.

Woodard, Chris M, Brian A Campos, Sheng-han Kuo, Melissa J Nirenberg, Michael W Nestor, Matthew Zimmer, Eugene Mosharov, et al. 2014. "iPS Cell-Derived Dopamine Neurons Reveal Differences between Monozygotic Twins Discordant for Parkinson's Disease." *Cell Reports* 9 (4): 1173–82. doi:10.1016/j.celrep.2014.10.023.iPS.

Wouters, Bradly G., Twan Van Den Beucken, Michael G. Magagnin, Marianne Koritzinsky, Diane Fels, and Constantinos Koumenis. 2005. "Control of the Hypoxic Response through Regulation of mRNA Translation." *Seminars in Cell and Developmental Biology* 16 (4–5): 487–501. doi:10.1016/j.semcdb.2005.03.009.

Wu, Bin, Carolina Eliscovich, Young J Yoon, and Robert H Singer. 2016. "Translation Dynamics of Single mRNAs in Live Cells and Neurons." *Science*, aaf1084. doi:10.1126/science.aaf1084.

Wu, J, X Tan, X Peng, J Yuan, and B Qiang. 2003. "Translocation and Phosphorylation of Calcyclin Binding Protein during Retinoic Acid-Induced Neuronal Differentiation of Neuroblastoma SH-SY5Y Cells." *Journal of Biochemistry and Molecular Biology* 36 (4): 354–58. doi:<ARTICLE_ID IdType=doi> [pii].

Xia, Zheng, Lawrence A Donehower, Thomas A Cooper, Joel R Neilson, David A Wheeler, Eric J Wagner, and Wei Li. 2014. "Dynamic Analyses of Alternative Polyadenylation from RNA-Seq Reveal a 3'-UTR Landscape across Seven Tumour Types." *Nature Communications* 5. Nature Publishing Group: 5274. doi:10.1038/ncomms6274.

Xiang, Chunchen, Yujia Wang, Han Zhang, and Fang Han. 2016. "The Role of Endoplasmic Reticulum Stress in Neurodegenerative Disease." *Apoptosis* 22 (1). Springer US: 1–26. doi:10.1007/s10495-016-1296-4.

Xu, Z, T A Patterson, J D Wren, T Han, L Shi, H Duhart, S F Ali, and W Slikker. 2005. "A

Microarray Study of MPP+-Treated PC12 Cells: Mechanisms of Toxicity (MOT) Analysis Using Bioinformatics Tools." *BMC Bioinformatics* 6 Suppl 2: S8. doi:10.1186/1471-2105-6-S2-S8.

Yamamoto, Koichi, Mari T. Furukawa, Kazuhiro Fukumura, Arisa Kawamura, Tomoko Yamada, Hitoshi Suzuki, Tetsuro Hirose, Hiroshi Sakamoto, and Kunio Inoue. 2016. "Control of the Heat Stress-Induced Alternative Splicing of a Subset of Genes by hnRNP K." *Genes to Cells* 21 (9): 1006–14. doi:10.1111/gtc.12400.

Yan, Xin, Hua Shen, Charles Loh, Jianzhong Shao, Yuhong Yang, and Chunling Lu. 2013. "A Longitudinal Study about the Effect of Practicing Yan Xin Qigong on Medical Care Cost with Medical Claims Data." *International Journal of Economic Research* 10 (2): 391–403. doi:10.3851/IMP2701.Changes.

Yana, Michael H., Xinglong Wang, and Xiongwei Zhu. 2013. "Mitochondrial Defects and Oxidative Stress in Alzheimer Disease and Parkinson Disease." *Free Radical Biology and Medicine* 62. Elsevier: 90–101. doi:10.1016/j.freeradbiomed.2012.11.014.

Yano, R., C. C. Yap, Y. Yamazaki, Y. Muto, H. Kishida, D. Okada, and T. Hashikawa. 2003. "SAST124, a Novel Splice Variant of Syntrophin-Associated Serine/threonine Kinase (SAST), Is Specifically Localized in the Restricted Brain Regions." *Neuroscience* 117 (2): 373–81. doi:10.1016/S0306-4522(02)00785-6.

Yenari, M A, and H S Han. 2012. "Neuroprotective Mechanisms of Hypothermia in Brain Ischaemia." *Nat Rev Neurosci* 13 (4). Nature Publishing Group: 267–78. doi:10.1038/nrn3174.

Yun, Hyung Mun, Kyung Ran Park, Mi Hee Park, Dae Hwan Kim, Mi Ran Jo, Ji Young Kim, Eun Cheol Kim, Do Young Yoon, Sang Bae Han, and Jin Tae Hong. 2015. "PRDX6 Promotes Tumor Development via the JAK2/STAT3 Pathway in a Urethane-Induced Lung Tumor Model." *Free Radical Biology and Medicine* 80. Elsevier: 136–44. doi:10.1016/j.freeradbiomed.2014.12.022.

Zawada, W M, G P Banninger, J Thornton, B Marriott, D Cantu, A L Rachubinski, M Das, W S Griffin, and S M Jones. 2011. "Generation of Reactive Oxygen Species in 1-Methyl-4-Phenylpyridinium (MPP+) Treated Dopaminergic Neurons Occurs as an NADPH Oxidase-Dependent Two-Wave Cascade." *J Neuroinflammation* 8 (1): 129. doi:10.1186/1742-2094-8-129.

Zhai, Huihong, Yongquan Shi, Xiong Chen, Jun Wang, Yuanyuan Lu, Faming Zhang, Zhengxiong Liu, Ting Lei, and Daiming Fan. 2017. "CacyBP/SIP Promotes the Proliferation of Colon Cancer Cells." *Plos One* 12 (2): e0169959. doi:10.1371/journal.pone.0169959.

Zhang, Chaolin, and Robert B Darnell. 2011. "Mapping in Vivo Protein-RNA Interactions at Single-Nucleotide Resolution from HITS-CLIP Data." *Nature Biotechnology* 29 (7): 607–14. doi:10.1038/nbt.1873.

Zhang, Cheng Cheng, Ang Xing, Meng Shan Tan, Lan Tan, and Jin Tai Yu. 2016. "The Role of MAPT in Neurodegenerative Diseases: Genetics, Mechanisms and Therapy." *Molecular Neurobiology* 53 (7). Molecular Neurobiology: 4893–4904. doi:10.1007/s12035-015-9415-8.

Zhang, Hai Tao, Jing Hui Xue, Zhi Wen Zhang, Hai Bo Kong, Ai Jun Liu, Shou Chun Li, and Dong Gang Xu. 2015. "Cold-Inducible RNA-Binding Protein Inhibits Neuron Apoptosis through the Suppression of Mitochondrial Apoptosis." *Brain Research* 1622: 474–83. doi:10.1016/j.brainres.2015.07.004.

Zhang, H, J Y Lee, and B Tian. 2005. "Biased Alternative Polyadenylation in Human Tissues." *Genome Biol* 6 (12): R100. doi:10.1186/gb-2005-6-12-r100.

Zhang, Qian, Ya Zhou Wang, Wenbin Zhang, Xiaoming Chen, Jiye Wang, Jingyuan Chen, and Wenjing Luo. 2017. "Involvement of Cold Inducible RNA-Binding Protein in Severe Hypoxia-Induced Growth Arrest of Neural Stem Cells In Vitro." *Molecular Neurobiology* 54. Molecular Neurobiology: 2143–53. doi:10.1007/s12035-016-9761-1.

Zhang, Xu, Jian-Ying Zhou, Mark H Chin, Athena A Schepmoes, Vladislav A Petyuk, Karl K Weitz, Brianne O Petritis, et al. 2010. "Region-Specific Protein Abundance Changes in the Brain of

MPTP-Induced Parkinson's Disease Mouse Model." *Journal of Proteome Research* 9 (3): 1496–1509. doi:10.1021/pr901024z.

Zhou, Mian, Weng-lang Yang, Youxin Ji, Xiaoling Qiang, and Ping Wang. 2014. "Cold-Inducible RNA-Binding Protein Mediates Neuroinflammation in Cerebral Ischemia." *Biochimica et Biophysica Acta* 1840 (7): 2253–61. doi:10.1016/j.bbagen.2014.02.027.

Zhu, Hui, Hua Lin Zhou, Robert A. Hasman, and Hua Lou. 2007. "Hu Proteins Regulate Polyadenylation by Blocking Sites Containing U-Rich Sequences." *Journal of Biological Chemistry* 282 (4): 2203–10. doi:10.1074/jbc.M609349200.

Zhu, Min, Wenwei Li, and Chuanzhen Lu. 2012. "Role of Alpha-Synuclein Protein Levels in Mitochondrial Morphology and Cell Survival in Cell Lines." *PLoS ONE* 7 (4): 1–9. doi:10.1371/journal.pone.0036377.

Zhu, Xinzhou, Christoph Buhrer, and Sven Wellmann. 2016. "Cold-Inducible Proteins CIRP and RBM3, a Unique Couple with Activities Far beyond the Cold." *Cellular and Molecular Life Sciences* 73 (20): 3839–59. doi:10.1007/s00018-016-2253-7.

Zhu, Xinzhou, Andrea Zelmer, Josef P. Kapfhammer, and Sven Wellmann. 2016. "Cold-Inducible RBM3 Inhibits PERK Phosphorylation through Cooperation with NF90 to Protect Cells from Endoplasmic Reticulum Stress." *FASEB Journal* 30 (2): 624–34. doi:10.1096/fj.15-274639.

Zlokovic, Berislav V. 2011. "Neurovascular Pathways to Neurodegeneration in Alzheimer's Disease and Other Disorders." *Nature Reviews. Neuroscience* 12 (12). Nature Publishing Group: 723–38. doi:10.1038/nrn3114.